Modifying the Natural State of Nucleic Acids: Three-Dimensional DNA Lattices and Extended Deoxyribonucleosides

Author: Eric Hardter

Boston College

The Graduate School of Arts and Sciences

Department of Chemistry

MODIFYING THE NATURAL STATE OF NUCLEIC ACIDS: THREE-DIMENSIONAL DNA LATTICES AND EXTENDED DEOXYRIBONUCLEOSIDES

A dissertation

by

ERIC DIHLMANN HARDTER

Submitted in partial fulfillment of the requirements
for the degree of

Doctor of Philosophy

May 2014

Abstract

MODIFYING THE NATURAL STATE OF NUCLEIC ACIDS: THREE-DIMENSIONAL DNA LATTICES AND EXTENDED DEOXYRIBONUCLEOSIDES

Eric Dihlmann Hardter

Under the guidance of Dr. Larry W. McLaughlin

By virtue of encoding and transferring hereditary information, nucleic acids effectively represent the blueprint for life as we know it. Given the biological relevance of this class of polymers, it comes as no surprise that scientists are constantly striving to reach a greater understanding of the innumerable genetic corridors contained within the human genome. This has led to the rational design and synthesis of numerous nucleoside analogues in an attempt to alter and subsequently control native nucleic acid structure and function.

The first attempts at harnessing the latent abilities of DNA are described in Chapter 2. Multiple tetrahedral branching "hubs" were designed, synthesized and characterized, at which point single-stranded DNA could be elongated from each of the four points of origin. Ensuing hybridization studies were performed with the goal that the binding traits of these elongated tetrahedral lattices could be monitored, and that fully formed lattices could potentially function as means of drug encapsulation or molecular tethering.

Chapter 3 describes direct alteration of the standard DNA backbone. Successive synthetic efforts towards creating a 6'-extended deoxyadenosine

molecule are detailed, and its effects on the stability of duplexed DNA (along with sister molecules 6'-deoxythymidine and an elongated 3'-deoxythymidine) are also defined. Upon insertion into DNA, this class of extended nucleosides could ultimately lead to a new duplex structure, as well as novel binding properties.

For Andrea and Orion

Thank you for giving me a reason to smile every day

Acknowledgements

I want to first thank Dr. Larry McLaughlin for allowing me to join his laboratory and offering me guidance during my time at Boston College. He took a chance on me despite a total lack of an organic chemistry background, and was patient even through periods of time where success was minimal. It was due to my time in the McLaughlin lab that I was able to become a significantly more well rounded chemist.

I also want to thank my thesis committee of Dr. Mary Roberts, Dr. Jianmin Gao and Dr. Eranthie Weerapana. I greatly appreciate the time you've taken to help facilitate the conclusion of my Ph.D. candidacy. I especially want to thank Dr. Roberts for serving as my first reader for the past several years, and also as someone to talk to at times when I lost perspective.

Dr. Carl Christianson and Dr. Mark Schlegel were also both integral to my success. They were excellent sources of knowledge, and assisted greatly in the day-to-day operations of the lab, including with one-on-one and group meetings. It was partly due to their help that my progress was able to remain on track.

During my time at Boston College I've also had the pleasure of working with many excellent scientists. Dr. Allen Horhota was the strongest guiding force during my early years, and I benefited greatly from his experience, patience and teaching abilities. Dr. Nicholas Greco was another exemplary chemist, and I still regard him

as one of the hardest working people I've ever met. I worked side by side with Dr. Joseph Arico, and his attention to detail with regards to practical methodologies helped me drastically refine my technique. Dr. Ayan Pal is one of the most intelligent people I've met, and I always valued his advice and chemical intuition.

Dr. Chris Theile and Dr. Han Yueh joined the lab around the same time I did. In addition to being remarkable chemists, they each helped turn the work environment into a fun place to be. I consider both great friends to this day.

Dr. Rajat Das joined the lab towards the end of my tenure, and I view his assistance as one of the primary reasons I was able to get over the hump with my research. He possesses a wealth of knowledge with regards to DNA chemistry and is also one of the kindest people I've known. With his passion and dedication, the sky is the limit for the extended nucleoside project.

I've also had the privilege of working with several dedicated undergraduate researchers. William "Billy the Kid" Lee and Erin Wolf were instrumental in helping propagate my early research, and Amy Calhoun performed above and beyond the scope of her project. I have no doubt all three will aspire to do great things.

I was fortunate enough to make numerous friends within the BC graduate community. Dr. Kimberly Mendes and Dr. Gregory Cockrell were always great sources of conversation, as well as my partners in crime for perpetual caffeine consumption. I've also gotten to know Dr. Timothy Montavon, Dr. Jason Gavenonis,

Dr. Becca Goldstein, Dr. Christopher Pace, Dr. Kate Harris, Dr. Cheryl Gradziel, Nicholas Pace and Azade Hosseini very well, and hold each in the highest regard.

The Boston College support staff has been nothing short of incredible. Dr. John Boylan, Dr. Thusitha Jayasundera and Marek Domin were extremely helpful and kept the instrumental facilities running smoothly. Lori St. Peter, Steve Quinn Ginny Owens, Dale Mahoney, Terri Wallace and Lynne Pflaumer were always able to help when needed. Dr. Lynne O'Connell constantly found the right teaching placement for me, and Dr. Neil Wolfman was an amazing professor for whom I was able to assist. John Madden, Dr. Ian Parr and Jennifer Hanlon always made sure I worked in a safe environment, and finally, Bill Fogerty never failed to wish me "success" in my endeavors – I valued his positivity likely more than he'll ever know.

My friends from Pennsylvania and Delaware were extremely supportive, and always inquired about the progress of my research. Ed and Tracie Crowley were also constantly encouraging me in my undertakings. My family always believed in me, quite possibly more than I believed in myself at times – that sentiment alone was invaluable to my continued efforts.

Finally and most importantly, there's no way I'd be where I am today without the love and affection of my girlfriend, Andrea. Along with our "little man" Orion, I'm excited to start the next chapter of our lives together. I love you more than words can say, and will continue to do so for the rest of my days.

Table of Contents

List of Figures

List of Schemes

List of Tables

List of Abbreviations

6'-dA	(2*R*,3*S*,5*R*)-5-(6-amino-9*H*-purin-9-yl)-2-(2-hydroxyethyl)tetrahydrofuran-3-ol
6'-dT	1-((2*R*,4*S*,5*R*)-4-hydroxy-5-(2-hydroxyethyl)tetrahydrofuran-2-yl)-5-methylpyrimidine-2,4(1*H*,3*H*)-dione
9-BBN	9-borabicyclo[3.3.1]nonane
A	adenine
Ac	acetyl
ACN	acetonitrile
AIBN	azobis(isobutyronitrile)
BBr_3	boron tribromide
Bn	benzyl
Bu_3SnH	tributyltin hydride
Bz	benzoyl
C	cytosine
$CDCl_3$	deuterated chloroform
CD_3OD	deuterated methanol
$CHCl_3$	chloroform
CN	cyano
CPG	controlled pore glass
d	doublet
dd	doublet of doublets
DART	direct analysis in real time
dA	2'-deoxyadenosine
dC	2'-deoxycytidine
dG	2'-deoxyguanosine
dT	2'-deoxythymidine
DBU	1,8-diazabicyclo[5.4.0]undec-7-ene

DCM	dichloromethane
DIPEA	diisopropylethylamine
DMAP	4-(dimethylamino)pyridine
DMF	dimethylformamide
DMSO-d_6	deuterated dimethylsulfoxide
DMTr	4,4'-dimethoxytrityl
DNA	β-D-2'-deoxyribonucleic acid
ESI	electrospray ionization
EtOAc	ethyl acetate
EtOH	ethanol
EVE	ethyl vinyl ether
G	guanine
H_2	hydrogen
H_2O_2	hydrogen peroxide
$Hg(CH_3COO)_2$	mercuric acetate
HPLC	high performance liquid chromatography
HRMS	high resolution mass spectrum
K_2CO_3	potassium carbonate
lcaa	long chain aminoalkyl
M	molar
m	multiplet
MALDI-TOF	matrix-assisted laser desorption ionization – time of flight
Me	methyl
MeOH	methanol
$MgCl_2$	magnesium chloride
MHz	megahertz
mL	milliliter
mM	millimolar
MS	mass spectrometry

MTPB	methyltriphenylphosphonium bromide
$NaBH_4$	sodium borohydride
NaCl	sodium chloride
NaH	sodium hydride
$NaHCO_3$	sodium bicarbonate
NaOH	sodium hydroxide
NaOMe	sodium methoxide
NH_3	ammonia
NH_3/MeOH	ammonia in methanol
NH_4Cl	ammonium chloride
NH_4OH	ammonium hydroxide
nm	nanometer
NMO	*N*-methylmorpholine *N*-oxide
NMR	nuclear magnetic resonance
OH	hydroxyl
OsO_4	osmium (VIII) tetroxide
PAGE	polyacrylamide gel electrophoresis
Pd/C	palladium on activated charcoal
$Pd(OH)_2$	palladium hydroxide
pPTS	pyridinium *p*-toluenesulfonate
pyr	pyridine
q	quartet
R_f	retention factor
RNA	β-D-ribonucleic acid
s	singlet
$SOCl_2$	thionyl chloride
ssDNA	single stranded DNA
T	thymine
t	triplet

TBAF	tetrabutylammonium fluoride
TBDPS	*tert*-butyldiphenylsilyl
TBS	*tert*-butyldimethylsilyl
tBuOK	potassium *tert*-butoxide
TCA	trichloroacetic acid
TEA	triethylamine
TEAA	triethylammonium acetate
THF	tetrahydrofuran
TIPS	triisopropylsilyl
TLC	thin layer chromatography
Tm	thermal melting point
TMS	trimethylsilyl
tol	*para*-toluoyl
UV/Vis	ultraviolet and visible light
W	watt
Å	angstrom
δ	chemical shift in parts per million
µ	micro

Chapter 1

Introduction

1.1 Discovery of Deoxyribonucleic Acids and Main Structural Components

60 years ago a discovery was made that would ultimately redefine the way the scientific community perceived our main hereditary material, deoxyribonucleic acids (DNA).[1] At this time research performed by Watson and Crick presented a new model for DNA structure, asserting that two antiparallel phosphodiester chains are able to wind about one another in a helical fashion, with a hydrogen bonding core formed by planar nucleobases extending from each strand (Figure 1.1). This improved upon a previous model that suggested DNA existed in an alternative triplex structure, with internal phosphates and external nucleobases.[2, 3]

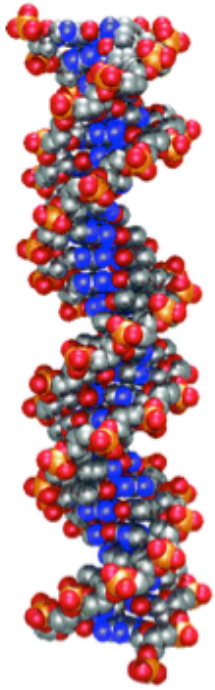

Figure 1.1: A molecular model of a B-form DNA duplex with two antiparallel phosphodiester backbones (red, silver and yellow chains) surrounding an internal core of hydrogen bonding nucleobases (blue).[4]

A two-dimensional view reveals a more simplified view of the DNA components (Figure 1.2). Within each ssDNA monomer exist three main components: the nucleobase (of which there are four primary species), the pentose sugar (2'-deoxy-D-ribose) and the phosphate moieties that help form the backbone.

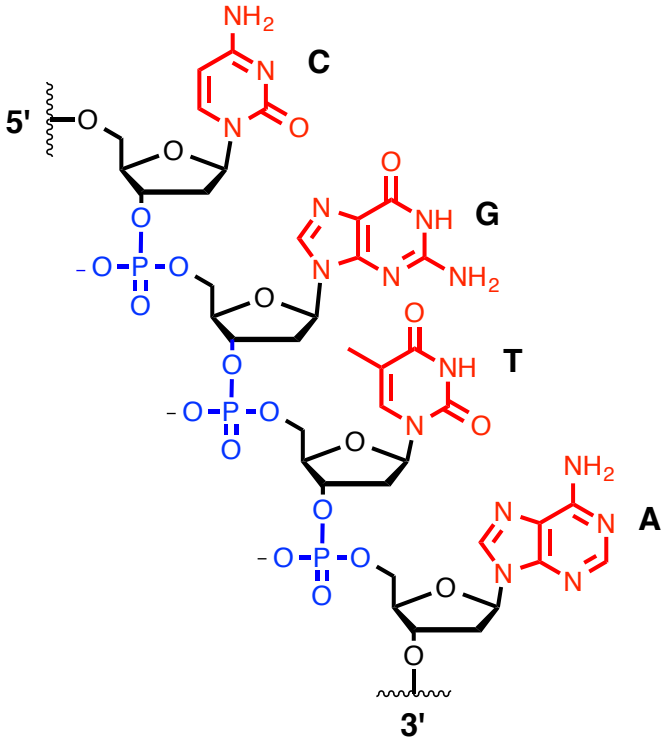

Figure 1.2: A simplified view of a ssDNA monomer. The three principal components include the nucleobases (red), sugar (black) and phosphate groups (blue). There are four main nucleobases: adenine (A), thymine (T), guanine (G) and cytosine (C).

The nucleobases include a pair apiece of purines (bicyclic molecules) and pyrimidines (single-ring heterocycles). As these pairs possess differing numbers of atoms, they are unsurprisingly numbered in a different manner (Figure 1.3).

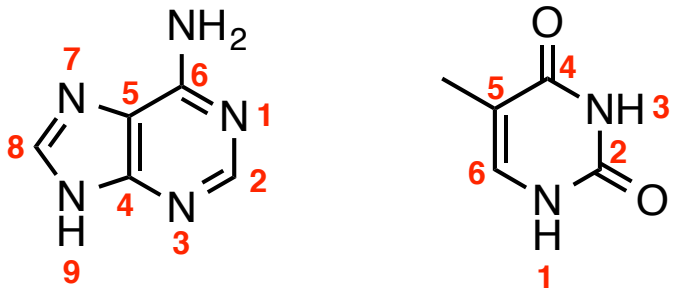

Figure 1.3: Standard numbering of purine (left) and pyrimidine (right) nucleobases.[5]

As mentioned previously, another vital component of DNA is the five-membered heterocyclic sugar. The 2'-deoxy-D-ribose sugar in DNA effectively serves as the branching point between the nucleobases and phosphodiester backbone, and its conformation also helps dictate the three-dimensional structure of ssDNA (Figure 1.4).

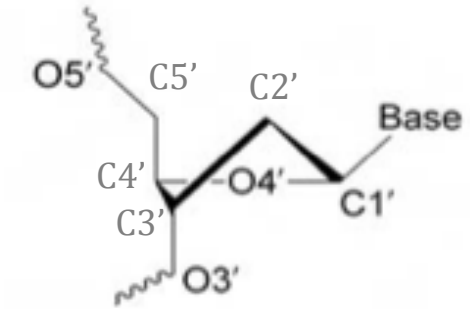

Figure 1.4: The puckering conformation adopted by 2'-deoxy-D-ribose in DNA. Numbering of the sugar also noted.[6]

The C2'-*endo* conformation of the sugar effectively serves to order the phosphodiester backbone in a manner conducive to minimizing steric clash and charge-charge interaction. In RNA oligomers, this pucker is reversed due to the presence of a hydroxyl moiety on the 2'-carbon, yielding a C3'-*endo* conformation.[7]

When a nucleobase is coupled to a sugar the resultant molecule is known as a nucleoside. Given the degrees of freedom of the nucleobase-sugar bond, as well as the two planes of bonding relative to the sugar, it's possible for multiple nucleoside conformations to exist. It's known, however, that the bonding preference is for a conformation that is both beta (β) and anti about the C1'-N9 (purine) and C1'-N1 (pyrimidine) glycosidic bond (Figure 1.5).

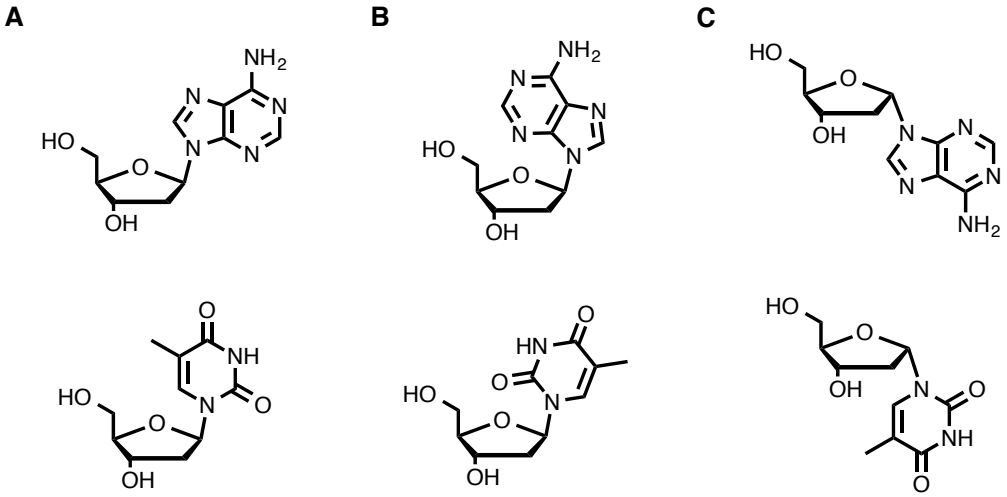

Figure 1.5: 2'-deoxyadenosine and 2'-deoxythymidine nucleosides in A) β/anti conformations, B) β/syn conformations and C) α-conformations.

While the syn-conformation can be adopted if bulky substituents are placed on the nucleobase (7/8/9-positions on purines or 5/6-positions on pyrimidines), it's not generally seen in unmodified duplexed DNA.[8, 9] Similarly, though α-nucleosides have been probed for medicinal value, they remain an undesired DNA conformation.[10] The β/anti conformation not only eliminates the majority of steric clash between the nucleobase and sugar, but also helps promote hydrogen bonding between nucleobases (see section 1.2.1).

The final ssDNA component shown in Figure 1.2 is the phosphodiester backbone. In addition to serving as linkages between the 2'-deoxyribose sugars, phosphate groups are also known to be resistant to exogenous nucleophiles such as water.[11] They can also be recognized and hydrolyzed through enzymatic mediation, a vital trait when it comes to DNA repair.[12]

1.2 DNA Duplex Characteristics

1.2.1 Forces Driving DNA Duplex Formation

Due to the asymmetry of the phosphodiester backbone (Figure 1.2), there exist two distinct concluding points on each ssDNA oligomer – the 5'-phosphate and 3'-hydroxyl termini. However, duplex formation between two complementary strands of DNA must occur in an antiparallel fashion such that the 3'-terminus of one strand is opposite the 5'-terminus of the other, and vice versa (Figure 1.6). This specific coordination allows for concurrent genomic replication, a feat that would be impossible if the polarity of both strands aligned.[13]

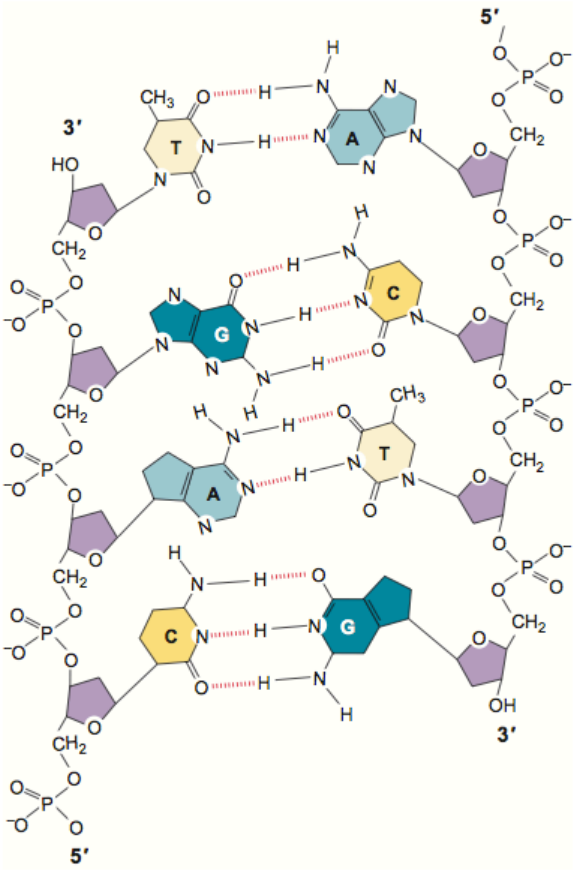

Figure 1.6: A simplified view of the antiparallel nature of a DNA duplex.[14]

The main factor that draws two lengths of ssDNA together is their base-pair complementarity. It's been noted above that there exist four distinct nucleobases in DNA (five total, including the RNA base uracil), but their ability to hydrogen bond in a complete and specific manner is what dictates whether two strands can ultimately form a duplex. During DNA renaturation, small tracts of complementary bases can recognize one another, functioning as nucleation sites and anchors for subsequent annealing.[15] The standard base pairs seen in DNA are shown below (Figure 1.7).

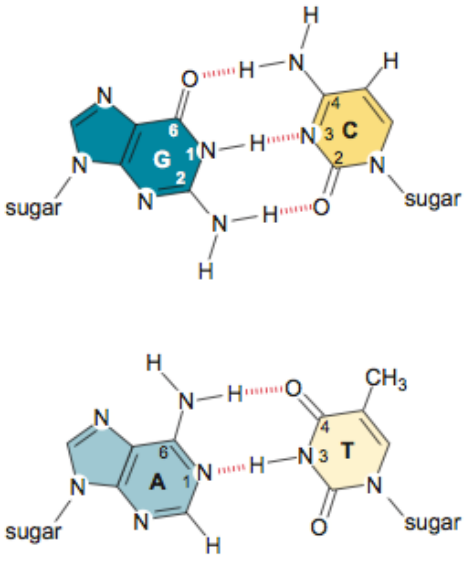

Figure 1.7: Standard DNA base-pairing exists between guanine (G) and cytosine (C) nucleobases, as well as adenine (A) and thymine (T) nucleobases.[16]

The G-C base pair forms due to hydrogen bonds between the O6, N1 and N2 of G with the N4, N3 and O2 of C, respectively. The A-T base pair forms due to hydrogen bonding interactions between the N6 of A and O4 of T, along with the N1 of A and N3 of T. As the G-C base pair forms three hydrogen bonds relative to the two of A-T, it stands as the stronger bonding pair.

Another necessary requirement for duplex formation is the mitigation of the negatively charged phosphate groups. As shown in Figure 1.2, each phosphate group in DNA contains an oxyanion, resulting in a highly negatively charged species. Without the presence of a counterion, both intra- and intermolecular repulsion would preclude DNA from forming a duplex. Simple addition of cations such as magnesium, sodium and potassium has proven to aid in duplex formation.[17]

Once in its duplex form, one of the main factors of stability is the successive stacking of base pairs. As the base pairs represent planar, aromatic and electrostatic systems, they present an ability to act in concert with one another. This ability manifests itself in the form of π-π interactions, London dispersion forces and electrostatic interactions. The totality of these beneficial exchanges results in the primary reason as to why the duplex is held together.[18] Even if perturbed, these base pairs possess a robust ability to adjust their positions relative to one another in order to minimize steric clash (Figure 1.8).

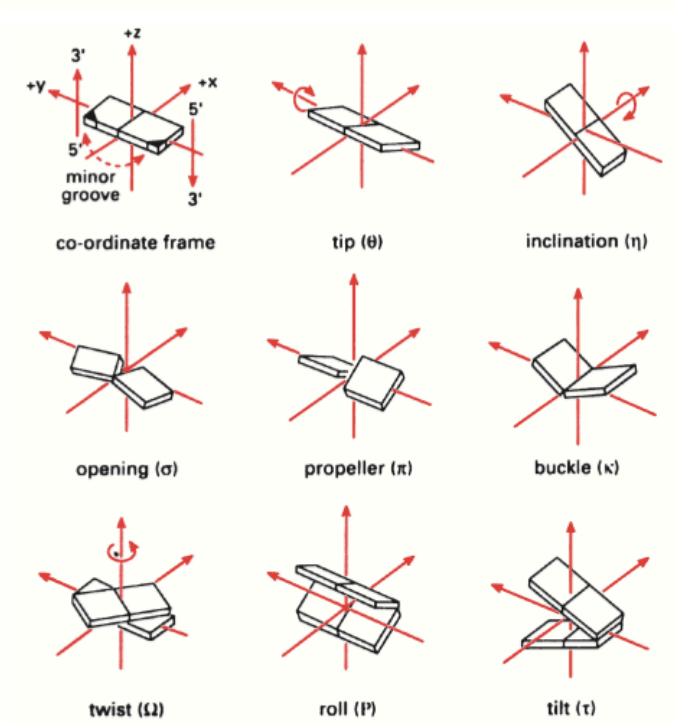

Figure 1.8: A pseudo-top down look at how a base pair can move in concert (top row), how the base-pairing partners can move relative to one another (middle row), and how two sets of base pairs can reset themselves in a three-dimensional plane.[19]

Finally, the spacing patterns in duplexed DNA allow for external molecules to act upon certain functionalities of the internal base-pairing core. Given the helical nature of DNA, the winding of the complementary strands occurs in a fashion so as to allow for two distinct persistent fissures, noted as the major and minor grooves (Figure 1.9).

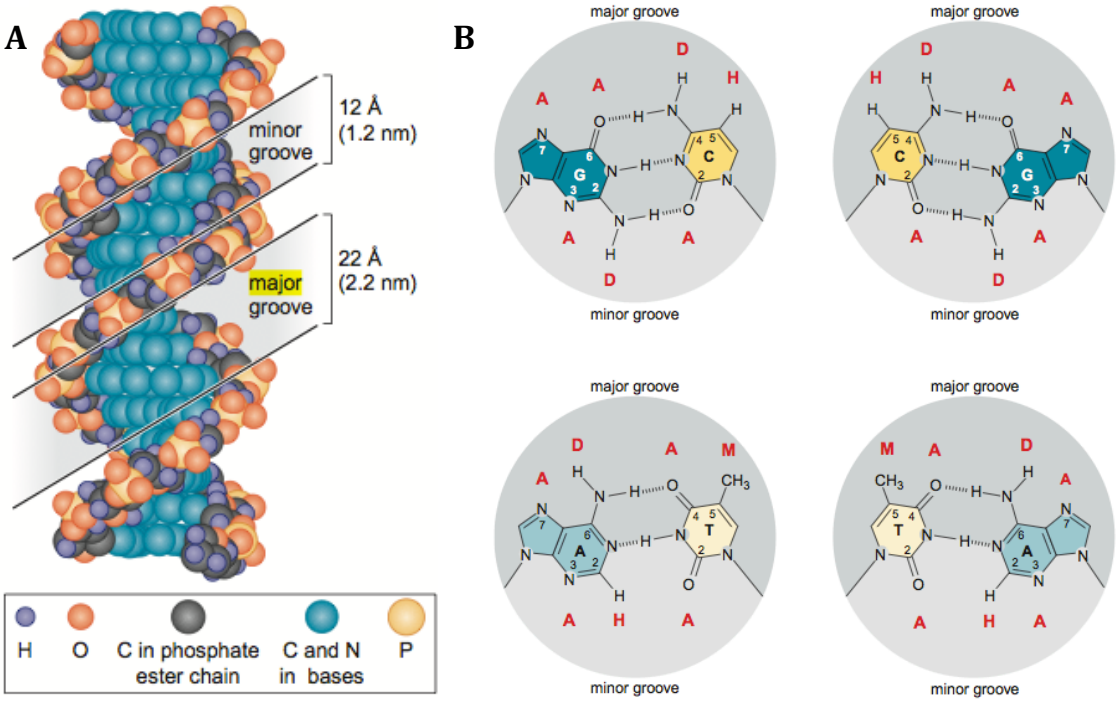

Figure 1.9: A) A simplified depiction of a B-form DNA duplex, with major and minor grooves resulting from gaps in the helical winding, and B) the exposed functional groups of each possible base pair in the major and minor grooves, with hydrogen bond donors (D) and acceptors (A) noted.[16]

As can be seen above, A-T and T-A base pairs allow for a greater intrusion into the minor groove, while also presenting two hydrogen-bond acceptors. As such, in poly A-T regions it's been shown that water molecules coordinate both with the bases and each other to form a spine of hydration, providing further stabilizing measures.[20] Our lab has even probed the potential of mimicking the spine of

hydration with hydroxymethyl functionalized 3-deazadeoxyadenosine in order to determine if this stabilization could be obtained in a pseudo-intramolecular manner (Figure 1.10).[21]

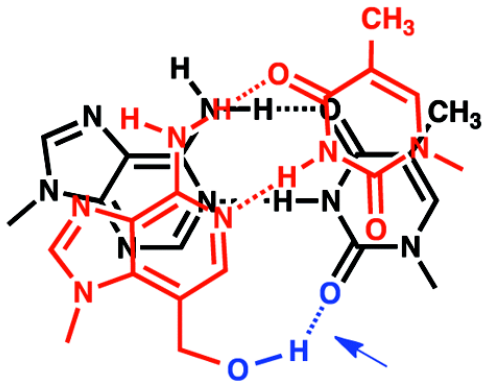

Figure 1.10: A simplified view of a deoxyadenosine derivative containing a hydroxymethyl extension at the 3-position, as well as it's potential to aid in forming a hydrogen bonding network.

1.2.2 Main Classes of Duplexed DNA

Thus far many of the explanatory measures above (2'-endo sugar pucker, major and minor groove interactions) have described B-form DNA, which is viewed as the standard DNA-DNA duplex. As revealed by crystallographic measures, B-form DNA is also defined by several other characteristics.[22] These include, but are not limited to nucleosides existing in the anti-conformation, a helical rise per base-pair of 3.4 Å (and therefore 10 base pairs per each 3.4-nm helical turn), and also a right-handed formation which prefers a larger relative humidity. Other qualifiers include relatively equal depths of the major and minor grooves (8.5 Å and 8.2 Å

respectively), and a nearly two-fold difference between their widths (11.6 Å and 6.0 Å respectively).[23]

Another known helical structure is the A-form assembly, which is also a right-handed helix. It's more compact relative to B-form DNA, with a smaller base-pair rise (2.5 Å) and 11 base pairs per turn (2.8 nm). This tightly packed formation also results in drastically different major and minor grooves, with a much deeper major groove (13.0 Å versus 2.6 Å for the minor groove), and a much wider minor groove (11.1 Å versus 2.2 Å for the major groove). Continuing, the sugar pucker is reversed in A-DNA, with a 3'-endo conformation versus the 2'-endo pucker seen in B-DNA. A-form DNA is seen most commonly in RNA-DNA and RNA-RNA duplexes.[24]

Relatively speaking, the structure of a third type of DNA duplex doesn't come close to resembling that of either A- or B-form DNA. Z-form DNA duplexes exist in a left-handed fashion and are typically formed between complementary strands rich in dG and dC residues, where nucleosides adopt anti and syn conformations in an alternating manner.[25] This also results in a combination of C2'-endo and C3'-endo sugar conformations. Similar to A-form DNA there is a large inequity in the depths of the major and minor grooves (3.7 Å and 13.8 Å, respectively), though the directionality is reversed. High salt concentration is also required for formation due to the proximity of adjacent phosphate groups.

These major differences in duplex characteristics are summed up pictorially below (Figure 1.11):

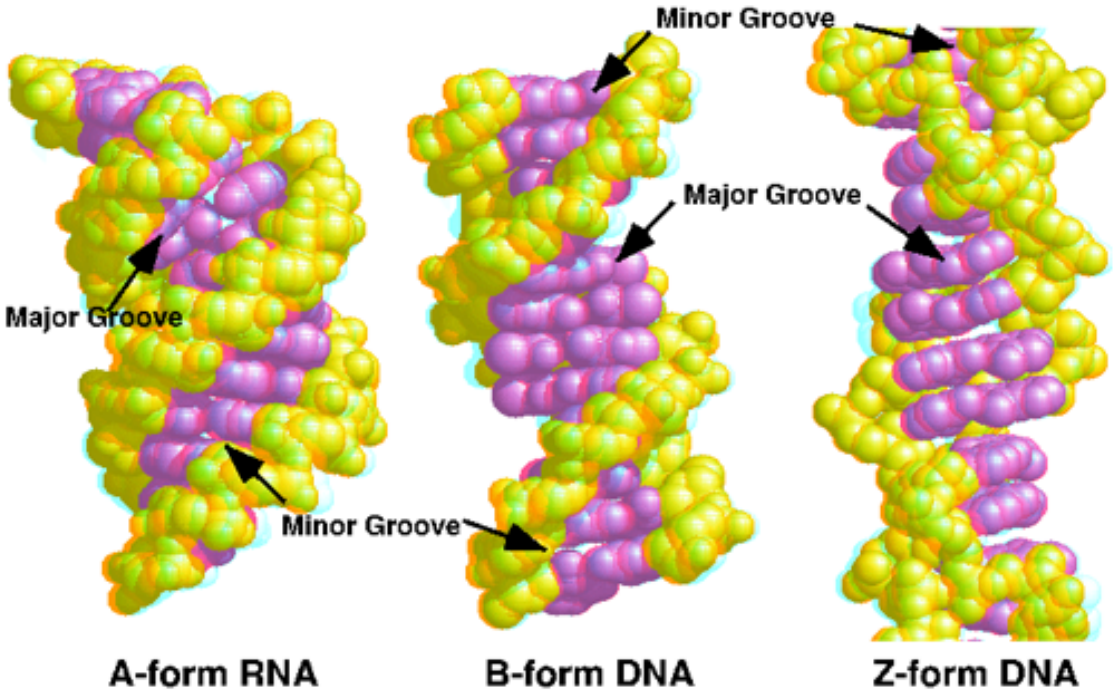

Figure 1.11: Space-filling views of the three main forms of nucleic acids. Yellow tracts represent the phosphodiester backbones and the purple atoms represent the base-pairs. Major and minor grooves are noted for each duplex.[26]

1.3 General Target Sites for DNA Modification

As mentioned previously (Figure 1.2), there exist three main components of nucleic acids: the sugar, the nucleobase and the phosphodiester backbone. As such, when it comes to transforming nucleosides, it's unsurprising that these represent three distinct modification sites. Alteration to the phosphodiester backbone of DNA will be covered in detail in Chapter 3, so this section will focus on modifications to the nucleobase and sugar.

Simple addition of an amine moiety to the 2-position of the adenine base yields the more functionalized 2,6-diaminopurine (DAP). This subtle change allows for a third hydrogen bond between the C2-amine of DAP and C2-oxygen of thymine, thereby enhancing the stability of the base pair (Figure 1.12). It's been shown that Cyanophage S-2L takes advantage of this higher level of stability, as it has been found to use DAP-nucleosides instead of 2'-deoxyadenosine.[27]

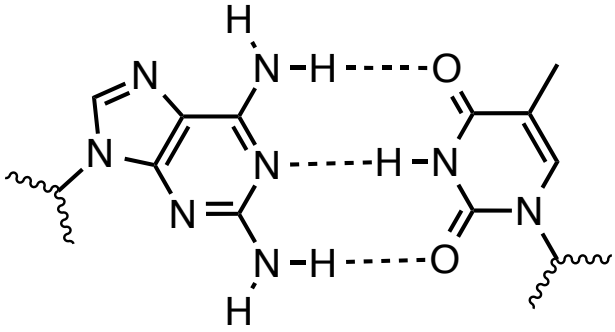

Figure 1.12: A DAP-thymine base pair contains an additional hydrogen bond.

Other simple modifications to the canonized quartet of adenine, guanine, cytosine and thymine (and their corresponding nucleosides) have been reported as well. 5'-methylcytidine has known origin in plants and bacteria, and has been previously isolated from *E. coli*.[28] Xanthosine, an inosine derivative with an extra carbonyl moiety in the 2-position is a known intermediate in production of caffeine.[29] 7-methylguanosine has been isolated from human urine and is believed to potentially function as a biomarker for certain types of cancer.[30]

Higher levels of nucleobase functionalization have also been reported. Addition of a thiophene moiety to the 6-position of a purine nucleobase yielded a

base-pairing entity that could also function as a fluorescent reporter (Figure 1.13).[31] Inclusion of a metal-binding ligand system between base pairs has allowed for the ability to bind copper ions.[32] Finally, expansion of the nucleobase has been reported by Kool et al., as addition of a benzene ring to adenine and thymine nucleobases has allowed for a more robust set of potential base pairs.[33]

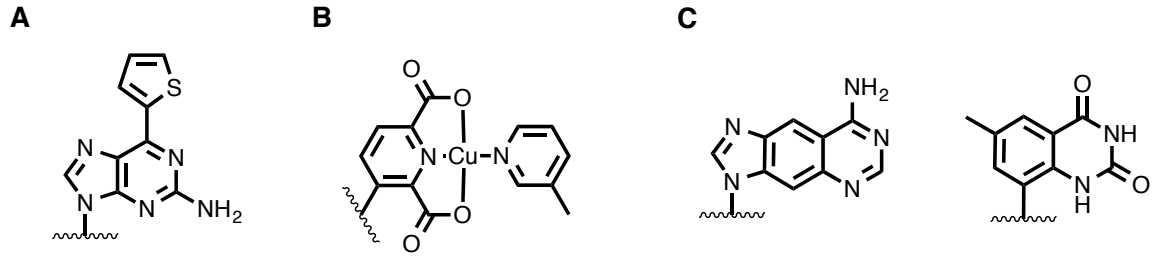

Figure 1.13: Modified nucleobases include A) a thiophene containing fluorescent system, B) a copper binding base-pair including an acidic modified pyrimidine opposite a pyridine derivative and C) a pair of expanded adenine and thymine nucleobases.

As mentioned above, another modification site is the 2'-deoxy-D-ribose sugar entity. This has included bi-and tricyclic systems, as well as extended six-member rings (Figure 1.14).[34,35] The O4' atom has also served as a substitution site, including displacement with a sulfur atom.[36] Many of these non-natural nucleosides have been probed for uses in antisense therapeutics.

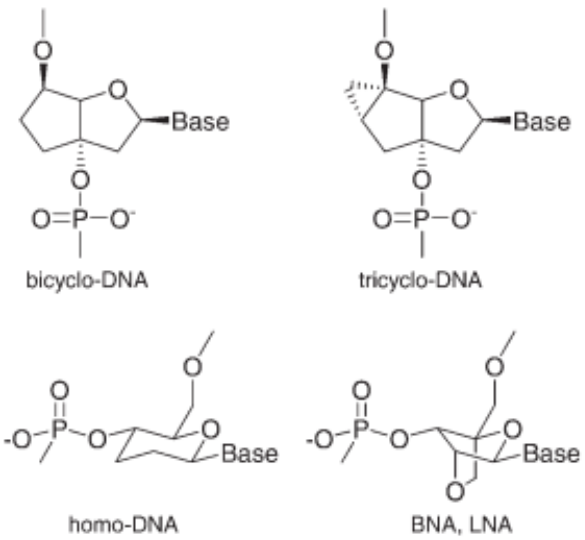

Figure 1.14: Examples of modified sugars include bi- and tricyclic systems and larger heterocycles.[34]

1.4 Known Methods of External DNA Synthesis

In order to perform DNA-based studies, it's crucial to have a robust means of propagation. Molecular cloning is arguably the predominant *in vitro* methodology, generally affording recombinant DNA in an appreciable yield.[37] Polymerase chain reaction (PCR) is a newer technique that can take a few strands of DNA and ultimately generate a quantity several orders of magnitude higher.[38] In PCR, DNA duplexes are constantly denatured and replicated through use of a thermally stable polymerase enzyme (ex. *Taq* polymerase) that can survive the heating process.

While these methods are useful for gaining large amounts of potentially lengthy DNA, they lack the ability to incorporate any sort of non-natural functionality. Continuing, while standard solution phase methodologies allow for insertion of non-natural nucleosides, the successive reactions would necessitate an

untenable amount of purification. This would render synthesis of even a short oligomer as a time-consuming process.

These issues were rectified with the advent of solid-phase DNA synthesis (SPDS). In SPDS, oligomers are elongated from a controlled pore glass resin of fixed pore-size, with an upper limit of approximately 50 nucleosides. Continuous deprotection/coupling/capping/oxidation reactions occur with high fidelity, ensuring that the desired product is obtained in a predominant yield (Figure 1.15). The resultant crude ssDNA can then be cleaved from the resin and segregated via HPLC, detritylated and desalted to afford pure monomer. More importantly, nucleosides containing non-natural functionalities can be inserted into ssDNA with ease. This methodology was vital to research described in the following chapters.

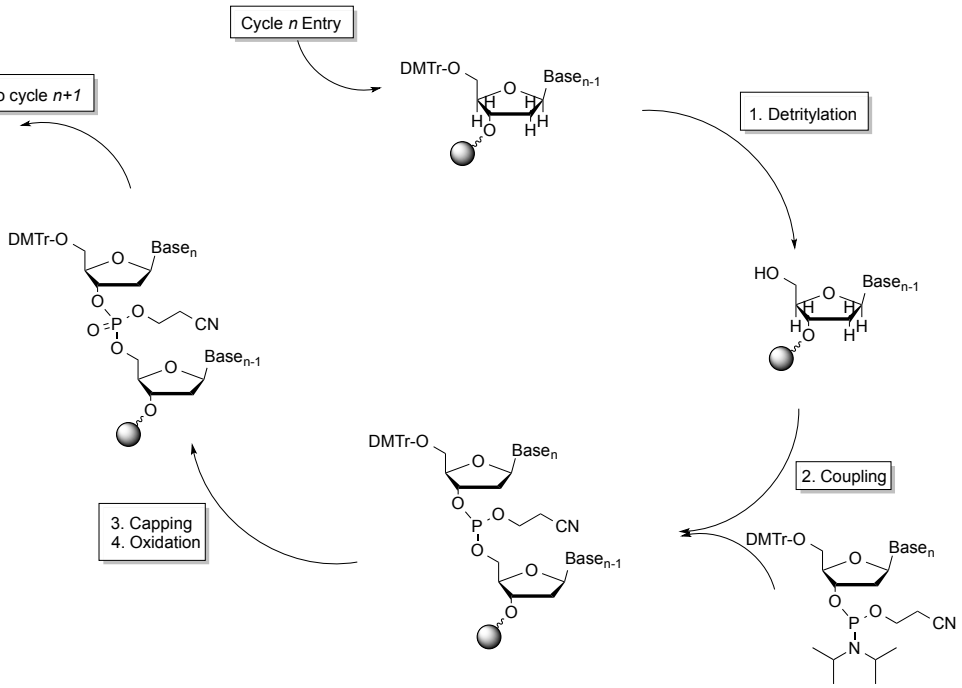

Figure 1.15: Generic cycle for solid-phase DNA synthesis.

1.5 Introduction to Subsequent Chapters

While direct modification of nucleosides was not performed, Chapter 2 describes attempts towards creation of three-dimensional DNA lattices. Synthetic methods were used to create novel tetrahedral hubs functionalized for multiple sites of DNA elongation, and SPDS played a vital role in the oligomer propagation. Chapter 3 details synthetic efforts towards a family of extended nucleosides, most notably a 6'-deoxyadenosine molecule. Insertion of these molecules into ssDNA afforded a novel family of potential hybridization products, which were then tested for salt dependence and thermal stability.

1.6 References

1. J. D. Watson and F. H. C. Crick, *Nature*, **1953**, *171*, 737-738.

2. L. Pauling and R. B. Corey, Nature, 1953, 171, 346.

3. L. Pauling and R. B. Corey, *Proceedings of the National Academy of the Sciences of the Unites States of America*, **1953**, *39*, 84.

4. T. J. Bandy, A. Brewer, J. R. Burns, G. Marth, T. Nguyen and E. Stulz, *Chemical Society Reviews*, **2011**, *40*, 138-148.

5. W. Saenger, *Principles of Nucleic Acid Structure*, Springer-Verlag: New York, 1984.

6. S. Neidle, *Principles of Nucleic Acid Structure*, Elsevier: London, 2008.

7. L. J. Murray, W. B. Arendall III, D. C. Richardson and J. S. Richardson, *Proceedings of the National Academy of the Sciences of the Unites States of America,* **2003**, *100*, 13904-13909.

8. D. W. Miles, L. B. Townsend, D. L. Miles and H. Eyring, *Proceedings of the National Academy of the Sciences of the Unites States of America*, **1979**, *76*, 553-556.

9. S. K. Mahto and C. S. Chow, *Bioorganic and Medicinal Chemistry*, **2008**, *16*, 8795-8800.

10. M. T. Migawa, J. L. Girardet, J. A. Walker II, G. W. Koszalka, S. D. Chamberlain, J. C. Drach and L. B. Townsend, *Journal of Medicinal Chemistry*, **1998**, *41*, 1242-1251.

11. F. H. Westheimer, *Science*, **1987**, *235*, 1173-1178.

12. X. G. Zhou and H. B. Gray, *Biochimica Et Biophysica Acta*, **1990**, *1049*, 83-91.

13. K. Sakabe and R. Okazaki, *Biochimica et Biophysica Acta*, **1966**, *129*, 651–654.

14. R. E. Dickerson, *Scientific American*, **1983**, *249*, 94-111.

15. J. G. Wetmur and N. Davidson, *Journal of Molecular Biology*, **1968**, *31*, 349-370.

16. J. D. Watson, *Molecular Biology of the Gene*, Benjamin Cummings Publishing: San Francisco, 2013.

17. R. Owczarzy, B. G. Moreira, Y. You, M. A. Behlke and J. A. Walder, *Biochemistry*, **2008**, *47*, 5336-5353.

18. P. Yakovchuk, E. Protozanova and M. D. Frank-Kamenetskii, *Nucleic Acids Research*, **2006**, *34*, 564-574.

19. G. M. Blackburn, M. J. Gait, D. Loakes and D. M. Williams, *Nucleic Acids in Chemistry and Biology*, RSC Publishing: Cambridge, 2006.

20. Y. Z. Chen and E. W. Prohofsky, *Nucleic Acids Research*, **1992**, *20*, 415-419.

21. K. J. Salandria, J. W. Arico, A. K. Calhoun and L. W. McLaughlin, *Journal of the American Chemical Society*, **2011**, *133*, 1766-1768.

22. H. R. Drew, R. M. Wing, T. Takano, C. Broka, S. Tanaka, K. Itakura and R. E. Dickerson, *Proceedings of the National Academy of the Sciences of the Unites States of America*, **1981**, *78*, 2179-2183.

23. S. Arnott, *Oxford Handbook of Nucleic Acid Structure*, Oxford University Press: Oxford, 1999.

24. Y. Xiong, J. Deng, C. Sudarsanakumar and M. Sundaralingam, *Journal of Molecular Biology*, **2001**, *313*, 573-582.

25. M. de Rosa, D. de Sanctis, A. L. Rosario, M. Archer, A. Rich, A. Athanasiadis and M. A. Carrondo, *Proceedings of the National Academy of the Sciences of the Unites States of America*, **2010**, *107*, 9088-9092.

26. R. E. Dickerson, *Methods in Enzymology*, **1992**, *211*, 67-111.

27. M. D. Kirnos, I. Y. Khudyakov, N. I. Alexandrushkina and B. F. Vanyushin, *Nature*, **1977**, *270*, 369–70.

28. D. B. Dunn, *Biochimica et Biophysica Acta*, **1960**, *38*, 176-178.

29. H. Ashihara, T. Yokota and A. Crozier, *Advances in Botanical Research*, **2013**, *68*, 111-138.

30. C. Reynaud, C. Bruno, P. Boullanger, J. Grange, S. Barbesti and A. Niveleau, *Cancer Letters*, **1992**, *61*, 255-262.

31. M. Kimoto, T. Mitsui, Y. Harada, A. Sato, S. Yokoyama and I. Harao, *Nucleic Acids Research*, **2007**, *35*, 5360-5369.

32. N. Zimmerman, E. Meggers and P. Schultz, *Bioorganic Chemistry*, **2004**, *32*, 13-25.

33. H. Liu, J. Gao, S. R. Lynch, Y. D. Saito, L. Maynard and E. T. Kool, *Science*, **2003**, *302*, 868-871.

34. C. Leumann, *Nucleic Acids Symposium Series*, **2006**, *50*, 55-56.

35. C. Zhou, O. Plashkevych and J. Chattopadhyaya, *Journal of Organic Chemistry*, **2009**, *74*, 3248-3265.

36. M. Faria and H. Ulrich, *Current Opinions in Molecular Therapeutics*, **2008**, *10*, 168-175.

37. J. D. Watson, *Recombinant DNA: Genes and Genomes, a Short Course*, W. H. Freeman Publishers: Gordonsville, 2007.

38. J. M. S. Bartlett and D. Stirling, *PCR Protocols*, **2003**, *226*, 3-6.

Chapter 2

Synthesis of Tetrahedral Branching Points and Attempts Towards Lattice Formation

2.1 Introduction

2.1.1 General Introduction to Controlled Nucleic Acid Complexes

The concept of ordered nucleic acid complexes that can supersede standard conformations is nothing new to the scientific community. On the genetic level, it's well known that chromosomal DNA is compacted due to a controlled, circular arrangement around histone proteins, thereby forming the nucleosome superstructure.[1] Another example is the "G-quadruplex" arrangement adopted by guanine-rich sequences (in both DNA and RNA) in the presence of a metal cation.[2] Continuing, ssRNA is known to adopt a specific tertiary structure that allows for it to play a pivotal role in protein synthesis as transfer RNA (tRNA).[3]

The desire to comprehend and subsequently harness the ability to create these molecular scaffolds is understandable, given the biological relevance of the monomers in question. As such, conformers of RNA have been probed in order to understand the kinetics and potential folding triggers.[4-6] Likewise, analysis has also been performed in order to gauge additional variants to the commonly accepted A, B and Z-forms of DNA.[7]

It should therefore come as little surprise that *in vitro* efforts represent the next step towards understanding and utilizing non-natural nucleic acid superstructures in order to perform a wide multitude of biochemical tasks. Solid phase synthesis allows for the ability to mass produce the requisite nucleic acid

strands, which can then also be combined with organically synthesized molecules to be used in a variety of ways. The section below will attempt to provide a brief summary of these pertinent endeavors.

2.1.2 Previous Efforts Towards Nucleic Acid Molecular Assemblies

Seeman and associates have been amongst the foremost pioneers into the world of nucleic acid molecular assemblies. His rational design and usage of double crossover (DX) DNA enabled formation of nanoscale assemblies that could be visualized using atomic force microscopy (Figure 2.1).[8] Similar techniques were utilized where the crossover patterns were regulated to form repeating triangular motifs, which could then be propagated and studied.[9]

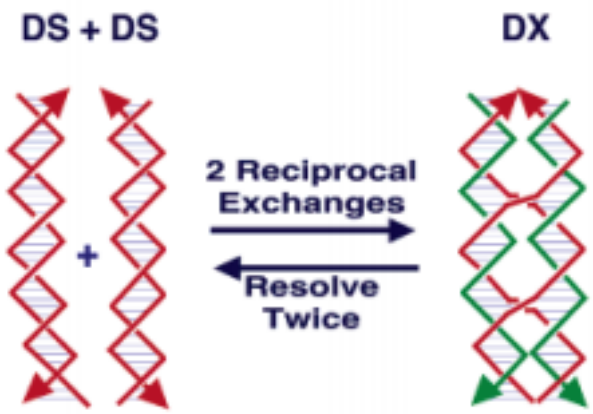

Figure 2.1: The simplest way to form DX DNA with strands of the same polarity.[10]

In an analogous manner, a controlled B-form to Z-form DNA transition of DX crossover duplexes was used to bring two attached fluorescent dye molecules closer together, a feat which was monitored by fluorescence resonance energy transfer spectroscopy.[11] In another example of a microassembly, a DNA tiling technique was

utilized in conjunction with an attached tetraphenylporphyrin derivative in order to create a "tunnel," which could then be used as a nanoscale scaffold.[12] Continuing this trend of functionalization, DX motifs were modified to terminate in a self-cleaving DNAzyme hairpin that could be triggered by the presence of copper (II) ions.[13]

Another example of nucleic acid functionalization is Szostak's use of ssDNA as an aptamer.[14] By virtue of screening a large pool of sequences, he was able to discover which ones could fold into a desired conformation, and could then isolate them using a DNA affinity column. He was also able to discover a conserved 18-mer sequence that could potentially fold into a stem-loop structure. Similarly, RNA was found to form 3D aptamers, which could then target specific proteins using the "presenter protein strategy."[15]

Mirkin and associates took another step forward by using thiolated ssDNA in conjunction with gold nanoparticles, as sulfur and gold are known to have a strong binding affinity (a fact which is of direct relevance to the work shown below).[16] One example includes separating DNA-bound gold particles of differing sizes by virtue of using their respective duplex melting points.[17] By changing the sequences of ssDNA attached to the gold nanoparticles, it was also shown that crystallographic arrangements could be ordered as desired.[18]

Given the controllable and programmable nature of nucleic acids, it's no surprise the work noted above is far from totally inclusive. With that said, it represents a great snapshot of the designs of and uses for nucleic acid constructs. The next section continues with the description of another family of DNA superassemblies.

2.1.3 Synthesis of Multi-Arm Metal Centered DNA Conjugates

While the research mentioned in the previous section is tangentially related to the goals of this project, direct antecedent work was performed by Dr. Kristen Stewart in the our lab.[19-21] Through the use of metal-bound ligands of a fixed geometry, building blocks for linear, tetrahedral and octahedral complexes were achieved (Figure 2.2). In order to create these hubs, ruthenium and nickel were utilized as the central atoms, with the coordinated ligands presenting sites for DNA attachment.

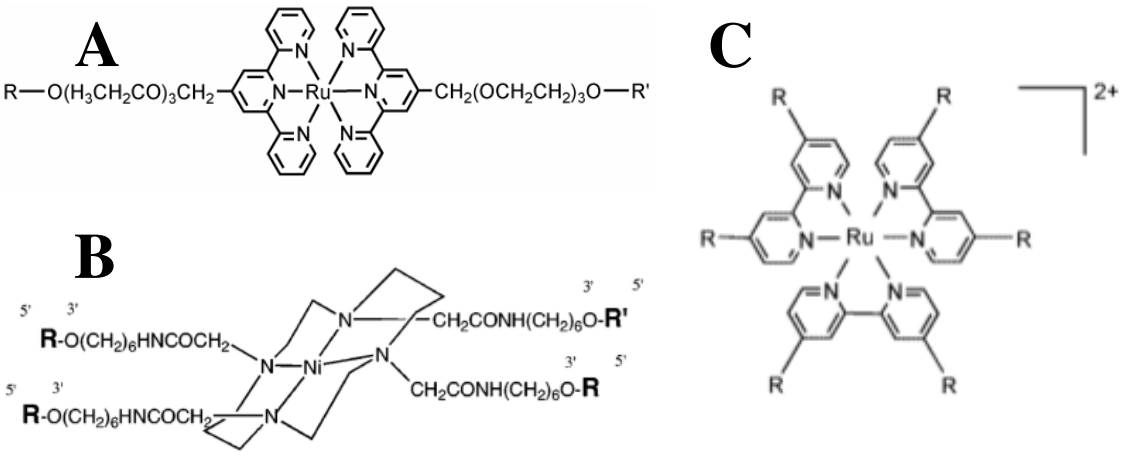

Figure 2.2: Summary of the metal-bound ligand complexes used for the formation of linear (A), tetrahedral (B) and octahedral (C) lattices.

Of particular relevance to the work presented in the following sections is the nickel-cyclam hub shown in Figure 2.2-B. Following synthesis of the metal-containing branching ligand and elongation of four identical ssDNA arms, it was shown that the branching monomers could associate both with complementary ssDNA and tetrahedral monomers to afford higher-order complexes (Figure 2.3). However, this method of potential lattice formation also had its drawbacks.

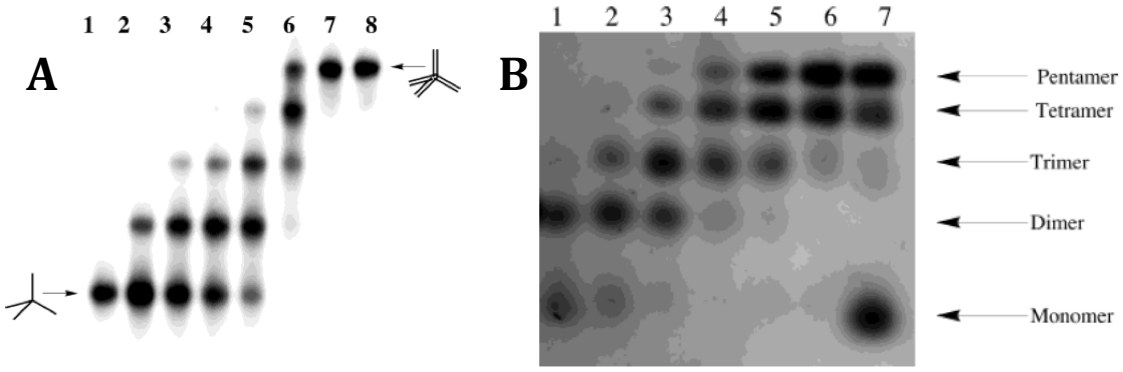

Figure 2.3: Stepwise addition of ssDNA complement (A; Lanes 1 – 8 = addition of 0, 0.25, 0.50, 1, 2, 3, 4 and 8 equivalents) and a tetrahedral monomer containing one complementary ssDNA arm (B; Lanes 1 – 7 = addition of 0.5, 1, 2, 3, 4, 5 and 10 equivalents).

Though the nickel-cyclam branching moiety was able to hybridize to its ssDNA complements in a sequential fashion, forming a complete construct with four other tetrahedral monomers proved challenging. Even with a 2.5:1 excess of complementary monomer, a large presence of the triply bound assembly (tetramer) and non-negligible amount of the doubly bound construct (trimer) remained. This is suggestive of an ultimate inability for total assembly in a successive manner, and it therefore became essential to embark upon an undertaking to create a more functional tetrahedral monomer.

2.1.4 Targeted Tetrahedral Ideas, Applications and General Goals

One of the potential problems with the nickel-cyclam hub is its size and flexibility. In what can be viewed as an inherent contradiction, the rigidity of the 1,4,8,11-tetraazacyclotetradecane-1,4,8,11-tetraacetic acid moiety necessitated a derivatized hexyl extension on each acidic terminus. Because of this, multiple degrees of flexibility were added to each "arm," creating an overlarge, floppy branching agent. This could have led to the issues forming a defined, higher-weight molecular assembly.

Additionally, the differing lengths of the hydrocarbon chains between nitrogen atoms in the cyclic core present an inequity in the spacing of the tetrahedral monomer. Though the molecule is symmetrical, the arms are unevenly spaced and the presence of the nickel (II) cation is necessitated for rigidity during the tetrahedral preformation. While this doesn't present a challenge *in vitro*, applications towards drug encapsulation and delivery could be hampered as nickel has been tabbed as a carcinogen.[22]

The most straightforward solution to the above issues is to create a smaller tetrahedral monomer using carbon as the central atom. Through use of standard synthetic methods, such a compound should be readily attainable. Moreover, specific functionalization should yield a construct suitable for standard solid-phase DNA synthesis.

If the solid phase synthesis utilizes a resin containing a disulfide moiety, the terminal sulfhydryl group needed for binding to a gold surface can also be attained. Subsequent arrangement and hybridization can then be achieved (Figure 2.4).

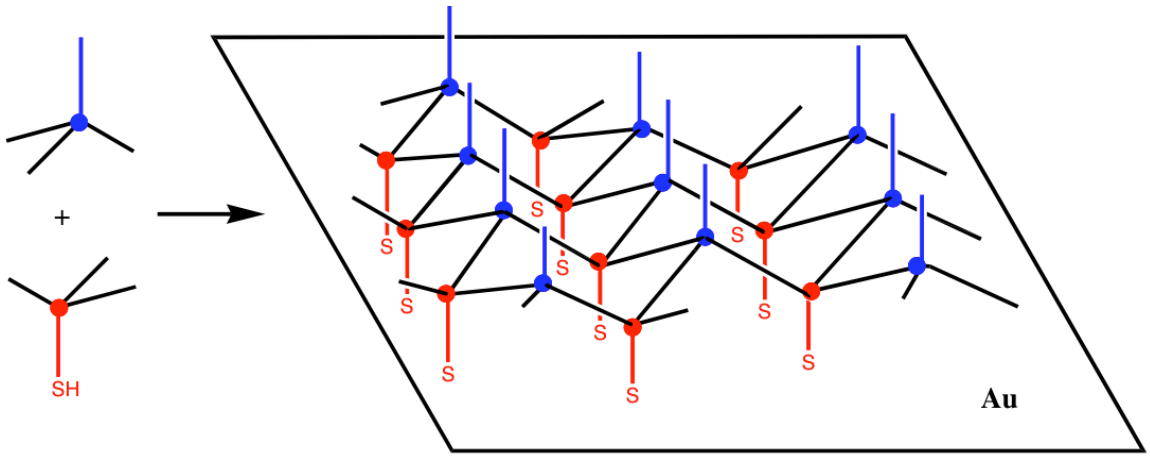

Figure 2.4: A bilayer tetrahedral assembly formed on a gold surface using hybridization of complementary ssDNA sequences (black arms).

If desired, the lattice could also be extended past the initial bilayer phase by virtue of successive binding events. Eventually, the lattice could be grown to a theoretically infinite size, providing a uniform scaffold for the binding of proteins or ligands for structural analysis. Other potential uses could include molecular tethering and encapsulation (Figure 2.5).

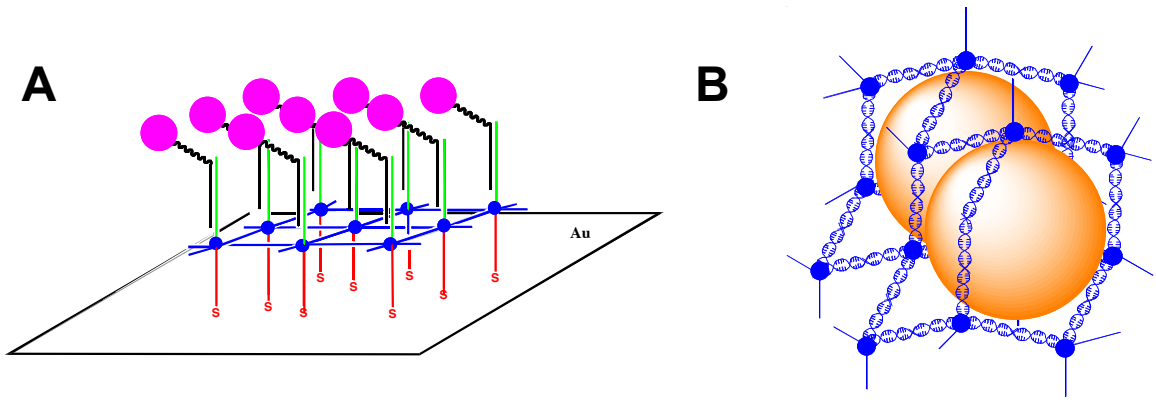

Figure 2.5: (A) Tethering a molecule of interest (pink circle) to a terminal ssDNA arm and (B) encapsulating a molecule of interest based on pore size discrimination.

Another luxury afforded by the gold-sulfur interaction is the ability to perform surface plasmon resonance (SPR) studies. SPR can be used to monitor the kinetics of assembly, as well as the extent of binding of DNA monomers. Electromagnetic fluctuations (plasmons) on a gold surface are continually perturbed by successive binding events, and monitoring these perturbations should ultimately shed insight on the formation of these types of superstructures. Previous attempts have already proven SPR has the ability to elucidate the kinetics of nucleic acid binding events to a gold surface, setting a standard for future efforts.[23] Moreover, given the surface binding ability it's fair to believe other surface studies such as atomic force microscopy and scanning electron microscopy can be utilized.

Through rational design and synthesis, a novel tetrahedral hub with the ability to grow four arms of ssDNA is attainable. Following solid phase DNA synthesis, resultant tetrahedral monomers can be purified, and hybridization to both complementary ssDNA and complementary tetrahedral monomers should provide an upgrade to previous efforts. From there, multiple practical applications

(including but not limited to those mentioned above) will be attempted, and surface studies using SPR and other methodologies should provide insight into the extent, kinetics and uniformity of lattice formation.

2.2 Synthesis of a Modified Disulfide Resin

As mentioned in the previous section, SPR surface studies are one of the many potential applications of the formation of a tetrahedral lattice. However, in order to perform these studies, the presence of a terminal thiol moiety is necessitated. While resins modified to include a disulfide bond are commercially available, the high cost presents an obstacle.

As such we set out to synthesize a more cost-effective alternative. To begin, 3-mercaptopropanol was oxidized in the presence of an iodine solution, affording the disulfide bond seen in compound **2** (Scheme 2.1).

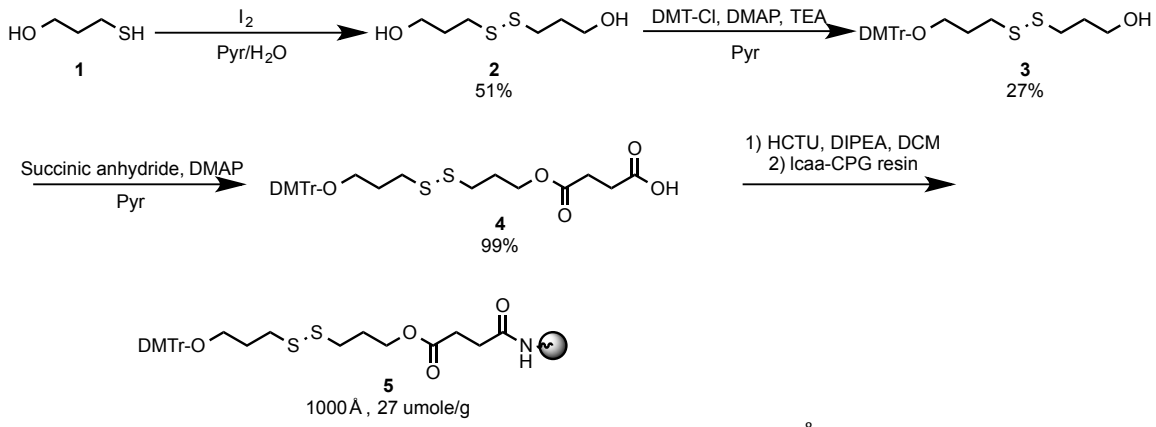

Scheme 2.1: Disulfide functionalization of a 1000 Å CPG resin.

DMT-derivatization afforded the mono-protected species **3**, and the remaining hydroxyl was reacted with succinic anhydride to form the acid **4** in a virtually quantitative yield. Following installation of the 1-[Bis(dimethylamino)methylene]-1H-1,2,3-triazolo[4,5-b]pyridinium 3-oxid hexafluorophosphate (HCTU) leaving group, an amide bond was formed to yield the desired resin **5**. Leftover amines were capped with an activated acetic anhydride solution, and quantitation through a detritylation assay showed the loading capacity of the resin to be 27 μmole/gram. As a test, a short oligomer was synthesized on the resin with a high yield, proving it to be a viable building block.

2.3 Synthesis of a Reverse 2'-deoxyadenosine Phosphoramidite

The next hurdle to overcome in building a tetrahedral monomer containing four identical ssDNA "arms" involved ensuring uniform strand polarity. In solid phase DNA synthesis, oligomers are generally synthesized in the 3' to 5' direction due solely to synthetic accessibility of the nucleoside phosphoramidites. Therefore each monomer is rationally designed to contain a phosphorus (III) electrophile on the 3'-OH and a DMT-protected 5'-OH, which can function as a nucleophile upon detritylation (Figure 2.6).

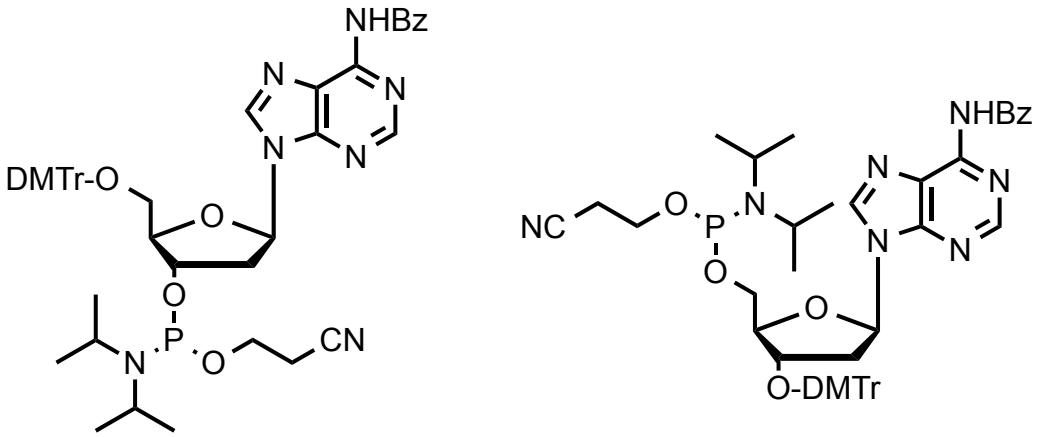

Figure 2.6: A standard 2'-dA phosphoramidite (left) and a "reverse" 2'-dA phosphoramidite (right).

Standard solid phase synthetic methods will be used to elongate the three strands stemming from the branch point of the tetrahedral hub, but the fourth strand needs to be grown directly from the resin. If it is also synthesized in a 3' to 5' manner, its directionality will oppose that of the other three strands (Figure 2.7). Therefore, a series of "reverse" phosphoramidites corresponding to the four natural nucleobases (ex. Figure 2.6 – right side) were synthesized in order to counterbalance this potential inequity.

Figure 2.7: Respective directionalities of the initial ssDNA elongated from the resin if standard phosphoramidites (left) and "reverse" phosphoramidites (right) are used.

Similar to the commercially available disulfide resin mentioned above, "reverse" phosphoramidites are prohibitively expensive. As such, a series of 5' to 3' phosphoramidites was synthesized, including "reverse" dA, dG, dC and dT. Given

the lesser costs of the reagents needed for synthesis, this provided an economical alternative to ordering the necessary DNA building blocks.

In order to make the "reverse" dA phosphoramidite (Scheme 2.2), the exocyclic amine in the 6-position was first protected to afford the benzoylated compound **7**. The more reactive primary 5'-OH was then silylated, followed by a DMT-protection of the 3'-OH and subsequent desilylation to provide the mono-protected compound **10**. This penultimate product was then phosphitylated to give compound **11** in a 75% yield. "Reverse" dA, along with the other "reverse" phosphoramidites, was now able to be utilized for solid phase DNA synthesis.

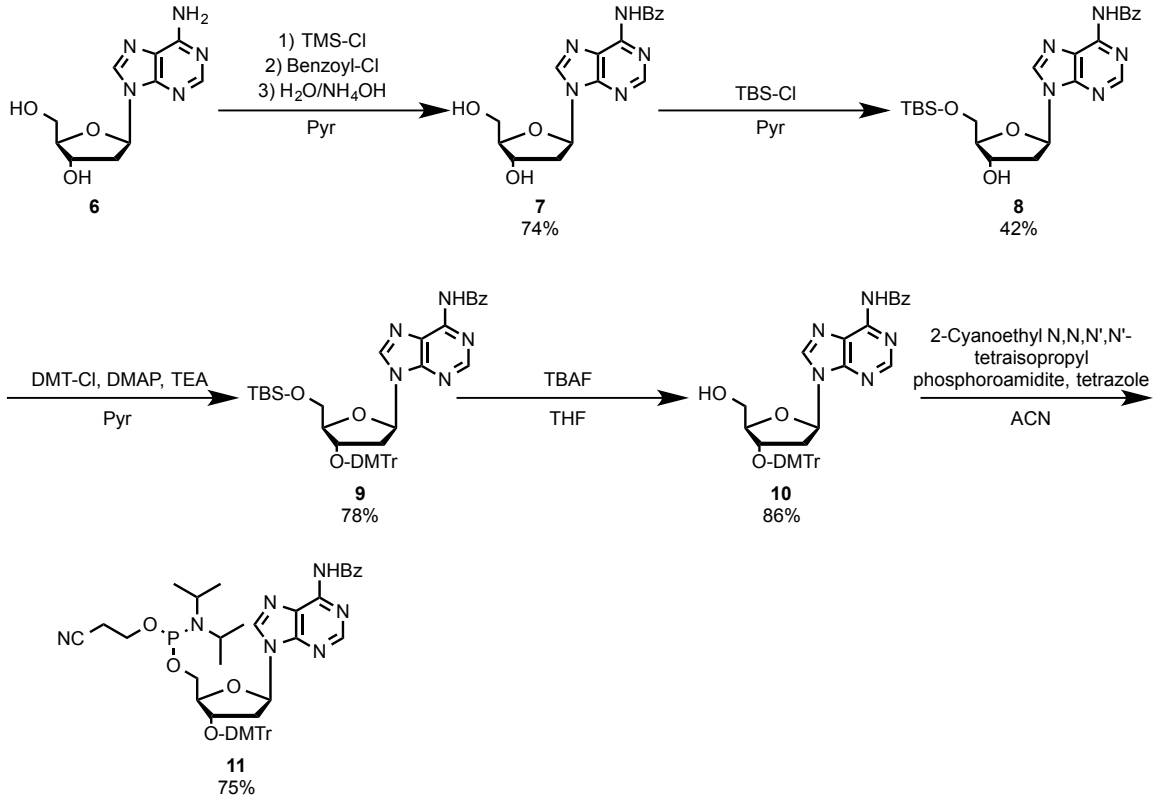

Scheme 2.2: Synthesis of the "reverse" 2'-deoxyadenosine phosphoramidite.

2.4 Attempts at DNA Scaffolds Using the Long Trebler Phosphoramidite

With the "reverse" phosphoramidites and modified disulfide resin **5** in hand, initial efforts towards creating the tetrahedral monomers began. The first attempts utilized the commercially available Long Trebler phosphoramidite (Figure 2.8), an extended pentaerythritol analogue modified to contain three DMT-protected hydroxyl groups as well as a phosphoramidite moiety.

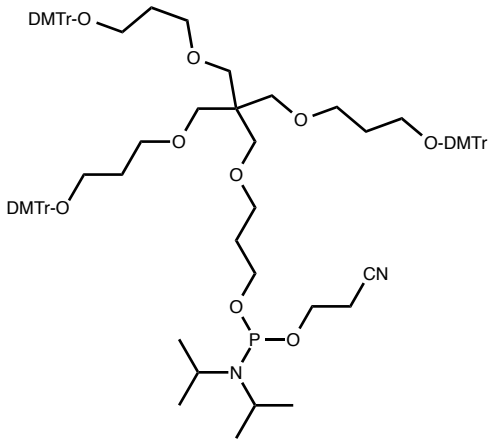

Figure 2.8: Molecular structure of the Long Trebler phosphoramidite purchased from Glen Research.

The initial ssDNA growth from resin **5** utilized the "reverse" phosphoramidites, with the 3'-terminal nucleoside ultimately coupling to the Long Trebler phosphoramidite (the complete protocol can be found in section 2.8). Once coupling of the branching hub was achieved, three more ssDNA oligomers, identical both to one another as well as the initial ssDNA monomer grown from the resin (Table 2.1), were elongated to afford the tetrahedral monomer (LT-1). A second, complementary tetrahedral monomer (LT-2) was also synthesized, as well as a pair of ssDNA complements.

Strand	Type	Sequence
1	ssDNA	5'-d(GCACCTGGAATTCACTCCGC)-3'
2	ssDNA	5'-d(GCGGAGTGAATTCCAGGTGC)-3'
LT-1	Tetrahedral Monomer	$[5'\text{-d(GCACCTGGAATTCACTCCGC)-3'}]_4$
LT-2	Tetrahedral Monomer	$[5'\text{-d(GCGGAGTGAATTCCAGGTGC)-3'}]_4$

Table 2.1: Sequences and nomenclature of the monomer building blocks.

Upon purification, it was imperative to ascertain the viability of the branching monomers. The simplest way to gauge the efficacy of DNA synthesis on the Long Trebler phosphoramidite was via hybridization analysis. If a *completely* synthesized tetrahedral monomer was subjected to increasing concentrations of complementary ssDNA, the result should be a stepwise hybridization pattern ultimately terminating in a superassembly containing four identical duplexes. A native PAGE gel using the intercalator ethidium bromide as a staining agent could then be used as a qualitative measure (Figure 2.9).

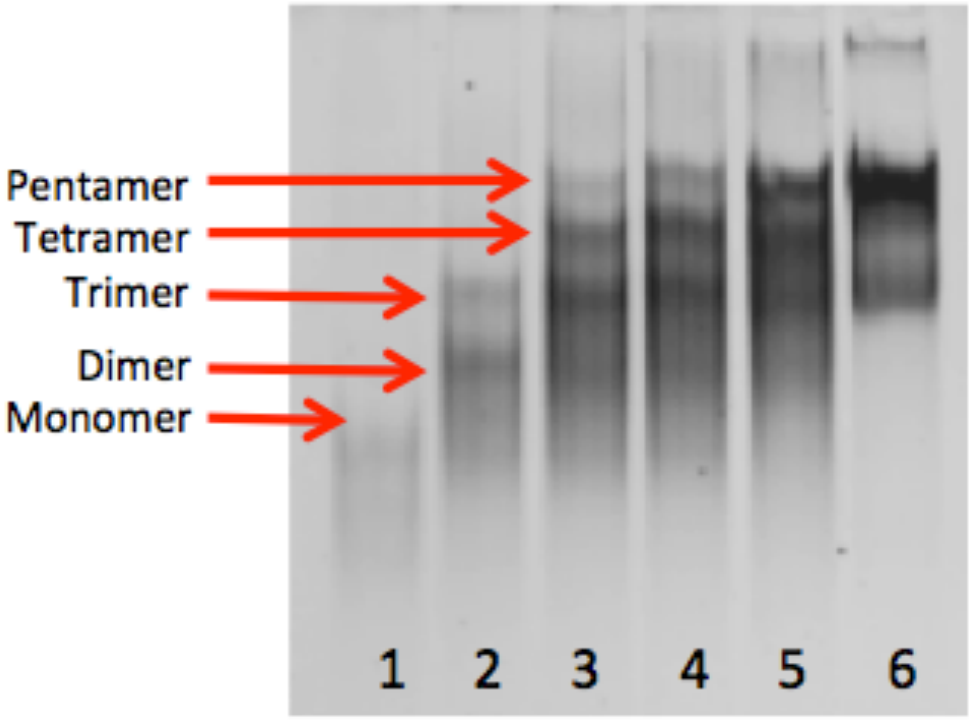

Figure 2.9: An ethidium bromide stained native PAGE gel (10%) containing the following ratios of ssDNA 1 relative to one equivalent of LT-2 (lanes numbered from left to right) – no ssDNA 1 (Lane 1), 1:1 (Lane 2), 2:1 (Lane 3), 3:1 (Lane 4), 4:1 (Lane 5), 8:1 (Lane 6).

Though a concentration-based stepwise duplexing pattern is readily detected, it's clear that the branching monomer LT-2 lacks the ability to hybridize in a complete or efficient manner. Even when a 2:1 excess of ssDNA 1 relative to the four ssDNA arms of tetrahedral monomer LT-2 (lane 9) is used during the annealing process, a significant portion of the Long Trebler complex remains unhybridized. In an attempt to rationalize the poor hybridization pattern, a Bio-Rad sequencing gel was run on purified LT-2 to determine the cause (Figure 2.10).

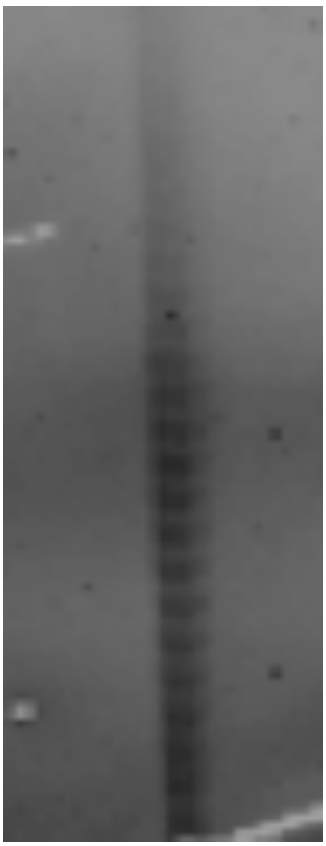

Figure 2.10: Ethidium bromide stained Bio-Rad sequencing gel (15% denaturing PAGE, 420 mm x 250 mm x 1 mm, 48 W power, 15 hours) of pure LT-2. Note that the gel ripped prior to imaging, but after the run was complete.

As can be seen above in the expanded snapshot of a denaturing PAGE gel, the seemingly pure tetrahedral monomer was actually a distribution of "N – *x*" (*x* = any whole number integer greater than or equal to one) deletion products. As a complete tetrahedral monomer would contain 80 nucleosides, it's not surprising that these failed sequences weren't readily detected given the ambiguity of the HPLC traces and gels. With the high proportion of truncated products, as well as 60 possible points of failure (3 x 20-mer ssDNA), it was determined that DNA synthesis on the Long Trebler phosphoramidite was an untenable proposition.

2.5 Creation of and DNA Elongation on Synthetic Tetrahedral Linkers

2.5.1 Synthesis of a More Rigid Tetrahedral Linker

One of the likeliest culprits in the synthetic failures on the Long Trebler phosphoramidite was steric hindrance. Though a resin with 1000 Å pores was used to mitigate interactions between the different growth sites, each arm of the commercially available branching agent contained six bonds between the central carbon and the terminal oxygen. This potentially resulted in an excess of flexibility, and it's possible the elongation of the latter three ssDNA arms was compromised due to intramolecular interference.

In order to combat this issue, it was decided that a more rigid hub should be synthesized and utilized (Scheme 2.3). The same pentaerythritol core seen in the Long Trebler reagent was modified by the addition of 4-hydroxybenzaldehyde to form the tetra-aldehyde **13**. Total reduction yielded terminal hydroxyl moieties on each arm, at which point limiting amounts of TBDPS-Cl afford the mono-silylated compound **15**.

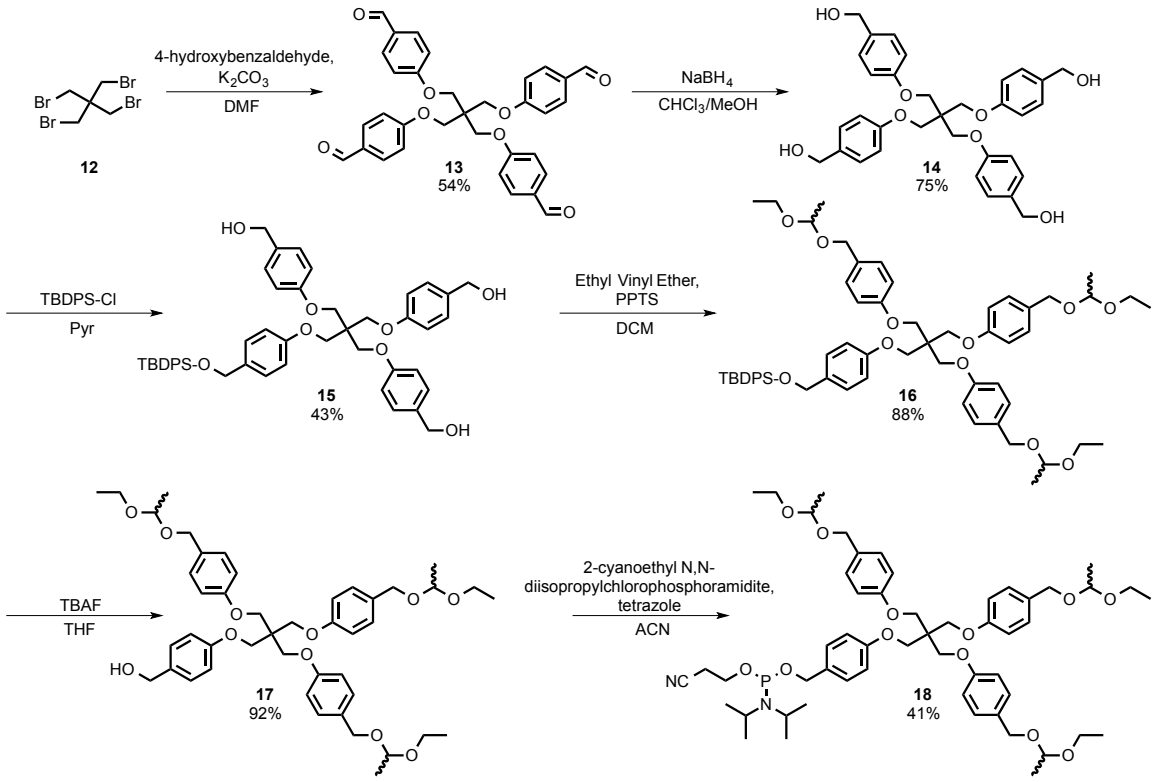

Scheme 2.3: Synthesis of an inflexible tetrahedral branching agent.

Though it's customary for solid phase phosphoramidite building blocks to incorporate the acid-labile DMT group to protect the hydroxyl nucleophiles, multiple synthetic efforts proved the installation of three additional bulky protecting groups wasn't feasible (a standard nucleoside phosphoramidite only has one DMT-group). Therefore the smaller, but also acid-labile ethyl vinyl ether (EVE) moiety was used, producing the tris-EVE product **16** in a high-yielding reaction. Following desilylation, the remaining hydroxyl was phosphitylated, providing phosphoramidite **18** as a new tetrahedral hub accessible for solid phase DNA synthesis.

2.5.2 Attempts at DNA Scaffolds Using a More Rigid Tetrahedral Hub

Given the many potential failure points in the Long Trebler synthesis, it was determined that the first trial should function more as a diagnostic. Therefore the initial ssDNA elongated from the resin (using the "reverse" phosphoramidites) was abandoned in favor of a direct coupling to the tetrahedral hub. This would reduce the total flexibility of the complex, thereby providing a better approximation of ssDNA growth from the latter three hydroxyl groups – in other words, it was an attempt to determine whether or not growth of three simultaneous ssDNA strands was possible.

The preliminary test utilized a similar protocol as the Long Trebler synthesis, and the DNA arms were of the sequence ssDNA 1 (Table 2.1). The average stepwise yield was in excess of 99%, and a subsequent HPLC trace showed a predominant product peak. Following standard detritylation and desalting protocol, PAGE analysis was then used to assess the purity and size of the resultant product Tet-1 (Figure 2.11).

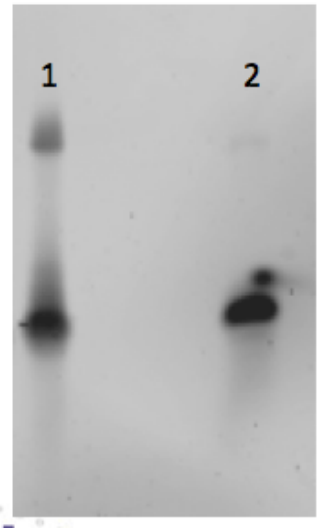

Figure 2.11: 10% denaturing PAGE gel stained with ethidium bromide. Lane 1 contains Tet-1 and Lane 2 contains ssDNA 1.

As shown above, what was perceived to be a pure 3 x 20-mer product (by HPLC) was actually predominantly a single-armed complex, with minor products likely coinciding with a poor EVE deprotection. This was affirmed by a hybridization study between the Tet-1 complex and ssDNA 1, showing an incomplete tetramer (all three ssDNA arms bound) complex (Figure 2.12).

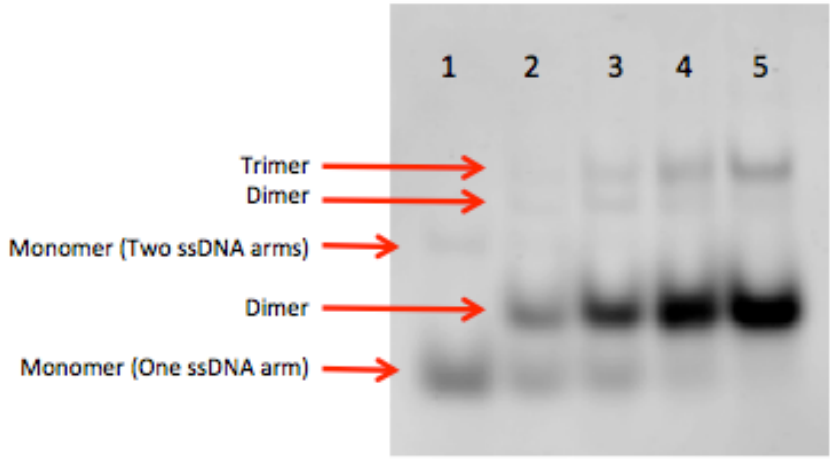

Figure 2.12: An ethidium bromide stained native PAGE gel (10%) containing the following ratios of ssDNA 1 relative to one equivalent of Tet-1 – no ssDNA 1 (Lane 1), 1:1 (Lane 2), 2:1 (Lane 3), 3:1 (Lane 4), 4:1 (Lane 5).

This was a confusing phenomenon, as the EVE moieties had previously shown a similar deprotection profile to the standard DMT group. Unfortunately, as seen above the largest proportion of the post-synthetic product corresponded to only one ssDNA arm of growth, with all other products representing the vast minority. It therefore became imperative to discover a better means of EVE deprotection.

The first attempted method involved a slight deviation from the standard protocol. Instead of 85 seconds of uninterrupted flow of a 3% trichloroacetic acid solution in DCM, the delivery was halted four times for three minutes apiece in order to let the resin-bound complexes soak under acidic conditions for a longer period of time. The totality of this methodology ensured that the EVE groups would be subjected to over 12 minutes of an acidic environment.

This "stop and go" protocol proved no better at EVE deprotection than the standard procedure, so it was determined that a stronger alternative should be explored. As such, the next iteration used trifluoroacetic acid (TFA) as the deprotecting agent. Unfortunately, exposure to TFA only served to destroy the resin-bound tetrahedral construct, rendering further synthesis impossible.

Finally, a 0.05 M solution of aqueous hydrochloric acid was tested as a viable means of EVE deprotection. This too failed to yield acceptable results, and it was determined that the EVE moiety was an undesirable means of protecting the

hydroxyl nucleophiles. Oligomer synthesis on the tetrahedral hub **18** was ultimately deemed an impractical approach.

2.5.3 Synthesis of a New Tris-DMT Protected Branching Hub

Between failing efforts using the Long Trebler phosphoramidite and tetrahedral hub **18** it was noted that two factors appeared to be directly influencing ssDNA synthesis: the flexibility of the branching "arms" and the choice of the protecting group on the hydroxyl nucleophiles. The Long Trebler agent had no issues with hydroxyl deprotection, but likely suffered due to steric interference caused by an excess of flexibility at the branch point. Conversely, the presence of the inflexible phenyl groups in building block **18** should have mitigated this proximity-based clash, but its rigid and bulky nature also made it impossible to install DMT-groups on the trio of hydroxyl nucleophiles. The smaller, and also acid-labile EVE group was synthetically accessible, but its inability to completely deprotect hindered elongation of the ssDNA arms.

In order to potentially nullify these two problems, a synthetic design based upon a short, flexible tetrahedral hub was considered. Commercially available bis-homotris lacks the inflexibility of compound **18**, but also only contains four sp^3 hybrid bonds between the branch point and the terminal oxygen (compared to the six in the Long Trebler phosphoramidite). The hope is this rational design will allow

for the addition of three DMT groups, while also not yielding to the inherent steric constraints caused by the floppier Long Trebler arms during ssDNA synthesis.

Despite a relatively poor yield, the first potential pitfall was avoided as the tris-DMT compound **20** was synthesized (Scheme 2.4). The addition of 4-hydroxybenzaldehyde in a Dean Stark apparatus provided the intermediate Schiff base, which was then reduced to afford the derivatized amine **21**. Subsequent phosphitylation of the aromatic hydroxyl group yielded the branching monomer **22**.

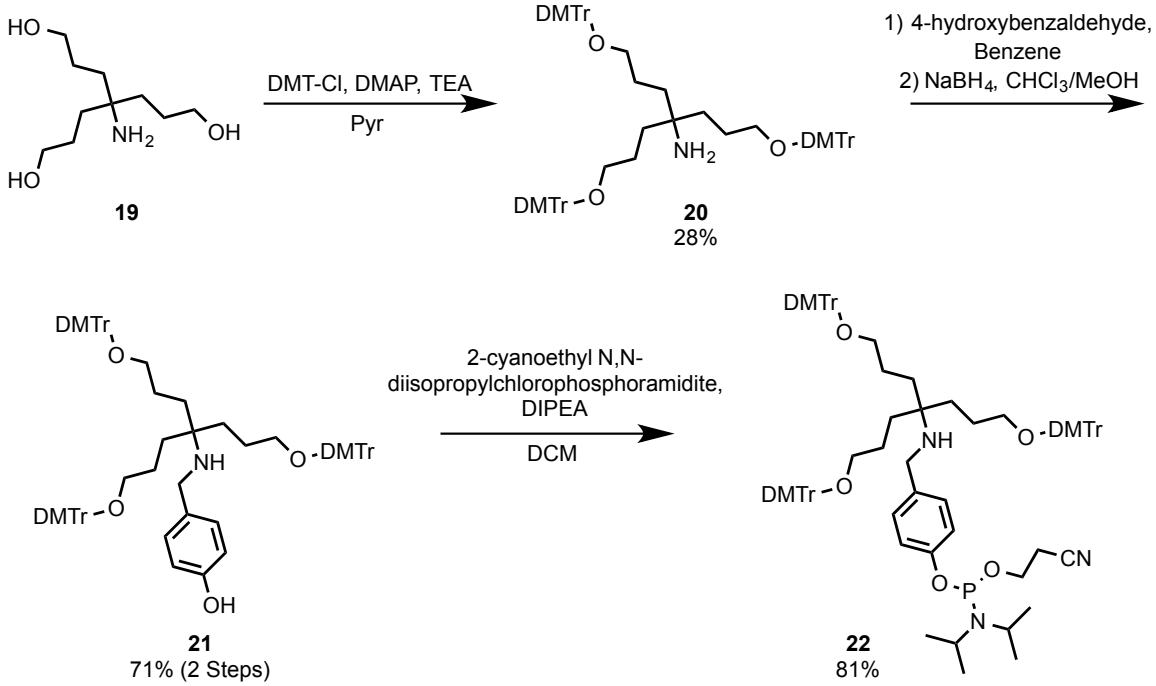

Scheme 2.4: Synthesis of a less flexible tris-DMT branching building block.

2.5.4 Efforts Towards a Bilayer Complex Using a New Tris-DMT Branching Agent

As can be discerned from Scheme 2.4, the four "arms" stemming from the central carbon of building block **22** lack the identical nature found in both the Long Trebler phosphoramidite and tetrahedral monomer **18**. While this deviation likely aided in the synthesis of the compound, it also renders the ability to construct a uniform tetrahedral scaffold impossible. As such, efforts with branching compound **22** were instead focused on building a complex terminating after one hybridization event (following binding to a gold surface – Figure 2.4). While this goal differs slightly from the intention of constructing a tetrahedral lattice, the desired end result would still function as a useful tool in helping gauge both the kinetics and extent of hybridization upon subjection to SPR analysis.

DNA synthesis began with the elongation of a short poly-$(dT)_4$ tract from disulfide resin **5**. Upon the coupling of hub **22**, attempts were made to grow three identical ssDNA oligomers (5'-d[GCAGAATTCGCA]-3') upon detritylation of the hydroxyl nucleophiles. Following purification, a denaturing PAGE gel was utilized to gauge the efficiency of the synthesis on the new branching construct.

As can be seen from the results (Figure 2.13), the output from the DNA synthesizer was nowhere near optimal. The fully elongated bilayer monomer should have contained 40 total nucleosides (3 x 12-mer ssDNA + $[dT]_4$ linker), yet

the product(s) contained in the main HPLC peak ran well past the smaller ssDNA standards.

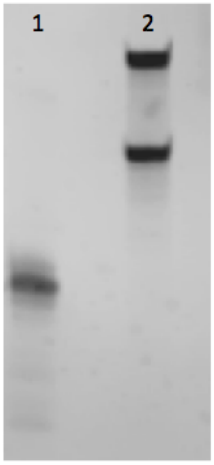

Figure 2.13: A 15% denaturing PAGE gel stained with ethidium bromide. Lane 1 contains the post-HPLC monomer and Lane 2 contains a mix of 24-mer and 36-mer ssDNA standards.

The major product appears to equate to a monomer containing one fully elongated ssDNA arm plus the $(dT)_4$ tract. Several minor products outpaced the main band, which is suggestive of capped deletion sequences. Given the apparent likelihood that two of the three ssDNA arms were unable to elongate significantly, or at all, it was determined that DNA synthesis on the branching monomer **22** was not a worthwhile endeavor.

2.6 Conclusions

During the course of this venture multiple synthetic targets were achieved. Synthesis of a functionalized CPG resin containing a disulfide moiety proved to be a cost-effective alternative to commercially available options, and the creation of a "reverse" dA phosphoramidite allowed for the same. Two unique branching

monomers were also rationally designed, synthesized and utilized as building blocks in solid phase DNA synthesis.

Unfortunately, creating fully grown, branching DNA monomers using the Long Trebler phosphoramidite, as well as hubs **18** and **22**, proved to be an exercise in futility likely due to a combination of steric clash and unusable deprotection profiles. Because the desired products were only present in trivial amounts, if at all, the goal of creating a tetrahedral lattice became impractical given the building blocks utilized. Additional fine tuning of the branching monomers, as well as enhanced solid phase synthetic ability (a microwave DNA synthesizer, perhaps) are needed in order for the primary objectives to be achieved.

2.7 Experimental

2.7.1 General Experimental Information

Starting materials, reagents and solvents were purchased from Sigma-Aldrich, Acros Organics, Oakwood, Glen Research, Chem-Impex, TCI International, Fisher, AK Scientific and Alfa Aesar. Flash chromatography utilized Silicycle SiliaFlash P60 silica gel (40 – 63 μm, 230 – 400 mesh) and thin layer chromatography used Silicycle glass-backed TLC plates (60 Å). TLC's were monitored by ultraviolet light (λ = 260 nm) and stained by 10% sulfuric acid or iodine where appropriate. Certain solvents (THF, DCM, diethyl ether, ACN, pyridine and DMF) were obtained from a Glass Contour solvent system using activated

alumina columns as an additional drying agent, while all other anhydrous solvents were commercially available. NMR studies were performed on a Varian VNMRS400, VNMRS500 or INOVA 500 instrument, with deuterated solvents (purchased from Cambridge Isotopes) noted where appropriate. Masses were obtained using either a Waters LCT or JEOL AccuTOF mass spectrometer, by way of electrospray ionization (positive) or DART (direct analysis in real time). HPLC studies were performed on a Waters 2487 Dual λ Absorbance Detector, and oligos were subsequently quantified using a Beckman DU640 UV/Vis spectrophotometer. Gel imaging used the ethidium bromide intercalating agent (5 μg/mL) and was visualized using a Bio-Rad FXpro Molecular Imager.

2.7.2 Synthetic Procedures

Compound 2

3-mercapto-1-propanol (1.00 mL, 11.58 mmol) was added to a flask containing pyridine (10 mL). Molecular iodine (3.52 g, 13.9 mmol) was dissolved in a solution of 9:1 pyridine/water (150 mL), and this solution was added drop-wise (two hours) to the flask containing the thiol. The reaction was stirred for 16 hours at room temperature, at which point the solvent was removed by rotary evaporation. The resultant white solid was dissolved in diethyl ether, washed twice with a sodium bicarbonate solution and dried over sodium sulfate. The organic layer was concentrated under vacuum to yield pure **2** as a red oil (540 mg, 51%). ^{1}H

NMR (500 MHz; D_2O): δ 1.90 – 2.00 (m, 4H), 2.77 – 2.82 (t, 4H), 3.66 – 3.70 (t, 4H), 4.82 (s, 2H). MALDI-TOF: 182.0449 $[M + H]^+$ (HSMS calculated 182.0435).

Compound 3

Pure **2** (540 mg, 2.97 mmol) was co-evaporated twice with anhydrous pyridine (20 mL) and then stirred under nitrogen at room temperature. DMT-Cl (1.20 g, 3.56 mmol), TEA (551 μL, 3.95 mmol) and catalytic DMAP were added, the temperature was increased to 60 °C and the reaction was stirred for 16 hours. The solution was quenched with water, concentrated under vacuum and co-evaporated three times with toluene. The red oil was re-dissolved in DCM, washed with three times with a sodium bicarbonate solution and concentrated. The crude was then purified via flash chromatography (0.5% TEA in DCM) to yield **3** as a white solid (390 mg, 27%). R_F = 0.49 (98:2 DCM/MeOH). ^1H NMR (400 MHz; $CDCl_3$): δ 1.86 – 1.98 (m, 4H), 2.72 – 2.76 (t, 2H), 2.76 – 2.81 (t, 2H), 3.10 – 3.16 (t, 2H), 3.68 – 3.76 (t, 2H), 3.76 (s, 6H), 6.78 – 6.82 (d, 4H), 7.16 – 7.19 (t, 1H), 7.25 – 7.27 (d, 4H), 7.27 – 7.30 (t, 2H), 7.38 – 7.42 (t, 2H).

Compound 4

Pure **3** (390 mg, 0.81 mmol) was dried overnight, dissolved in anhydrous pyridine (20 mL) and stirred under argon at room temperature. DMAP (48 mg, 0.39 mmol) and succinic anhydride (121 mg, 1.21 mmol) were added in a stepwise manner, and the reaction was stirred at room temperature for 14 hours. Volatiles

were removed via rotary evaporation and co-evaporate three times with toluene. The resultant oil was re-dissolved in DCM, washed twice with an ice-cold solution of citric acid (10% in water) and then twice with water, dried over sodium sulfate and evaporated to dryness to afford pure **4** (470 mg, 99%). ^{1}H NMR (500 MHz; $CDCl_3$): δ 1.90 – 2.02 (m, 4H), 2.60 – 2.68 (m, 4H), 2.74 – 2.78 (t, 2H), 3.10 – 3.14 (t, 2H), 3.76 (s, 6H), 4.14 – 4.18 (t, 2H), 6.78 – 6.82 (d, 4H), 7.16 – 7.19 (t, 1H), 7.25 – 7.27 (d, 4H), 7.27 – 7.30 (t, 2H), 7.38 – 7.42 (t, 2H).

Compound 5

To an argon-filled flask containing dry **4** (470 mg, 0.80 mmol) was added anhydrous DCM (30 mL). Re-distilled DIEA (571 μL, 3.28 mmol) and HCTU (624 mg, 1.64 mmol) were added consecutively and the reaction was stirred for 30 minutes at room temperature. Long-chain aminoalkyl controlled pore glass resin (1.00 g, 1111 Å pore diameter, 99.2 μmole/gram loading capacity) was added the mixture was stirred for an additional 18 hours at 25 °C. Volatiles were removed via filtration and the resin was washed with DMF (1x), MeOH (1x) and diethyl ether (1x) before being dried overnight under vacuum. Upon quantification (see below), the resin was washed with an activated acetic anhydride solution (8:1:1 THF/pyridine/acetic anhydride; activated with a 16% solution of 1-methylimidazole in THF) for 15 minutes in order to render all unmodified amines inert. The resin was then washed with anhydrous acetonitrile for 10 minutes and dried under vacuum.

Compound 7

2'-deoxyadenosine monohydrate (5 g, 19.9 mmol) was co-evaporated twice with anhydrous pyridine (200 mL) and cooled to 0 °C under nitrogen. Trimethylsilyl chloride (12.63 mL, 99.5 mmol) was added and the solution was stirred for 30 minutes at 0 °C. Benzoyl chloride (11.56 mL, 99.5 mmol) was added via syringe, and the solution was returned to room temperature and stirred for two hours. The solution was then quenched with cold water (40 mL) and stirred for 15 minutes, and then ammonium hydroxide (40 mL) was added and the solution was stirred for an additional 30 minutes. Volatiles were removed under vacuum and the crude mixture was co-evaporated three times with toluene. The resultant off-white solid was re-dissolved in water and washed once with diethyl ether. The aqueous layer was sequestered and the product was allowed to re-crystallize over the course of 16 hours at 20 °C. Pure **7** (5.21 g, 74%) was filtered off and dried under vacuum. ^{1}H NMR (500 MHz; DMSO-d_6): δ 2.36 – 2.40 (m, 1H), 2.78 – 2.82 (m, 1H), 3.52 – 3.58 (m, 1H), 3.62 – 3.66 (m, 1H), 3.90 – 3.92 (d, 1H), 4.42 – 4.46 (s, 1H), 5.00 – 5.04 (t, 1H), 5.38 – 5.40 (d, 1H), 6.48 – 6.52 (t, 1H), 7.56 – 7.59 (t, 2H), 7.63 – 7.66 (t, 1H), 8.02 – 8.05 (d, 2H), 8.70 (s, 1H), 8.78 (s, 1H). ^{13}C NMR (100 MHz; DMSO-d_6): δ 41.67, 68.19, 70.25, 71.70, 72.75, 76.13, 84.29, 91.38, 96.45, 98.83, 102.76, 133.72, 137.96, 150.92, 171.77.

Compound 8

Pure **7** (3.45 g, 9.71 mmol) was co-evaporated twice with anhydrous pyridine (110 mL) and stirred under nitrogen at room temperature. TBDMS-Cl (1.61 g, 10.68 mmol) was added and the reaction was stirred for 16 hours. The solution was reduced under pressure, co-evaporated with toluene and re-dissolved in chloroform. The organic layer was washed once with sodium bicarbonate and twice with water, dried over sodium sulfate and volatiles were removed via rotary evaporation. The crude was purified by flash chromatography (97:3 DCM/EtOH) and pure **8** was recovered as a white solid (1.90 g, 42%). R_F = 0.43 (9:1 DCM/MeOH). ^{1}H NMR (500 MHz; DMSO-d_6): δ 0.01 (s, 6H), 0.92 (s, 9H), 2.40 (m, 1H), 2.81 (m, 1H), 3.75 – 3.82 (m, 2H), 3.90 (m, 1H), 4.44 (s, 1H), 5.40 (s, 1H), 6.46 (t, 1H), 7.58 (t, 2H), 7.63 (t, 1H), 8.04 (d, 2H), 8.60 (s, 1H), 8.78 (s, 1H), 11.20 (s, 1H). ESI-MS (positive): 470.1859 $[M + H]^+$ (HSMS calculated 470.2224).

Compound 9

Pure **8** (1.90 g, 4.0 mmol) was dried overnight under vacuum and dissolved in anhydrous pyridine (60 mL). DMT-Cl (2.00 g, 5.9 mmol) and catalytic DMAP were added and the solution was heated to 60 °C and stirred for 18 hours under nitrogen. The reaction was quenched with MeOH and volatiles were removed under vacuum. The crude slurry was then co-evaporated with toluene and re-dissolved in DCM. The organic layer was washed twice with sodium carbonate and once with brine, dried over sodium sulfate and reduced under vacuum. The remaining crude was

purified via flash chromatography (98:1:1 DCM/MeOH/TEA), yielding pure **9** as a white solid (2.41 g, 78%). R_F = 0.52 (97:3 DCM/MeOH). ^{1}H NMR (500 MHz; DMSO-d_6): δ 0.00 (s, 6H), 0.78 (s, 9H), 1.99 (d, 1H), 2.40 (m, 1H), 3.39 (m, 1H), 3.56 (d, 1H), 3.78 (s, 6H), 3.99 (s, 1H), 4.18 (d, 1H), 6.49 (t, 1H), 6.91 (d, 4H), 7.26 (t, 2H), 7.35 (d, 6H), 7.48 (d, 2H), 7.55 (t, 2H), 7.63 (t, 1H), 8.02 (d, 2H), 8.43 (s, 1H), 8.71 (s, 1H). ESI-MS (positive): 772.4 $[M + H]^+$ (HSMS calculated 772.3531).

Compound 10

Pure, dry **9** (300 mg, 0.39 mmol) was dissolved in anhydrous THF (10 mL) and stirred under nitrogen at room temperature. Tetrabutylammonium fluoride (1.95 mL, 1.95 mmol – 1.0 M in THF) was added and the solution was allowed to react for 15 minutes at room temperature. At that point TLC showed complete consumption of the starting material and the volatiles were reduced under pressure. The crude was purified through flash chromatography (99:1 DCM/TEA) and pure **10** was recovered as a white solid (220 mg, 86%). R_F = 0.43 (97:3 DCM/MeOH). ^{1}H NMR (500 MHz; $CDCl_3$): δ 2.62 (m, 1H), 2.96 (m, 1H), 3.30 (d, 1H), 3.70 (d, 1H), 3.78 (s, 6H), 4.04 (s, 1H), 4.60 (d, 1H), 6.36 (t, 1H), 6.81 (d, 4H), 7.21 (t, 1H), 7.24 – 7.28 (t, 2H), 7.36 (d, 4H), 7.44 (d, 2H), 7.46 (d, 2H), 7.56 (t, 1H), 7.98 (d, 2H), 8.06 (s, 1H), 8.68 (s, 1H).

Compound 11

Pure, dry **10** (1.00 g, 1.52 mmol) was dissolved in anhydrous ACN (25 mL) and the solution was stirred under argon at room temperature. 2-Cyanoethyl N,N,N',N'-tetraisopropyl phosphoroamidite (962 μL, 3.03 mmol) was added via syringe, followed by addition of tetrazole (3.20 mL, 1.44 mmol – 0.45 M solution in ACN). The reaction mixture was allowed to stir for 16 hours at room temperature. The solution was quenched with MeOH, reduced under pressure and re-dissolved in DCM. The organic layer was washed three times with sodium bicarbonate, dried over sodium sulfate and diminished via rotary evaporation. The crude was initially purified via flash chromatography (95:4:1 DCM/MeOH/TEA) and the collected product was reduced under pressure and re-dissolved in DCM (4 mL). This aggregated fraction was added drop-wise to a volume of stirring hexanes (100 mL) and completely purified **11** precipitated out of the solution. The supernatant was removed via filtration, and pure **11** was collected as a white solid (983 mg, 75%). ^{31}P NMR (100 MHz; DMSO-d_6): δ 148.0.

Compound 13

To a dry, argon-filled flask containing 4-hydroxybenzaldehyde (7.54 g, 61.8 mmol) was added anhydrous DMF (80 mL). The mixture was stirred at room temperature and potassium carbonate (8.54 g, 61.8 mmol) was added. Pentaerythritol tetrabromide (3.00 g, 7.74 mmol) was next added and the reaction mixture was refluxed at 120 °C for 16 hours. The solution was allowed to cool to

room temperature, and volatiles were removed *in vacuo*. The crude mixture was then dissolved in water and extracted three times with ethyl acetate. The combined organic fractions were washed twice with sodium bicarbonate, dried over sodium sulfate and concentrated under reduced pressure. The resultant red oil was subjected to flash chromatography (11:9 EtOAc/Hexanes) and pure **13** was isolated as a crystalline solid (2.32 g, 54%). R_F = 0.31 (3:2 Hexanes/EtOAc). ^{1}H NMR (500 MHz; $CDCl_3$): δ 4.43 (s, 8H), 7.01 (d, 8H), 7.81 (d, 8H), 9.85 (s, 4H). ESI-MS (positive): 553.1852 $[M + H]^+$ (HSMS calculated 553.1863).

Compound 14

Dry **13** (2.32 g, 4.20 mmol) was dissolved in a solution of chloroform (30 mL) and MeOH (10 mL), cooled to -10 °C and stirred. Sodium borohydride (1.91g, 50.5 mmol) was added in a stepwise manner over five minutes and the reaction mixture was stirred for 30 minutes. The solution was then allowed to warm to room temperature, and was stirred for 14 hours. Volatiles were removed via rotary evaporation and the resultant crude was washed thoroughly with water. The remaining solid was dissolved in ethanol and pure **14** was recrystallized as a white solid (1.77 g, 75%). ^{1}H NMR (500 MHz; DMSO-d_6): δ 4.22 (s, 8H), 4.39 (s, 8H), 5.02 (s, 4H), 6.90 (d, 8H), 7.20 (d, 8H). ESI-MS (positive): 821.3 $[M + Na]^+$ (HSMS calculated 821.3486).

Compound 15

To a flask containing dry **14** (1.77 g, 3.16 mmol) was added anhydrous pyridine (30 mL), and the solution was stirred under nitrogen at room temperature. Tertbutyldiphenylsilyl chloride (889 μL, 3.47 mmol) was added via syringe and the reaction mixture was stirred for 12 hours. The reaction was quenched with MeOH, and volatiles were removed *in vacuo* and co-evaporated three times with toluene. The crude was re-dissolved in DCM and washed three times with water. The organic layer was then dried over sodium sulfate and reduced under pressure. Flash chromatography (7:3 EtOAc/Hexanes) afforded pure **15** as a white foam (1.08 g, 43%). R_F = 0.40 (3:1 EtOAc/Hexanes). ^{1}H NMR (500 MHz; $CDCl_3$): δ 1.02 (s, 9H), 4.33 (s, 8H), 4.59 (s, 6H), 4.65 (s, 2H), 6.88 (d, 8H), 7.20 (t, 2H), 7.26 (d, 8H), 7.38 (t, 4H), 7.66, (d, 4H).

Compound 16

Dry **15** (193 mg, 0.24 mmol) was combined with pyridinium *p*-toluenesulfonate (73 mg, 0.29 mmol) and both were dissolved in anhydrous DCM (5 mL) and stirred under nitrogen at room temperature. Ethyl vinyl ether (417 μL, 4.35 mmol) was added and the solution was stirred for 2.5 hours. The reaction mixture was washed three times with sodium bicarbonate, dried over sodium sulfate and evaporated. Drying under high pressure (0.0 torr) for an additional 12 hours removed excess ether reagent and pure **16** was obtained as a clear yellow oil

(215 mg, 88%). R_F = 0.56 (97:3 DCM/MeOH). ^{1}H NMR (500 MHz; $CDCl_3$): δ 1.02 (s, 9H), 1.18 (t, 9H), 1.30 (d, 9H), 3.44 (m, 4H), 3.62 (m, 4H), 4.30 (s, 8H), 4.40 (d, 3H), 4.52 (d, 3H), 4.64 (s, 2H), 4.73 (q, 3H), 6.86 (d, 8H), 7.20 (d, 8H), 7.33 (t, 4H), 7.35 (t, 2H), 7.64 (d, 4H).

Compound 17

Dry **16** (215 mg, 0.21 mmol) was dissolved in anhydrous THF (8 mL) and the solution was stirred under nitrogen at room temperature. Tetrabutylammonium fluoride (1.06 mL, 1.06 mmol – 1.0 M in THF) was added via syringe and the reaction was allowed to proceed for 15 minutes. The reaction was quenched with MeOH and reduced under pressure. The crude was then re-dissolved in DCM and washed with sodium bicarbonate (1x) and brine (1x), dried over sodium sulfate and reduced via rotary evaporation. Pure **17** was achieved via flash chromatography (11:9 EtOAc/Hexanes, 0.5% TEA) as a clear oil (150 mg, 92%). R_F = 0.51 (1:1 EtOAc/Hexanes). ^{1}H NMR (400 MHz; $CDCl_3$): δ 1.20 (t, 9H), 1.30 (d, 9H), 3.44 (m, 4H), 3.62 (m, 4H), 4.31 (s, 8H), 4.42 (d, 3H), 4.50 (s, 2H), 4.56 (d, 3H), 4.76 (q, 3H), 6.86 (d, 8H), 7.21 (d, 8H).

Compound 18

To a dry, argon-filled flask containing **15** (236 mg, 0.30 mmol) was added anhydrous DCM (8 mL). Re-distilled diisopropylethylamine (212 μL, 1.22 mmol) was then added, followed by addition of 2-cyanoethyl N,N-

diisopropylchlorophosphoramidite (136 µL, 0.61 mmol). The reaction was stirred at room temperature for two hours and then quenched with water. The reaction mixture was washed three times with sodium bicarbonate, dried over sodium sulfate and volatiles were removed via rotary evaporation. Pure **18** was obtained via flash chromatography (11:9 EtOAc/Hexanes, 0.5% TEA) as a clear oil (122 mg, 41%). R_F = 0.68 (1:1 EtOAc/Hexanes). ^{1}H NMR (400 MHz; $CDCl_3$): δ 1.18 (t, 9H), 1.20 (d, 12H), 2.59 (t, 2H), 3.46 (q, 6H), 3.61 (t, 6H), 3.80 (q, 2H), 4.30 (s, 8H), 4.41 (d, 4H), 4.54 (d, 4H), 4.77 (q, 3H), 6.86 (d, 8H), 7.22 (d, 8H). ^{31}P NMR (100 MHz; $CDCl_3$): δ 149.0.

Compound 20

To a flask containing dry bis-homotris (1.00 g, 4.80 mmol) was added anhydrous pyridine (50 mL), and the solution was stirred under argon at room temperature. DMT-Cl (9.88 g, 29.2 mmol) and dimethylaminopyridine (59 mg, 0.48 mmol) were added and the mixture was stirred at 70 °C for 14 hours. The solution was allowed to return to room temperature, quenched with water and concentrated under low pressure. The crude was re-dissolved in DCM, washed with sodium bicarbonate (2x) and brine (1x), dried over sodium sulfate and reduced *in vacuo*. Flash chromatography (9:1 DCM/MeOH, 0,5% TEA) afforded pure **20** as a white solid (1.47 g, 28%). R_F = 0.70 (9:1 DCM/MeOH). ^{1}H NMR (500 MHz; $CDCl_3$): δ 1.38 (m, 2H), 1.58 (t, 6H), 1.75 (m, 6H), 3.02 (t, 6H), 3.78 (s, 18H), 6.81 (d, 12H), 7.16 (d, 12H), 7.27 (d, 6H), 7.30 (d, 6H), 7.41 (t, 3H).

Compound 21

Pure **20** (1.47 g, 1.32 mmol) was dissolved in benzene (32 mL), and 4-hydroxybenzaldehyde (323 mg, 2.64 mmol) was added. The reaction mixture was refluxed at 110 °C in a Dean-Stark apparatus for 15 hours and then allowed to return to room temperature. Volatiles were removed *in vacuo* and the crude was taken up in DCM and washed with sodium bicarbonate (2x) and brine (1x). The organic layer was dried over sodium sulfate and reduced under low pressure. Following the work-up protocol, the crude was dissolved in a 3:1 mixture of chloroform/MeOH (40 mL) and the temperature was lowered to 0 °C. Sodium borohydride (220 mg, 5.82 mmol) was added and the solution was stirred at 0 °C for 30 minutes. The solution was allowed to warm to room temperature and then stirred for 16 hours. Volatiles were then removed via rotary evaporation and the crude was washed with water. The resultant solid was purified with flash chromatography (97:3 DCM/MeOH, 0.5% TEA) yielding pure **21** as a white solid (1.15 g, 71% over two steps). R_F = 0.67 (9:1 DCM/MeOH). ^{1}H NMR (500 MHz; $CDCl_3$): δ 1.40 (t, 6H), 1.60 (m, 6H), 3.05 (t, 6H), 3.50 (s, 2H), 3.78 (s, 18H), 6.80 (d, 12H), 6.84 (d, 2H), 7.18 (d, 6H), 7.24 (t, 3H), 7.29 (d, 2H), 7.33 (d, 12H), 7.44 (d, 6H). MALDI-TOF: 1218.6208 $[M + H]^+$ (HSMS calculated 1218.6096).

Compound 22

To as flask containing pure **21** (1.09 g, 0.893 mmol) was added anhydrous DCM (40 mL). Re-distilled diisopropylethylamine (1.26 mL, 7.14 mmol) and 2-

cyanoethyl N,N-diisopropylchlorophosphoramidite (794 µL, 3.57 mmol) were added in a stepwise manner at 0 °C, and then the solution was allowed to warm to room temperature and stirred for 3 hours. The reaction was quenched with water, washed three times with sodium bicarbonate, dried over sodium sulfate and reduced under vacuum pressure. Flash chromatography (99:1 DCM/MeOH, 0.5% TEA) yielded pure **22** (1.02 g, 81%) as a clear oil. R_F = 0.59 (97:3 DCM/MeOH). ^{1}H NMR (500 MHz; $CDCl_3$): δ 1.20 (d, 12H), 1.40 (m, 6H), 1.60 (t, 6H), 2.62 (q, 2H), 3.05 (t, 6H), 3.54 (s, 2H), 3.78 (s, 18H), 3.88 (t, 2H), 6.78 (d, 12H), 6.97 (d, 2H), 7.17 (t, 3H), 7.23 (d, 6H), 7.29 (s, 2H), 7.31 (d, 12H), 7.43 (d, 6H), 7.68 (s, 2H). ^{31}P NMR (100 MHz; $CDCl_3$): δ 147.0.

2.7.3 Synthesis, Purification and Quantification of Solid-Phase DNA Materials

Quantification of the Loading Capacity of Disulfide Resin 5

Pure **5** (3.0 mg) was placed in a 25-mL volumetric flask, which was then diluted to the mark with a mixture of HCl/ethanol (3:2). The flask was shaken for seven minutes, and an aliquot (1.00 mL) of the resultant orange solution was measured on a UV/vis spectrophotometer at a wavelength of 495 nm. Subsequent calculations via Beer's Law yielded an average loading capacity for **5** of 27 µmole/gram.

Standard DNA Synthesis and Purification

Reagents, resins and phosphoramidites were purchased from Glen Research. Native sequences were synthesized on an Applied Biosystems 394 DNA/RNA synthesizer using standard solid phase techniques on a one-μmole scale. Average stepwise yields were determined through UV absorption (λ = 495 nm) by way of measuring the cleaved DMT groups (the 5'-terminal DMT moiety was left attached). Sequences were generally synthesized with yields exceeding 97%.

Upon completion of synthesis, oligomers were cleaved from the resin by being subjected to 12 hours of ammonium hydroxide at 55 °C. The supernatant was sequestered and volatiles were removed with a Jouan RC1010 vacuum concentrator. The cleaved DNA was dissolved in MilliQ water (5 mL) and any remaining resin was removed via syringe filtration.

Full-length oligomers were separated from truncated sequences and cleaved protecting groups via HPLC using an Oligo R3 column (0.46 cm x 10 cm). The two mobile phases used were defined as Standard A (50 mM triethylammonium acetate, 5% ACN, pH = 7) and Standard B (50 mM triethylammonium acetate, 70% ACN, pH = 7), and the generic solvent gradient is shown below.

Time (min)	Flow Rate (mL/min)	% Standard A	% Standard B
0	5.0	100	0
2	5.0	100	0
24	5.0	50	50

Table 2.2: HPLC Gradient utilized for purification of standard oligomers.

Collected fractions containing the desired product were aggregated, and volatiles were removed via rotary evaporation.

Next, the 5'-terminal DMT group was removed by dissolving the remaining crude in a 4:1 mixture of acetic acid/water (10 mL) and letting it react for 30 minutes at 0 °C. Remaining acetic acid was removed under vacuum pressure and the detritylated DNA was co-evaporated with ethanol five times. The remaining white powder was dissolved in MilliQ water (2 mL) and desalted on a Sephade G-10 column. Purified ssDNA was collected, dried on a VirTis Benchtop lyophilizer, re-dissolved in a measured volume of water and quantified using UV analysis at 260 nm.

Long Trebler DNA Synthesis and Purification

Disulfide resin **5** (37 mg, 1.0 μmol) was utilized in lieu of the commercially available standard. Oligomers were elongated using "reverse" phosphoramidites (5' to 3' directed synthesis), with all other solid-phase variables remaining the same. Upon completion of the "reverse" sequence, the 3'-terminal DMT group was removed using standard methods. Next, the Long Trebler phosphoramidite (Glen Research) was coupled using an extended one-hour coupling time.

The three terminal DMT groups on the Long Trebler moiety were removed and the remaining oligomers were elongated in the standard 3' to 5' direction. Due to potential lower yields based on steric hindrance the coupling protocols were run

three times for each nucleoside addition (see solid phase synthetic cycle in section 1.4) before the capping step was allowed to occur. The coupling steps were also elongated to 15 minutes apiece.

Cleavage from the resin was achieved in the same manner as described previously, although it was performed at room temperature. In order to cleave the disulfide bond, dithiothreitol (50 mM) was added to the ammonium hydroxide solution. Liberated DNA was prepped for the HPLC as described previously.

Separation of the desired crude product from all other artifacts was performed via HPLC utilizing the gradient shown below (Standards A and B as described above).

Time (min)	Flow Rate (mL/min)	% Standard A	% Standard B
0	5.0	100	0
2	5.0	100	0
28	5.0	30	70

Table 2.3: Purification gradient for the Long Trebler constructs.

Volatiles were then evaporated and the DMT groups were removed as described in the previous section. The detritylated product was taken up in MilliQ water, washed once with diethyl ether and then the aqueous layer was sequestered and concentrated under vacuum. The crude DNA complex was then re-purified with a 10% polyacrylamide (19:1 acrylamide/bis-acrylamide) denaturing gel (7.5 M urea) run with the following specifications: 240 mm x 175 mm x 1.5 mm gel cast, 22

W power for 8.5 hours at 4 °C. Oligos were liberated from the gel using an Elutrap electroelution system, then desalted, dried and quantified as described previously.

DNA Synthesis and Purification of Tetrahedral Hub 18

Disulfide resin **5** (37 mg, 1.0 μmol) was used instead of the commercially available standard. **18** was diluted in anhydrous ACN (0.1 M) and loaded onto the DNA synthesizer. It was coupled to the resin using an extended one-hour coupling time.

The ethyl vinyl ether moieties were cleaved using the various acidic conditions described in section 2.5.2 and the 3'-terminal nucleoside phosphoramidites were coupled using the same 3 x 15 minute protocol as noted previously. As the ethyl vinyl ether groups are not UV-active, subsequent nucleoside phosphoramidites were coupled using a new program with the same protocol so as to utilize the synthesizer's monitoring of the average yield.

Cleavage from the resin and reduction of the disulfide bond was achieved with the methodology described in the previous section. HPLC purification was accomplished using the following gradient (Standards A & B as previously defined):

Time (min)	Flow Rate (mL/min)	% Standard A	% Standard B
0	3.0	100	0
5	3.0	60	40
25	3.0	0	100

Table 2.4: HPLC gradient for DNA grown from hub **18**.

Volatiles were removed via rotary evaporation and the DMT groups were removed in a manner analogous to the previous section. The crude product was desalted using a Sephade G-10 column, and the branching complex was dried and quantified as described previously.

DNA Synthesis and Purification of Tetrahedral Hub 22

From disulfide resin **5** (37 mg, 1 μmol) was elongated a tract of $(dT)_4$ using the normal synthetic protocol, at which point **22** (0.1 M solution in anhydrous ACN) was attached using a one-hour coupling time. Subsequent strands were elongated from the trio of detritylated 3'-terminal hydroxyl moieties using the 3 x 15 minute coupling protocol. The branched product was cleaved from the resin and the disulfide bond was reduced using previously mentioned methodology.

The crude DNA construct was then purified on the HPLC using the following gradient (Standards A & B as previously defined):

Time (min)	Flow Rate (mL/min)	% Standard A	% Standard B
0	3.0	100	0
2	3.0	100	0
35	3.0	0	100

Table 2.5: HPLC gradient for the DNA construct grown on hub **22**.

Collected fractions were reduced under pressure and detritylated as previously described. The remaining crude product was desalted using a Sephade G-10 column, and the branching complex was dried as described previously.

DNA Hybridization Studies

An aliquot of purified ssDNA (or one of the branching DNA monomers) in MilliQ water (of known concentration) was combined with an aliquot of its complement (ratios noted where appropriate). To this mixture was added 15 μL of hybridization buffer (80 mM Tris, 80 mM boric acid, 1 mM $MgCl_2$, pH = 8.3), and the resultant solution was mixed vigorously, centrifuged and heated at 95 °C for five minutes. The buffered solution was then allowed to return to room temperature over the course of an hour. Subsequent analysis of the annealed duplex DNA was performed via native PAGE or agarose gels where appropriate.

2.8 References

1. K. Luger, A. W. Mäder, R. K. Richmond, D. F. Sargent and T. J. Richmond, *Nature*, **1997**, *389*, 251–60.

2. T. Simonsson, *Biological Chemistry*, **2001**, *382*, 621–628.

3. F. Crick, *Journal of Molecular Biology*, **1968**, *38*, 367–379.

4. K. A. LeCuyer and D. M. Crothers, *Proceedings of the National Academy of the Sciences of the United States of America*, **1994**, *91*, 3373-3377.

5. X. Xu and S. Chen, *Journal of the American Chemical Society*, **2012**, *134*, 12499–12507.

6. M. Egli, G. Minasov, L. Su and A. Rich, *Proceedings of the National Academy of the Sciences of the United States of America*, **2002**, *99*, 4302-7.

7. D. Svozil, J. Kalina, M. Omelka and Bohdan Schneider, *Nucleic Acids Research*, **2008**, *36*, 3690-3706.

8. E. Winfree, F. Liu, L. Wenzler and N. Seeman, *Nature*, **1998**, *394*, 539-544.

9. J. Zheng, P. E. Constantinou, C. Micheel, A. P. Alivisatos, R. A. Kiehl and N. C. Seeman, *Nano Letters*, **2006**, *6*, 1502–1504.

10. N. C. Seeman, *Biochemistry*, **2003**, *42*, 7259-7269.

11. C. Mao, W. Sun, Z. Shen and N. C. Seeman, *Nature*, **1999**, *397*, 144-146.

12. M. Endo, N. C. Seeman and T. Majima, *Angewandte Chemie International Edition*, **2005**, *44*, 6074-6077.

13. A. V. Garibotti, S. M. Knudsen, A. D. Ellington and N. C. Seeman, *Nano Letters*, **2006**, *6*, 1505-1507.

14. A. D. Ellington and J. W. Szostak, *Nature*, **1992**, *355*, 850-852.

15. A. D. Ellington and J. W. Szostak, *Nature*, **1990**, *346*, 818-22.

16. P. D. Jadzinsky, G. Calero, C. J. Ackerson, D. A. Bushnell and R. D. Kornberg, *Science*, **2007**, *318*, 430-433.

17. J. Lee, S. I. Stoeva and C. A. Mirkin, *Journal of the American Chemical Society*, **2006**, *128*, 8899-8903.

18. S. Y. Park, A. K. R. Lytton-Jean, B. Lee, S. Weigand, G. C. Schatz and C. A. Mirkin, *Nature*, **2008**, *451*, 553-556.

19. K. M. Stewart, J. Rojo and L. W. McLaughlin, *Chemical Communications*, **2003**, 2934-2935.

20. K. M. Stewart and L. W. McLaughlin, *Journal of the American Chemical Society*, **2004**, *126*, 2050-2057.

21. K. M. Stewart, J. Rojo and L. W. McLaughlin, *Angewandte Chemie International Edition*, **2004**, *43*, 5808-5811.

22. United States Environmental Protection Agency, *Health Assessment Document for Nickel*, **1986**.

23. R. J. Heaton, A. W. Peterson and R. M. Georgiadis, *Proceedings of the National Academy of Sciences of the United States of America*, ***2001**, 98,* 3701-3704.

2.9 Pertinent HPLC Traces

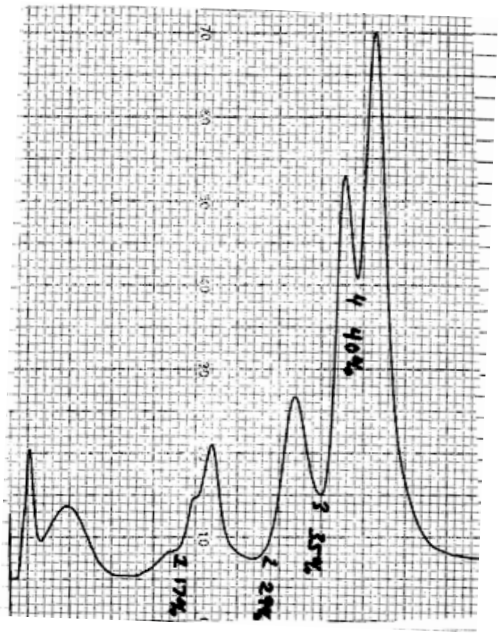

Figure 2.14: HPLC trace of DNA grown on the Long Trebler Phosphoramidite. Gradient shown above.

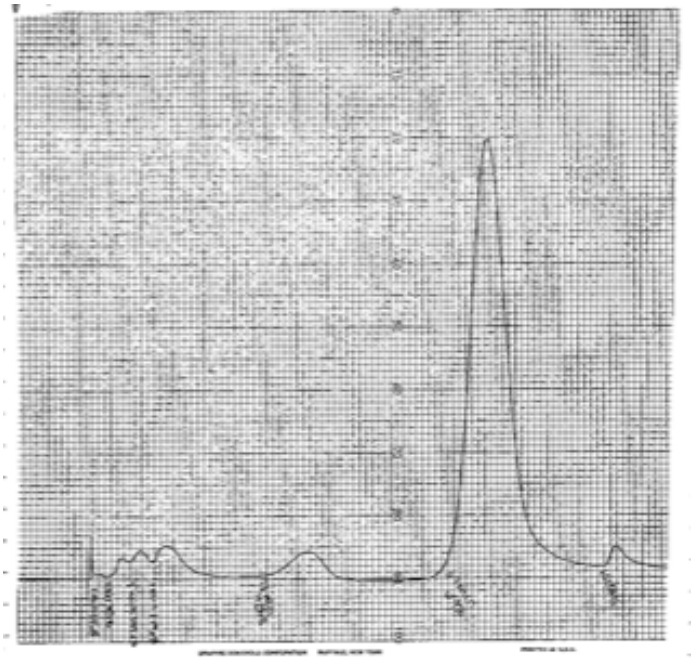

Figure 2.15: HPLC trace of DNA grown on tetrahedral hub **18**. Gradient described previously.

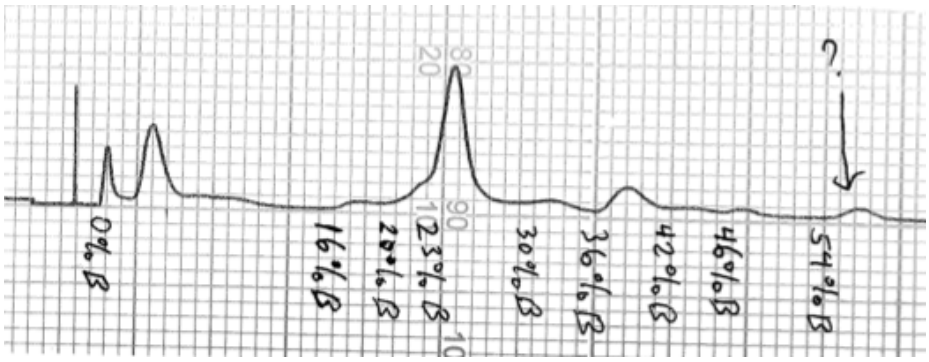

Figure 2.16: HPLC trace of DNA grown on tetrahedral hub 22. Gradient described previously.

2.10 ^{1}H, ^{13}C and ^{31}P NMR Spectra

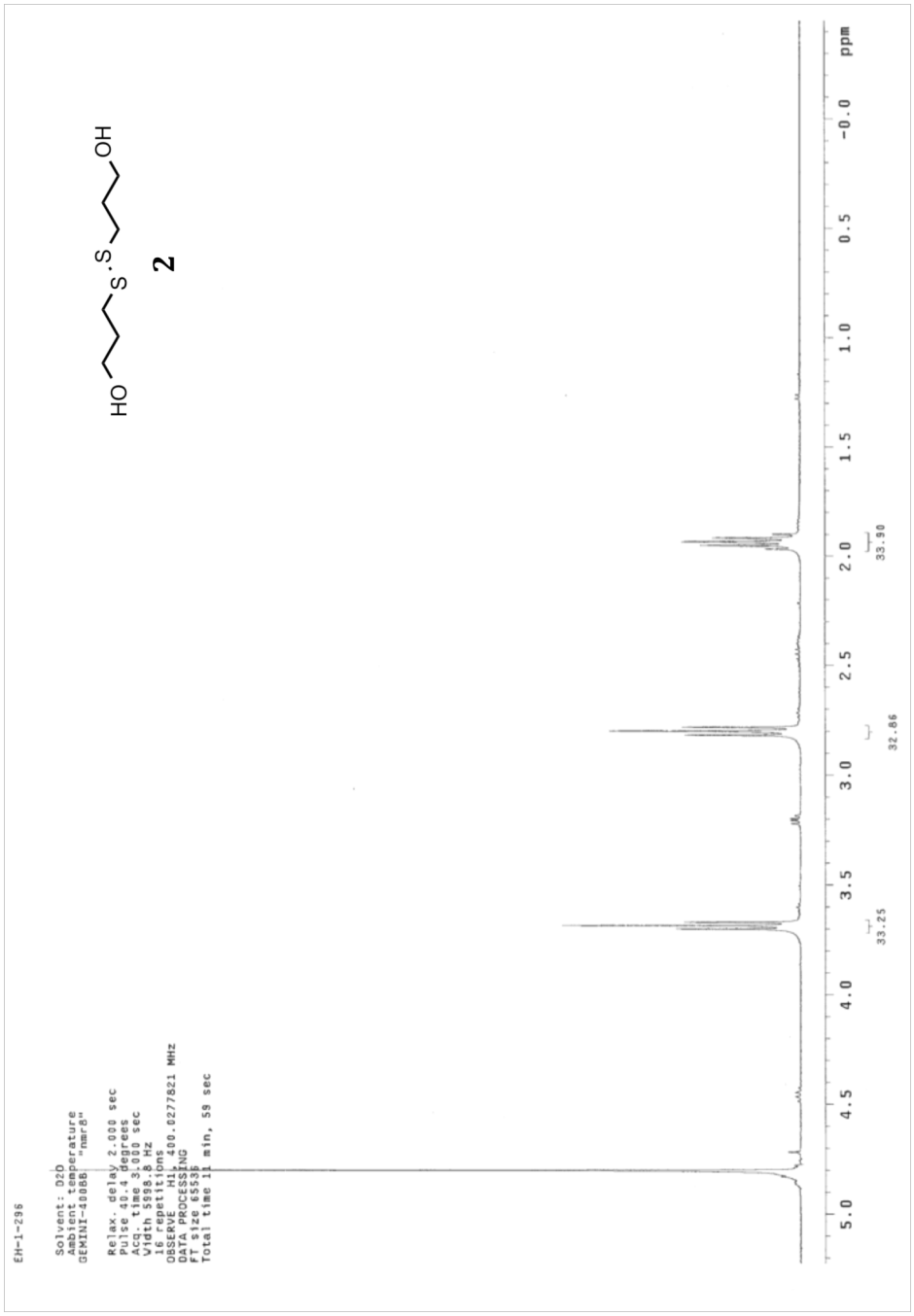

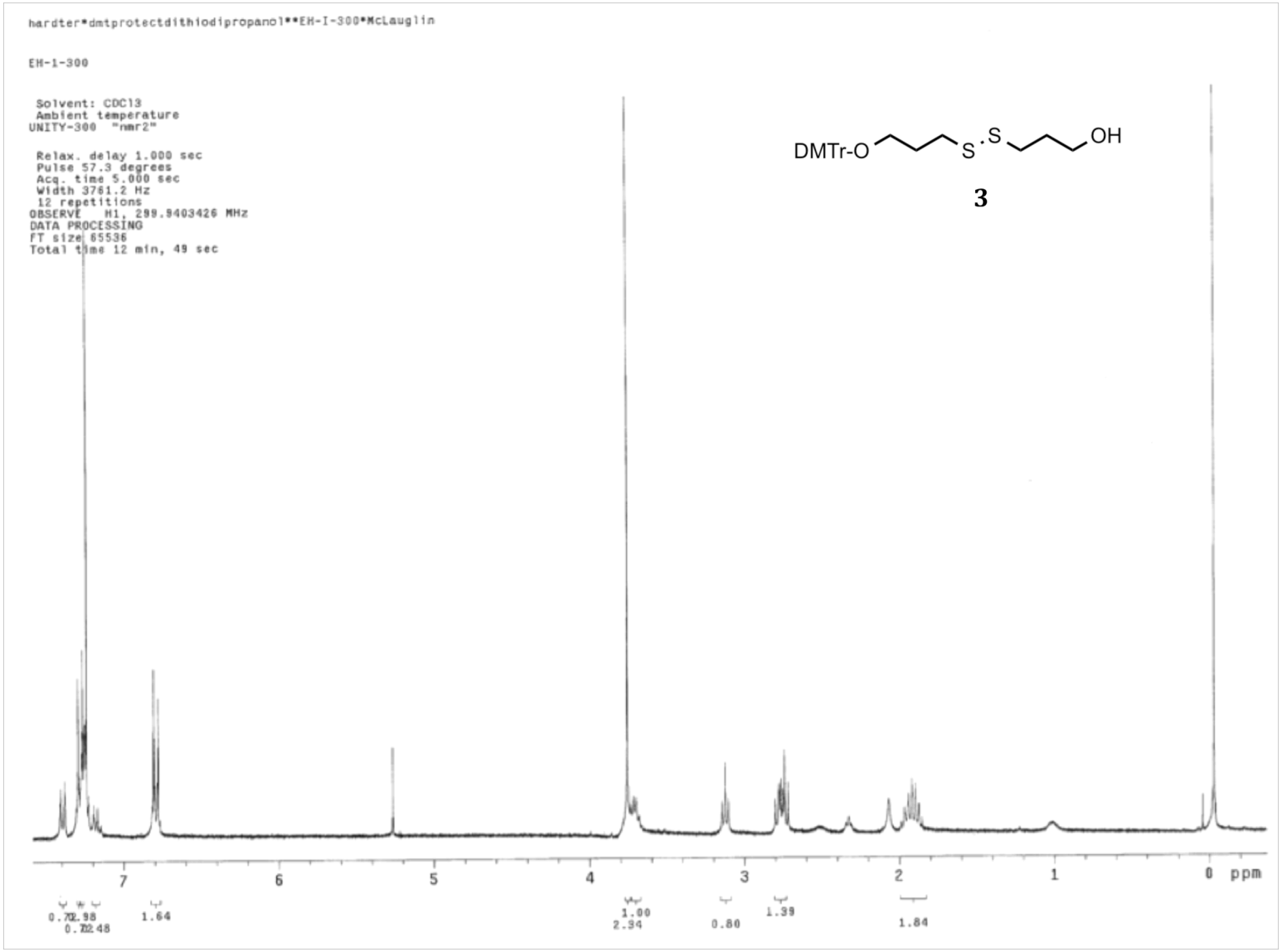
hardter*dmtprotectdithiodipropanol**EH-I-300*McLauglin
EH-1-300
Solvent: CDCl3
Ambient temperature
UNITY-300 "nmr2"
Relax. delay 1.000 sec
Pulse 57.3 degrees
Acq. time 5.000 sec
Width 3781.2 Hz
12 repetitions
OBSERVE H1, 299.9403426 MHz
DATA PROCESSING
FT size 65536
Total time 12 min, 49 sec
DMTr-O
S
S
OH
3
7
6
5
4
3
2
1
0 ppm
0.70
2.98
0.70
2.48
1.64
1.00
2.34
0.80
1.39
1.84

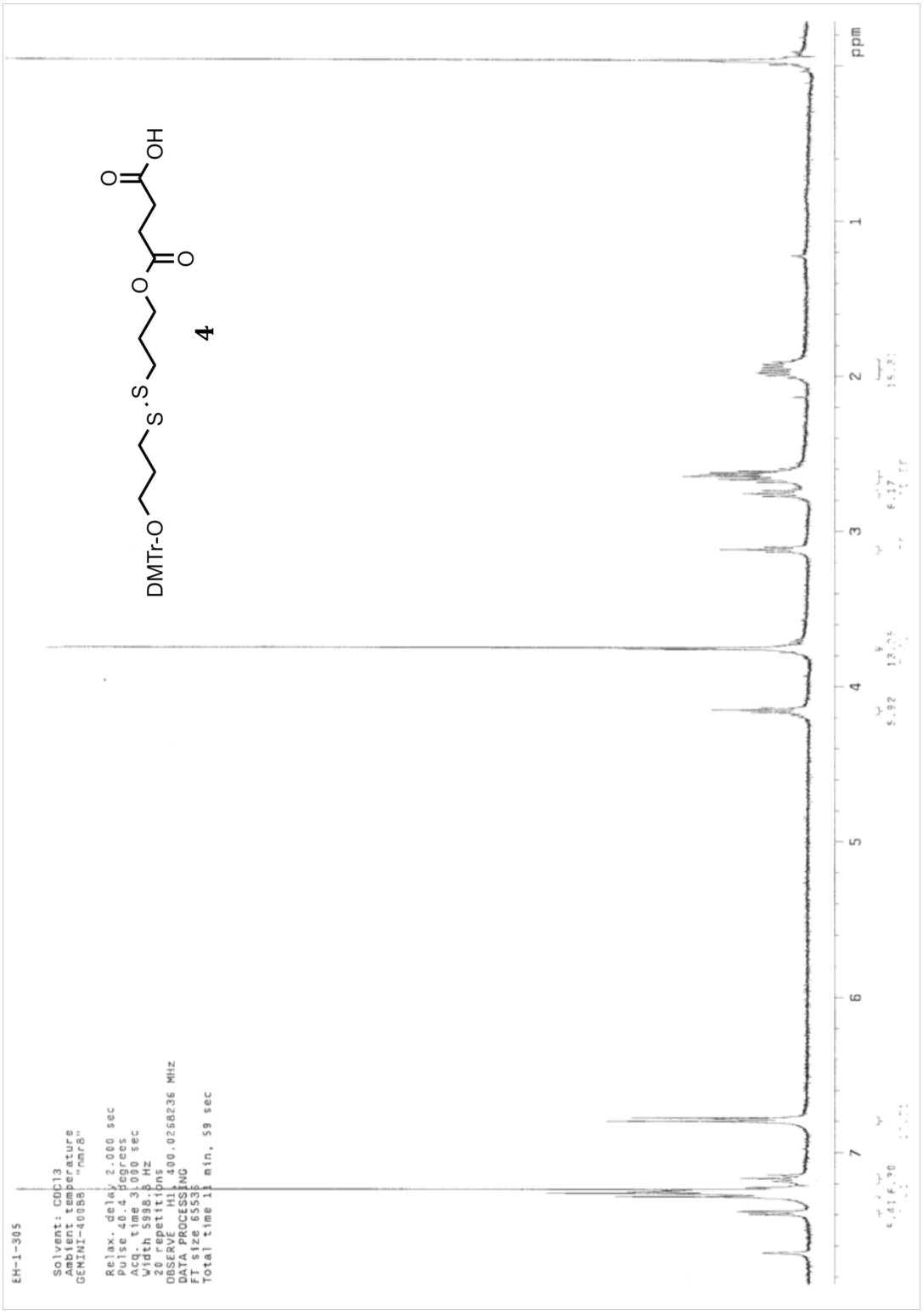
EM-1-305
Solvent: CDCl3
Ambient temperature
GEMINI-400BB "nmr8"
Relax. delay 2.000 sec
Pulse 40.4 degrees
Acq. time 3.090 sec
Width 5998.8 Hz
20 repetitions
OBSERVE H1 400.0268236 MHz
DATA PROCESSING
FT size 65536
Total time 11 min, 59 sec
DMTr-O
S
S
O
O
O
OH
4
ppm

Pulse Sequence: s2pul
Solvent: DMSO
Ambient temperature
GEMINI-400BB "nmr8"
Relax. delay 2.000 sec
Pulse 45.6 degrees
Acq. time 3.000 sec
Width 5938.8 Hz
20 repetitions
OBSERVE H1, 400.0287083 MHz
DATA PROCESSING
FT size 65536
Total time 0 min, 0 sec
NHBz
HO
OH
7
ppm

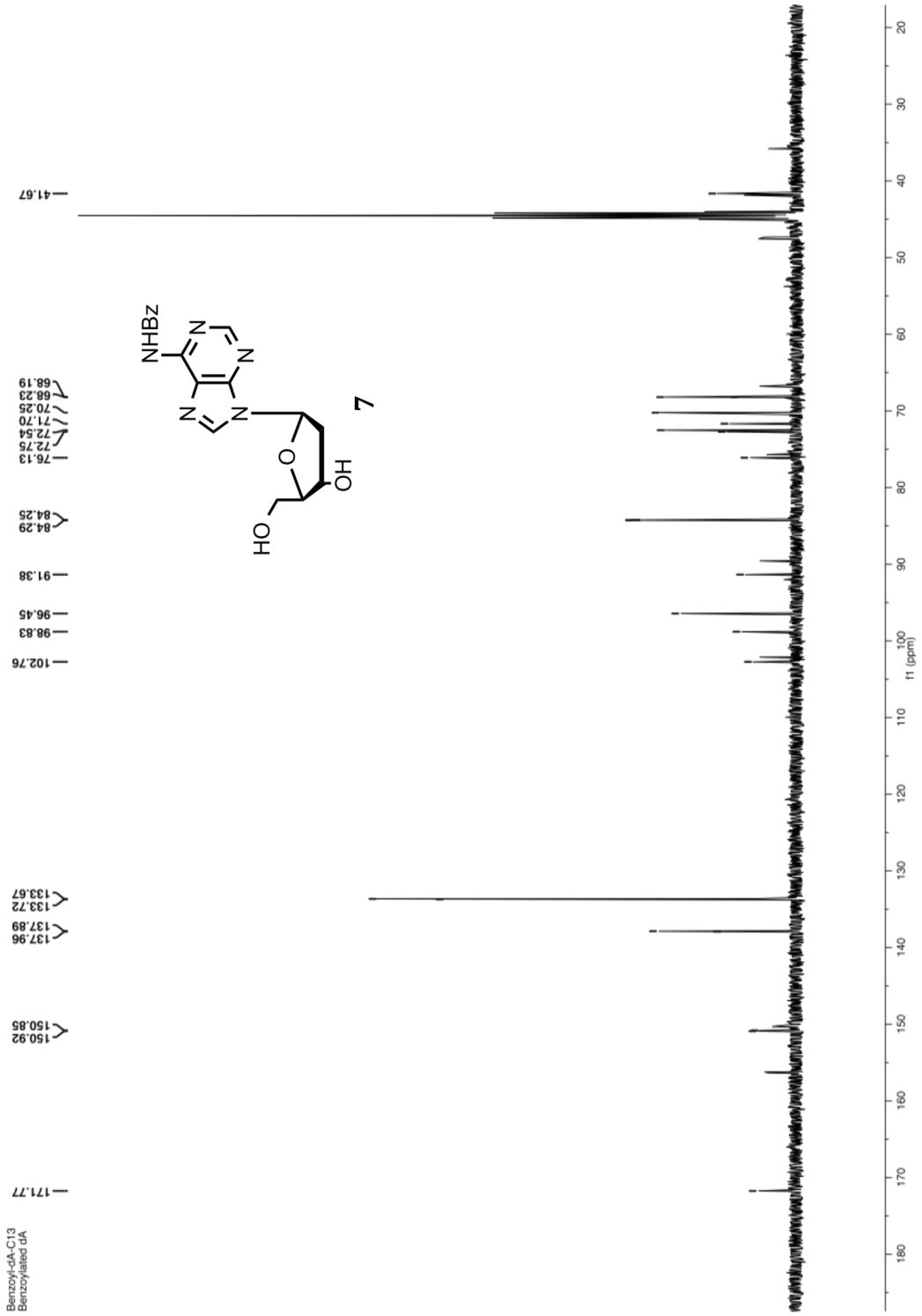
Benzoyl-dA-C13
Benzoylated dA
171.77
150.92
150.85
137.96
137.89
133.72
133.67
102.76
98.83
96.45
91.38
84.29
84.25
76.13
72.75
72.54
71.70
70.25
68.23
68.19
41.67
NHBz
HO
OH
O
7
f1 (ppm)

EM-1-157
Pulse Sequence: s2pul
Solvent: DMSO
Ambient temperature
GEMINI-400BB "nmr8"
Relax. delay 2.000 sec
Pulse 45.0 degrees
Acq. time 3.000 sec
Width 5998.8 Hz
8 repetitions
OBSERVE H1, 400.0287087 MHz
DATA PROCESSING
FT size 65536
Total time 11 min, 59 sec
NHBz
TBS-O
OH
8
ppm

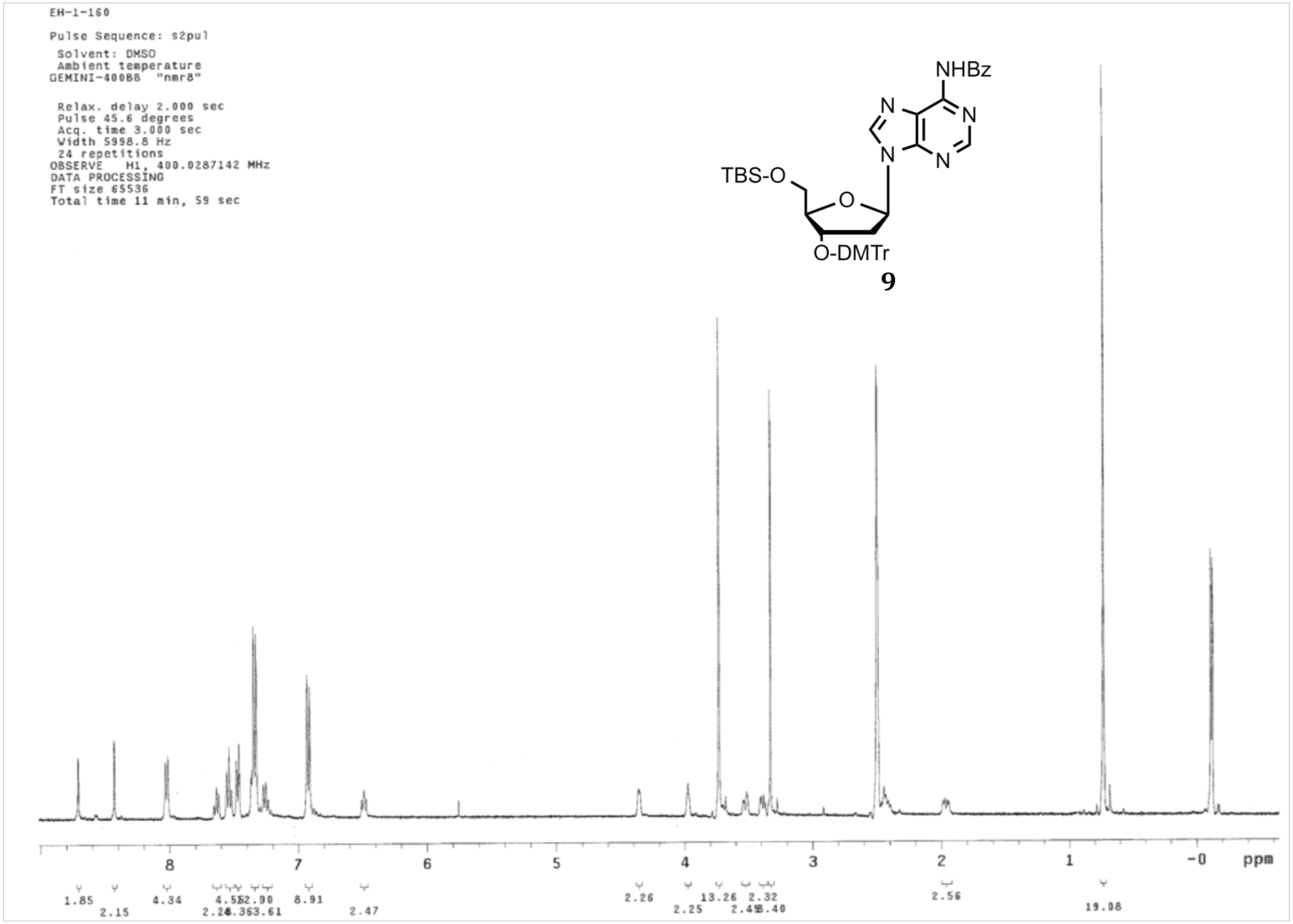
EH-1-160
Pulse Sequence: s2pul
Solvent: DMSO
Ambient temperature
GEMINI-400BB "nmr8"
Relax. delay 2.000 sec
Pulse 45.6 degrees
Acq. time 3.000 sec
Width 5998.8 Hz
24 repetitions
OBSERVE H1, 400.0287142 MHz
DATA PROCESSING
FT size 65536
Total time 11 min, 59 sec
NHBz
N
N
N
N
TBS-O
O
O-DMTr
9
8
7
6
5
4
3
2
1
-0
ppm
1.85
2.15
4.34
2.90
8.91
2.47
2.26
2.25
13.26
2.32
2.56
19.08

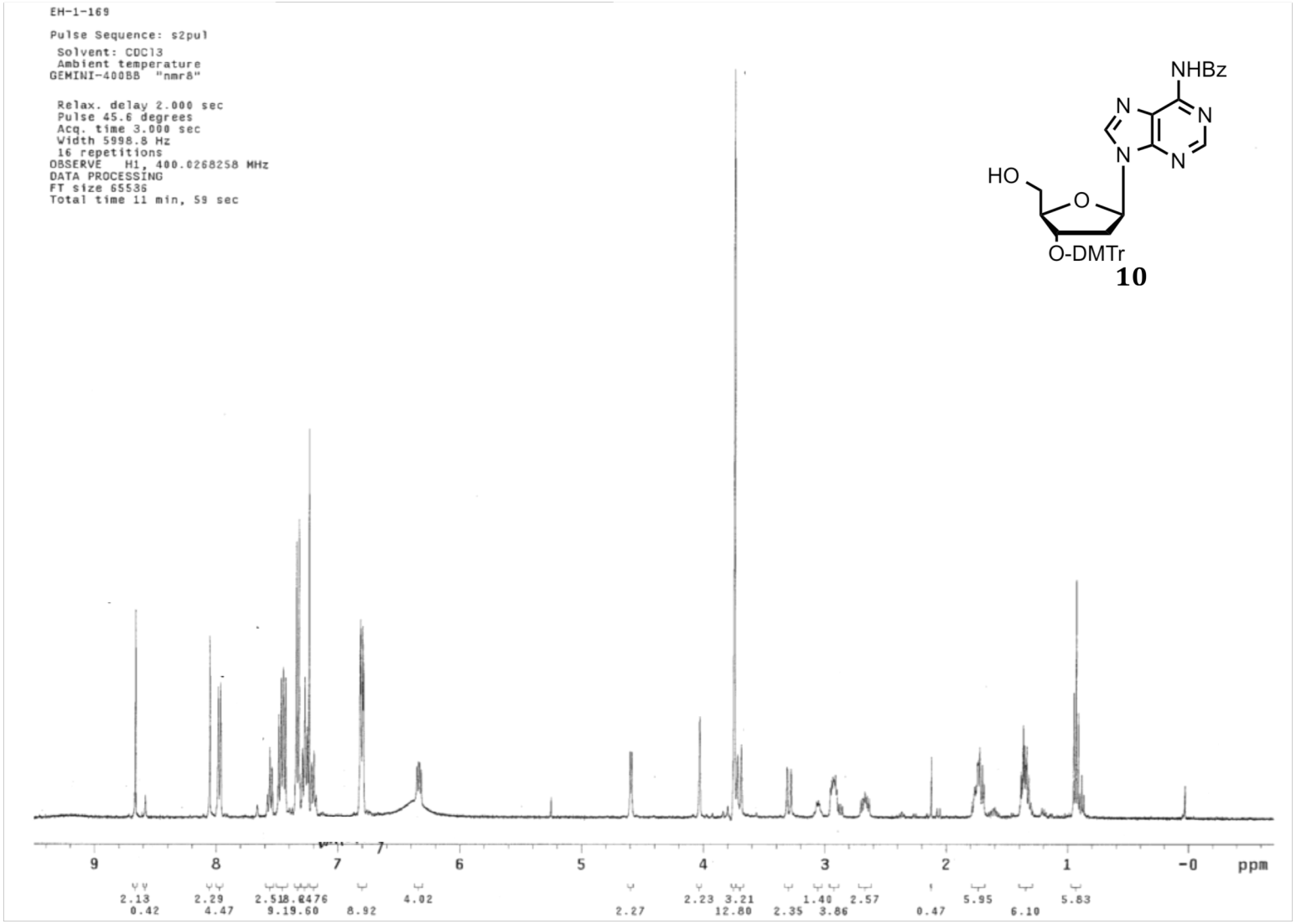
EH-1-169
Pulse Sequence: s2pul
Solvent: CDCl3
Ambient temperature
GEMINI-400BB "nmr8"
Relax. delay 2.000 sec
Pulse 45.6 degrees
Acq. time 3.000 sec
Width 5998.8 Hz
16 repetitions
OBSERVE H1, 400.0268258 MHz
DATA PROCESSING
FT size 65536
Total time 11 min, 59 sec
NHBz
N
N
N
N
HO
O
O-DMTr
10
9
8
7
6
5
4
3
2
1
-0
ppm
2.13
0.42
2.29
4.47
2.51
8.64
76
9.19
60
8.92
4.02
2.27
2.23
12.80
3.21
2.35
1.40
3.86
2.57
0.47
5.95
6.10
5.83

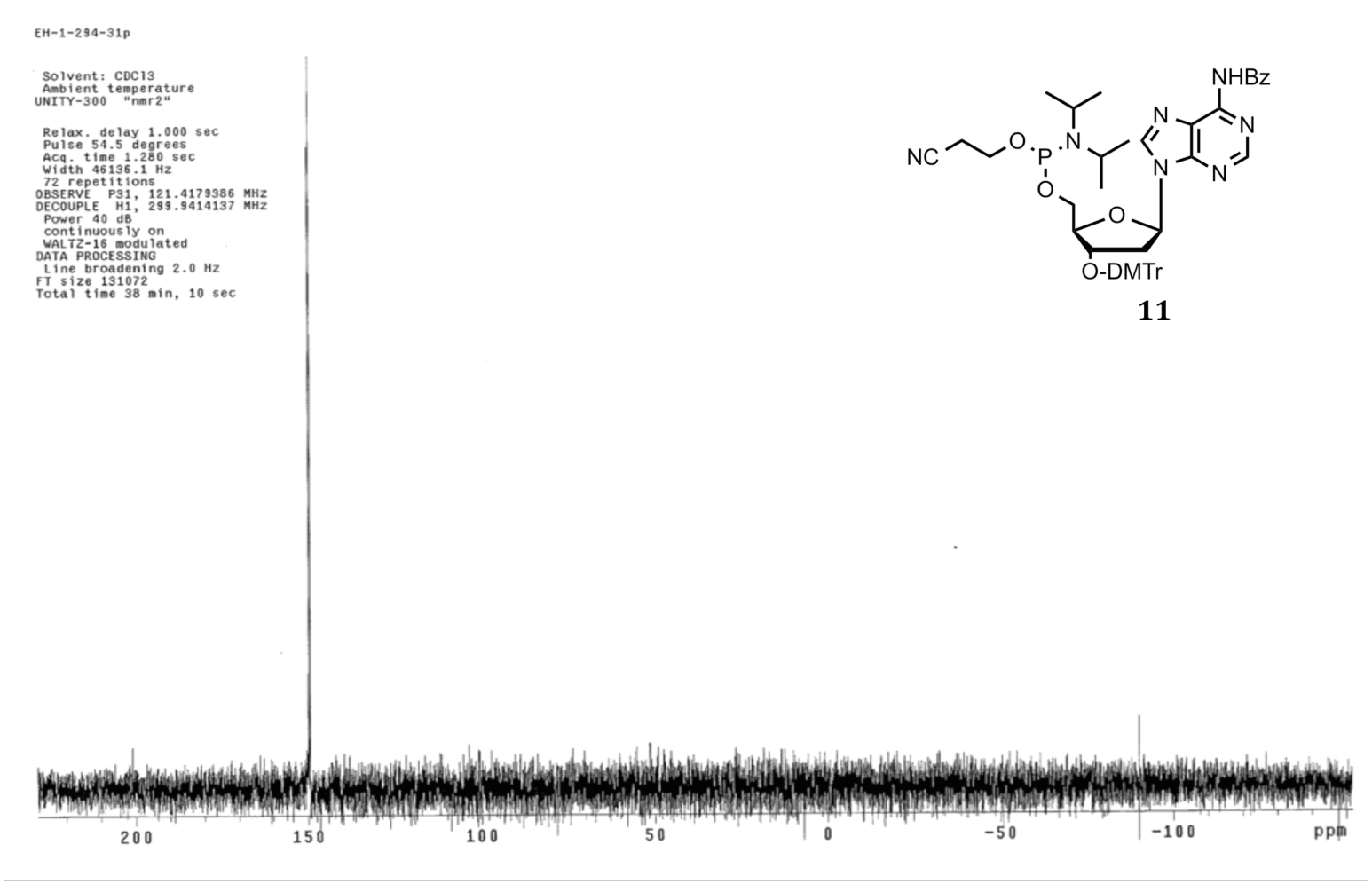
EH-1-294-31p
Solvent: CDCl3
Ambient temperature
UNITY-300 "nmr2"
Relax. delay 1.000 sec
Pulse 54.5 degrees
Acq. time 1.280 sec
Width 46136.1 Hz
72 repetitions
OBSERVE P31, 121.4179386 MHz
DECOUPLE H1, 299.9414137 MHz
Power 40 dB
continuously on
WALTZ-16 modulated
DATA PROCESSING
Line broadening 2.0 Hz
FT size 131072
Total time 38 min, 10 sec
NHBz
NC
O
P
N
N
N
N
O
O
O-DMTr
200
150
100
50
0
-50
-100
ppm

11

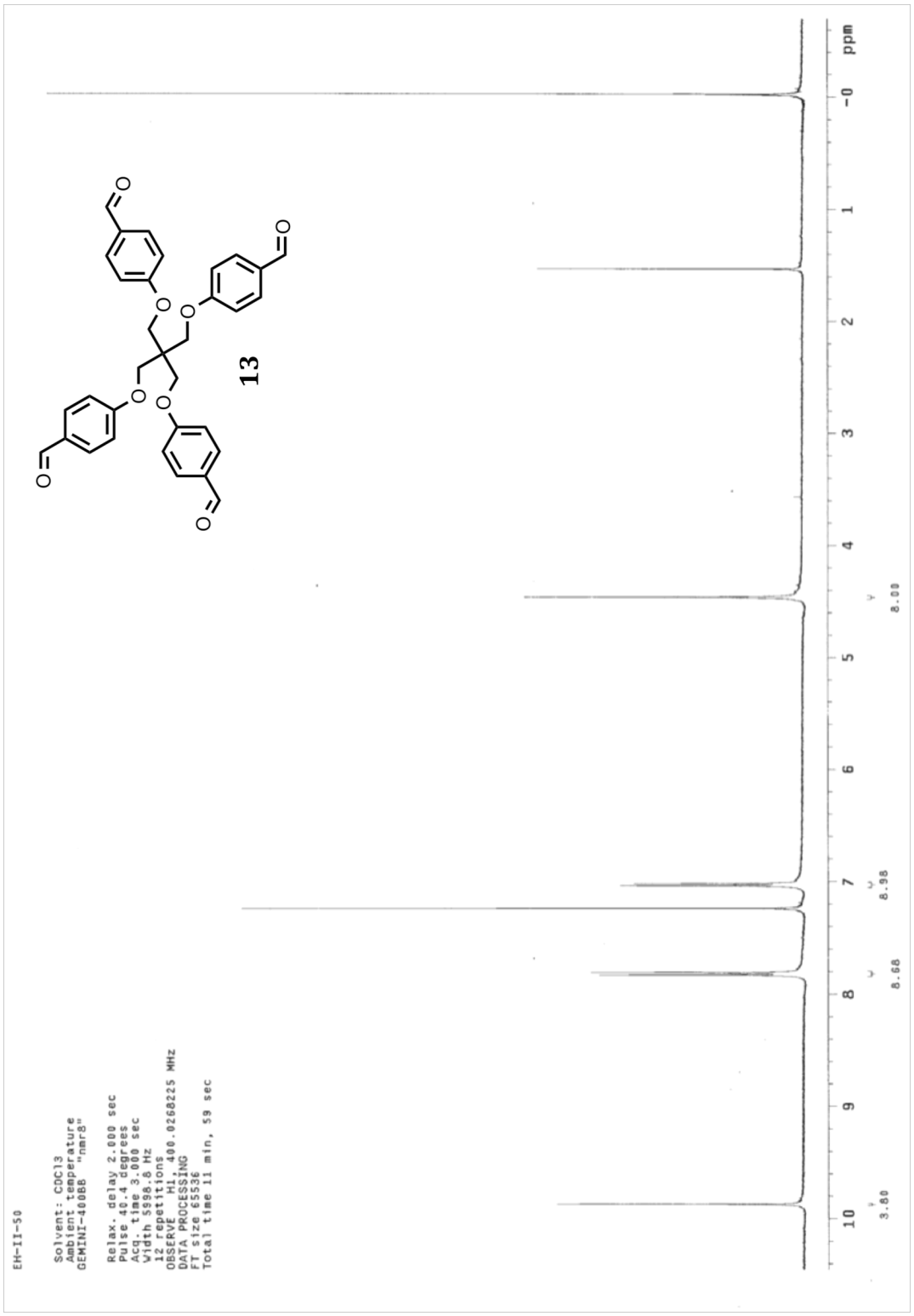
EH-II-50
Solvent: CDCl3
Ambient temperature
GEMINI-400BB "mar8"
Relax. delay 2.000 sec
Pulse 40.4 degrees
Acq. time 3.000 sec
Width 5998.8 Hz
12 repetitions
OBSERVE H1, 400.0260225 MHz
DATA PROCESSING
FT size 65536
Total time 11 min, 59 sec
13
ppm
3.80
8.68
8.98
8.88

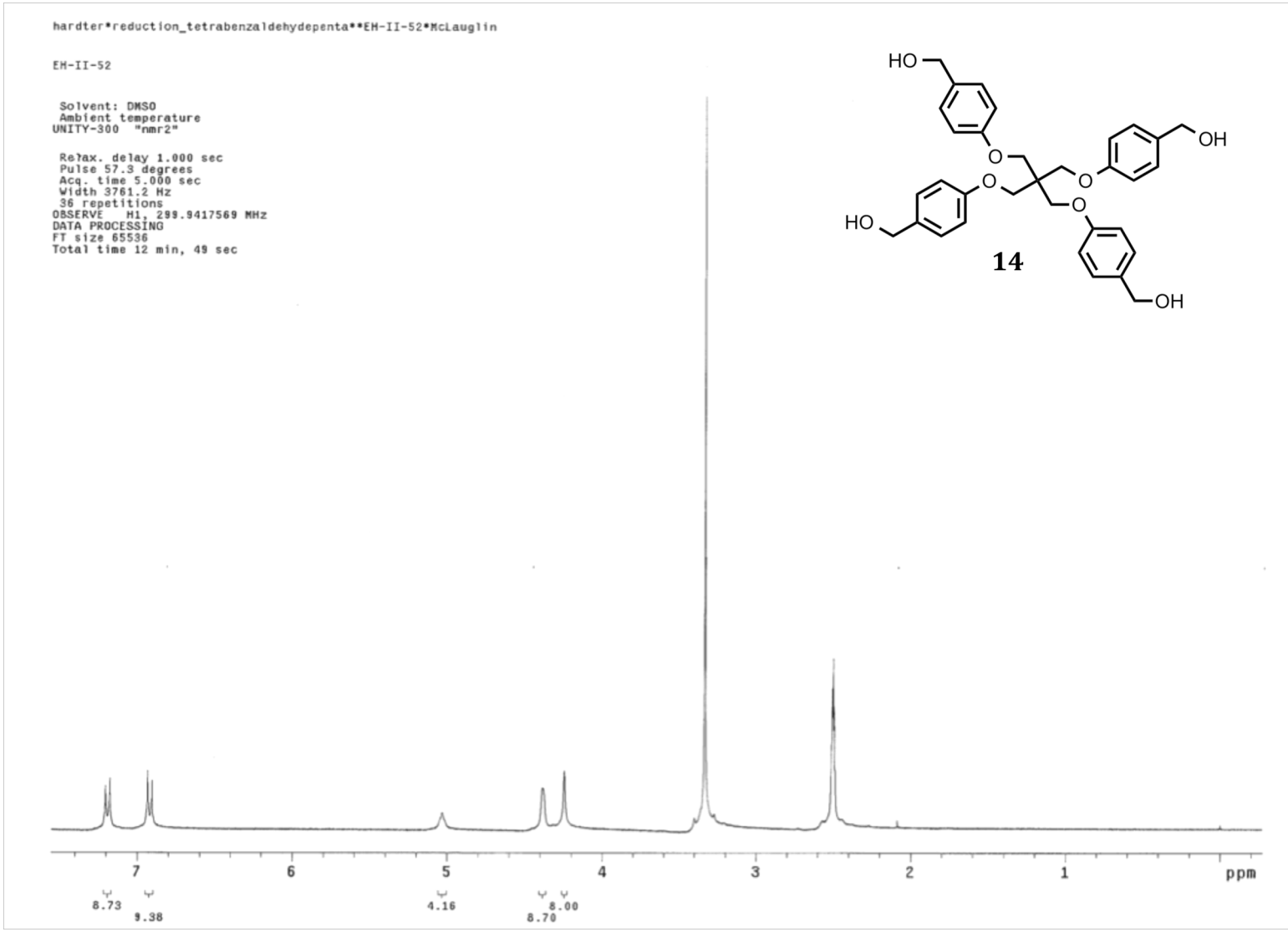
hardter*reduction_tetrabenzaldehydepenta**EH-II-52*McLauglin
EH-II-52
Solvent: DMSO
Ambient temperature
UNITY-300 "nmr2"
Relax. delay 1.000 sec
Pulse 57.3 degrees
Acq. time 5.000 sec
Width 3761.2 Hz
36 repetitions
OBSERVE H1, 299.9417569 MHz
DATA PROCESSING
FT size 65536
Total time 12 min, 49 sec
HO
OH
HO
OH
O
O
O
O
14
7
6
5
4
3
2
1
ppm
8.73
9.38
4.16
8.70
8.00

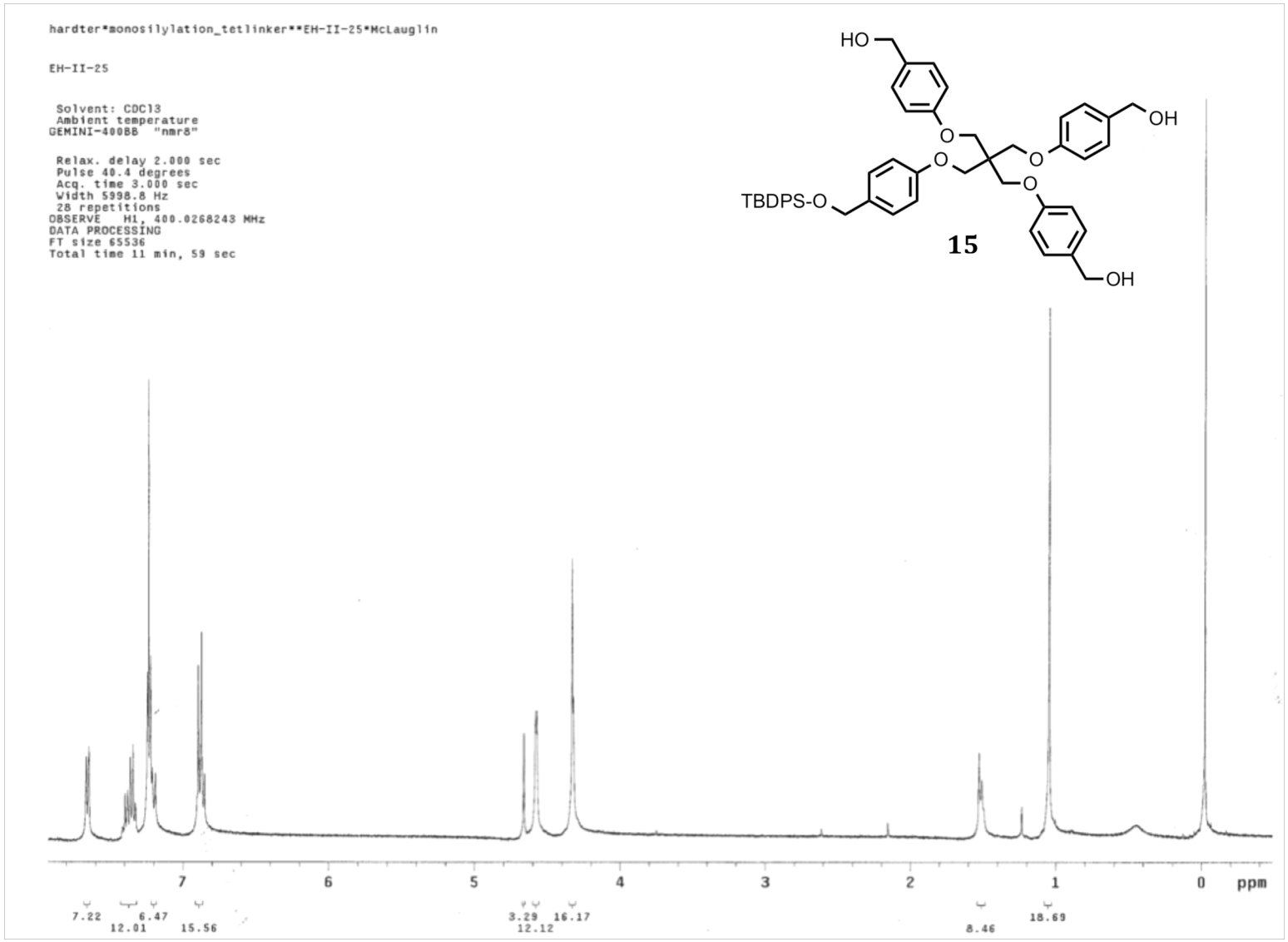
hardter*monosilylation_tetlinker**EH-II-25*McLauglin
EH-II-25
Solvent: CDCl3
Ambient temperature
GEMINI-400BB "nmr8"
Relax. delay 2.000 sec
Pulse 40.4 degrees
Acq. time 3.000 sec
Width 5998.8 Hz
28 repetitions
OBSERVE H1, 400.0268243 MHz
DATA PROCESSING
FT size 65536
Total time 11 min, 59 sec
HO
OH
TBDPS-O
OH
O
O
O
O
15
7
6
5
4
3
2
1
0
ppm
7.22
12.01
6.47
15.56
3.29
12.12
16.17
8.46
18.69

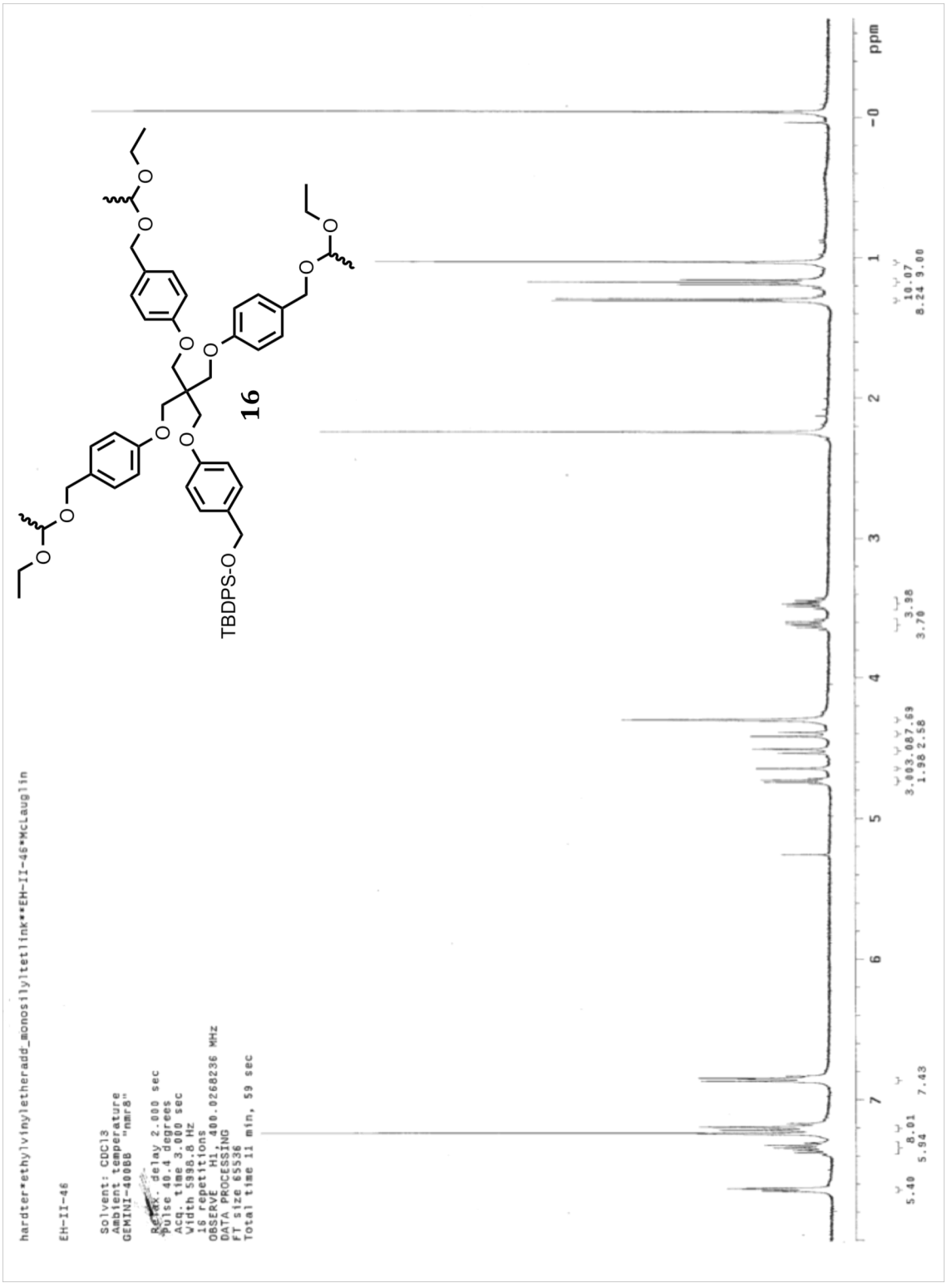
hardter*ethylvinylethera dd_monosilyltetlink**EH-II-46*McLaughlin
EH-II-46
Solvent: CDCl3
Ambient temperature
GEMINI-400BB "nmr8"
Relax. delay 2.000 sec
Pulse 40.4 degrees
Acq. time 3.000 sec
Width 5398.8 Hz
16 repetitions
OBSERVE H1, 400.0268236 MHz
DATA PROCESSING
FT size 65536
Total time 11 min, 59 sec
TBDPS-O
16
ppm
5.40
8.01
5.94
7.43
3.00
3.08
7.69
1.98
2.58
3.98
3.70
10.07
8.24
9.00

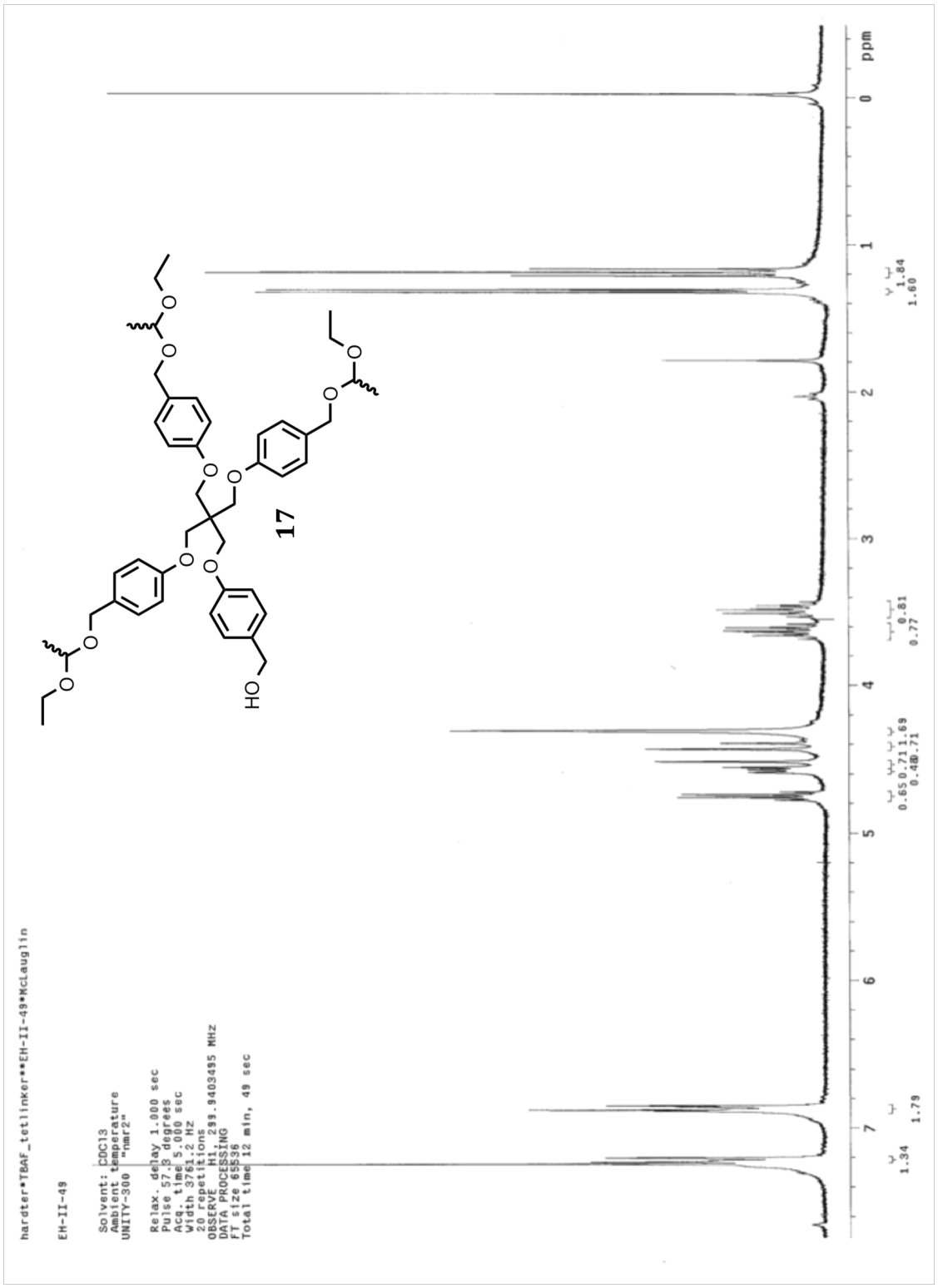
harder*TBAF_tetlinker**EH-II-49*McLaughlin
EH-II-49
Solvent: CDCl3
Ambient temperature
UNITY-300 'rmr2'
Relax. delay 1.000 sec
Pulse 57.3 degrees
Acq. time 5.000 sec
Width 3761.2 Hz
20 repetitions
OBSERVE H1, 299.9403495 MHz
DATA PROCESSING
FT size 65536
Total time 12 min, 49 sec
HO
17
ppm

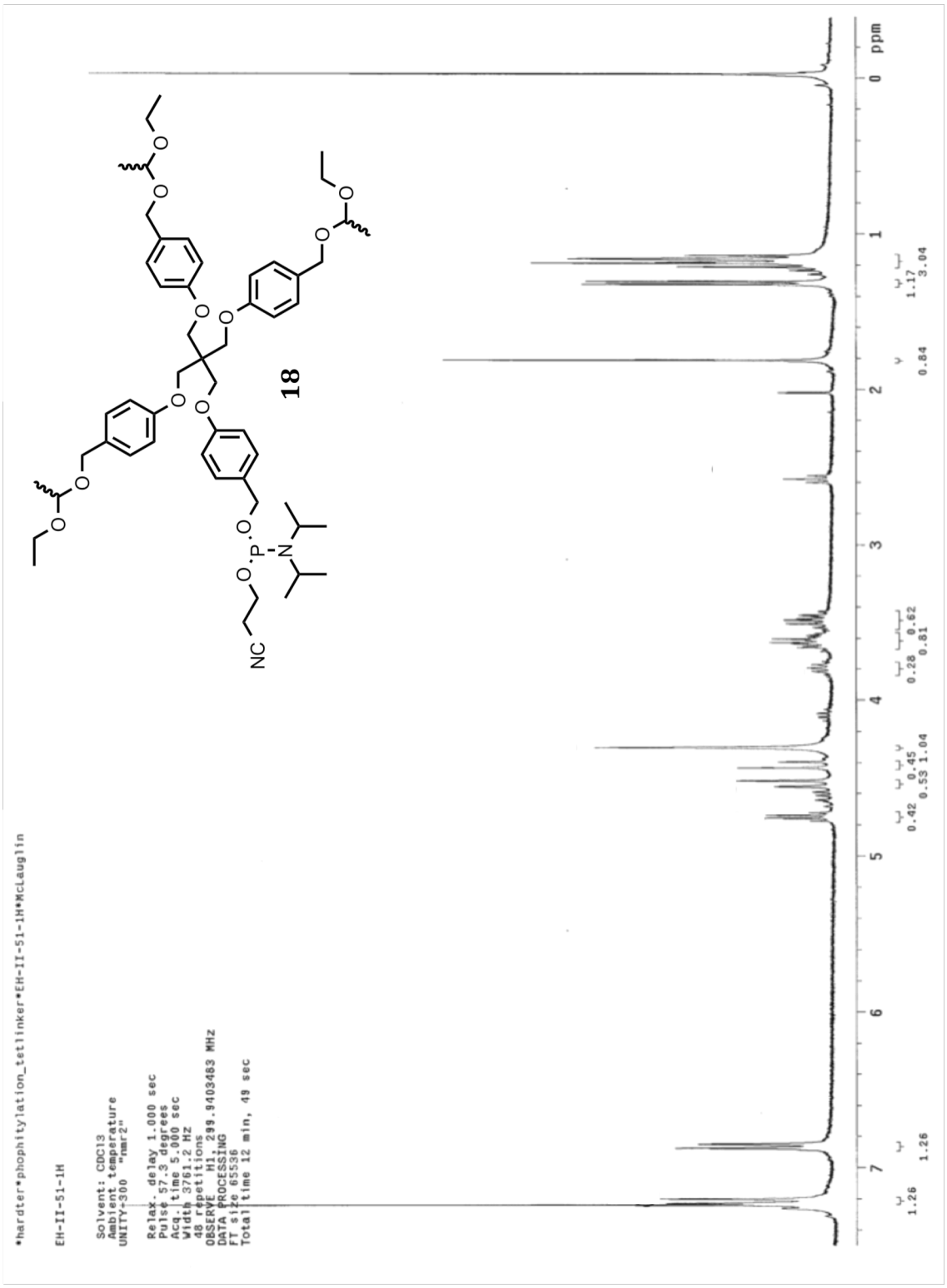
*hardter*phophitylation_tetlinker*EH-II-51-1H*McLaughlin
EH-II-51-1H
Solvent: CDCl3
Ambient temperature
UNITY-300 "nmr2"
Relax. delay 1.000 sec
Pulse 57.3 degrees
Acq. time 5.000 sec
Width 3761.2 Hz
48 repetitions
OBSERVE H1, 299.9403483 MHz
DATA PROCESSING
FT size 65536
Total time 12 min, 49 sec
18
NC
P
N
O
ppm
0
1
2
3
4
5
6
7
1.26
1.26
0.42
0.45
0.53
1.04
0.28
0.62
0.81
0.84
1.17
3.04

hardter*phosphitylation_tetlinker**EH-II-51*McLaughlin
EH-II-51
Solvent: CDCl3
Ambient temperature
UNITY-300 "nmr2"
Relax. delay 1.000 sec
Pulse 54.5 degrees
Acq. time 1.280 sec
Width 46136.1 Hz
100 repetitions
OBSERVE P31, 121.4179386 MHz
DECOUPLE H1, 299.9414137 MHz
Power 40 dB
continuously on
WALTZ-16 modulated
DATA PROCESSING
Line broadening 2.0 Hz
FT size 131072
Total time 38 min, 10 sec
18
NC
200
150
100
50
0
-50
-100
ppm

Sample: EM-II-183
File: exp
Pulse Sequence: s2pul
Solvent: cdcl3
Temp. 25.0 C / 298.1 K
Operator: lwm
VNMRS-400 "nmr14"
Relax. delay 1.000 sec
Pulse 45.0 degrees
Acq. time 2.049 sec
Width 6410.3 Hz
32 repetitions
OBSERVE H1, 399.7662768 MHz
DATA PROCESSING
Resol. enhancement -0.0 Hz
FT size 65536
Total time 3 min, 21 sec
DMTr
O
NH2
O-DMTr
DMTr-O
20
ppm

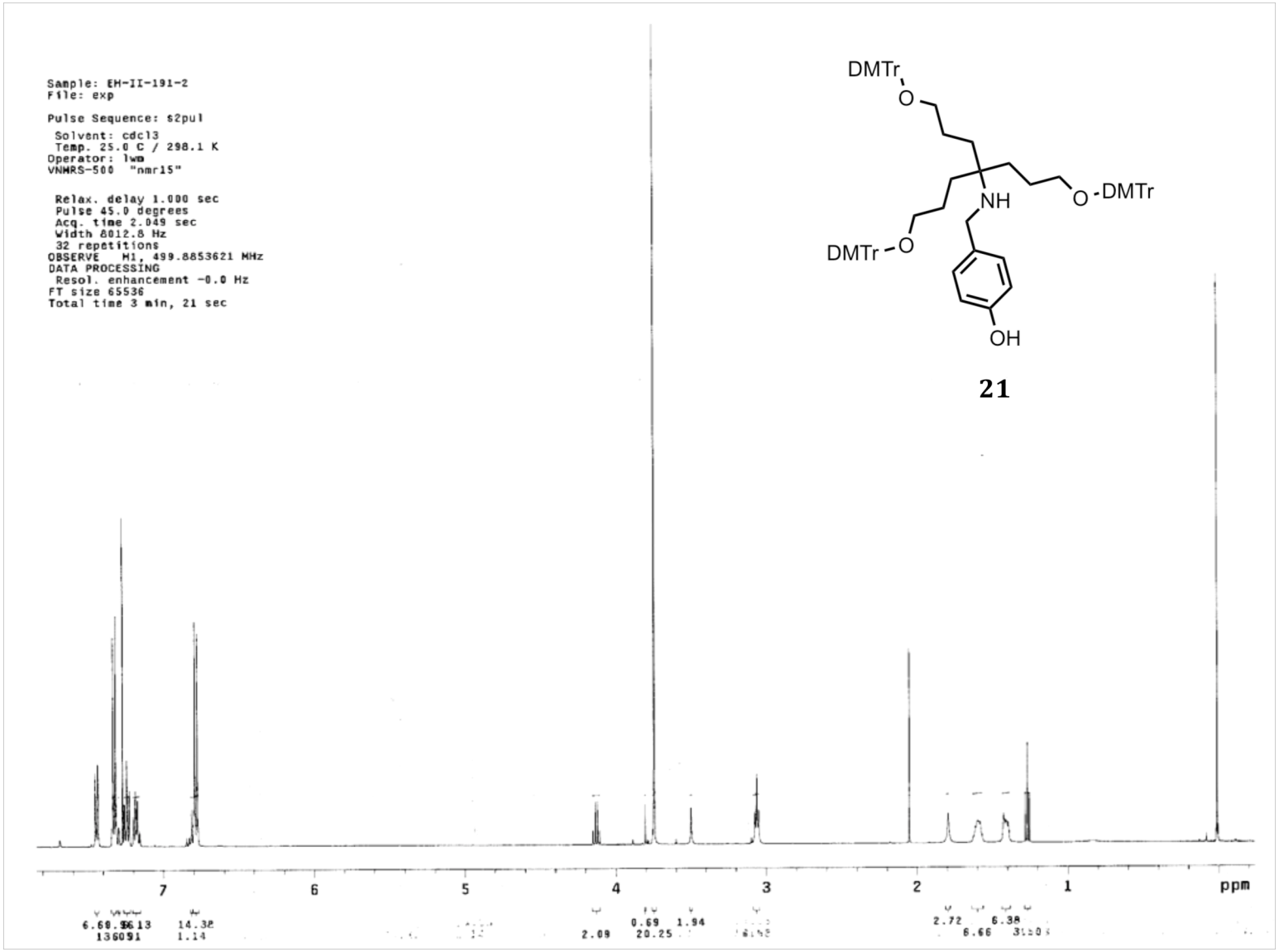
Sample: EH-II-191-2
File: exp
Pulse Sequence: s2pul
Solvent: cdcl3
Temp. 25.0 C / 298.1 K
Operator: lwa
VNMRS-500 "nmr15"
Relax. delay 1.000 sec
Pulse 45.0 degrees
Acq. time 2.049 sec
Width 8012.8 Hz
32 repetitions
OBSERVE H1, 499.8853621 MHz
DATA PROCESSING
Resol. enhancement -0.0 Hz
FT size 65536
Total time 3 min, 21 sec
DMTr
O
NH
O-DMTr
DMTr-O
OH
21
7
6
5
4
3
2
1
ppm
14.38
1.14
2.09
0.69
1.94
20.25
2.72
6.38
6.66

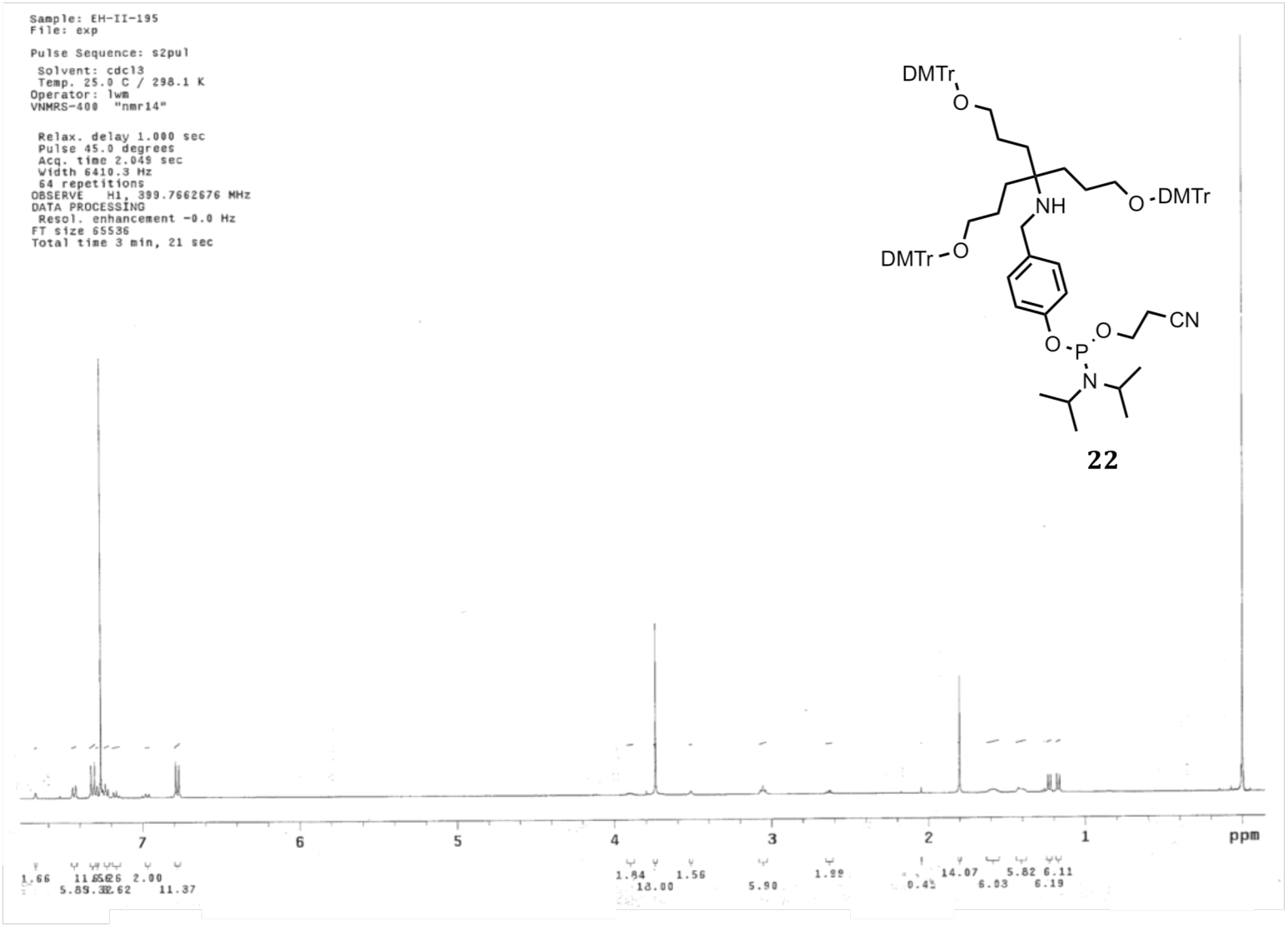
Sample: EH-II-195
File: exp
Pulse Sequence: s2pul
Solvent: cdcl3
Temp. 25.0 C / 298.1 K
Operator: lwm
VNMRS-400 "nmr14"
Relax. delay 1.000 sec
Pulse 45.0 degrees
Acq. time 2.049 sec
Width 6410.3 Hz
64 repetitions
OBSERVE H1, 399.7662676 MHz
DATA PROCESSING
Resol. enhancement -0.0 Hz
FT size 65536
Total time 3 min, 21 sec
DMTr
O
NH
O-DMTr
DMTr-O
O
O-P
O
CN
N
22
7
6
5
4
3
2
1
ppm
1.66
11.37
2.00
1.94
18.00
1.56
5.90
1.99
14.07
6.03
5.82
6.19
6.11

Sample: EH-II-195
File: exp
Pulse Sequence: s2pul
Solvent: cdcl3
Temp. 25.0 C / 298.1 K
Operator: lwm
VNMRS-400 "nmr14"
Relax. delay 1.000 sec
Pulse 45.0 degrees
Acq. time 1.600 sec
Width 37878.8 Hz
100 repetitions
OBSERVE P31, 161.8283551 MHz
DECOUPLE H1, 399.7682756 MHz
Power 40 dB
continuously on
WALTZ-16 modulated
DATA PROCESSING
Line broadening 1.0 Hz
FT size 131072
Total time 43 min, 20 sec
DMTr
O
O-DMTr
NH
O-P
N
O
CN
DMTr-O
22
180
160
140
120
100
80
60

2.11 Mass Spectra

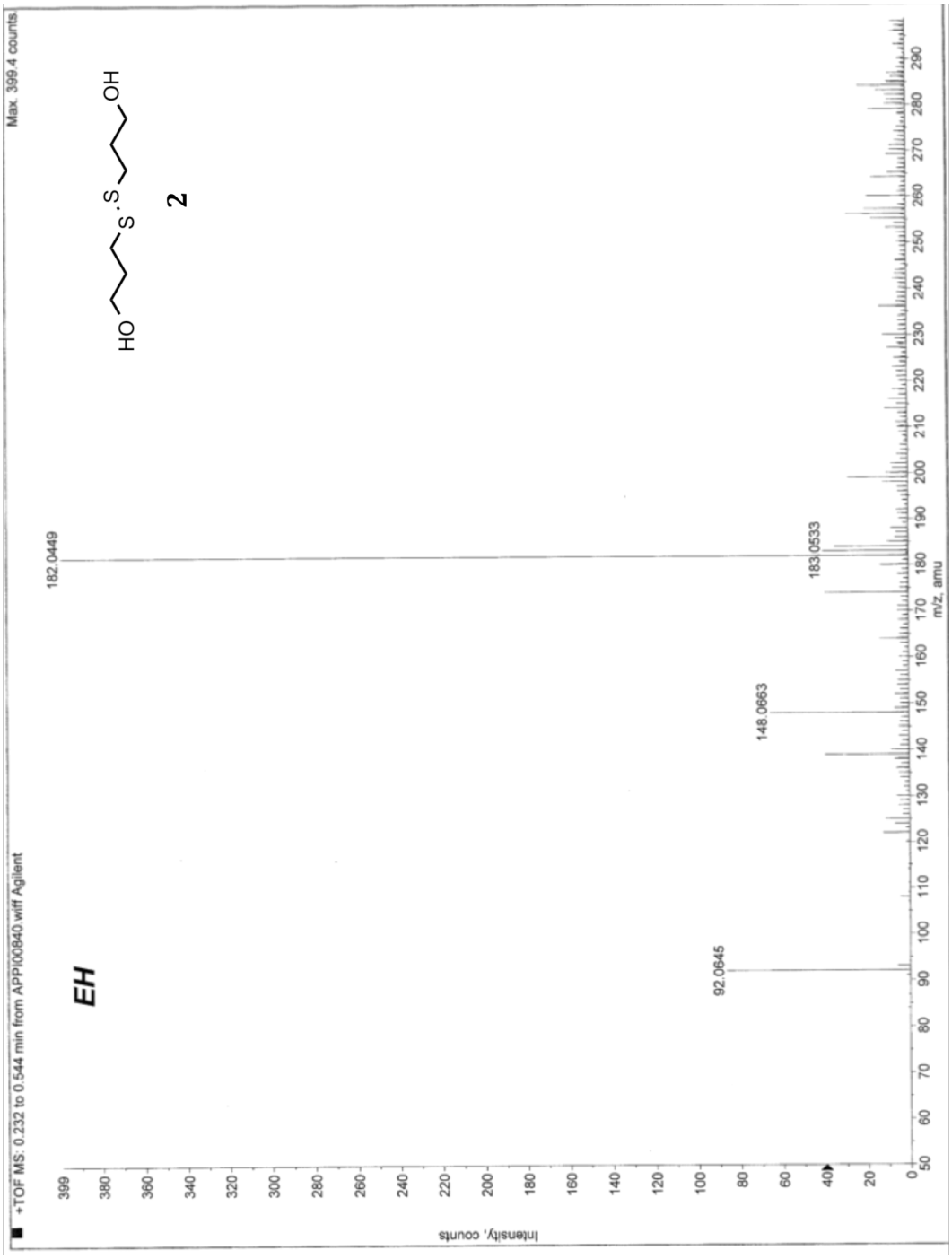

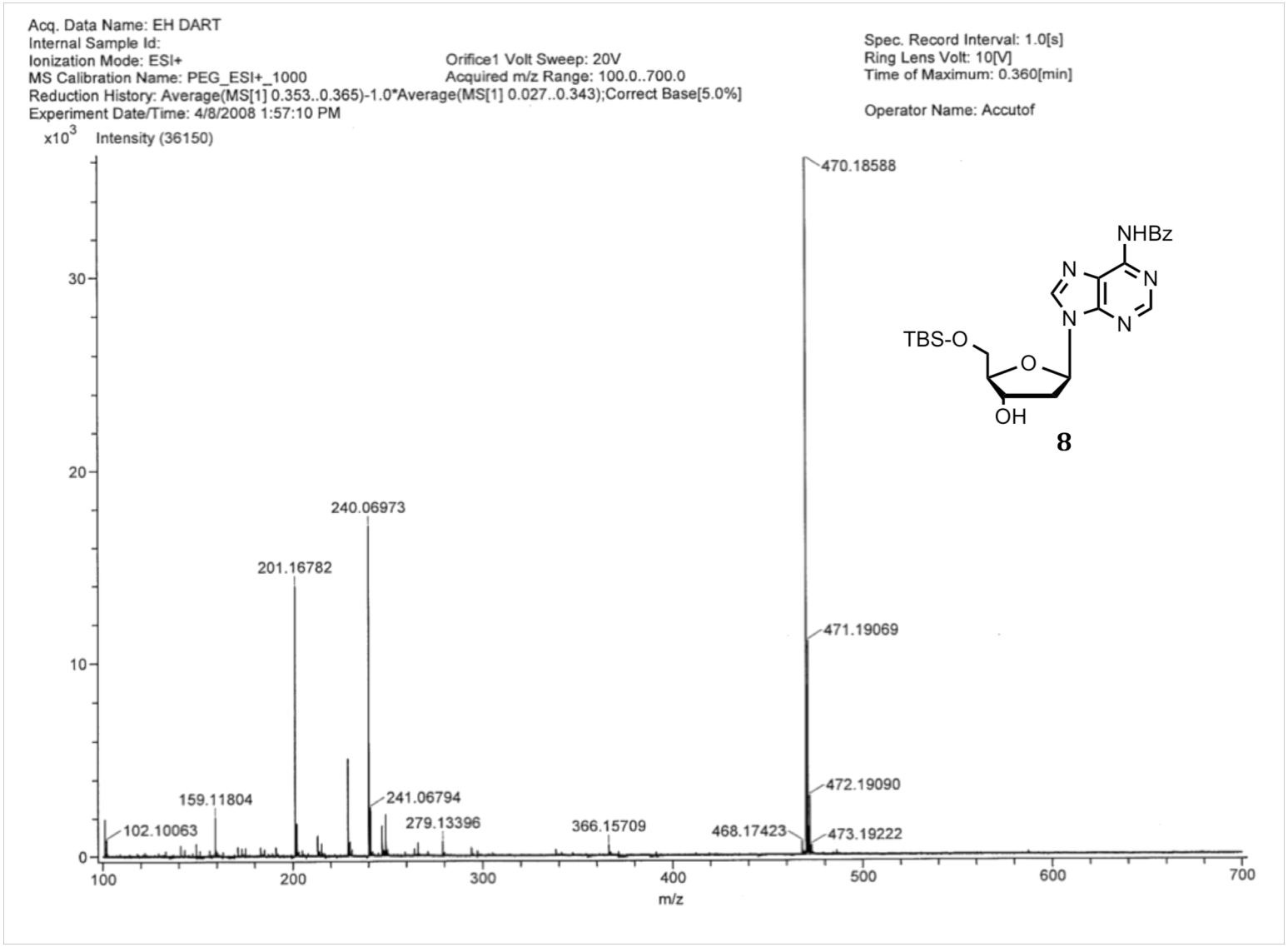
Acq. Data Name: EH DART
Internal Sample Id:
Ionization Mode: ESI+
MS Calibration Name: PEG_ESI+_1000
Reduction History: Average(MS[1] 0.353..0.365)-1.0*Average(MS[1] 0.027..0.343);Correct Base[5.0%]
Experiment Date/Time: 4/8/2008 1:57:10 PM
Orifice1 Volt Sweep: 20V
Acquired m/z Range: 100.0..700.0
Spec. Record Interval: 1.0[s]
Ring Lens Volt: 10[V]
Time of Maximum: 0.360[min]
Operator Name: Accutof
x10^3 Intensity (36150)
470.18588
471.19069
472.19090
473.19222
240.06973
201.16782
159.11804
241.06794
279.13396
366.15709
468.17423
102.10063
NHBz
N
N
N
N
TBS-O
O
OH
8
m/z

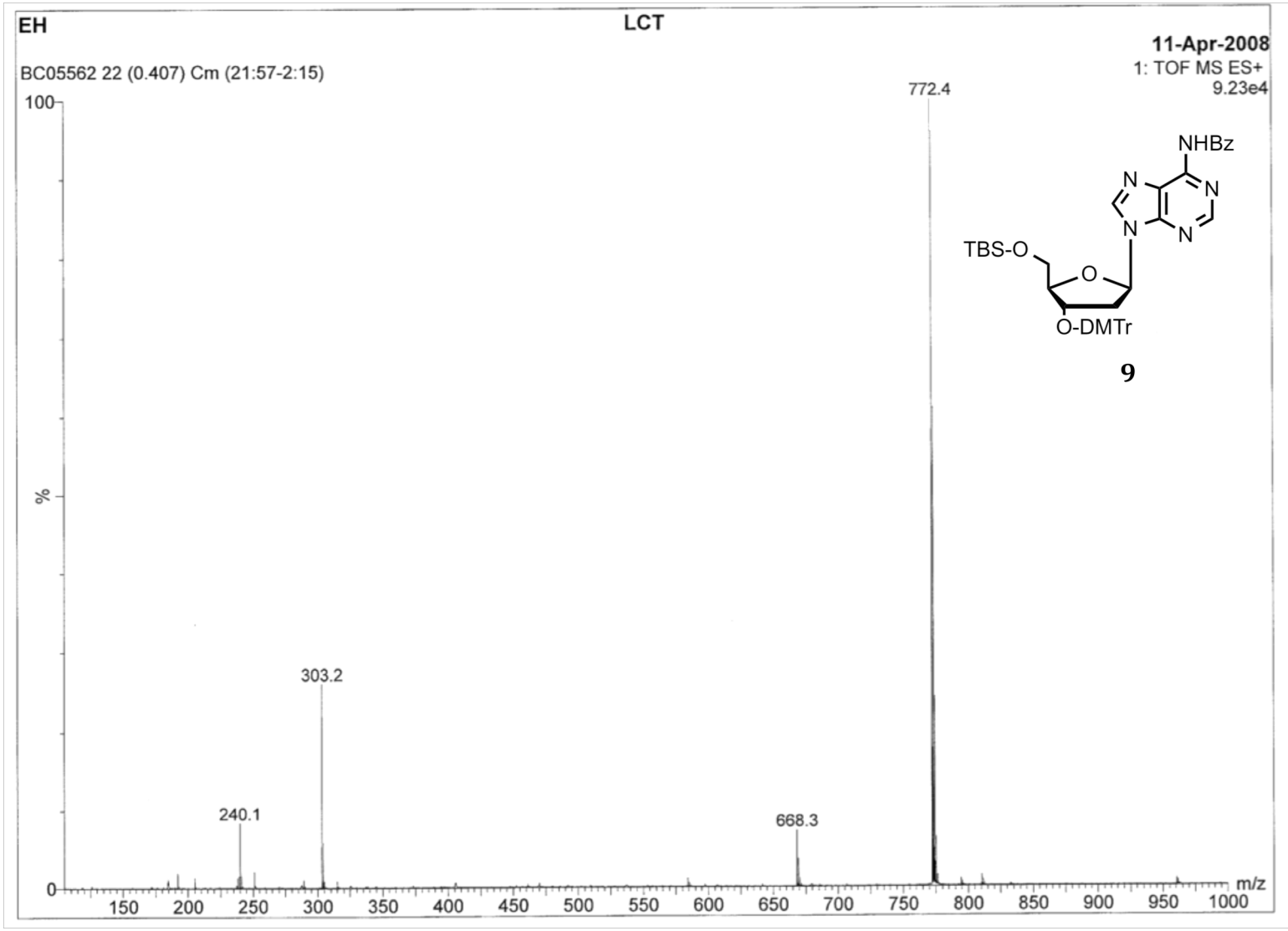
EH
LCT
11-Apr-2008
1: TOF MS ES+
9.23e4
BC05562 22 (0.407) Cm (21:57-2:15)
100
%
0
772.4
303.2
240.1
668.3
m/z
150 200 250 300 350 400 450 500 550 600 650 700 750 800 850 900 950 1000
NHBz
N
N
N
N
TBS-O
O
O-DMTr

9

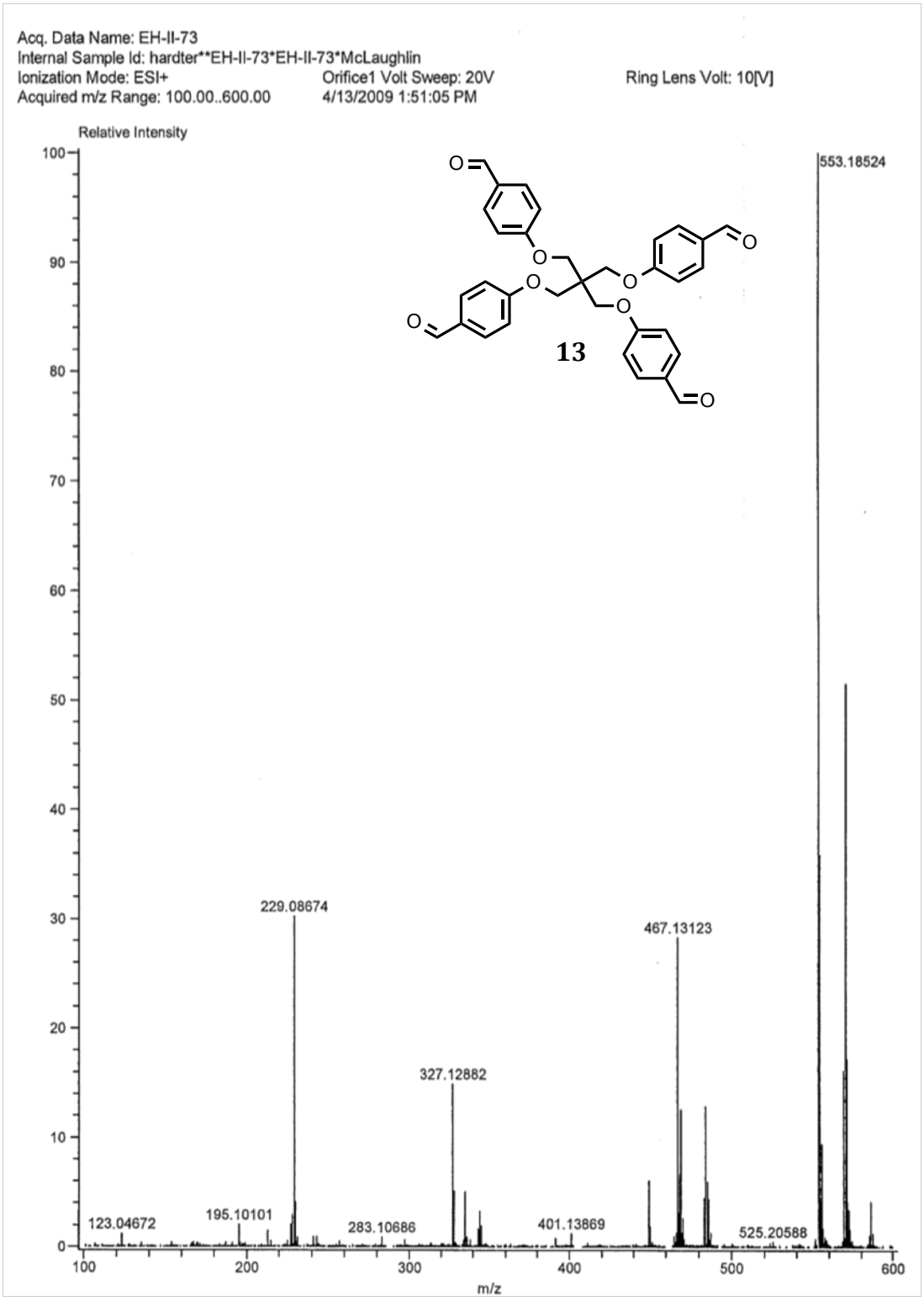
Acq. Data Name: EH-II-73
Internal Sample Id: hardter**EH-II-73*EH-II-73*McLaughlin
Ionization Mode: ESI+
Orifice1 Volt Sweep: 20V
Ring Lens Volt: 10[V]
Acquired m/z Range: 100.00..600.00
4/13/2009 1:51:05 PM
Relative Intensity
553.18524
229.08674
467.13123
327.12882
123.04672
195.10101
283.10686
401.13869
525.20588
m/z
13

EH-II-23
Waters0000348 40 (0.735) Cm (40:55-3:32)
LCT
1: TOF MS ES+
681
100
%
0
821.3
822.3
858.4
859.5
736.5
300.0
325.0
200
300
400
500
600
700
800
900
1000
1100
1200
1300
1400
1500
1600
1700
m/z
HO
OH
OH
TBDPS-O
15

Sample Name	EH-II-191 Matrix : A	**Position**	P1-A1	**Instrument Name**	Instrument 1	**User Name**	Marek A. Domin
Inj Vol	-1	**InjPosition**		**SampleType**	Sample	**IRM Calibration Status**	Success
Data Filename	Agilent0000417.d	**ACQ Method**		**Comment**	hardter*Reduction Schiff bis homotris*Ag	**Acquired Time**	1/11/2010 1:40:39 PM

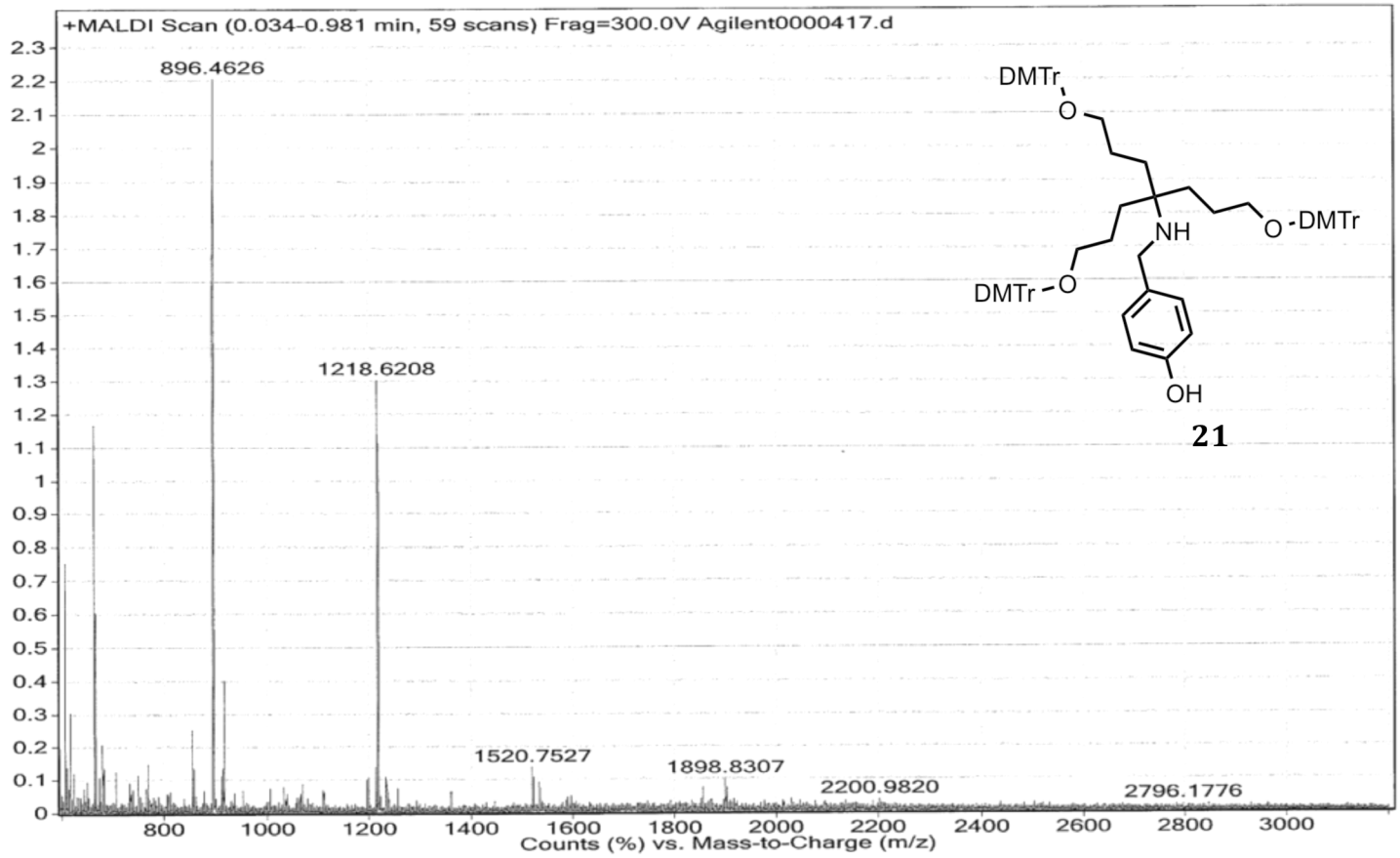

21

Chapter 3

Synthesis of Backbone-Extended Deoxyribonucleosides and Effects of Their Insertion into Duplexed DNA

3.1 Introduction

3.1.1 Modifying the DNA Backbone, Introduction to 6'-nucleosides and General Goals

As mentioned in the first chapter, one of the three main target sites for nucleic acid modification is an oligomer's backbone. Previous studies include both increasing and decreasing the complexity of standard phosphodiester linkage, as well as selective atomic-level replacement. Depending on the methodologies utilized, examples have shown novel and useful properties.

The creation of a phosphorothioate linkage between two nucleosides has been previously described, providing a blueprint for incorporating a sulfur atom into the DNA backbone.[1] More recently, templated elongation using a 3'-phosphorothioate in conjunction with 5'-iodonucleosides has enabled researchers to create a phosphorothioester linkage in DNA.[2] Resultant assays showed a resistance to the T4 exonuclease, as well as a decrease in duplex melting temperatures.

Similarly, templated duplex creation using a 2'-amino nucleophile coupled with a 5'-phosphoimidizolide has been documented.[3] Fully synthesized duplexes were achieved, and couplings opposite RNA and locked-nucleic acid (LNA) primers were completed in under ten minutes. Most importantly, this mechanism was completed in a non-enzymatic fashion (Figure 3.1).

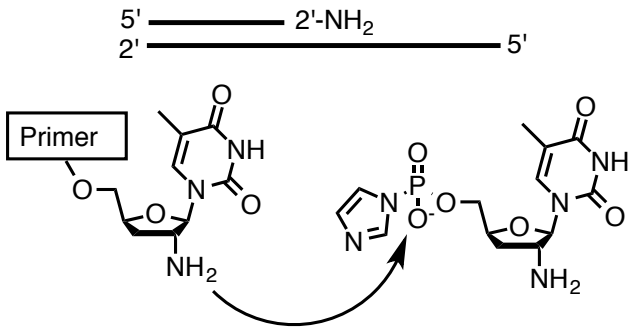

Figure 3.1: Templated, non-enzymatic polymerization with a 2'-amino nucleophile.

It's also been previously shown that shortening and simplifying the backbone can result in viable nucleic acid oligomers. To that end, our lab has previously described the synthesis and propagation of threose nucleic acids (TNA) and glycol nucleic acids (GNA), each of which involves a pseudo 2'-3' phosphodiester linkage between adjacent nucleosides (Figure 3.2).[4-9]

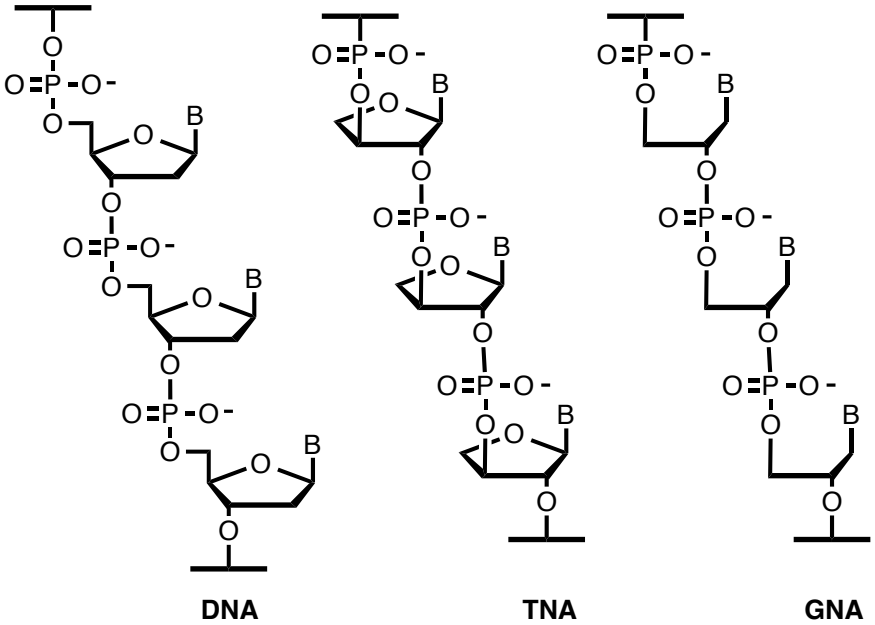

Figure 3.2: The shorter lengths and relatively unsophisticated natures of the TNA and GNA backbones relative to that of DNA.

This bonding pattern results in the omission of a carbon-carbon linkage relative to the DNA standard, thereby truncating the phosphodiester backbone. In the case of GNA, the cyclic sugar moiety is eliminated altogether, resulting in one less atom apiece of carbon and oxygen, as well as the absence of a stereocenter at the 3'-position. Given their simplistic natures, as well as the ability for triphosphates of both GNA and TNA to be accepted by certain DNA polymerase enzymes, it's entirely possible that these classes of molecules could have served as precursors to the "RNA World."[10]

Similar to the above, we set about continuing with the trend of backbone modification. However, unlike with the backbone truncation of the GNA and TNA nucleosides, our goal was to create a new class of nucleosides which extend upon the conventional 3'-5' phosphodiester linkage. In order to do so, standard DNA building blocks (efforts began with 2'-deoxyadenosine and 2'-deoxythymidine) would have an additional methylene moiety added to either the 5'-carbon or 3'-carbon, affording a new family of elongated molecules. These monomers will also be functionalized in such a way that they are accessible for solid phase DNA synthesis (Figure 3.3).

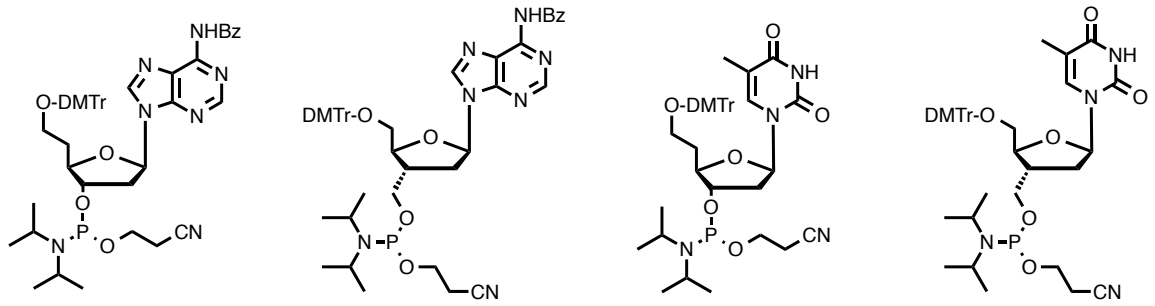

Figure 3.3: 2'-dA and 2'-dT were modified to afford extensions at the 3' and 5'-carbons, as well as functionalized to be used for solid phase DNA synthesis.

Given the numerous factors at play in DNA hybridization, it will be interesting to see if the addition of a carbon atom (per substituted residue) to the backbone will result in the formation of a new type of duplex. With increased spacing it could be inferred that the ability of the base pairs to stack will be compromised, but this could also lead to less charge-charge interaction between phosphate groups, as well as locally expanded major and minor grooves. Another potential result could be a change to the DNA's turn length, which stands at 10 base pairs per turn for B-form DNA.

In order to answer these questions, the family of molecules shown in Figure 3.3 will be synthesized. Of particular relevance to this research are the synthetic efforts towards the 6'-extended deoxyadenosine nucleoside ("6'-dA" – left-most molecule in Figure 3.3), which are highlighted in great detail below. These nucleoside phosphoramidites will then be inserted into ssDNA and paired against native complements, as well as complements containing additional extended 6'- and 3'-nucleosides. Finally, melting points for each duplex will be obtained in order to see if the backbone elongation results in any change in stability.

3.1.2 Previous Efforts Towards Extended Nucleosides

Though relatively sparse, there have been multiple reported syntheses of extended deoxyribonucleosides. Langen and associates are credited with the earliest synthesis of 6'-deoxythymidine, proceeding through a 5'-cyano moiety which was ultimately reduced to the desired product (Scheme 3.1).[11] However, reaction yields were poor and no spectral data was reported. Additionally, studies never proceeded past the synthetic phase.

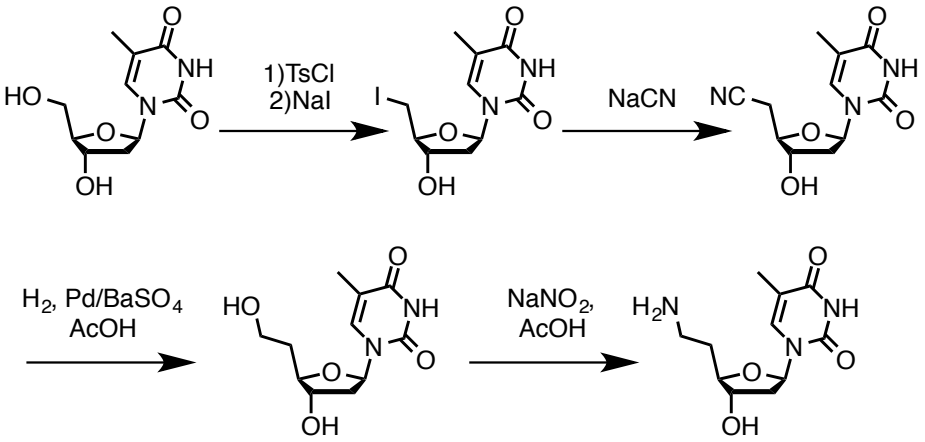

Scheme 3.1: Synthetic efforts towards 6'-dT by Langen et al.

More recently, Pederson and colleagues completed the dual syntheses of the extended 6'-deoxythymidine and 3'-deoxythymideine molecules.[12,13] The former involved key oxidation/Wittig and hydroboration steps, affording the free 6'-hydroxyl group (Scheme 3.2 - Top).

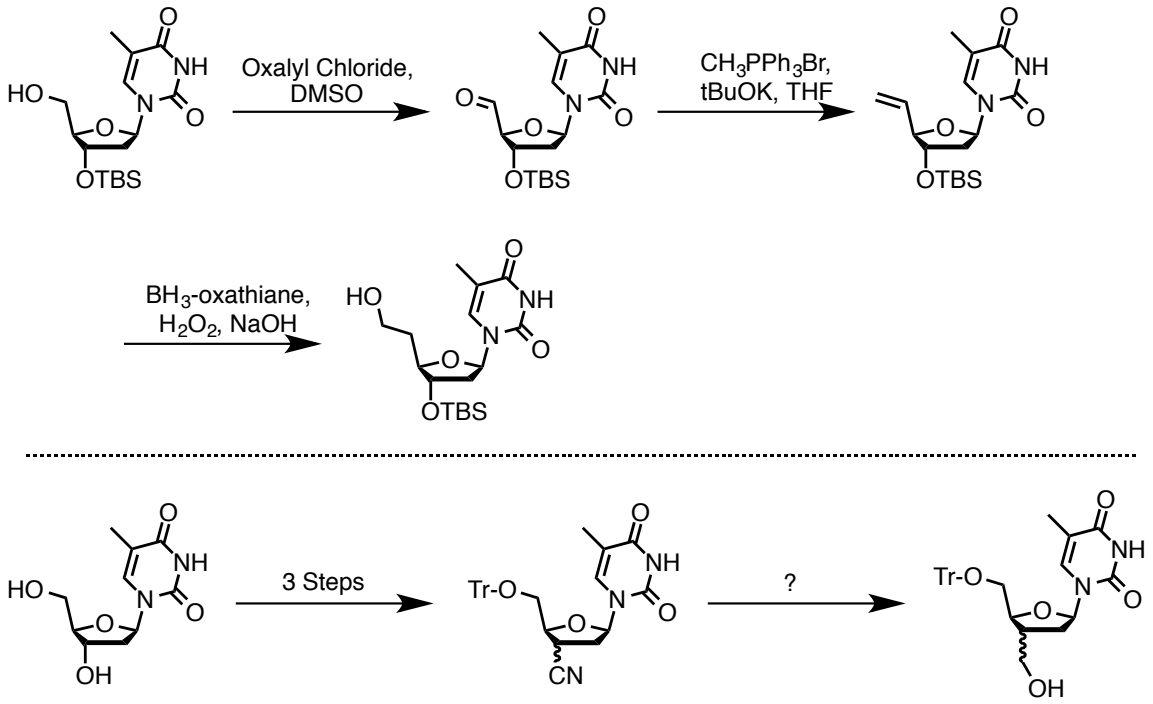

Scheme 3.2: Highlighting the key steps towards extended 6'- and 3'-dT performed by Pederson et al.

Synthesis of the 3'-extended deoxythymidine molecule, however, encountered multiple problems (Scheme 3.2 – Bottom). Displacement of the protected 3'-hydroxyl moiety by a cyano-nucleophile couldn't possibly have maintained any sort of stereospecificity about the 3'-carbon, and it's more than likely there was a racemic mixture present. Continuing, protocol for the reduction to the hydroxymethyl species was not presented in any detail, and the reference cited did not contain any sort of methodology either. It's entirely possible that the expected product was never actually created.

The only known synthesis of a derivatized (2*R*,3*S*,5*R*)-5-(6-amino-9*H*-purin-9-yl)-2-(2-hydroxyethyl)tetrahydrofuran-3-ol ("6'-deoxyadenosine" or "6'-dA") molecule was put forward by Hecht and associates, and follows a pathway starting

with a protected α-D-allofuranose sugar. Subsequent key steps include a coupling reaction by a protected adenine base and deoxygenation via Barton-McCombie protocol, ultimately yielding the protected 6'-deoxyadenosine derivative (Scheme 3.3).

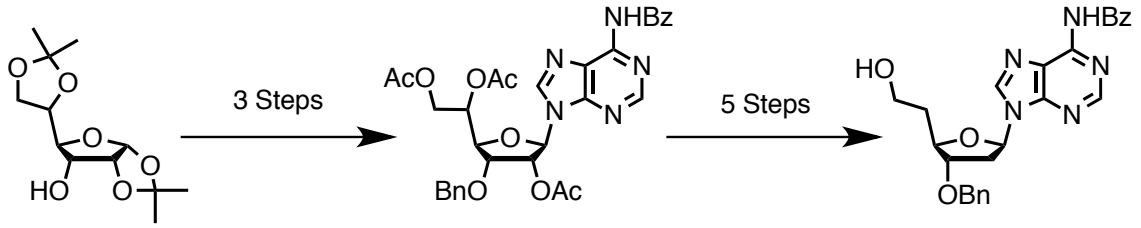

Scheme 3.3: Synthetic efforts towards a 6'-dA nucleoside by Hecht et al.

The main drawbacks of this pathway involve purification and believability. According to the methods, flash chromatography is required after every step, increasing the efforts necessary to obtain purified intermediates. To that end, given the high yields presented, it's fair to wonder if an aggregate of product and recovered starting material was reported for each stepwise yield.

Finally, the coupling between the protected sugar and a bis-TMS-N6-benzoyladenine was supposedly achieved in a 71% yield despite the possibility of N7/N9 coupling products in potential α- and β-conformations. Having performed similar chemistry in the past, only the presence of a 2,2,3,3-tetramethylsuccinamide protecting group (see section 3.4) on the N6-amine moiety resulted in the desired coupling fidelity. For these reasons, it is believed a more facile chemical approach is possible.

3.2 Our Synthetic Approaches for Extended Deoxythymidine Derivatives

Dr. Christopher Theile enhanced the work performed by Pederson and associates by using Dess-Martin protocol to oxidize the 5'-hydroxyl group, and also achieved greater success in generating the 6'-OH through use of 9-BBN. Compared to the Swern oxidation and use of BH_3 preferred by Pederson during these two key steps, Dr. Theile was able to enhance the respective yields by 18% and 25% (Scheme 3.4).

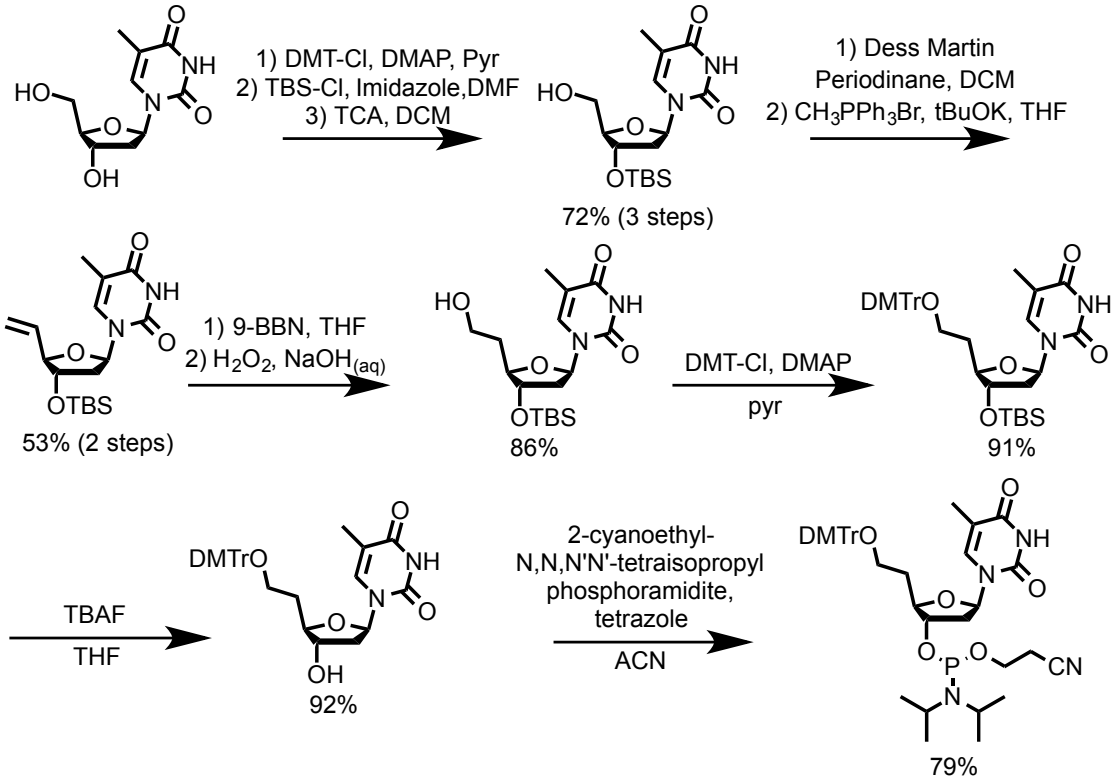

Scheme 3.4: A more efficient synthesis of the 6'-dT phosphoramidite. Work done by Dr. Christopher Theile.

More recently, Dr. Rajat Das has been able to achieve a stereoselective extension of deoxythymidine by adding a methylene group between the 3'-carbon

and 3'-hydroxyl. This is once again an improvement on Pederson's work, as his pathway undoubtedly yielded a racemic mixture on the 3'-carbon, versus Dr. Das' *S*-selectivity (Scheme 3.5).

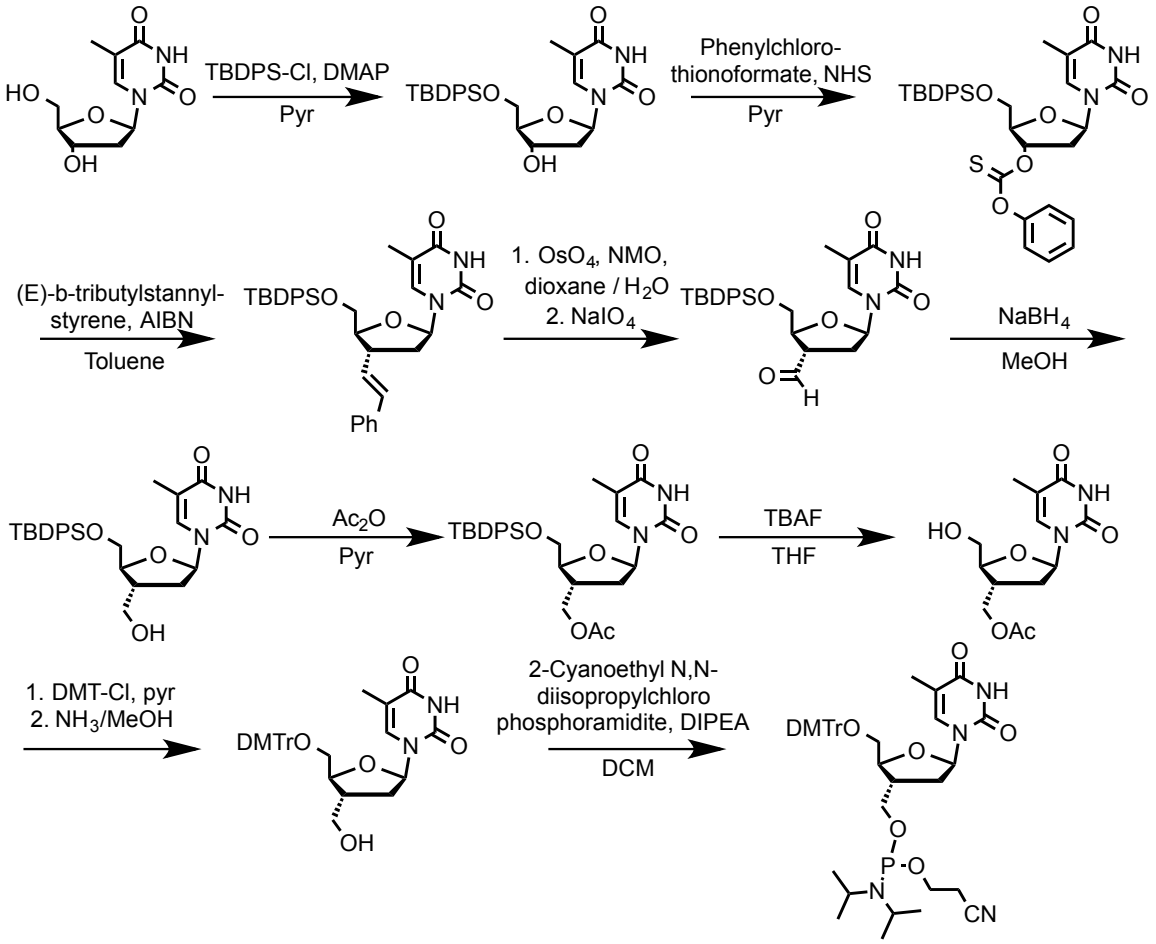

Scheme 3.5: Synthesis of an extended 3'-dT phosphoramidite. Work performed by Dr. Rajat Das.

Dr. Das' pathway utilized a key series of steps where he installed a styrene moiety onto the 3'-carbon, which was then converted to an aldehyde and subsequently reduced to yield the extended hydroxyl group. Subsequent protection/deprotection chemistry was followed by phosphitylation, providing the solid-phase synthetically accessible phosphoramidite.

3.3 Initial Efforts Towards a 6'-deoxyadenosine Phosphoramidite

Preliminary trials for generating the extended 6'-deoxyadenosine molecule sought to mimic the protocol used for synthesis of the 6'-deoxythymidine nucleoside phosphoramidite. Benzoylation of the exocyclic amino group was followed by protection/deprotection chemistry, affording the silylated compound **3** (Scheme 3.6). A Dess-Martin oxidation provided the crude 5'-aldehyde, which was immediately subjected to Wittig conditions yielding the olefin-containing intermediate **4**.

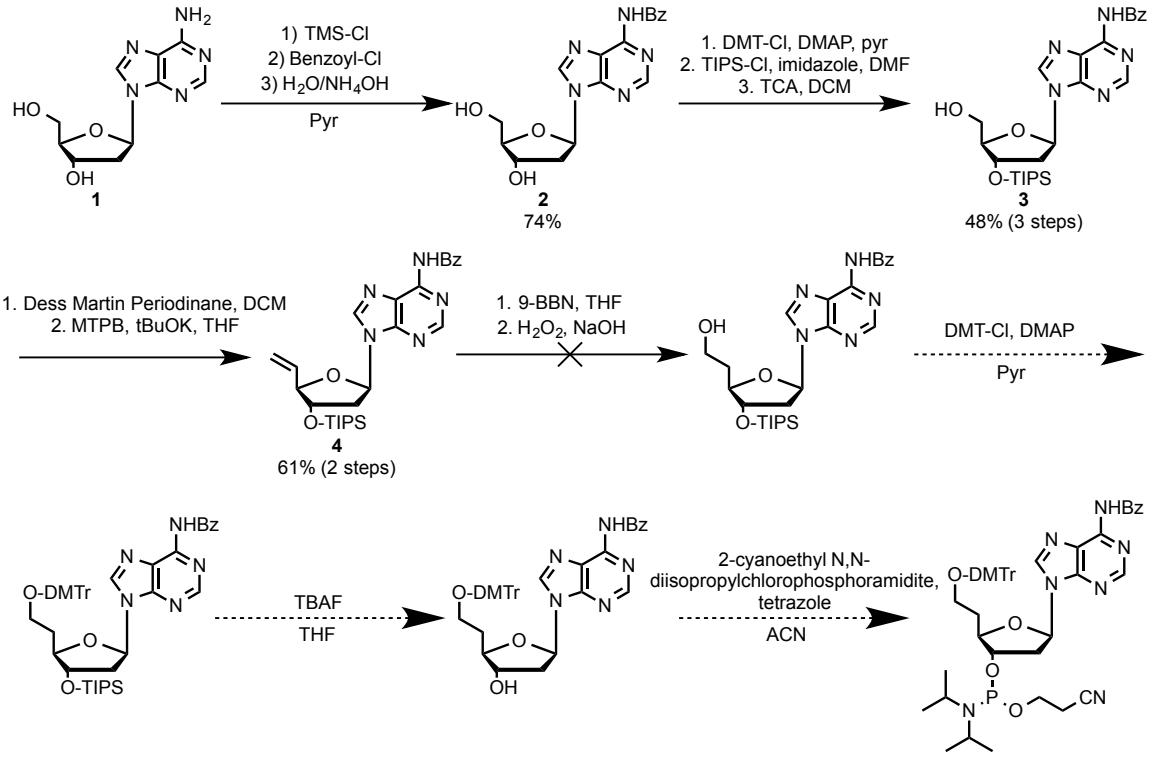

Scheme 3.6: The initial synthetic scheme towards the 6'-deoxyadenosine phosphoramidite.

Unfortunately, the subsequent hydroboration and attempted installation of the 6'-hydroxyl group did not generate the desired product. 9-BBN was utilized as

the initial hydroboration agent, and alternatively borane dimethyl sulfide was tested as well. The reactions were also run with increasing equivalents of reagent and at varying temperatures. None of these conditions proved to be acceptable means of conversion.

It was theorized that the benzoyl moiety might have been reacting or coordinating with the hydroboration agent, so on the next set of trials it was cleaved with ammonium hydroxide to afford the free amine in the 6-position. Ensuing hydroboration and attempts at installation of the 6'-OH nevertheless proved to be fruitless. After numerous failing attempts, it was determined this route was not worth pursuing.

3.4 Modifying the Protection Profile on the Adenine Base

The next logical step was to alter the functionality of the nucleobase. As the intermediates containing either an amide bond or free amine proved unreactive, it stood to reason that an alternative design should be pursued. In an effort to diversify this line of reasoning, multiple strategies were enacted.

One method employed the tetramethylsuccinic anhydride (TMSA) protecting/directing group. It had been previously shown that when nucleobases containing free amines were protected with a TMSA moiety, they adequately prevented against any unwanted side reactions during coupling to a modified furanose sugar.[15] Moreover, the TMSA group also directed coupling in such a way

that virtually only the preferred N9-product was achieved. Finally, TMSA was proven to be labile when exposed to ammonia, confirming an ability to be utilized in solid phase DNA synthesis.

Cyclization of 2,2,3,3-tetramethylsuccinonitrile under acidic conditions afforded the TMSA product in a 90%, one-step yield. Since installing the TMSA group involved harsh conditions, direct protection of a nucleoside was eschewed in favor of protecting only the adenine nucleobase. Not all of the protected product was cyclized, so the remainder was refluxed in thionyl chloride to provide the pyrrolidine **8** (Scheme 3.7).

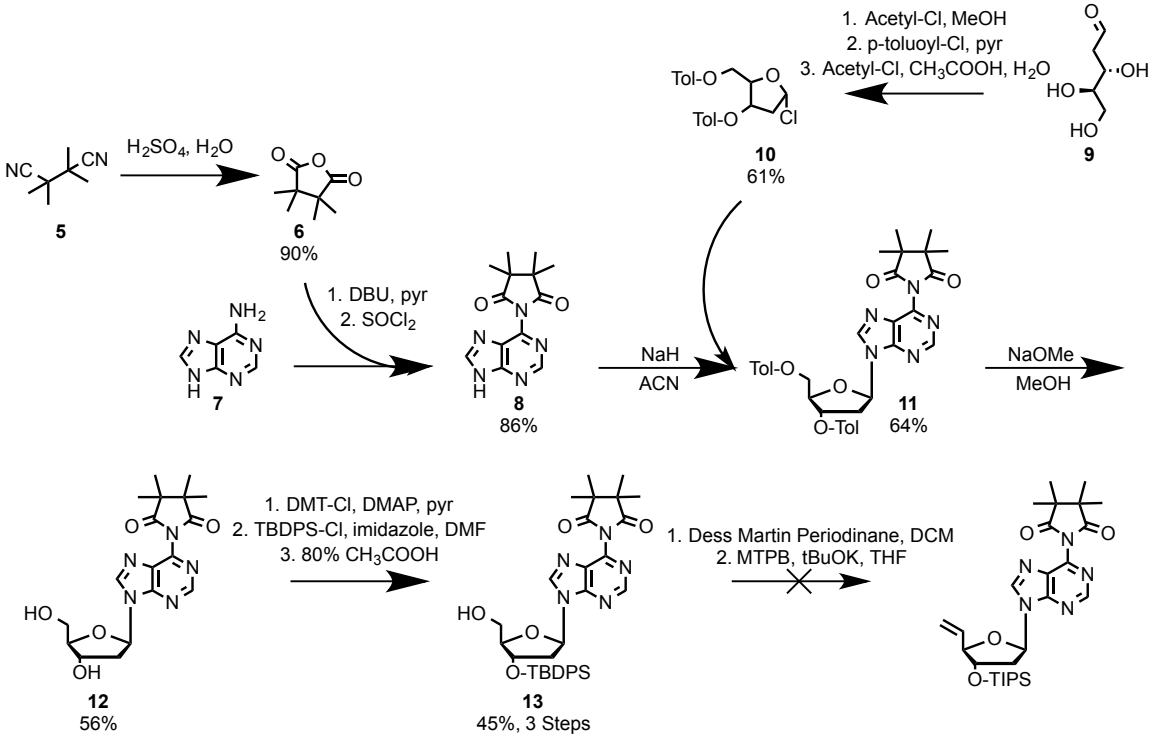

Scheme 3.7: Attempted synthesis of a TMSA-protected 6'-dA nucleoside.

In order to form the coupling product, a bis-toluoyl 2'-deoxyribose sugar containing an α-chlorine in the 1'-position was synthesized with a 61% yield over three steps (compound **10**).[16] When combined with the protected base **8**, the desired β, N9-nucleoside was obtained in a 64% yield. Subsequent deprotection of the toluoyl groups afforded the TMSA-protected analogue to the previously shown benzoylated compound **2**.

Further protection/deprotection chemistry afforded the 3'-silylated compound **13** in a 45% yield over three steps. Regrettably, the TMSA pathway was rendered unusable following the Dess-Martin oxidation when the subsequent Wittig reaction failed, presumably because unreacted potassium tert-butoxide deprotected the TMSA moiety. As it was previously mentioned that amine-containing nucleosides could not be directly TMSA-protected, there was no way to attempt consequent hydroboration chemistry.

Another strategy employed was the use of the N,N-dimethylformamide dimethyl acetal (DMFDMA) protecting group (Scheme 3.8). This is the same protection often used with commercially available 2'-deoxyguanosine phosphoramidites, suggesting it could be utilized on the 6'-dA substrate as well. The resultant imine functionality also presented another test study for the accessibility of hydroboration and hydroxyl installation.

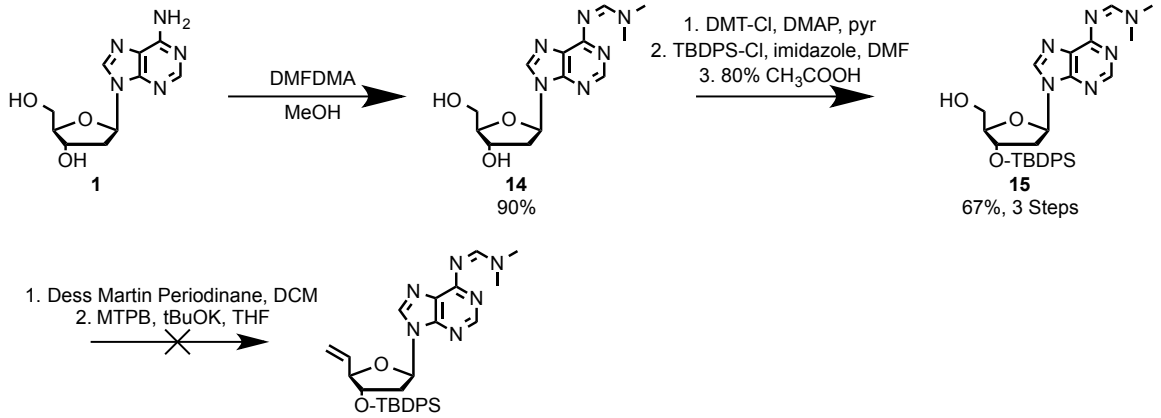

Scheme 3.8: Initial steps of the attempted synthesis of 6'-dA using the DMFDMA protecting group.

Direct DMFDMA addition to 2'-deoxyadenosine proceeded with a quick and efficient yield, resulting in the protected imine **14**. Following the standard three-step protection/deprotection chemistry, the silylated compound **15** was obtained and then subjected to the consecutive Dess-Martin and Wittig reactions. Once again the desired product failed to form, as it was shown that the DMFDMA group was cleaved and the olefin wasn't produced. At this point enough empirical evidence existed to suggest the presence of any type of amine (protected or not) was essentially poisoning the reaction pathway.

3.5 A Bottom-Up Approach Utilizing a 6-chloropurine Nucleobase

Given the results shown above, it was determined that the next iteration of reactions should exclude the exocyclic amine until after the 6'-hydroxyl moiety was installed. As such, a less reactive functional group in the 6-position was desired. To achieve this goal, commercially available 6-chloropurine was utilized in a "bottom

up" approach similar to that of the TMSA-protected adenine base shown previously (Scheme 3.9).

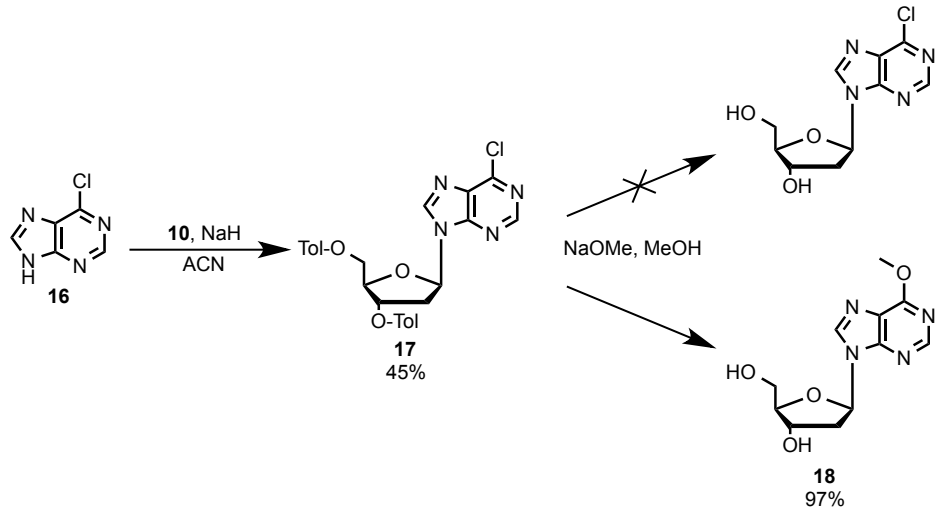

Scheme 3.9: Toluoyl deprotection of chloropurine nucleoside unexpectedly resulted in displacement and installation of a methoxy group. Work performed with Dr. Christopher Theile.

Coupling of the chloropurine nucleobase proceeded with a lower yield than shown with TMSA-protected adenine, affording the N9-product **17** in a 45% yield. This is due to the lack of steric bulk possessed by the chlorine atom, allowing for an additional 35% yield of the undesired N7-coupled nucleoside due to a lack of "directing" ability. Fortunately, these two isomers were easily separated via flash chromatography.

Toluoyl groups were next cleaved in the same manner as previously described, but instead of yielding the unprotected chloropurine nucleoside, nuclear magnetic resonance studies verified the presence of a methoxy group at the 6-position of the base. This was an unintended byproduct of using sodium methoxide (NaOMe) as the deprotecting nucleophile, and actions were taken to rectify the loss

of the chlorine atom. Reactions, both at 25 °C and elevated temperatures, using alternative nucleophiles were attempted in collaboration with Dr. Christopher Theile, but these resulted in either no toluoyl deprotection (sodium hydroxide) or the same methoxy installation (ammonia in methanol). Alteration of the NaOMe reactions (including reduced temperatures and limiting equivalents of reagent) also showed no specificity for toluoyl cleavage versus chlorine displacement.

Regardless of the intent, having the methoxy functionality did not derail subsequent planned reactions (Scheme 3.10). Protection/deprotection chemistry provided the silylated compound **19**, and oxidation and olefination afforded the alkene **20** in a 59% two-step yield. Most importantly, hydroboration with 9-BBN and ensuing hydroxyl installation proceeded as planned, providing the backbone-extended demi-product **21**.

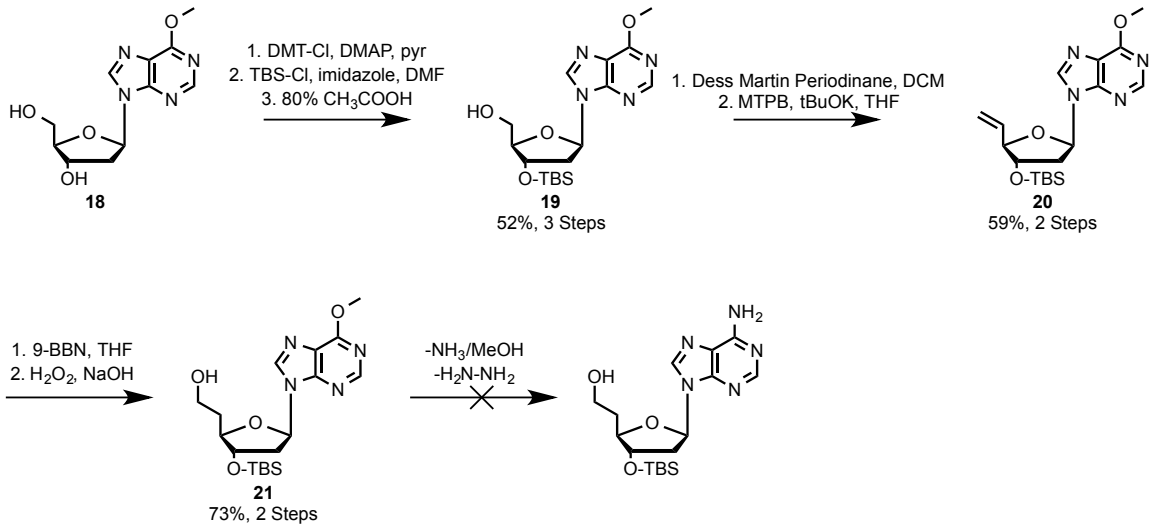

Scheme 3.10: Successful hydroboration and addition of a 6'-hydroxyl group to the protected methoxy-containing nucleoside.

Sadly, ensuing attempts to introduce the amine moiety via nucleophilic displacement were unsuccessful. Both ammonia in methanol and hydrazine proved unable to displace the methoxy group, including at increased temperatures as well as in a pressure vessel. As such, the 6-chloropurine pathway was abandoned and it was determined that efforts should focus on regulating controllable factors outside of nucleobase modification.

3.6 Synthetic Attempts Involving Alternative Wittig Reagents

Thus far the efforts described have shown that success of the hydroboration reaction and the presence of the exocyclic amino group (protected or not) in the 6-position are mutually exclusive concepts. The lone trial where hydroboration and hydroxyl installation were effective exploited the absence of the amino functionality, but subsequent downstream displacement attempts were rendered fruitless. Because of these facts, it was determined that creation of the 6'-OH should be achieved in a different fashion, preferably one which is performed on a protected 2'-deoxyadenosine molecule.

One of the key steps in each pathway shown above is the Wittig reaction, which both adds a 6'-carbon and olefinates the 5'-6' carbon-carbon bond. The Wittig reactions described in previous schemes employed the methyltriphenylphosphonium bromide (MTPB) reagent as a means of alkenation, "simply" replacing the oxygen atom of the terminal aldehyde (the Dess-Martin

intermediate) with a carbon. However, it's also possible to use more elegant Wittig reagents in place of MTPB, thereby allowing for the ability to functionalize the intermediate compound even further.

One such commercially available Wittig reagent is (methoxymethyl)triphenylphosphonium chloride (MOMTPC). Unlike MTPB, the MOMTPC reagent not only installs the 6'-carbon atom, but also a methylated 6'-hydroxyl group as well. Following Dess-Martin oxidation, this methodology was employed to gain compound **22** with a 60% yield over two steps (Scheme 3.11).

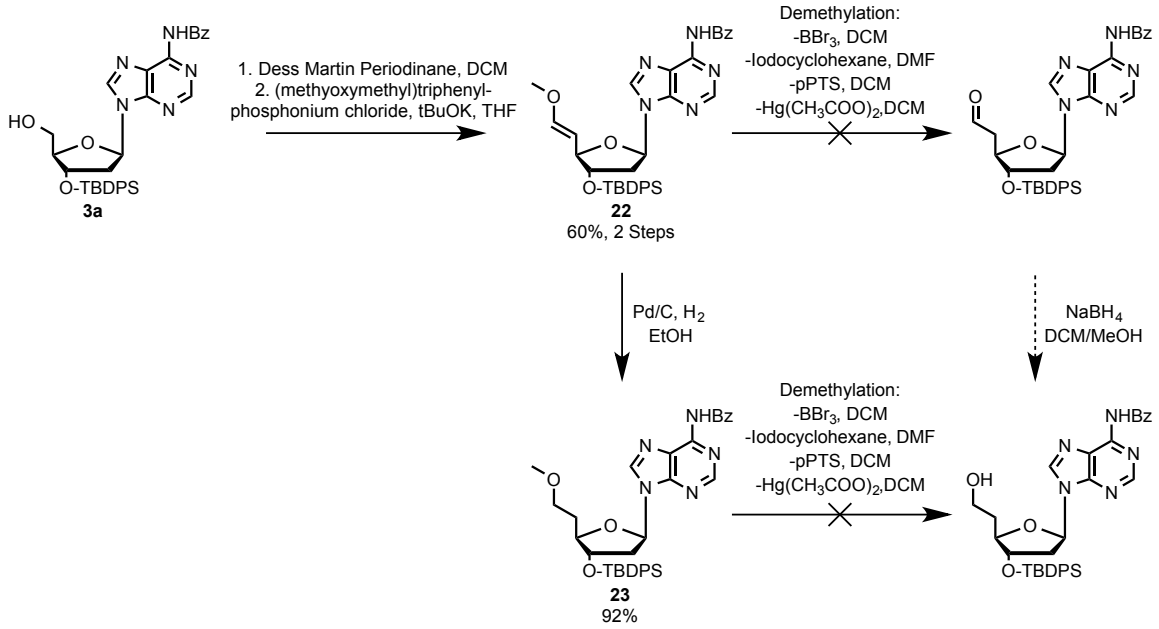

Scheme 3.11: Addition of a functionalized 6'-OH and attempts towards demethylation.

Subsequent demethylation of the 6'-hydroxyl moiety would afford the tautomerized terminal aldehyde, which could then be reduced using sodium borohydride. However, despite numerous attempts, the various reagents used

resulted in either decomposition/depurination (boron tribromide, iodocyclohexane and pyridinium *p*-toluenesulfonate) or no reaction (mercuric acetate).[17, 18] These procedures were replicated on the reduced alkane **22** (achieved via hydrogenation), but the results were no different.

Since purine nucleosides are susceptible to decomposition when subjected to acidic conditions or temperatures greater than 80 °C, it was decided that a protecting group which could be labilized under milder conditions would be preferable. As no such Wittig reagent was commercially available (at a non-prohibitive cost, at least), it became necessary to synthesize one. A simple reaction of triphenylphosphine with benzyl chloromethyl ether accomplished just that, providing the benzyloxy-Wittig reagent **24** in a substantive yield (Scheme 3.12).[19]

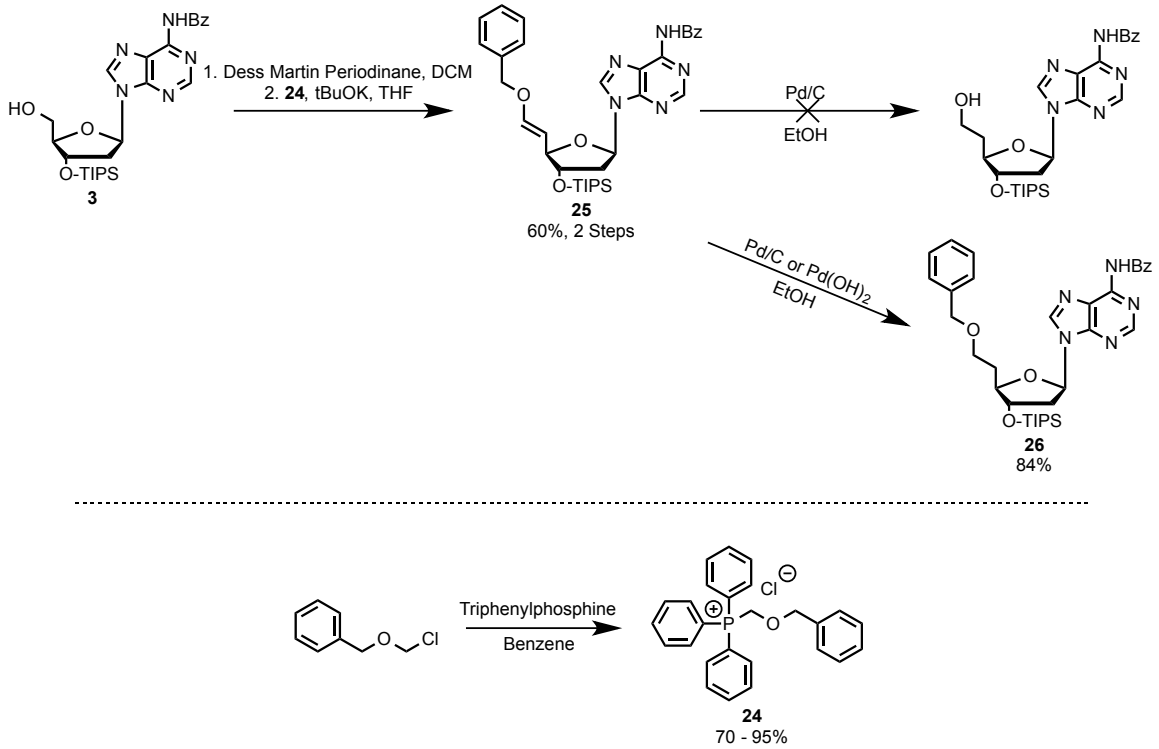

Scheme 3.12: Synthesis of a benzyl-protected Wittig reagent and consequent efforts towards the 6'-dA nucleoside.

Following application of the Dess-Martin periodinane, Wittig reagent **24** was used to create the benzyl-protected alkene **25**. Conveniently enough benzyl moieties can be removed via hydrogenation conditions, which should simultaneously reduce the 5'-6' carbon-carbon double bond as well, effectively killing two birds with one synthetic stone. However, when subjected to multiple activated palladium reagents the benzyl group remained intact, despite reduction of the double bond.

Multiple examples of benzyl groups being cleaved from adenosine analogues exist in literature, and in each instance the amine on the adenine base was unprotected.[20, 21] This methodology was going to be attempted with compound **25**,

but for an unknown reason the benzyl-Wittig reaction wasn't able to be replicated again, despite exhaustive efforts. With an absence of the benzylated alkene, no further attempts were able to be made.

3.7 A 2'-deoxyinosine Conversion Methodology

3.7.1 Previous Efforts with a 2'-deoxyinosine Conversion Pathway

With other avenues failing, Dr. Christopher Theile attempted another method towards "masking" the effect of the exocyclic amine, this time via a 2'-deoxyinosine conversion (Scheme 3.13). The premise was similar to that of the previously seen "methoxy" scheme (section 3.5), where successful hydroboration chemistry was performed on a purine nucleoside that didn't contain any sort of amine functionality.

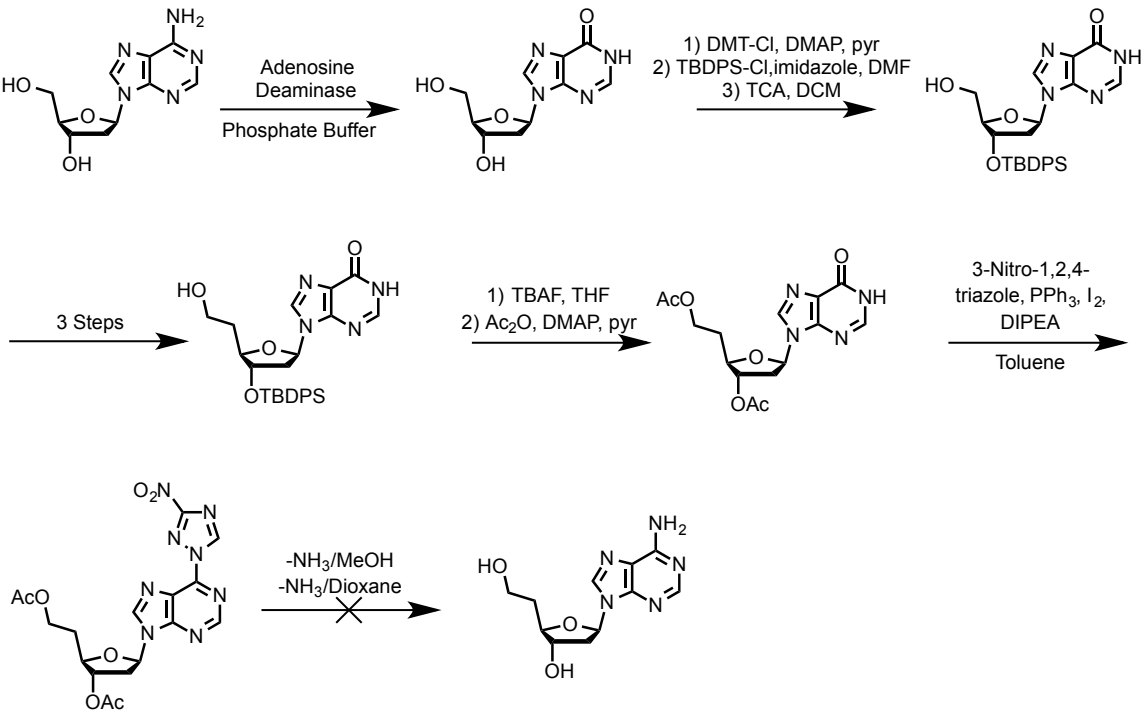

Scheme 3.13: An attempted synthesis of 6'-dA using through temporary elimination of the amino moiety in the 6-position. Work performed by Dr. Christopher Theile.

Synthesis began with an enzymatic conversion of 2'-deoxyadenosine to 2'-deoxyinosine, at which point the protection/deprotection chemistry shown previously was performed to afford the Dess-Martin precursor. Oxidation, olefination and installation of the 6'-hydroxyl were then successfully performed, followed by desilylation and per-acylation. At this point a nitro-triazole leaving group was utilized to displace the O6 moiety and afford a good leaving group for nucleophilic displacement. Lamentably, the ammonia reagents used weren't strong enough to remove the nitro-triazole moiety, and it was determined a more labile group was needed.

3.7.2 Modifications to the 2'-deoxyinosine Conversion

Continuing the work of Dr. Theile, additional means of amine installation were attempted by way of altering the leaving group at the 6-position on the nucleobase. However, as the acylated 6'-deoxyinosine intermediate was only possessed in limited quantity, tests were performed on a commercially available inosine analogue (Scheme 3.14).

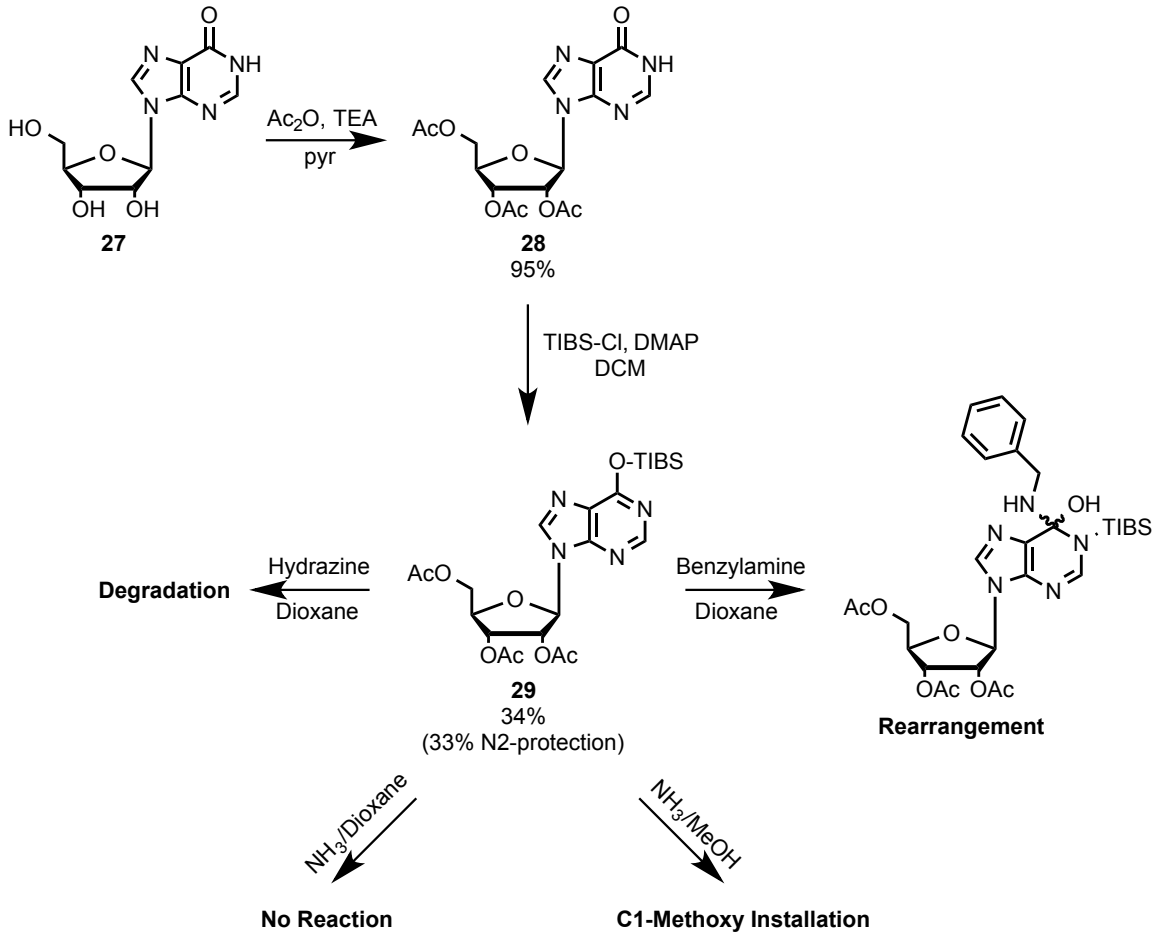

Scheme 3.14: Multiple attempts using a TIBS-protected, per-acylated inosine failed to result in a desired conversion to the corresponding adenosine analogue.

Per-acylation yielded the protected intermediate **28**, followed by addition of the 2,4,6-triisopropylbenzenesulfonyl chloride (TIBS) protecting group. The O6-protected isomer was achieved in a 34% yielded and separated from the undesired N2-protected side-product. As TIBS-protected oxygen atoms on pyrimidine nucleosides have previously been shown to act as leaving groups in the presence of a nucleophile, it was surmised the same could be done with purines.[22]

The first displacement attempt utilized re-distilled benzylamine as a nucleophile.[22] Similar to the plan for the benzylic oxygen atoms shown before (section 3.6), the thought was upon addition, the benzyl functionality could be cleaved using hydrogenation conditions. However, despite multiple, varying conditions (changes include benzylamine concentration and dilution of the starting material), the only product achieved was that of an intramolecular rearrangement.

When other reagents were used, the desired product still remained unachieved. Depending on the reaction conditions, results ranged from installation of a methylated oxygen (NH_3/MeOH) to degradation (hydrazine) to simply no reaction (NH_3/dioxane).[23] Once again, it was determined other possibilities needed to be explored.

Along those lines, Verdine and associates had established the concept of "convertible nucleosides."[24] These were essentially defined as nucleoside phosphoramidites that could be incorporated into RNA, and modified *after* the solid

phase synthetic process. This was done by virtue of having a *p*-chlorophenol leaving group on the nucleobase, which could be displaced as necessary.

While Verdine performed his modifications on an entire ssRNA oligomer, this was viewed as an untenable option for our efforts, as the efficacy of the conversion wouldn't be determined until a mass of the pure ssDNA was obtained. Therefore, analogous chemistry was performed directly on the TIBS-protected inosine nucleoside **29** in order to explore the potential reactivity (Scheme 3.15).

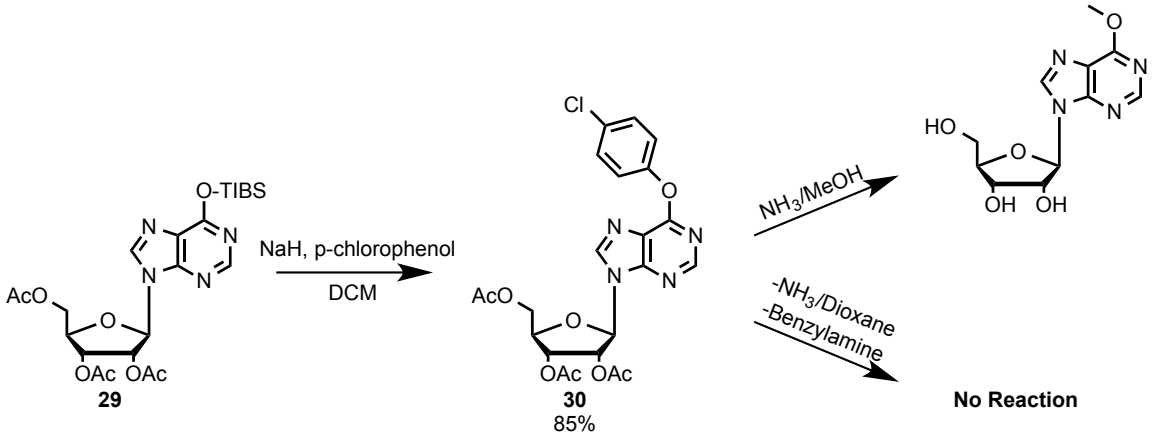

Scheme 3.15: Attempts to obtain an adenosine analogue using "convertible nucleoside" chemistry.

TIBS-displacement using *p*-chlorophenol provided the intermediate **30** in an 85% yield, but the downstream conversion attempts proved unsuccessful. Conditions involving NH_3/MeOH as the nucleophile resulted in the all-too-familiar methoxy displacement, and neither NH_3/dioxane nor benzylamine resulted in any kind of reaction. At this point it was decided that the inosine conversion methodology was unlikely to ultimately achieve the desired results.

3.8 A Dihydroxylation/Deoxygenation Scheme Affords 6'-deoxyadenosine

As sections 3.3 – 3.7 have now shown, synthesis of the 6'-deoxyadenosine nucleoside was resistant to chemistry that worked for 6'-deoxythymidine, as well as to a series of more elaborate pathways. The key step of delivering the 6'-hydroxyl entity only worked with intermediates that didn't contain an amino (protected or not) functionality on the nucleobase, and on said molecules the conversion back to a deoxyadenosine analogue proved unachievable. Ultimately, it appeared as though an alternative means of hydroxyl installation was necessitated, and that it should take place on an amine-containing nucleoside.

During synthesis of his cyclic deoxyadenosine compounds, Dr. Han Yueh in our lab used an aqueous osmium (VIII) tetroxide solution in order to install vicinal hydroxyl moieties on the olefin **4**. Though the newly created 5'-OH would eventually need to be eliminated, the framework for a new pathway was now in place (Scheme 3.16).

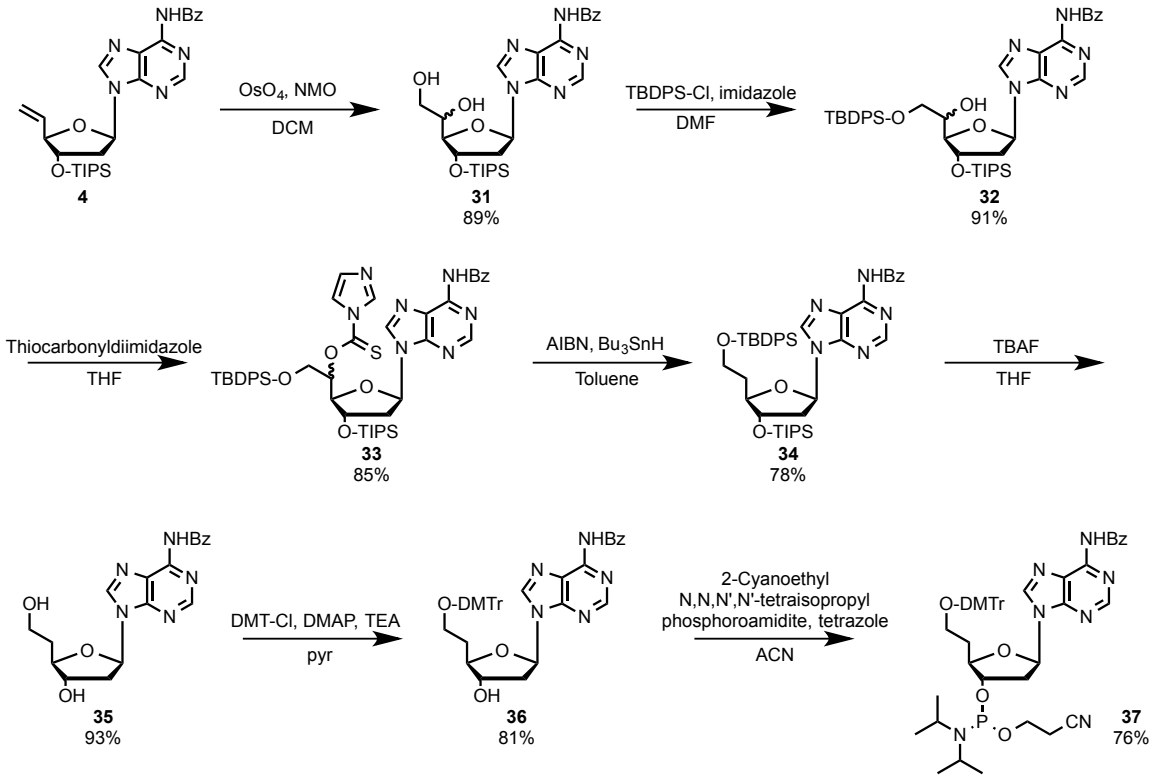

Scheme 3.16: A new synthetic pathway involving dihydroxylation and deoxygenation key steps yielded the desired 6'-dA phosphoramidite.

The diol-installation was achieved in an 89% yield to afford intermediate **31** in a racemic mixture, due to the stereocenter at the 5'-carbon. The 6'-hydroxyl was then silylated, and thiocarbonyldiimidazole was used to turn the 5'-oxygen into a leaving group for completion of the Barton-McCombie deoxygenation process. Radicalization then resulted in elimination of the protected 5'-hydroxyl to afford the bis-silylated 6'-deoxyadenosine analogue **34** in a 78% yield.

Tetrabutylammonium fluoride was next used to desilylate both the 3' and 6'-hydroxyl groups, at which point the 6'-OH was selectively protected with DMT-Cl. Phosphitylation then yielded the desired phosphoramidite **37** in a 76% yield. At long last, the target molecule was achieved and ready for solid phase DNA synthesis.

3.9 DNA Studies

3.9.1 Incorporation of Extended Nucleosides into DNA

With the extended 6'-dA phosphoramidite **37** in hand, along with the complementary 6'-dT phosphoramidite (synthesized using Dr. Theile's method detailed in section 3.2) and extended 3'-dT phosphoramidite (synthesized by Dr. Das, shown in section 3.2), efforts towards incorporation into ssDNA were undertaken. The sequences utilized resembled the expansively studied Dickerson dodecamer (5'-d[CGCGAATTCGCG]-3'), maintaining the internal "d(GAATTC)" core. Modifications were made to the termini, where dC and dG residues were re-ordered in order to nullify any self-complementarity or potential hairpin formation, thereby necessitating the synthesis of two unique strands. Upon substitution of the extended nucleosides, a family of eight distinct strands was created (Table 3.1).

Strand Name	Strand Sequence	Calculated Mass (Da)	Experimental Mass (Da)
G-Control	5'-d(GGCGAATTCCGG)-3'	3685.5	3691.4
C-Control	5'-d(CCGGAATTCGCC)-3'	3606.4	3612.1
GA_62	5'-d(GGCGA_6A_6TTCCGG)-3'	3713.6	3720.2
CA_62	5'-d(CCGGA_6A_6TTCGCC)-3'	3634.5	3640.3
GT_62	5'-d(GGCGAAT_6T_6CCGG)-3'	3713.6	3721.7
CT_62	5'-d(CCGGAAT_6T_6CGCC)-3'	3634.5	3641.3
GT_32	5'-d(GGCGAAT_3T_3CCGG)-3'	3713.6	3720.0
CT_32	5'-d(CCGGAAT_3T_3CGCC)-3'	3634.5	3641.0

Table 3.1: Names, sequences and masses (obtained via MALDI) of the ssDNA strands utilized. Substituted nucleosides are denoted with a subscript number corresponding to the extension site. The first letter of the strand name indicates which control sequence it mimics, and the terminal number references the total amount of substitutions.

ssDNA was synthesized, purified and quantitated as described in section 3.12.3, at which point it was possible to perform hybridization studies and ascertain the melting temperatures (Tm) of the various DNA duplexes. Duplexes were formed in accordance with complementarity constraints, with every possible match utilized. Subsequent temperature studies (described in section 3.12.3) resulted in a series of Tm values for the duplexes tested.

3.9.2 Tm Determinations of Duplexes Containing 6'-nucleosides

The standard for these studies was the annealing of the thermally denatured G-Control and C-Control sequences in the specified hybridization buffer (20 mM phosphate, 100 mM NaCl, pH = 7; all thermal data reflect these conditions unless otherwise noted). As can be discerned from the melting curve, this duplex was found to possess a Tm value of 53 °C, a temperature which shall be denoted as the standard and subsequent point of comparison (Figure 3.4).

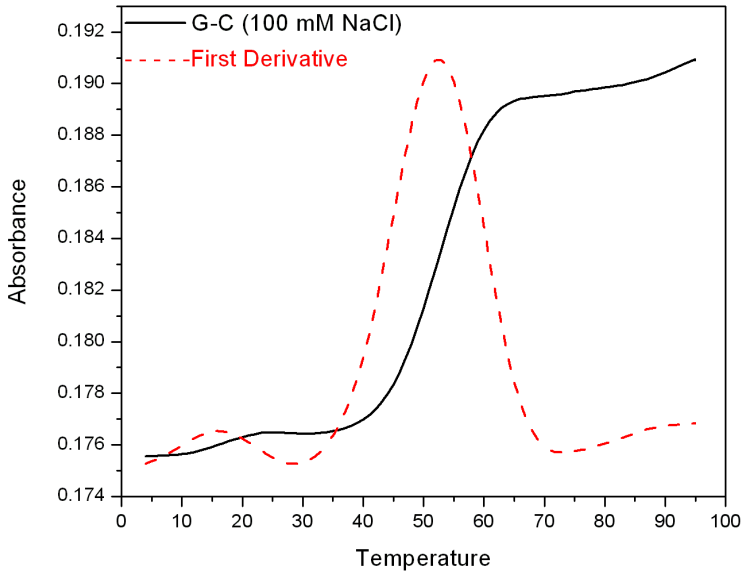

Figure 3.4: Melting curve of the control duplex (solid black line) in terms of absorbance versus temperature (°C), as well as the first derivative calculations (red dashed line).

Next, the sequences containing the 6'-extended substitutions (GA_62, CA_62, GT_62 and CT_62) were analyzed. First, they were paired with the control sequences to determine if any decrease in stability would be brought about by the addition of the extra carbon atom (per nucleoside) to only one half of the duplex. As can be seen in the melting curves, this was indeed the case. The duplexes containing the 6'-deoxyadenosine substitutions presented Tm values of 49 °C, while the duplexes including the 6'-deoxythymidine nucleosides dropped to even lower Tm values of 44 °C (Figure 3.5).

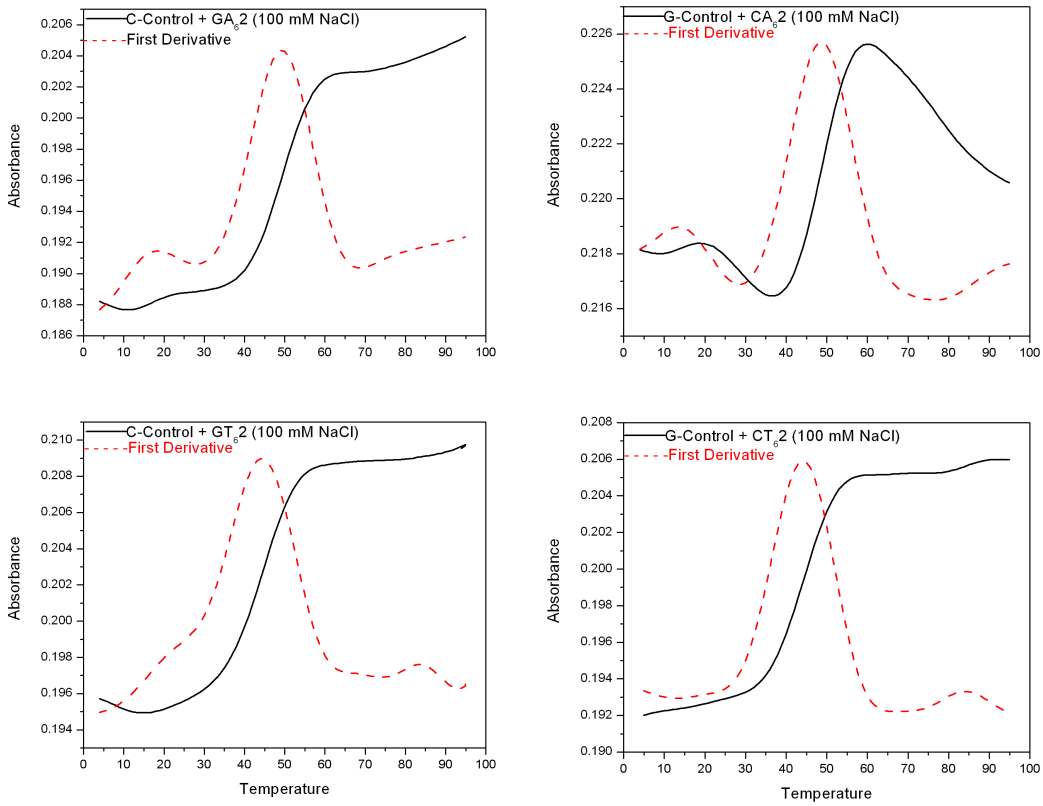

Figure 3.5: Melting curves of the duplexes formed when ssDNA containing 6'-substitutions was paired with the control sequences (sequences utilized shown in the legend).

This destabilization intensified when ssDNA containing extended nucleosides were annealed with similarly-substituted, complementary ssDNA. In these cases, duplexed DNA wasn't achieved unless hybridization conditions involved a concentration of sodium chloride equal to 1 M. The duplexes created from pairing GA_62 with CA_62 and GT_62 with CT_62 correlated to Tm values of 52 °C and 44 °C respectively, which in turn equated to drop-offs of 7 °C and 15 °C relative to the native control of 59 °C at 1 M salt (Figure 3.6).

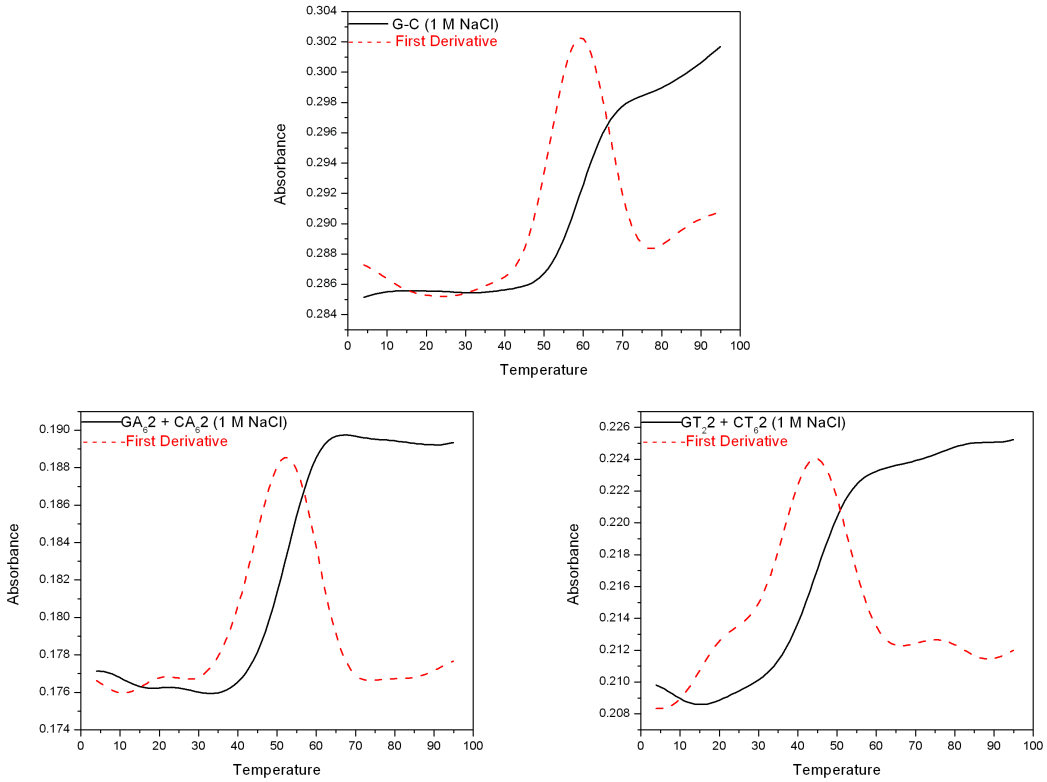

Figure 3.6: 1 M NaCl melting profiles for the control sequence (top), GA_62/CA_62 pair (lower left) and GT_62/CT_62 pair (lower right).

Hybridizing ssDNA containing 6'-deoxyadenosine nucleosides with complementary ssDNA containing 6'-deoxythymidine nucleosides formed the final series of duplexes. These duplexes also didn't achieve complete hybridization at low salt concentration, and in these instances a pseudo two-step denaturation profile was observed. Duplexes formed at a higher salt concentration were also found to melt at lower temperatures than the control (Figure 3.7).

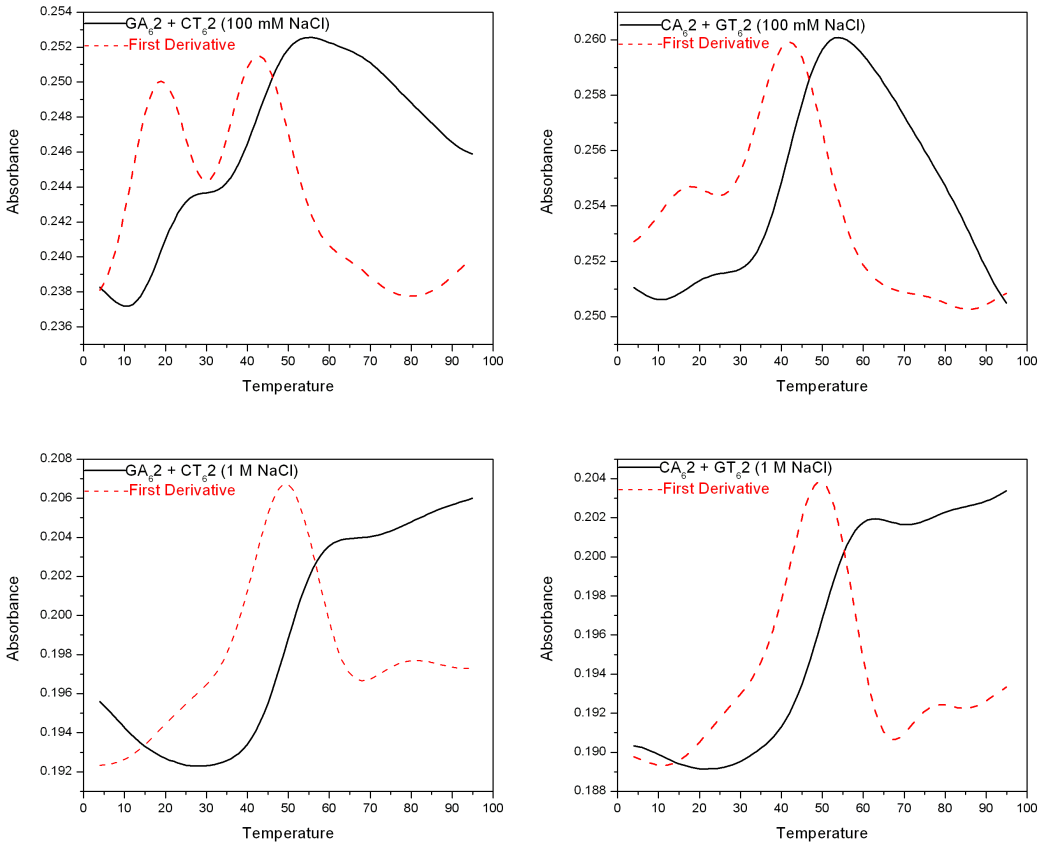

Figure 3.7: Melting curves of duplexes containing both extended 6'-dA and 6'-dT nucleosides. Sequences and salt concentrations noted in the individual legends.

In the low salt studies, the first transitions occur between approximately 19-20 °C. This is likely suggestive of a fraction of duplexes which were unable to form all twelve base pairs. The next transitions occurred between 42-43 °C, or approximately 10 degrees lower than the control duplex. At higher salt concentration the duplexes were seemingly able to fully form, but Tm values of 49 °C also remain 10 degrees lower than the measured standard. All data was shown to be reversible upon cooling back down to 4 °C.

The hybridization and stability results are summarized below (Table 3.2):

Strand 1	Strand 2	[NaCl]	Tm (± 1 °C)	Delta Tm from Standard (°C)
G-Control	C-Control	100 mM	53	N/A
G-Control	C-Control	1 M	59	N/A
GA_62	C-Control	100 mM	49	4
GA_62	C-Control	1 M	55	4
CA_62	G-Control	100 mM	49	4
CA_62	G-Control	1 M	55	4
GT_62	C-Control	100 mM	44	9
GT_62	C-Control	1 M	52	7
CT_62	G-Control	100 mM	44	9
CT_62	G-Control	1 M	52	7
GA_62	CA_62	100 mM	N/A	N/A
GA_62	CA_62	1 M	52	7
GT_62	CT_62	100 mM	N/A	N/A
GT_62	CT_62	1 M	44	15
GA_62	CT_62	100 mM	19, 43	34, 10
GA_62	CT_62	1 M	49	10
CA_62	GT_62	100 mM	20, 42	33, 11
CA_62	GT_62	1 M	49	10

Table 3.2: A summary of every combination of complementary sequences utilizing 6'-nucleosides, as well as hybridizing conditions and Tm values.

3.9.3 Discussion of Tm Studies for DNA Containing 6'-nucleosides

One major observed trend is the difference in destabilization brought about by 6'-deoxyadeonsine nucleosides relative to their 6'-deoxythymidine complements. Regardless of salt concentration, duplexes containing only the extended purines showed a drop in Tm value equivalent to 2 °C per substitution. For the pyrimidine analogue, that number jumped twofold to approximately 4 °C per replacement.

This can potentially be explained by the relative steric bulk of the adenine base versus the smaller thymine. Due to the bicyclic nature of purine nucleobases, they encompass a larger area within the core of the DNA duplex, stretching past the

midpoint of the space occupied by a hydrogen-bonding pair (Figure 3.8-A). While it's disingenuous to assert that the purine nucleobases impart a greater impact unto duplex stability, their relative bulk could be a key factor in play.

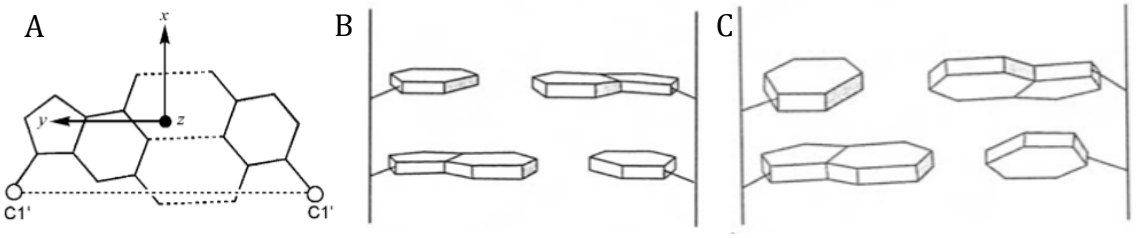

Figure 3.8: A) A top-down view of a purine-pyrimidine base pair within a duplex, B) base-pair stacking when little propeller twist is present, and C) the impact a high propeller twist has on successive base pairs.

Given the extra carbon inserted into the phosphodiester scaffold by the 6'-nucleosides, it's possible that the backbone is kinking and flipping out of position. This could subsequently alter the relative position of the sugar, and therefore the base. Should the nucleobase be removed from its usual position within the duplex, it could result in a higher propeller twist than normal, or disengage from hydrogen bonding altogether (Figure 3.8-B/C).

As purine nucleobases are set deeper into the hydrogen bonding axis, a kink in the backbone could potentially result in a less impactful relative positional shift. Though still not ideal, an offset purine could still possibly afford a greater conservation of the standard conformation, and henceforth a relatively higher amount of preserved base-stacking. While the full truth is likely more complicated, this qualitative observation would seem to mesh with the gathered data.

In terms of the general trend of duplex destabilization, it isn't altogether unsurprising. Apart from the control duplex, no pair of complementary ssDNA shown in Table 3.1 possesses the exact same combination of backbone length and polarity as its partner. As such, the duplex is likely forced to adopt a new, relatively unstable conformation in order to account for these differences (Figure 3.9).

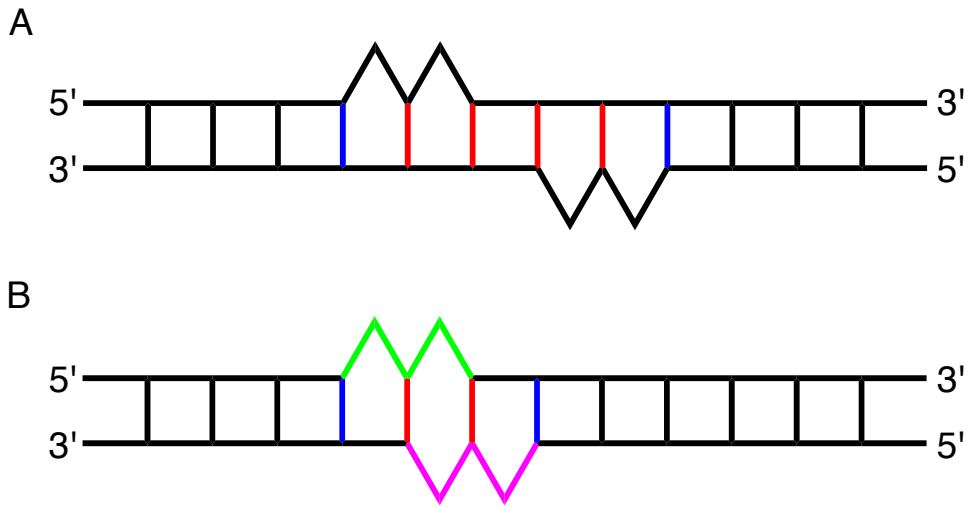

Figure 3.9: A simplified view of duplexes containing 6'-extended nucleosides (triangular bulges) A) opposite natural nucleosides and B) opposite other 6'-extended nucleosides (green = 6'-dA and pink = 6'-dT). Red bonds represent hydrogen bonding pairs involving at least one 6'-nucleoside, and blue bonds signify adjacent base pairs that could be affected as well.

Duplexes that include the extended 6'-nucleosides opposite their native complements present an obstacle for annealing, as the local backbone lengths of the two strands don't align. Should this result in displacement of the nucleobase, a loss of π-π stacking could be realized, as well as an offsetting of the hydrogen bonding pairs (Figure 3.9-A, red and blue bonds). In the duplexing pairs of GA_62/CA_62 and GT_62/CT_62 there are four potential sites for this to occur, and it therefore comes as no surprise that the annealing process failed to proceed at low salt concentration.

Typical base-pairing integrity remains compromised even when the 6'-nucleosides are placed directly opposite one another (GA_62/CT_62 and CA_62/GT_62). Despite the fact that the local backbone lengths are now the same, the difference in strand polarity ensures that pseudo-normal duplex conditions cannot be achieved (Figure 3.9-B). An enhanced view of the region containing "extended" base-pairs helps explain the potential issues caused by this inequity (Figure 3.10).

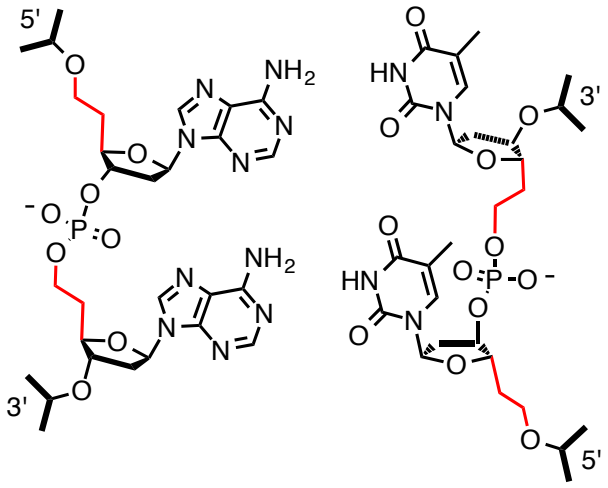

Figure 3.10: A local view of the substituted duplex core, highlighting the extension inequality caused by opposing strand polarities. The red bonds signify the extension sites.

Though each ssDNA contains the same extension, the opposing directionalities render duplex formation challenging, as the bonding pairs are more than likely thrown off their traditional axes. Moreover, given the offset nature of the two ssDNA strands, it's possible that the adjacent base pairs have difficulty forming as well. As such, it comes as little surprise that a reasonable fraction of each duplexing pair melted below 20 °C, implying that the central tract of nucleosides never fully formed. Even at higher salt concentrations, a Tm value of 49 °C means

that, on average, each substituted nucleoside destabilized the duplex by approximately 2.5 °C.

3.9.4 Tm Determinations of Duplexes Containing Both 6'-deoxyadenosine and Extended 3'-deoxythymidine

In order to rectify the continuing issues with strand length/polarity, ssDNA incorporating the extended 3'-deoxythymidine nucleoside (shown in section 3.2) was synthesized. These strands (GT_32 and CT_32) were then paired with complementary sequences containing 6'-deoxyadenosine nucleosides (GA_62 and CA_62) in an effort to create a more uniform local backbone (Figure 3.11).

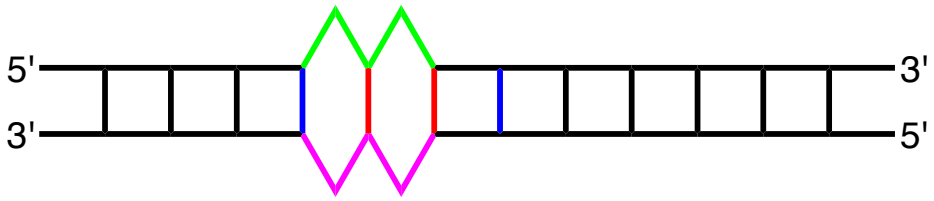

Figure 3.11: A simplified blueprint of a duplex containing 6'-dA nucleosides (green bulges) opposite extended 3'-dT nucleosides (pink bulges). Red bonds represent hydrogen bonding pairs between extended nucleosides, and blue bonds signify adjacent base pairs that could be affected as well.

Upon hybridization, melting curves were obtained and Tm values were determined for the duplexes described above. Similar to before, a destabilizing effect was observed (Figure 3.12).

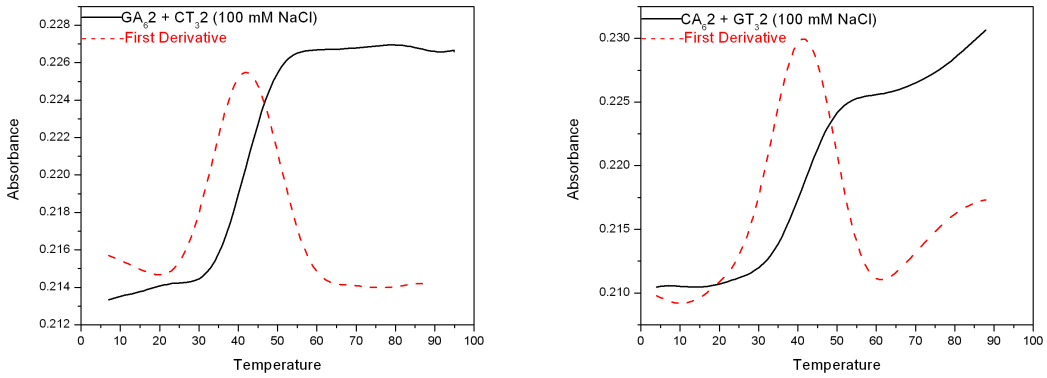

Figure 3.12: Melting curves (100 mM NaCl) for duplexes containing the 6'-dA and extended 3'-dT nucleosides.

Temperature scans were also run at higher salt concentration, with similar relative destabilization effects. The data for this family of duplexes is summarized below (Table 3.3).

Strand 1	Strand 2	[NaCl]	Tm (± 1 °C)	Delta Tm from Standard (°C)
GA62	CT32	100 mM	42	11
GA62	CT32	1 M	49	10
CA62	GT32	100 mM	42	11
CA62	GT32	1 M	48	11

Table 3.3: Summary of the duplex pairs, salt concentrations and Tm values for strands containing 6'-dA and extended 3'-dT nucleosides.

3.9.5 Discussion of Tm Studies for DNA Containing 6'-deoxyadenosine and Extended 3'-deoxythymidine nucleosides

Despite the backbone length/polarity issue being rectified, complementary insertion of the 6'- and extended 3'-nucleosides still produced a destabilizing effect on duplexed DNA. To that point, an average decrease of 11 °C (2.75 °C per substituted nucleoside) to the duplex Tm value was noticed across the four trials.

This aligns with the trends observed with the A_6/T_6 pairs, though it should be noted that the A_6/T_3 duplexes were able to fully form at low salt concentration.

Without a crystallographic interpretation it's impossible to know precisely why the insertion of the additional carbon atoms has a deleterious effect, but potential reasons include loss of base stacking, or a moderate change to the backbone conformation (outward kink versus an even tighter coil). Another potential rationale involved the number of substitutions, as only two of the 12 nucleosides (per strand) possessed the additional carbon atom. These "extended" base pairs are only 20% of the length of B-form DNA's "unit cell" of 10 base-pairs per turn, resulting in an inability to gauge the effects of the extended nucleosides over a full turn-length. As such, future studies should include longer internal tracts of the complementary elongated nucleosides.

3.9.6 Intercalation of the Extended Duplexes

Given the likely perturbation of the π-π interactions generated by successive base stacking events, it was reasoned that the stability of these substituted duplexes could benefit from the addition of an intercalating agent. Generally planar and aromatic, DNA intercalators are a class of molecules that possess an ability to insert themselves within the base stacking hierarchy of the duplex core. Furthermore, as intercalators are known to change the conformation of duplexed DNA by slightly

unwinding its phosphodiester backbone, the extended duplexes described above seem like a logical fit.

Often used as a finishing stain for gel electrophoresis, ethidium bromide (EtBr) is one of the most common DNA intercalators (Figure 3.13). Its interactions with DNA have been extensively scrutinized, including binding constant determination, as well as binding efficiency as a function of temperature and salt concentration.[25, 26] Continuing, given EtBr's relatively minor absorbance at λ = 260 nm, there should be little if any interference with the UV absorption of the DNA nucleobases.

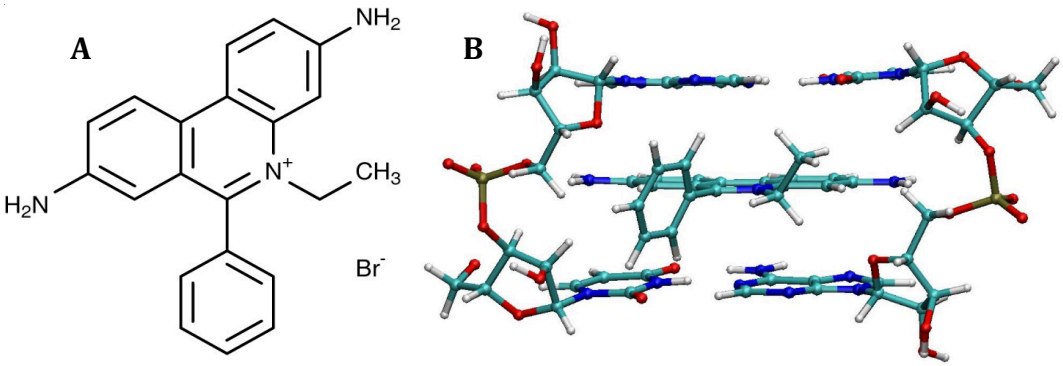

Figure 3.13: A) structure of EtBr and B) a three-dimensional depiction of its insertion between two A-U base pairs.

Initial EtBr intercalation attempts focused on duplexes containing 6'-extended nucleosides placed opposite native nucleosides (Table 3.4). As these duplexes were either destabilized, or didn't form at all at low salt concentration, the goal was to see if EtBr addition could have a positive effect on stability. These preliminary trials afforded mixed results (see Section 3.12.3 for a detailed experimental protocol).

ssDNA Pair	Tm Without EtBr (± 1 °C)	Tm With EtBr (± 1 °C)
C-Control/$GA_6$2	49	50
C-Control/$GT_6$2	44	45
$GA_6$2/$CA_6$2	N/A	N/A
$GT_6$2/$CT_6$2	N/A	42

Table 3.4: Tm values for a quartet of duplexes both with and without the presence of EtBr. All studies were performed with a salt concentration of 100 mM NaCl.

Duplexes containing substitutions on only one strand (top two entries in Table 3.4) saw a marginal increase in their respective Tm values. As these were already the most stable and afforded the least amount of base-pair interruption, it's not wholly unsurprising that the presence of an intercalator provided little gain in stability. According to the first-derivative plots, the Tm value for each duplex only increased by 1 °C.

Conversely, the DNA pair where both strands contained two 6'-deoxyadenosine nucleoside substitutions still failed to form a duplex. Given the combination of the bulk and potential spatial rearrangement of the adenine nucleobases, it's possible there wasn't any room for EtBr to insert itself into the modified core. With the spacing of the extended nucleosides presenting a tract spanning one-third of the sequence length (Figure 3.9-A), it's possible the inclusion of the intercalator still wasn't enough to promote annealing.

The lone "success story" to come from these initial trials was the final entry in the table. The difficulty of duplex formation between the $GT_6$2/$CT_6$2 pair (at low salt concentration) was described earlier (Section 3.9.2), and it was postulated that

the requisite core base pairs had failed to form. However, addition of EtBr provided a semblance of stability to the previously disrupted duplex (Figure 3.14).

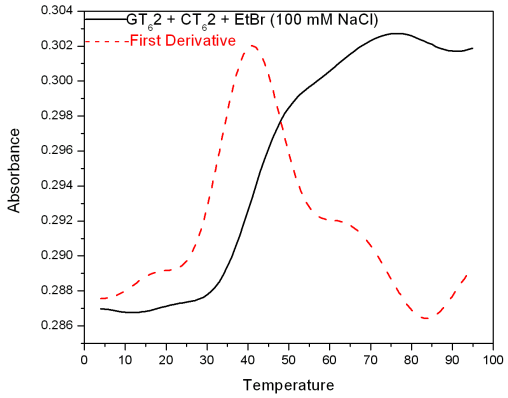

Figure 3.14: Temperature scan for the GT_62/CT_62 pair with the presence of EtBr (100 mM NaCl).

These findings align with the previous assertion that the thymine nucleobase was drawn out of its base pairing position in a more complete fashion than the adenine analogue (Figure 3.8). The space afforded by the combination of the extended backbone and displaced nucleobases could have provided the an opening for EtBr binding, which in turn may have precipitated an energetically favorable restructuring of the internal hydrophobic core. The resultant intercalated duplex displayed a Tm value of 42 °C, which was only two degrees lower than the duplex formed at a 1 M salt concentration (without the presence of an intercalator).

Subsequent studies were then performed with duplexes containing the 6'-deoxyadenosine nucleosides opposite either the 6'-deoxythymidine or extended 3'-deoxythymidine molecules. Regardless of the pairing, the increased local backbone spacing on both strands could present an additional impetus for intercalation

(Figures 3.9-B and 3.11). However, the intercalator provided little to no change in the duplex melting profiles.

ssDNA Pair	Tm Without EtBr (°C)	Tm With EtBr (°C)
$CA_6 2/GT_6 2$	19, 43	N/A
$CA_6 2/GT_3 2$	42	43

Table 3.5: Comparative Tm values for the annealing processes of $CA_6 2$ paired with both $GT_6 2$ and $GT_3 2$, with and without the presence of EtBr. Studies were performed at 100 mM NaCl.

Once again, the results show very little change in duplex stability. This isn't wholly unsurprising, as it's been shown previously that vicinal EtBr binding is anticooperative and rarely occurs.[27] Even though there were two extension sites on each ssDNA, and therefore two potential elongated pockets of space between base pairs, it's highly unlikely EtBr would've occupied both.

Nevertheless, the work with the $GT_6 2/CT_6 2$ duplexing pair remains promising and could ultimately yield multiple potential applications. First, as DNA intercalators are gaining traction as anticancer drugs, extended DNA sequences containing such molecules could theoretically be used as a means of drug delivery.[28] Given the controllable nature of the extended duplex formation, it's fair to reason the ssDNA components could be prompted to disengage in regions of lower salt concentration, thereby releasing the therapeutic agent.

Another possible use lies in assay development. If a molecule of interest is a known DNA intercalator, extended ssDNA's could be prompted to anneal through by means of binding the molecule in question. If each of the complementary sequences

were tagged with a fluorophore and quenching agent respectively, a vast difference in the fluorescence of the solution would be detected (Figure 3.15).

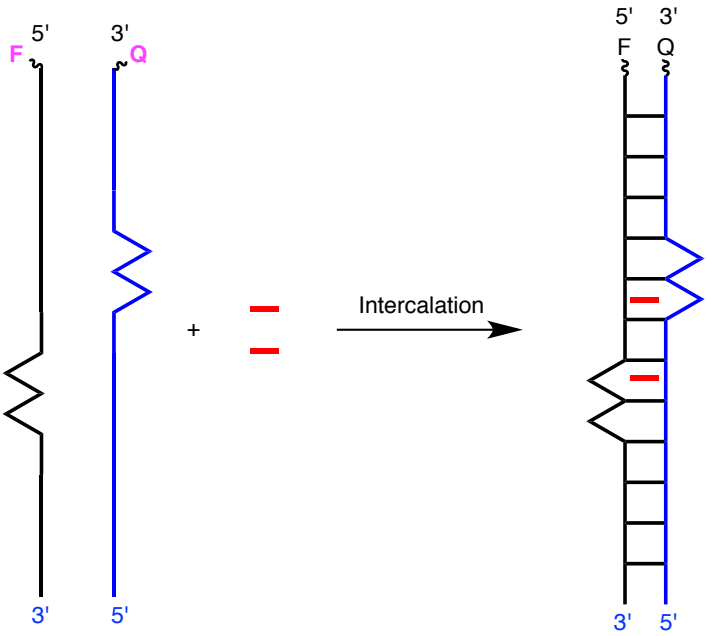

Figure 3.15: A potential fluorescence-based assay using DNA intercalation as the trigger. Binding of the intercalator (red line) precipitates duplex formation, drawing the fluorophore (F) and quencher (Q) closer together.

3.10 Conclusions

A novel synthesis of the 6'-deoxyadenosine nucleoside phosphoramidite **37** was detailed, incorporating dihydroxylation and deoxygenation key steps. While the number of total reactions matches that of the synthesis described by Hecht and coworkers, the purification is significantly more facile – flash chromatography is only necessitated twice between the 2'-deoxyadenosine starting material and the olefin intermediate **4**, a tract that encompasses nearly half of the synthetic pathway. Moreover, no single-step yield fell below 74%, including averages from the multi-

step reactions. The phosphoramidite was also shown to be compatible with solid phase DNA synthesis.

Upon insertion into ssDNA, the extended family of nucleosides displayed a destabilizing effect with every duplex pair tested. Thermal stabilities decreased with increased substitutions, but placing the extended nucleosides opposite one another appeared to at least somewhat mitigate this effect. It was also shown that the deoxyadenosine analogues had roughly half the destabilizing effect as their deoxythymidine counterparts.

Ethidium bromide intercalation was shown to have a marginal effect on the stabilities of the majority of duplexes. The GT_62/CT_62 pairing proved to be an exception to this trend, as a previous inability to anneal was supplanted by a more thermally stable, intercalated duplex. It's possible this system could provide useful applications such as those described in Section 3.9.6.

3.11 Future Directions

Upon completion of the extended 3'-deoxyadenosine nucleoside (shown in Figure 3.3), the central 5'-d(AATT)-3' cores of each sequence can be fully substituted. This will allow for a larger tract of extension, potentially aiding in a restructuring of the DNA turn. Subsequent syntheses of extended deoxycytidine and deoxyguanosine derivatives would ultimately make creating a fully substituted duplex possible, which could possibly yield an entirely new form of DNA.

3.12 Experimental

3.12.1 General Experimental Information

Starting materials, reagents and solvents were purchased from Sigma-Aldrich, Acros Organics, Oakwood, Glen Research, Chem-Impex, TCI International, Fisher, AK Scientific and Alfa Aesar. Flash chromatography utilized Silicycle SiliaFlash P60 silica gel (40 – 63 μm, 230 – 400 mesh) and thin layer chromatography used Silicycle glass-backed TLC plates (60 Å). TLC's were monitored by ultraviolet light (λ = 260 nm) and stained by 10% sulfuric acid or iodine where appropriate. Certain solvents (THF, DCM, diethyl ether, ACN, pyridine and DMF) were obtained from a Glass Contour solvent system using activated alumina columns as an additional drying agent, while all other anhydrous solvents were commercially available. NMR studies were performed on a Varian VNMRS400, VNMRS500 or INOVA 500 instrument, with deuterated solvents (purchased from Cambridge Isotopes) noted where appropriate. Masses were obtained using either a Waters LCT or JEOL AccuTOF mass spectrometer, by way of electrospray ionization (positive), MALDI-TOF or DART. HPLC studies were performed on a Waters 2487 Dual λ Absorbance Detector, and oligos were subsequently quantified using a Beckman DU640 UV/Vis spectrophotometer.

3.12.2 Synthetic Procedures

Compound 3

To a flask containing dry **2** (19.06 g, 53.64 mmol – synthesis and characterization described in section 2.8.1) was added anhydrous pyridine (700 mL), DMT-Cl (22.73 g, 67.55 mmol), dimethylaminopyridine (647 mg, 5.36 mmol) and TEA (9.72 mL, 69.73 mmol) in a stepwise manner. The reaction was stirred under nitrogen at room temperature for 16 hours and then quenched with MeOH. Volatiles were removed *in vacuo* and the crude was co-evaporated with toluene (3x). The resultant red oil was taken up in DCM, washed with $NaHCO_3$ (2x) and brine (1x), dried over sodium sulfate and reduced to dryness.

The DMT-protected intermediate was then dissolved in anhydrous DMF (750 mL). Imidazole (9.13 g, 134.1 mmol) was added and the stirring mixture was chilled to 0 °C. Triisopropylchlorosilane (25.83 mL, 120.69 mmol) was added and the reaction was allowed to return to room temperature and stir for 14 hours. The reaction was quenched with MeOH and volatiles were reduced under vacuum pressure. The crude material was re-dissolved in DCM, washed with $NaHCO_3$ (2x) and brine (1x), dried over sodium sulfate and concentrated under pressure.

Due to excessive mass the DMT/TIPS protected intermediate was split into two separate half-reactions. Each half was dissolved in DCM (750 mL) and stirred at 0 °C, at which time trichloroacetic acid (21.90 g, 134.1 mmol) was added. The

mixtures were stirred for 45 minutes and then quenched with TEA (22.43 mL, 160.92 mmol). The reaction mixtures were then combined, washed with $NaHCO_3$ (1x) and brine (1x), dried over sodium sulfate and reduced under pressure. The combined crude material was purified via flash chromatography (7:3 EtOAc/hexanes), and pure **3** was obtained as a white foam (13.16 g, 48% over three steps). R_F = 0.15 (3:1 EtOAc/hexanes). ^1H NMR (500 MHz; $CDCl_3$): δ 1.10 (s, 18H), 1.62 (s, 3H), 2.37 (m, 1H), 3.10 (m, 1H), 3.81 (t, 1H), 4.01 (d, 1H), 4.24 (s, 1H), 4.82 (d, 1H), 5.88 (d, 1H), 6.40 (m, 1H), 7.55 (t, 2H), 7.64 (t, 1H), 8.05 (d, 2H), 8.13 (s, 1H), 8.80 (s, 1H), 9.03 (s, 1H). ^{13}C NMR (100 MHz; $CDCl_3$): δ 11.90, 17.91, 41.55, 63.12, 74.09, 74.57, 87.58, 90.45, 124.38, 127.90, 128.37, 133.46, 142.73, 150.23, 150.75, 151.99, 165.03. ESI-MS (positive): 512.15 $[M + H]^+$ (HSMS calculated 512.2694).

Compound 4

To a flask containing pure, dry **3** (7.75 g, 15.14 mmol) was added anhydrous DCM (310 mL) and Dess-Martin periodinane (12.85 g, 30.3 mmol). The solution was stirred under nitrogen at room temperature for two hours and then quenched with equal parts of $NaHCO_3$ and sodium thiosulfate (saturated solutions in water). The organic layer was sequestered and washed with brine (2x), dried over sodium sulfate and concentrated under pressure.

In a separate flask, methyltriphenylphosphonium bromide (21.63 g, 60.56 mmol) and potassium tert-butoxide (5.52 g, 49.21 mmol) were dissolved in

anhydrous THF (250 mL) and stirred under nitrogen for one hour at room temperature. At that point, the dried crude from the Dess-Martin reaction was dissolved in anhydrous THF (100 mL) and added to the stirring mixture via cannula. The solution was stirred at room temperature for 18 hours and then quenched with a saturated solution of NH_4Cl.

Volatiles were removed *in vacuo* and the crude was taken up in DCM, washed with $NaHCO_3$ (1x) and brine (1x), dried over sodium sulfate and reduced under pressure as a red oil. Pure **4** was obtained via column chromatography (3:1 EtOAc/hexanes) as a white foam (4.70 g, 61% over two steps). R_F = 0.40 (3:1 EtOAc/hexanes). ^1H NMR (500 MHz; $CDCl_3$): δ 1.05 (d, 18H), 1.11 (q, 3H), 2.52 (d, 1H), 2.85 (m, 1H), 4.49 (d, 1H), 4.59 (d, 1H), 5.24 (d, 1H), 5.31 (d, 1H), 6.00 (m, 1H), 6.47 (d, 1H), 7.49 (t, 2H), 7.55 (t, 1H), 8.02 (d, 2H), 8.18 (s, 1H), 8.75 (s, 1H), 9.27 (s, 1H). ^{13}C NMR (100 MHz; $CDCl_3$): δ 12.03, 17.93, 40.27, 53.41, 76.05, 84.96, 88.95, 118.06, 127.90, 128.77, 132.69, 135.57, 141.69, 149.58, 152.55, 164.75. ESI-MS (positive): 508.2770 $[M + H]^+$ (HSMS calculated 508.2745).

Compound 6

To a flask containing 2,2,3,3-tetramethylsuccinonitrile (5.00 g, 36.7 mmol) was added a 3:2 mixture of H_2O/H_2SO_4 (100 mL), and the mixture was heated to 100 °C and stirred for 15 minutes. The reaction was then heated to 140 °C and refluxed for an additional two hours. The mixture was next returned to room temperature,

and the product was extracted using diethyl ether. The organic layer was then dried over sodium sulfate and concentrated under pressure to yield pure 6 as a white solid (5.16 g, 90%). ^{1}H NMR as described in literature.

Compound 8

To a flask containing dry adenine (3.00 g, 22.2 mmol) was added anhydrous pyridine (20 mL) and **6** (6.93 g, 44.4 mmol). The reaction was heated to 90 °C, stirred under nitrogen for 14 hours, lowered to room temperature and quenched with water. Volatiles were removed and the crude then was co-evaporated with toluene (3x). Flash chromatography (9:1 DCM/MeOH) yielded a combination of desired product and non-cyclized protected adenine.

This mixture of products was dissolved in re-distilled thionyl chloride (10 mL) and refluxed at 80 °C for two hours. Volatiles were removed via rotary evaporation and the crude was co-evaporated with ethyl acetate (5x). Subsequent flash chromatography (9:1 DCM/MeOH) afforded pure **8** as a white solid (5.18 g, 86%). R_F = 0.52 (9:1 DCM/MeOH). ^{1}H NMR (500 MHz; DMSO-d_6): δ 1.29 (s, 12H), 8.82 (s, 1H), 8.98 (s, 1H).

Compound 10

To a flask containing dry 2-deoxy-d-ribose (30.00 g, 223.5 mmol) was added anhydrous MeOH (360 mL) and the mixture was stirred under nitrogen at room

temperature. A solution of methanolic HCl (60 mL – made by combining 1.7 mL of acetyl chloride in 100 mL of MeOH) was added via syringe and the reaction was stirred for 25 minutes before being quenched with $NaHCO_3$ (12 g). Particulates were filtered off and the supernatant was reduced under low pressure.

The crude was then co-evaporated with anhydrous pyridine (3x), reduced to a volume of 90 mL and stirred under nitrogen at 0 °C. In a separate flask, p-toluoyl chloride (66 mL, 154.6 mmol) was dissolved in anhydrous pyridine (90 mL), and the mixture was added to the crude via cannula. The solution was allowed to warm to room temperature and react for 16 hours.

The mixture was quenched with cold water (360 mL), extracted with DCM (3x) and then washed successively with $NaHCO_3$ (2x), 2N HCl (1x) and water (1x). The crude was dried over sodium sulfate, concentrated under diminished pressure and the resultant orange-brown oil was dried under high vacuum pressure.

The crude was then dissolved in acetic acid (120 mL), and an aliquot of HCl in acetic acid (189 mL – formed by combining 48.9 mL acetyl chloride, 243 mL acetic acid and 12 mL water at 0 °C) was added in three equivalent volumes over the course of five minutes. Upon an additional 10 minutes of stirring, the desired α-chloro sugar precipitated out as a white solid. The filtrate was removed, and pure **10** was sequestered (53.00 g, 61%). ^1H NMR (500 MHz; $CDCl_3$): δ 2.40 (s, 6H), 2.76

(d, 1H), 2.85 (m, 1H), 4.59 (d, 1H), 4.67 (d, 1H), 4.84 (m, 1H), 5.58 (m, 1H), 6.46 (d, 1H), 7.24 (q, 4H), 7.90 (d, 2H), 8.00 (d, 2H).

Compound 11

Pure, dry **8** (5.18 g, 19.0 mmol) was dissolved in anhydrous ACN (500 mL). Sodium hydride (1.60 g, 33.3 mmol) was added and the solution was stirred under nitrogen at room temperature for one hour. Pure, dry **10** (12.95 g, 33.3 mmol) was then added and the solution was allowed to react for an additional two hours. Solids were removed via filtration and the supernatant was reduced under diminished pressure. The desired N9-coupled product **11** was achieved using flash chromatography (3:2 EtOAc/hexanes) as a white foam (8.94 g, 64%). R_F = 0.60 (1:1 EtOAc/hexanes). ^{1}H NMR (500 MHz; $CDCl_3$): δ 1.39 (s, 12H), 2.39 (s, 3H), 2.43 (s, 3H), 2.84 (m, 1H), 3.19 (m, 1H), 4.65 (d, 2H), 4.78 (t, 1H), 5.82 (d, 1H), 6.60 (t, 1H), 7.21 (d, 2H), 7.26 (d, 2H), 7.90 (d, 2H), 7.96 (d, 2H), 8.30 (s, 1H), 8.93 (s, 1H).

Compound 12

To a flask containing pure, dry **11** (8.94 g, 14.3 mmol) was added anhydrous MeOH (400 mL) and sodium methoxide (114.32 mL, 57.2 mmol – 0.50 M solution in MeOH), and the reaction was stirred at room temperature for one hour. Silica gel (60 g) was then added, and the solution was concentrated under pressure. Dry-packed flash chromatography yielded pure **12** as a white foam (3.10 g, 56%). R_F = 0.10 (3:1 EtOAc/hexanes). ^{1}H NMR (500 MHz; Acetone-d_6): δ 1.39 (s, 12H), 2.58 (m,

1H), 3.00 (m, 1H), 3.79 (d, 1H), 3.84 (d, 1H), 4.15 (t, 1H), 4.76 (t, 1H), 6.65 (m, 1H), 8.78 (s, 1H), 8.98 (s, 1H). ESI-MS (positive): 390.18 $[M + H]^+$ (HSMS calculated 390.1778).

Compound 13

Synthesis of **13** was performed in an analogous fashion to compound **3**, with the following quantities of reagents:

5'-OH DMT-protection – **12** (3.10 g, 8.0 mmol), DMT-Cl (3.37 g, 10.0 mmol), dimethylaminopyridine (98 mg, 0.8 mmol), TEA (1.45 mL, 10.4 mmol) and anhydrous pyridine (80 mL)

3'-OH Silylation – Tertbutyldiphenylchlorosilane (4.14 mL, 15.9 mmol), imidazole (1.08 g, 15.9 mmol), anhydrous DMF (80 mL)

Detritylation – 80% acetic acid in water (100 mL), DCM (50 mL)

Through flash chromatography (1:1 EtOAc/hexanes) pure **13** was afforded as a white foam (2.26 g, 45% over three steps). R_F = 0.65 (3:1 EtOAc/hexanes). ^{1}H NMR (500 MHz; $CDCl_3$): δ 1.04 (s, 9H), 1.39 (s, 12H), 2.56 (m, 1H), 2.82 (m, 1H), 3.80 (d, 1H), 3.87 (m, 2H), 4.10 (t, 1H), 4.75 (m, 1H), 6.44 (t, 1H), 7.39 (t, 4H), 7.42 (t, 2H), 7.63 (d, 4H), 8.25 (s, 1H), 8.90 (s, 1H).

Compound 14

To a flask containing pure, dry 2'-deoxyadenosine (3.00 g, 11.1 mmol) was added anhydrous MeOH (130 mL). N,N-dimethylformamide dimethyl acetal (7.44 mL, 55.7 mmol) was added via syringe and the reaction was allowed to stir under nitrogen at room temperature for two hours. Volatiles were removed in vacuo and pure **14** was re-crystallized out of ethyl acetate as a white solid (3.24 g, 95%). ^{1}H NMR (500 MHz; CD_3OD): δ 2.41 (m, 1H), 2.81 (m, 1H), 3.24 (s, 6H), 3.74 (dd, 1H), 3.82 (dd, 1H), 4.07 (q, 1H), 4.59 (m, 1H), 5.58 (s, 1H), 6.50 (m, 1H), 8.43 (d, 1H), 8.92 (s, 1H). ESI-MS (positive): 307.1688 $[M + H]^+$ (HSMS calculated 307.1519).

Compound 15

Synthesis of **15** was performed in an analogous fashion to compound **3**, with the following quantities of reagents:

5'-OH DMT-protection – **14** (3.24 g, 10.6 mmol), DMT-Cl (4.66 g, 13.8 mmol), dimethylaminopyridine (129 mg, 1.1 mmol), TEA (1.92 mL, 13.8 mmol) and anhydrous pyridine (105 mL)

3'-OH Silylation – Tertbutyldiphenylchlorosilane (5.50 mL, 21.2 mmol), imidazole (1.44 g, 21.2 mmol), anhydrous DMF (110 mL)

Detritylation – 80% acetic acid in water (150 mL), DCM (60 mL)

Following flash chromatography (3:1 EtOAc/hexanes), pure **15** was afforded as a white foam (3.87 g, 67% over three steps). R_F = 0.25 (3:1 EtOAc/hexanes). ^{1}H NMR (500 MHz; $CDCl_3$): δ 1.10 (s, 9H), 1.60 (s, 6H), 2.22 (m, 1H), 2.93 (m, 1H), 3.20 (dd, 1H), 3.75 (m, 2H), 4.17 (s, 1H), 4.76 (d, 1H), 5.57 (s, 1H), 6.34 (d, 1H), 7.40 (t, 4H), 7.42 (t, 2H), 7.63 (d, 4H), 7.82 (s, 1H), 8.20 (s, 1H).

Compound 17

Synthesis of **17** was performed in an analogous manner to compound **11**, using the following quantities of reactants, reagents and solvents: 6-chloropurine (2.00 g, 12.9 mmol), sodium hydride (932 mg, 19.4 mmol), α-chloro sugar **10** (7.54 g, 19.4 mmol) and anhydrous ACN (340 mL). Flash chromatography (3:1 EtOAc/hexanes) yielded the desired N9-coupled product **17** as a white solid (3.31 g, 51%) along with the N7-coupled side product (2.00 g, 31%). R_F = 0.34. ^{1}H NMR (500 MHz; $CDCl_3$): δ 2.39 (s, 3H), 2.41 (s, 3H), 2.86 (dd, 1H), 3.18 (m, 1H), 4.63 (d, 2H), 4.80 (m, 1H), 5.81 (d, 1H), 6.56 (t, 1H), 7.20 (d, 2H), 7.25 (d, 2H), 7.81 (d, 2H), 7.96 (d, 2H), 8.26 (s, 1H), 8.65 (s, 1H). ESI-MS (positive): 507.1777 $[M + H]^+$ (HSMS calculated 507.1436).

Compound 18

Pure, dry **17** (3.31 g, 6.53 mmol) was dissolved in anhydrous MeOH (180 mL) and sodium methoxide (45.71 mL, 22.86 mmol – 0.5 M solution in MeOH) was added via syringe. The reaction was stirred for two hours at room temperature and then

silica gel (40 g) was added. Volatiles were removed by rotary evaporation to afford the dry-pack crude, and flash chromatography (19:1 DCM/MeOH) yielded pure **18** as a white foam (1.69 g, 97%). R_F = 0.30 (19:1 DCM/MeOH). ^{1}H NMR (500 MHz; acetone-d_6): δ 2.42 (dd, 1H), 2.85 (m, 1H), 3.76 (d, 1H), 3.81 (d, 1H), 4.10 (s, 1H), 4.16 (s, 3H), 4.63 (d, 1H), 6.53 (t, 1H), 8.41 (s, 1H), 8.48 (s, 1H). ESI-MS (positive): 267.1154 $[M + H]^+$ (HSMS calculated 267.1094).

Compound 19

Synthesis of **19** was performed in an analogous fashion to compound **3**, with the following quantities of reagents:

5'-OH DMT-protection – **18** (1.69 g, 6.2 mmol), DMT-Cl (3.17 g, 9.4 mmol), dimethylaminopyridine (76 mg, 0.6 mmol), TEA (1.31 mL, 9.4 mmol) and anhydrous pyridine (95 mL)

3'-OH Silylation – Tertbutyldiphenylchlorosilane (3.19 mL, 12.5 mmol), imidazole (850 mg, 12.5 mmol), anhydrous DMF (65 mL)

Detritylation – 80% acetic acid in water (75 mL), DCM (30 mL)

Following flash chromatography (3:1 EtOAc/hexanes), pure **19** was afforded as a white foam (1.63 g, 52% over three steps). R_F = 0.35 (3:1 EtOAc/hexanes).

Compound 20

Synthesis of **20** was performed in an analogous manner to compound **4**, with the following quantities of reactants, reagents and solvents utilized:

Dess-Martin oxidation – **20** (1.00 g, 1.98 mmol), Dess-Martin periodinane (1.68 g, 3.96 mmol), anhydrous DCM (40 mL)

Wittig reaction – methyltriphenylphosphonium bromide (2.83 g, 7.92 mmol), potassium tert-butoxide (722 mg, 6.44 mmol), anhydrous THF (20 mL – activation of Wittig reagent, 10 mL – dissolution of Dess-Martin intermediate)

Flash chromatography (1:1 EtOAc/hexanes) yielded pure **20** as a white foam (585 mg, 59% over two steps). R_F = 0.32 (1:1 EtOAc/hexanes).

Compound 21

To a flask containing pure, dry **20** (240 mg, 0.48 mmol) was added anhydrous THF (10 mL), and the reaction was stirred under nitrogen at room temperature. 9-BBN (2.85 mL, 1.43 mmol – 0.5 M solution in THF) was added via syringe and the solution was stirred for two hours at room temperature. The reaction temperature was then reduced to 0 °C and hydrogen peroxide (61 μL, 0.72 mmol – 35 weight % solution in water) and sodium hydroxide (713 μL, 0.72 mmol – 1 M solution) were added concurrently. The reaction was allowed to warm to room temperature and was stirred for an additional 30 minutes. Volatiles were removed

in vacuo and the crude was taken up in DCM, washed with $NaHCO_3$ (1x) and brine (1x), dried over sodium sulfate and reduced under pressure. Flash chromatography (4:1 EtOAc/hexanes) afforded pure **21** as a white foam (182 mg ,73%). R_F = 0.24 (3:1 EtOAc/hexanes). ^1H NMR (500 MHz; $CDCl_3$): δ 0.10 (s, 3H), 0.11 (s, 3H), 0.91 (s, 9H), 1.62 (t, 2H), 1.95 (m, 1H), 2.40 (m, 1H), 2.85 (m, 1H), 3.80 (t, 2H), 4.20 (s, 3H), 4.55 (m, 1H), 6.37 (t, 1H), 8.01 (s, 1H), 8.57 (s, 1H). ESI-MS (positive): 395.4 $[M + H]^+$ (HSMS calculated 395.2115).

Compound 22

To pure **3a** (analogous to compound **3**, but with a 3'-TBDPS protection – 4.00 g, 6.74 mmol) was added anhydrous DCM (85 mL) and Dess-Martin periodinane (21 mL, 10.12 mmol – 0.48 M solution in DCM). The solution was stirred under nitrogen for two hours, and the reaction was then quenched and worked up as described for compound **4**.

In a separate flask, (methoxymethyl)triphenylphosphonium chloride (9.24 g, 26.96 mmol) and potassium tert-butoxide (2.65 g, 23.59 mmol) were dissolved in anhydrous THF (70 mL) and stirred under nitrogen at room temperature for one hour. The crude Dess-Martin product was then dissolved in anhydrous THF (20 mL) and added via cannula. The solution was stirred under nitrogen at room temperature for 16 hours, and then quenched and worked up as described previously. Flash chromatography (1:1 EtOAc/hexanes) yielded pure **22** as a white

foam (2.51 g, 60% over two steps). R_F = 0.45 (1:1 EtOAc/hexanes). ^{1}H NMR (500 MHz; $CDCl_3$): δ 1.01 (s, 9H), 2.41 (m, 1H), 2.62 (m, 1H), 3.38 (s, 3H), 3.50 (d, 1H), 4.30 (m, 1H), 4.40 (d, 1H), 4.58 (t, 1H), 6.15 (m, 1H), 7.30 (t, 4H), 7.35 (t, 2H), 7.41 (d, 2H), 7.59 (d, 4H), 7.90 (t, 2H), 7.95 (t, 1H), 8.61 (s, 1H), 8.95 (s, 1H).

Compound 23

Pure, dry **22** (90 mg, 0.15 mmol) was added to a 20-mL test tube and dissolved in anhydrous ethanol (5 mL). Palladium on activated charcoal (15 mg, 10% palladium basis) was added and the test tube was inserted into a flask and placed on a Parr hydrogenation apparatus. The system was filled with hydrogen gas and the reaction was allowed to take place over the course of 15 hours at room temperature. The palladium reagent was filtered off over celite and the filtrate was collected and reduced under vacuum pressure. Flash chromatography (1:1 EtOAc/hexanes) afforded pure **23** as a white foam (83 mg, 92%). R_F = 0.43 (1:1 EtOAc/hexanes). ^{1}H NMR (500 MHz; $CDCl_3$): δ 1.10 (s, 9H), 1.70 (m, 2H), 2.45 (m, 1H), 2.63 (dd, 1H), 3.20 (s, 3H), 3.27 (m, 1H), 4.20 (t, 1H), 4.46 (d, 1H), 6.45 (t, 1H), 7.40 (t, 4H), 7.44 (t, 2H), 7.52 (t, 2H), 7.60 (t, 1H), 7.67 (d, 4H), 8.01 (d, 2H), 8.03 (s, 1H), 8.75 (s, 1H), 8.91 (s, 1H).

Compound 24

To a nitrogen-filled pressure vessel containing dry triphenylphosphine (1.59 g, 6.07 mmol) was added anhydrous benzene (25 mL) and benzyloxychloromethyl

ether (1.00 mL, 7.28 mmol). The reaction was heated to 105 °C and stirred for 60 hours, during which time pure **24** precipitated out of solution. The reaction was quenched by reducing the temperature to 0 °C, at which point **24** was filtered off, washed with cold toluene and sequestered as a white powder (2.35 g, 70%). Melting point = 140 °C. ^{1}H NMR (500 MHz; $CDCl_3$): δ 5.01 (s, 2H), 6.06 (s, 2H), 7.28 (t, 1H), 7.30 (t, 3H), 7.63 (d, 2H), 7.66 (d, 6H), 7.74 (t, 2H), 7.80 (t, 6H).

Compound 25

To a flask containing pure, dry **3** (162 mg, 0.33 mmol) was added anhydrous DCM (15 mL) and Dess-Martin periodinane (242 mg, 0.57 mmol). The reaction was stirred under nitrogen at room temperature for two hours, and was then quenched and worked up as described previously.

In a separate flask, pure, dry **24** (500 mg, 1.30 mmol) and potassium tert-butoxide (128 mg, 1.14 mmol) were dissolved in a 2:1 mixture of anhydrous THF/DCM (15 mL) and stirred for under nitrogen for two hours at room temperature. The crude Dess-Martin product was then dissolved in anhydrous THF (10 mL) and added via cannula. The solution was stirred for 16 hours, and then quenched and worked up as described above. Flash chromatography (1:1 EtOAc/hexanes) afforded pure **25** as a white foam (120 mg, 60%). R_F = 0.42 (1:1 EtOAc/hexanes). ^{1}H NMR (500 MHz; $CDCl_3$): δ 1.06 (s, 18H), 1.25 (s, 3H), 2.55 (m, 1H), 2.99 (m, 1H), 4.60 (dd, 1H), 4.78 (s, 2H), 4.82 (dd, 1H), 5.08 (t, 1H), 6.39 (t, 1H),

7.30 – 7.40 (undefined, 5H), 7.55 (t, 2H), 7.60 (t, 1H), 8.02 (d, 2H), 8.18 (s, 1H), 8.80 (s, 1H), 9.16 (s, 1H). MALDI-TOF (positive): 614.4 $[M + H]^+$ (HSMS calculated 614.3163).

Compound 26

Pure, dry **25** (30 mg, 0.05 mmol) and palladium on activated charcoal (50 mg, 10% palladium basis) were placed in a nitrogen-filled 20-mL test tube, and dissolved in anhydrous ethanol (5 mL). The tube was then deposited in a flask and placed on a Parr apparatus. The system was filled with hydrogen gas, and the reaction was mixed for 16 hours. Solids were filtered off over celite, and the filtrate was concentrated under vacuum. Flash chromatography (1:1 EtOAc/hexanes) yielded pure **26** as a white foam (25 mg, 84%). R_F = 0.93 (3:1 EtOAc/hexanes). ^1H NMR (500 MHz; $CDCl_3$): δ 1.08 (s, 18H), 1.63 (s, 3H), 2.01 (dd, 2H), 2.48 (m, 1H), 2.91 (m, 1H), 3.60 (t, 2H), 4.20 (m, 1H), 4.49 (s, 2H), 4.63 (m, 1H), 6.41 (t, 1H), 7.30 - 7.38 (undefined, 5H), 7.52 (t, 2H), 7.61 (t, 1H), 8.02 (d, 2H), 8.12 (s, 1H), 8.79 (s, 1H), 8.98 (s, 1H). ESI-MS (positive): 616.3 $[M + H]^+$ (HSMS calculated 616.3320).

Compound 28

To a flask containing dry inosine (1.00 g, 3.73 mmol) was added anhydrous pyridine (50 mL), TEA (2.34 mL, 16.78 mmol) and acetic anhydride (1.59 mL, 16.78 mmol) in a stepwise manner. The solution was heated to 60 °C and stirred under nitrogen for two hours, then quenched with water. Volatiles were removed by

rotary evaporation and the resultant yellow oil was co-evaporated with toluene (3x). The crude was then taken up in DCM, washed with $NaHCO_3$ (1x) and brine (1x), dried over sodium sulfate and concentrated under pressure to afford pure 28 as a white solid (1.40 g, 95%). R_F = 0.08 (19:1 DCM/MeOH). ^1H NMR (500 MHz; $CDCl_3$): δ 2.10 (s, 3H), 2.14 (s, 3H), 2.15 (s, 3H), 4.37 (dd, 1H), 4.44 (dd, 2H), 5.60 (t, 1H), 5.87 (t, 1H), 6.15 (d, 1H), 7.99 (s, 1H), 8.13 (s, 1H).

Compound 29

Pure, dry **28** (200 mg, 0.51 mmol) was dissolved in anhydrous DCM (10 mL), and the solution was stirred under nitrogen at 0 °C. TEA (283 µL, 2.03 mmol) was added, followed by 2,4,6-triisopropylbenzenesulfonyl chloride (269 mg, 0.89 mmol) and dimethylaminopyridine (16 mg, 0.13 mmol). The reaction vessel was wrapped in aluminum foil and stirred for 3 hours at 0 °C, quenched with MeOH and then stirred for an additional 5 minutes. Volatiles were removed *in vacuo* and flash chromatography (1:1 EtOAc/hexanes) afforded pure **29** as a white solid (115 mg, 34%) along with the N1-protected byproduct (111 mg, 33%). R_F = 0.43 (1:1 EtOAc/hexanes). ^1H NMR (500 MHz; $CDCl_3$): δ 1.24 (s, 12H), 1.27 (s, 6H), 2.03 (s, 3H), 2.10 (s, 3H), 2.12 (s, 3H), 2.16 (s, 3H), 4.37 (dd, 1H), 4.44 (dd, 2H), 5.62 (t, 1H), 5.94 (t, 1H), 6.20 (d, 1H), 7.21 (s, 2H), 8.20 (s, 1H), 8.60 (s, 1H). ESI-MS (positive): 699.23 $[M + K]^+$ (HSMS calculated 699.3448).

Compound 30

4-chlorophenol (45 mg, 0.35 mmol) and sodium hydride (17 mg, 0.35 mmol – 50 weight % dispersion in mineral oil) were dissolved in anhydrous DCM (10 mL) and stirred under nitrogen for one hour at room temperature. Pure **29** (236 mg, 0.36 mmol) dissolved in anhydrous DCM (5 mL) was added via cannula, and the solution was allowed to react for 4 hours. Solids were removed via filtration and the filtrate was reduced under diminished pressure. Flash chromatography (1:1 EtOAc/hexanes) afforded pure 30 as a white solid (154 mg, 85%). R_F = 0.20 (1:1 EtOAc/hexanes). ^{1}H NMR (500 MHz; $CDCl_3$): δ 2.10 (s, 3H), 2.15 (s, 3H), 2.16 (s, 3H), 4.40 (dd, 1H), 4.45 (dd, 2H), 5.60 (t, 1H), 5.88 (t, 1H), 6.19 (d, 1H), 7.19 – 7.24 (undefined, 4H), 8.05 (s, 1H), 8.13 (s, 1H).

Compound 31

To a flask containing pure **4** (4.61 g, 9.08 mmol) was added DCM (140 mL), N-methylmorpholine N-oxide (4.64 mL, 22.7 mmol – 50 weight % aqueous solution) and osmium tetroxide (2.31 mL, 0.18 mmol – 2% solution in water) in a consecutive fashion. The reaction was stirred for 3 hours at room temperature, at which point it was quenched with a concentrated sodium thiosulfate solution (20 mL). The organic layer was sequestered, washed with water (2x) and brine (1x), dried over sodium sulfate and concentrated under reduced pressure. Flash chromatography (99:1 EtOAc/MeOH) yielded a racemic mixture of **31** as a white foam (4.40 g, 89%).

R_F = 0.05 (3:1 EtOAc/hexanes). ^{1}H NMR indecipherable due to a racemic mixture. ^{13}C NMR (100 MHz; $CDCl_3$): δ 12.03, 18.02, 41.43, 63.39, 72.63, 72.96, 86.95, 90.88, 124.38, 128.04, 128.73, 132.79, 133.45, 142.75, 150.29, 150.67, 151.93, 164.87 (some small side peaks noted due to the racemic mixture). ESI-MS (positive): 542.2810 $[M + H]^+$ (HSMS calculated 542.2799).

Compound 32

Pure **31** (3.16 g, 5.83 mmol) was dissolved in anhydrous DMF (100 mL), and imidazole (694 mg, 10.20 mmol) was then added. The reaction mixture was reduced to 0 °C and stirred under nitrogen, at which point tertbutyldiphenylchlorosilane (2.27 mL, 8.75 mmol) was added via syringe. The reaction temperature was returned to 25 °C and the solution was stirred for 15 hours, at which point the solution was quenched with MeOH. Volatiles were removed via rotary evaporation and the resultant yellow oil was taken up in DCM, washed with $NaHCO_3$ (1x) and brine (1x), dried over sodium sulfate and reduced under vacuum pressure. Flash chromatography (3:2 EtOAc/hexanes) provided pure **32** as a white foam (4.16 g, 91%). R_F = 0.55 (3:1 EtOAc/hexanes). ^{1}H NMR indecipherable due to a racemic mixture. ^{13}C NMR (100 MHz; $CDCl_3$) spectrum included, but also challenging to assign due to the presence of numerous side racemic side peaks. ESI-MS (positive): 780.29 $[M + H]^+$ (HSMS calculated 780.3977).

Compound 33

To a flask containing pure, dry **32** (4.16 g, 5.33 mmol) was added anhydrous THF (135 mL) and thiocarbonyldiimidazole (4.75 g, 26.62 mmol), and the reaction was refluxed at 65 °C in darkness for 18 hours. Volatiles were then removed under diminished pressure and the resultant red oil was taken up in DCM, washed with a 1% HCl solution (1x – 81 mL), $NaHCO_3$ (1x) and brine (1x), and then dried over sodium sulfate. The organic layer was concentrated via rotary evaporation and flash chromatography afforded a racemic mixture of **33** as a white foam (4.02 g, 85%). R_F = 0.20 (3:1 EtOAc/hexanes). ^1H NMR indecipherable due to a racemic mixture. ^1H NMR indecipherable due to a racemic mixture. ^{13}C NMR (100 MHz; $CDCl_3$) spectrum included, but also challenging to assign due to the presence of numerous side racemic side peaks. ESI-MS (positive): 890.95 $[M + H]^+$ (HSMS calculated 890.3916).

Compound 34

Pure **33** (3.98 g, 4.47 mmol) was dissolved in anhydrous toluene (160 mL), and tributyltin hydride (3.03 mL, 11.18 mmol) was next added. The reaction mixture was then heated to 75 °C and stirred under nitrogen. In a separate flask, AIBN (204 mg, 1.12 mmol) was dissolved in anhydrous toluene (24 mL), and this solution was added to the fully heated, stirring mixture above in three equivalent aliquots over the course of two hours. The reaction was then allowed to proceed at

75 °C for an additional 14 hours, at which point volatiles were removed *in vacuo*. Flash chromatography (1:1 EtOAc/hexanes) yielded pure **34** as a white foam (2.34 g, 78%). R_F = 0.65 (3:1 EtOAc/hexanes). ^{1}H NMR (500 MHz; $CDCl_3$): δ 1.03 (q, 3H), 1.06 (d, 18H), 1.11 (s, 9H), 1.85 (m, 1H), 1.98 (m, 1H), 2.50 (m, 1H), 2.87 (m, 1H), 3.78 (t, 2H), 4.31 (m, 1H), 4.57 (m, 1H), 6.40 (t, 1H), 7.35 (t, 4H), 7.40 (t, 2H), 7.49 (t, 2H), 7.58 (t, 1H), 7.65 (d, 4H), 8.03 (d, 2H), 8.06 (s, 1H), 8.75 (s, 1H), 9.33 (s, 1H). ^{13}C NMR (100 MHz; $CDCl_3$): δ 11.84, 12.60, 13.79, 17.05, 17.62, 17.98, 19.15, 26.86, 30.90, 36.90, 40.42, 60.36, 75.93, 85.15, 127.62, 127.77, 127.86, 128.83, 129.62, 132.72, 133.68, 135.51, 141.79, 152.46. ESI-MS (positive): 764.41 $[M + H]^+$ (HSMS calculated 764.4028).

Compound 35

To a flask containing pure, dry **34** (1.70 g, 2.22 mmol) was added anhydrous THF (100 mL) and tetrabutylammonium fluoride (13.35 mL, 13.35 mmol – 1.0 M solution in THF), and the reaction was stirred under nitrogen at room temperature for 15 minutes. Volatiles were then removed under reduced pressure, and the crude was re-dissolved in DCM, washed with $NaHCO_3$ (1x) and brine (1x), dried over sodium sulfate and concentrated under vacuum pressure. Flash chromatography afforded pure **35** as a white foam (766 mg, 93%). R_F = 0.45 (9:1 DCM/MeOH). ^{1}H NMR (500 MHz; CD_3OD): δ 1.95 (m, 2H), 2.49 (m, 1H), 2.90 (m, 1H), 3.26 (d, 1H), 3.60 (m, 2H), 4.05 (m, 1H), 4.49 (d, 1H) 6.48 (t, 1H), 7.52 (t, 2H), 7.60 (t, 1H), 8.05 (d, 2H), 8.50 (s, 1H), 8.70 (s, 1H). ^{13}C NMR (100 MHz; CD_3OD): δ 12.62, 19.74, 29.27,

36.15, 38.85, 44.07, 58.39, 74.10, 84.34, 124.02, 127.99, 128.32, 132.45, 142.96, 149.64, 151.71. ESI-MS (positive): 392.10 $[M + Na]^+$ (HSMS calculated 392.1335).

Compound 36

Pure **35** (766 mg, 2.07 mmol) was dissolved in anhydrous pyridine, and the resultant solution was stirred under nitrogen at room temperature. TEA (375 µL, 2.59 mmol), DMT-Cl (878 mg, 2.59 mmol) and dimethylaminopyridine (25 mg, 0.21 mmol) were then added in a stepwise manner and the solution was allowed to react for 16 hours before being quenched with MeOH. Volatiles were removed and the resultant orange oil was co-evaporated with toluene (3x). The crude was then re-dissolved in DCM, washed with $NaHCO_3$ (2x) and brine (1x), dried over sodium sulfate and concentrated under vacuum pressure. Flash chromatography (96:3.5:0.5 DCM/MeOH/TEA) was utilized to provide pure **36** as a white foam (1.12 g, 81%). R_F = 0.40 (19:1 DCM/MeOH). ^1H NMR (500 MHz; $CDCl_3$): δ 2.03 (m, 2H), 2.58 (m, 1H), 2.81 (m, 1H), 3.17 (m, 1H), 3.45 (d, 1H), 3.77 (s, 6H), 3.99 (d, 1H), 4.53 (d, 1H), 5.28 (s, 1H), 6.33 (t, 1H), 6.77 (d, 4H), 7.22 (t, 1H), 7.27 (t, 6H), 7.40 (d, 2H), 7.48 (t, 2H), 7.52 (t, 1H), 8.02 (d, 2H), 8.06 (s, 1H), 8.53 (s, 1H), 9.21 (s, 1H). ^{13}C NMR (100 MHz; $CDCl_3$): δ 33.92, 39.69, 55.22, 60.79, 74.30, 83.98, 85.85, 87.08, 113.30, 123.62, 126.96, 127.89, 128.00, 128.83, 129.84, 132.76, 133.67, 135.53, 135.62, 141.27, 144.41, 149.51, 151.31, 152.56, 158.56. ESI-MS (positive): 672.24 $[M + H]^+$ (HSMS calculated 672.2823).

Compound 37

To a flask containing pure, dry **36** (170 mg, 0.25 mmol) was added anhydrous ACN, and the mixture was stirred under nitrogen at room temperature. 2-Cyanoethyl *N,N,N′,N′*-tetraisopropylphosphordiamidite (155 µL, 0.50 mmol) was then added, followed by tetrazole (526 µL, 0.24 mmol – 0.45 M solution in ACN), and the reaction was stirred at room temperature. After 18 hours the solution was quenched with MeOH and volatiles were removed via rotary evaporation. The crude yellowish oil was re-dissolved in DCM, washed with $NaHCO_3$ (1x) and brine (1x), dried over sodium sulfate and reduced under pressure. The resultant oil was then dissolved in DCM (2 mL) and added dropwise to a beaker containing vigorously stirring hexanes (120 mL). A white precipitate was formed, filtered off, washed with hexanes and dried under high vacuum pressure to afford a racemic mixture of **37** as a white foam (166 mg, 76%). R_F = 0.48 (19:1 DCM/MeOH). ^{1}H NMR (500 MHz; $CDCl_3$): δ 1.25 (d, 12H), 2.04 (m, 2H), 2.60 (q, 3H), 2.87 (m, 1H), 3.25 (t, 2H), 3.68 (t, 2H), 3.75 (t, 2H), 3.76 (s, 6H), 3.82 (m, 1H), 4.35 (t, 1H), 4.58 (m, 1H), 6.40 (t, 1H), 6.77 (t, 4H), 7.24 (t, 1H), 7.26 (d, 1H), 7.27 (t, 4H), 7.40 (d, 2H), 7.52 (t, 2H), 7.60 (t, 1H), 8.02 (d, 2H), 8.03 (s, 1H), 8.52 (s, 1H), 9.03 (s, 1H). ^{13}C NMR (100 MHz; $CDCl_3$): δ 24.63, 43.10, 43.26, 43.47, 55.20, 84.69, 86.17, 112.43, 113.02, 113.62, 117.56, 123.64, 127.73, 127.90, 128.41, 129.30, 129.61, 130.34, 133.69, 136.22, 136.26, 141.49, 145.06, 149.46, 151.36, 152.49, 152.59, 158.35, 158.39, 164.54. ^{31}P NMR (100 MHz; $CDCl_3$): δ 148.46, 148.87.

3.12.3 Synthesis, Purification and Quantification of Solid-Phase DNA Materials

DNA Synthesis and Purification

Reagents, resins and phosphoramidites were purchased from Glen Research. Sequences were synthesized on an Applied Biosystems 394 DNA/RNA synthesizer using standard solid phase techniques on a one-μmole scale. A standard two-minute coupling protocol was used for all native nucleoside phosphoramidites (exceptions noted below), while a 10-minute coupling time was utilized for non-natural nucleoside phosphoramidites. All natural phosphoramidites coupling directly after a non-natural phosphoramidite were also provided with a 10-minute wait time. Non-natural nucleoside phosphoramidites were manually diluted with anhydrous ACN to a final concentration of 0.1 M. Average stepwise yields were determined through UV absorption (λ = 495 nm) by way of measuring the cleaved DMT groups (the 5'-terminal DMT moiety was left attached). Sequences were generally synthesized with yields exceeding 97%.

Upon completion of synthesis, oligomers were cleaved from the resin by being subjected to 12 hours of ammonium hydroxide at 55 °C. The supernatant was sequestered and volatiles were removed with a Jouan RC1010 vacuum concentrator. The cleaved DNA was dissolved in MilliQ water (5 mL) and any remaining resin was removed via syringe filtration.

Full-length oligomers were separated from truncated sequences and cleaved protecting groups via HPLC using a C18 column (0.46 cm x 23 cm). The two mobile phases used were defined as Standard A (50 mM triethylammonium acetate, 5% ACN, pH = 7) and Standard B (50 mM triethylammonium acetate, 70% ACN, pH = 7), and the generic solvent gradient is shown below.

Time (min)	Flow Rate (mL/min)	% Standard A	% Standard B
0	3.0	100	0
2	3.0	100	0
8	3.0	70	30
33	3.0	0	100

Table 3.6: HPLC gradient used for the purification of ssDNA sequences.

Collected fractions containing the desired product were aggregated, and volatiles were removed via rotary evaporation.

Next, the 5'-terminal DMT group was removed by dissolving the remaining crude in a 4:1 mixture of acetic acid/water (10 mL) and letting it react for 30 minutes at 0 °C. Remaining acetic acid was removed under vacuum pressure and the detritylated DNA was co-evaporated with ethanol five times. The remaining white powder was dissolved in MilliQ water (3 mL) and desalted over three GE Healthcare illustra Nap-10 columns (3 x 1 mL). Purified ssDNA was collected, dried on a VirTis Benchtop lyophilizer, re-dissolved in a measured volume of water and quantified using UV analysis at 260 nm.

Determination of DNA Duplex Melting Points

Complements of ssDNA were combined in an Eppendorf tube such that the final concentration of each strand was 0.5 μM. The mixture was diluted to a total volume of 1.25 mL with a 20 mM sodium phosphate hybridization buffer (pH = 7, either 100 mM or 1 M NaCl). Each sample was heated at 95 °C for five minutes, and was then allowed to return to room temperature over the course of an hour. Samples were then equilibrated at 4 °C for 60 minutes, and a 1.0 mL aliquot of each was utilized for each experiment.

Temperature scans were run on an Aviv Spectrophotometer Model 14DS UV-Vis. Samples were monitored from a range of 4 °C to 95 °C at a wavelength of 260 nm. Absorbance readings were recorded at every degree, with an equilibration time of 30 seconds corresponding to every step. Upon reaching the maximum temperature, samples were returned to 4 °C with wait times of 30 seconds per degree. Tm values were obtained from the data acquired by taking the first derivative of the melting curve.

Ethidium Bromide Intercalation Studies

Complementary pairs of ssDNA were diluted in a hybridization buffer (20 mM phosphate, 100 mM NaCl, pH = 7) to a final concentration of 0.5 μM and heated at 95 °C for five minutes. The DNA solutions were then allowed to cool to 50 °C, at which point ethidium bromide was added (final concentration = 0.5 μM). After

cooling to 25 °C, each DNA/EtBr solution was then stirred for 60 minutes. The solutions were next cooled to 4 °C and equilibrated at that temperature for 60 minutes, and then subjected to the temperature scans described in the section above.

3.13 References

1. A. F. Cook, *Journal of the American Chemical Society*, **1970**, *92*, 190–195.

2. Y. Xu and E. T. Kool, *Nucleic Acids Research*, **1998**, *26*, 3159-3164.

3. J. P. Schrum, A. Ricardo, M. Krishnamurthy, J. C. Blain and J. W. Szostak, *Journal of the American Chemical Society*, **2009**, *131*, 14560-14570.

4. J. J. Chen, C. H. Tsai, X. Cai, A. T. Horhota, L. W. McLaughlin and J. W. Szostak, *PLOS One*, **2009**, *4*.

5. A. T. Horhota, K. Y. Zou, J. K. Ichida, B. Yu, L. W. McLaughlin and J. W. Szostak, *Journal of the American Chemical Society*, **2005**, *127*, 7427-7434.

6. A. T. Horhota, J. W. Szostak and L. W. McLaughlin, *Organic Letters*, **2006**, *8*, 5345-5347.

7. J. K. Ichida, A. Horhota, K. Y. Zou, L. W. McLaughlin and J. W. Szostak, *Nucleic Acids Research*, **2005**, *33*, 5219-5225.

8. J. K. Ichida, A. Horhota, B. Yu, L. W. McLaughlin and J. W. Szostak, *Journal of the American Chemical Society*, **2005**, *127*, 2802-2803.

9. K. Y. Zou, A. Horhota, B. Yu, J. W. Szostak and L. W. McLaughlin, *Organic Letters*, **2005**, *7*, 1485-1487.

10. J. C. Chaput, J. K. Ichida and J. W. Szostak, *Journal of the American Chemical Society*, **2003**, *125*, 856-857.

11. G. Etzold, G. Kowollik and P. Langen, *Chemical Communications*, **1968**, *7*, 422.

12. T. Kofoed, P. B. Rasmussen, P. Valentin-Hansen and E. B. Pederson, *Acta Chemica Scandanavica*, **1997**, *51*, 318-324.

13. T. Kofoed and M. H. Caruthers, *Tetrahedron Letters*, **1996**, *37*, 6457-6460.

14. K. A. Henningfeld, T. Arslan and S. M. Hecht, *Journal of the American Chemical Society*, **1996**, *118*, 11701-11714.

15. J. W. Arico, A. K. Calhoun, K. J. Salandria and L. W. McLaughlin, *Organic Letters*, **2010**, *12*, 120-122.

16. V. Rolland, M. Kotera and J. Lhomme, *Synthetic Communications*, **1997**, *27*, 3505-3511.

17. J. G. Douglass, J. B. de Camp, E. H. Fulcher, W. Jones, S. Mahanty, A. Morgan, D. Smirnov, J. L. Boyer and P. S. Watson, *Bioorganic and Medicinal Chemistry Letters*, **2008**, *18*, 2167-2171.

18. R. Jasztold-Howorko, C. Landras, A. Pierré, G. Atassi, N. Guilbaud, L. Kraus-Berthier, S. Léonce, Y. Rolland, J. Prost and E. Bisagni, *Journal of Medicinal Chemistry*, **1994**, *37*, 2445-2452.

19. D. H. R. Barton, S. D. Géro, J. Cléophax, A. S. Machado and B. Quiclet-Sire, *Journal of the Chemical Communications*, **1988**, *17*, 1184-1186.

20. N. Chavain and P. Herdewijn, *European Journal of Organic Chemistry*, **2011**, *6*, 1140-1147.

21. S. G. Patching, S. A. Baldwin, A. D. Baldwin, J. D. Young, M. P. Gallagher, P. J. F. Henderson and R. B. Herbert, *Organic and Biomolecular Chemistry*, **2005**, *3*, 462-470.

22. S. R. Sarfati and V. K. Kansal, *Tetrahedron*, **1988**, *44*, 6367-6372.

23. T. Naito, K. Ueno and F. Ishikawa, *Chemical and Pharmaceutical Bulletin*, **1964**, *12*, 951-954.

24. C. R. Allerson, S. L. Chen and G. L. Verdine, *Journal of the American Chemical Society*, **1997**, *119*, 7423-7433.

25. S. Nafisi, A. A. Saboury, N. Keramat, J. Neault and H. Tajmir-Riahi, *Journal of Molecular Structure*, **2007**, *827*, 35-43.

26. C. Cuniberti and M. Guenza, *Biophysical Chemistry*, **1990**, *38*, 11-22.

27. L. D. Williams, M. Egli, Q. Gao and A. Rich, *Structure and Function Volume One*, Adenine Press: Albany, 1992.

28. M. F. Braña, M. Cacho, A. Gradillas, B. de Pascual-Teresa and A. Ramos, *Current Pharmaceutical Design*, **2001**, *7*, 1745-1780.

3.14 Pertinent HPLC Traces

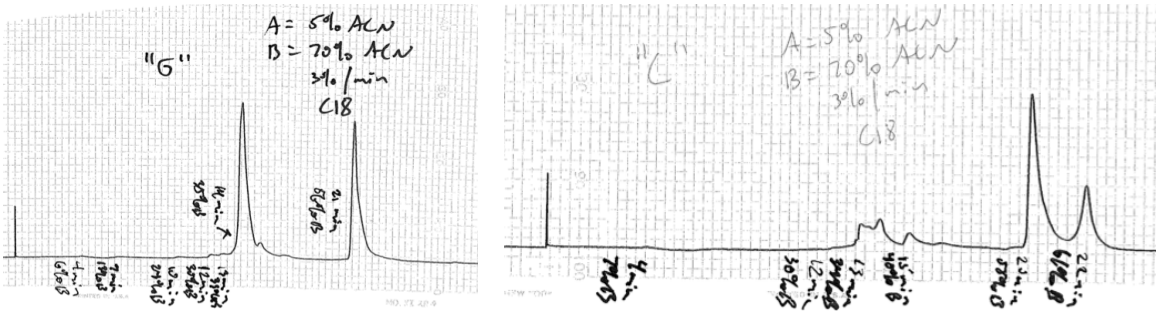

Figure 3.16: HPLC Traces for the control ssDNA sequences.

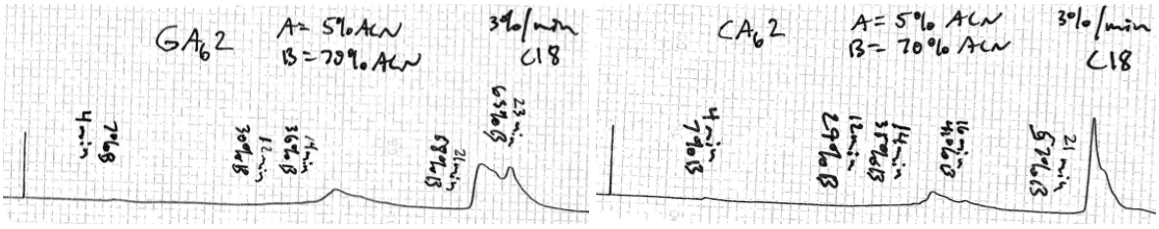

Figure 3.17: HPLC traces for ssDNA containing 6'-dA substitutions.

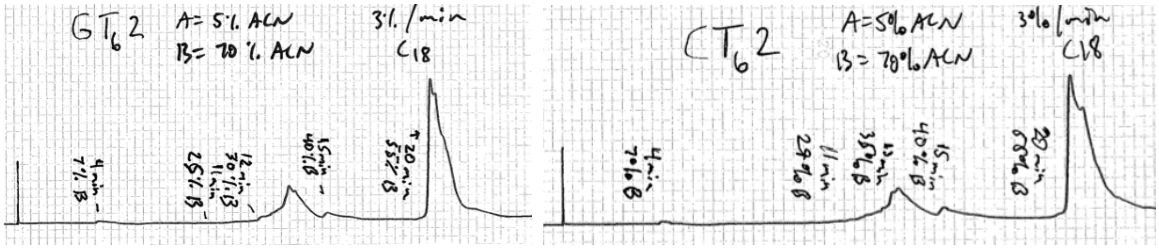

Figure 3.18: HPLC traces for ssDNA containing 6'-dT substitutions.

3.15 Additional Temperature Scans

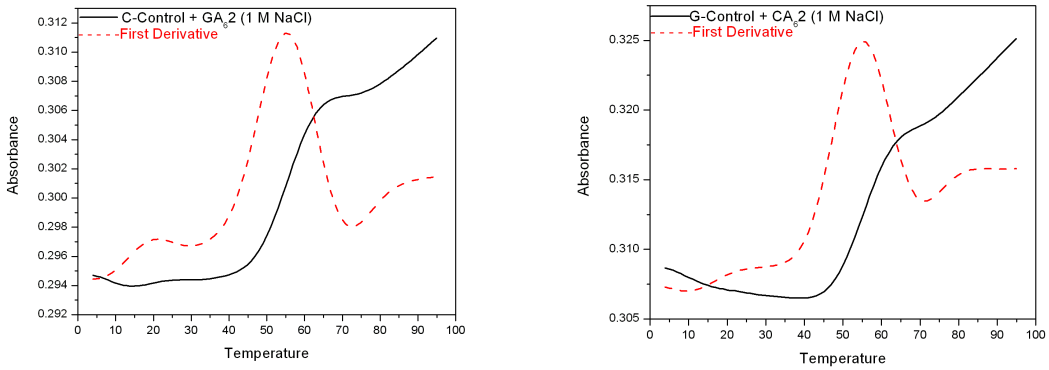

Figure 3.19: Melting curves of 6'-dA substituted ssDNA with control sequences at 1 M NaCl.

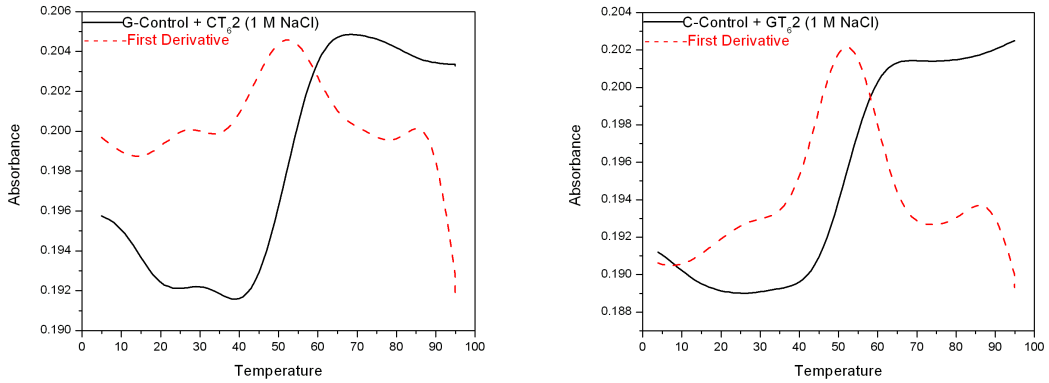

Figure 3.20: Melting curves of 6'-dT substituted ssDNA with control sequences at 1 M NaCl.

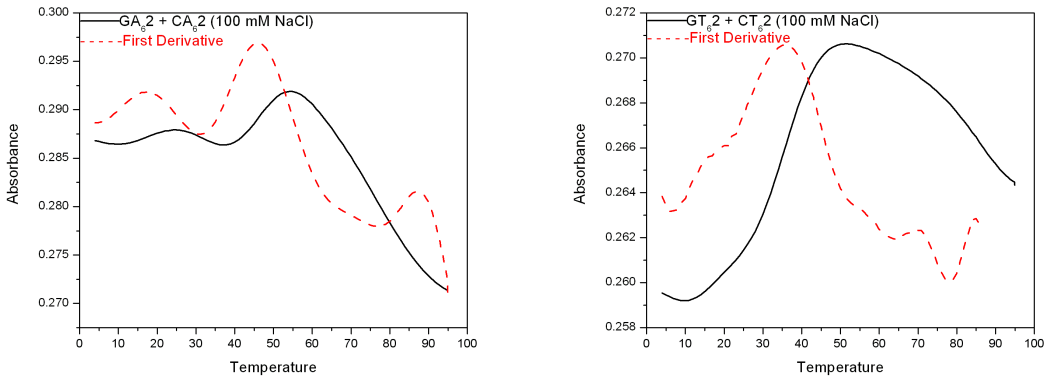

Figure 3.21: Melting curves of the efforts towards annealing GA_62 with CA_62 and GT_62 with CT_62 (100 mM NaCl).

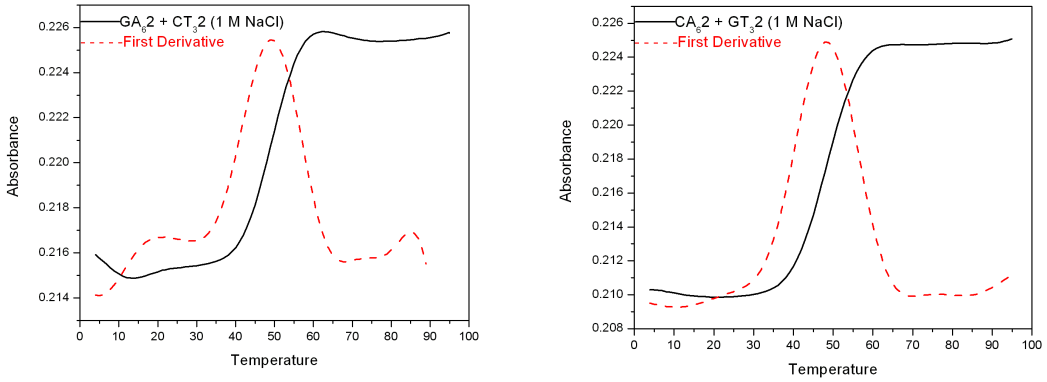

Figure 3.22: Melting curves of the duplexes formed between complementary ssDNA containing 6'-dA and extended 3'-dT substitutions at 1 M NaCl.

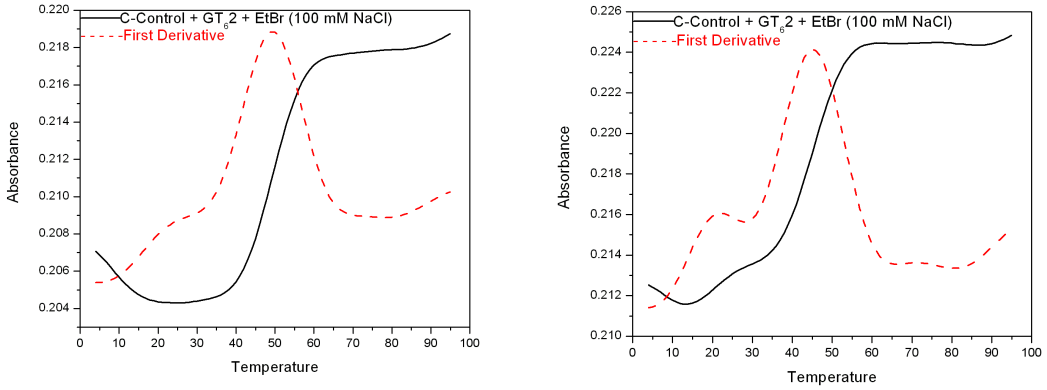

Figure 3.23: Melting curves of the C-Control paired with both GA_62 and GT_62 in the presence of ethidium bromide at 100 mM NaCl.

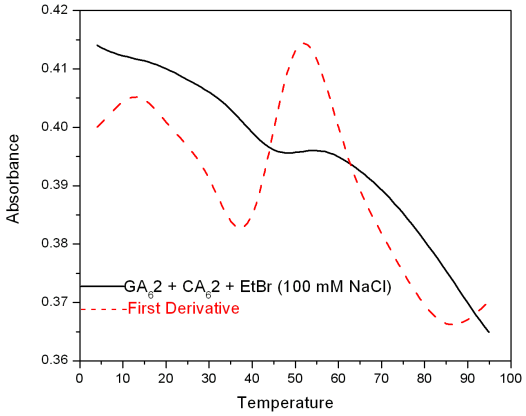

Figure 3.24: Melting curve of the post-annealing process of $GA_6 2$ and $CA_6 2$ in the presence of ethidium bromide at 100 mM NaCl.

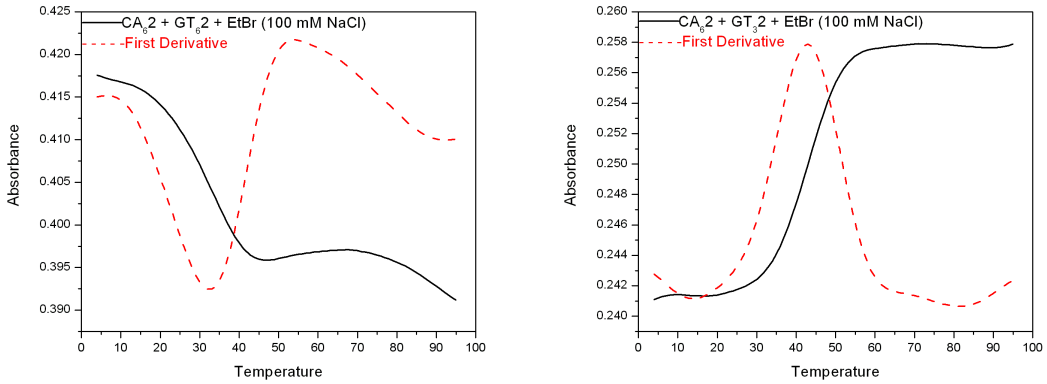

Figure 3.25: Melting curves of the post-annealing processes for $CA_6 2$ opposite both $GT_6 2$ and $GT_3 2$ in the presence of ethidium bromide at 100 mM NaCl.

3.16 ^{1}H, ^{13}C and ^{31}P NMR Spectra

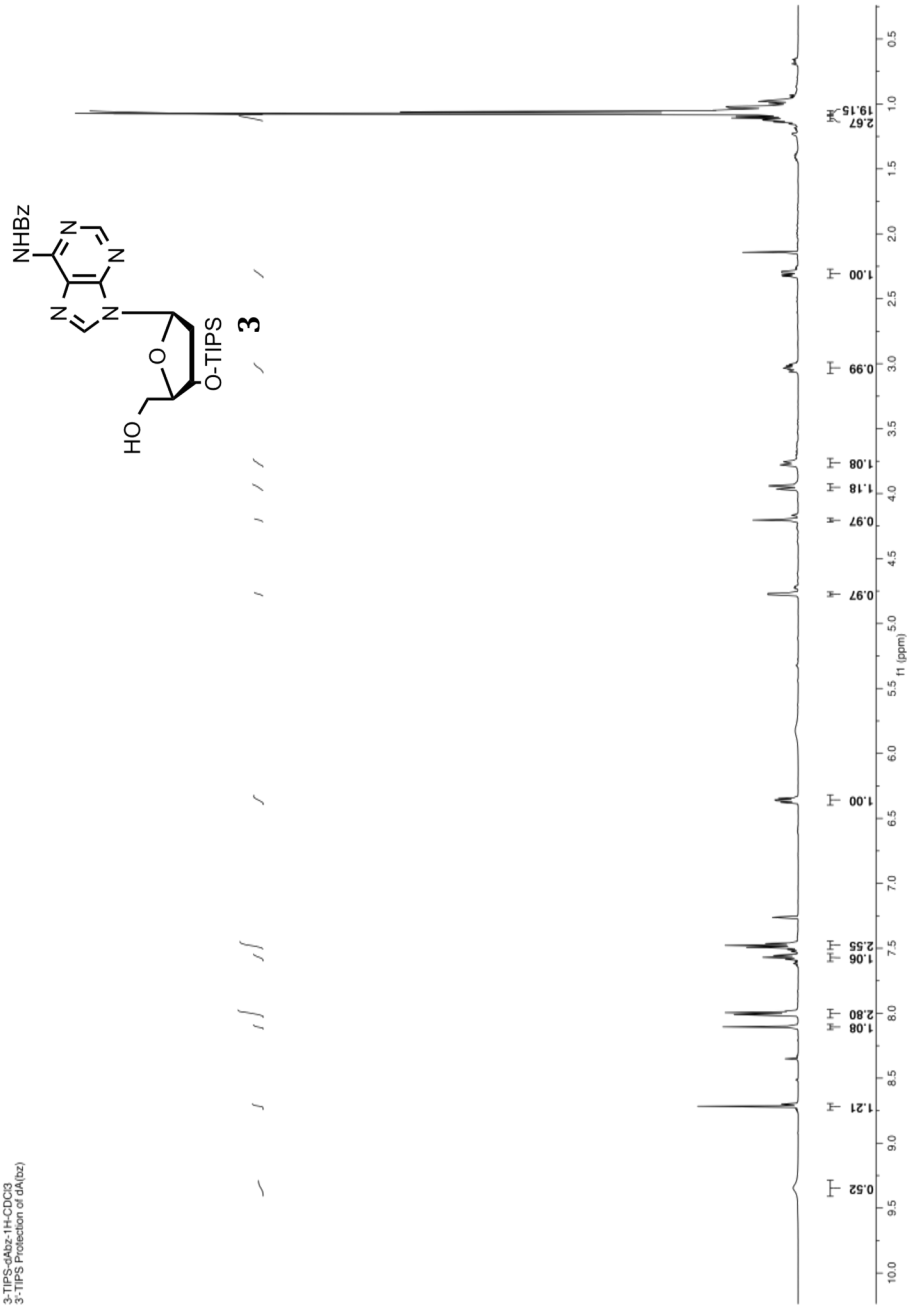

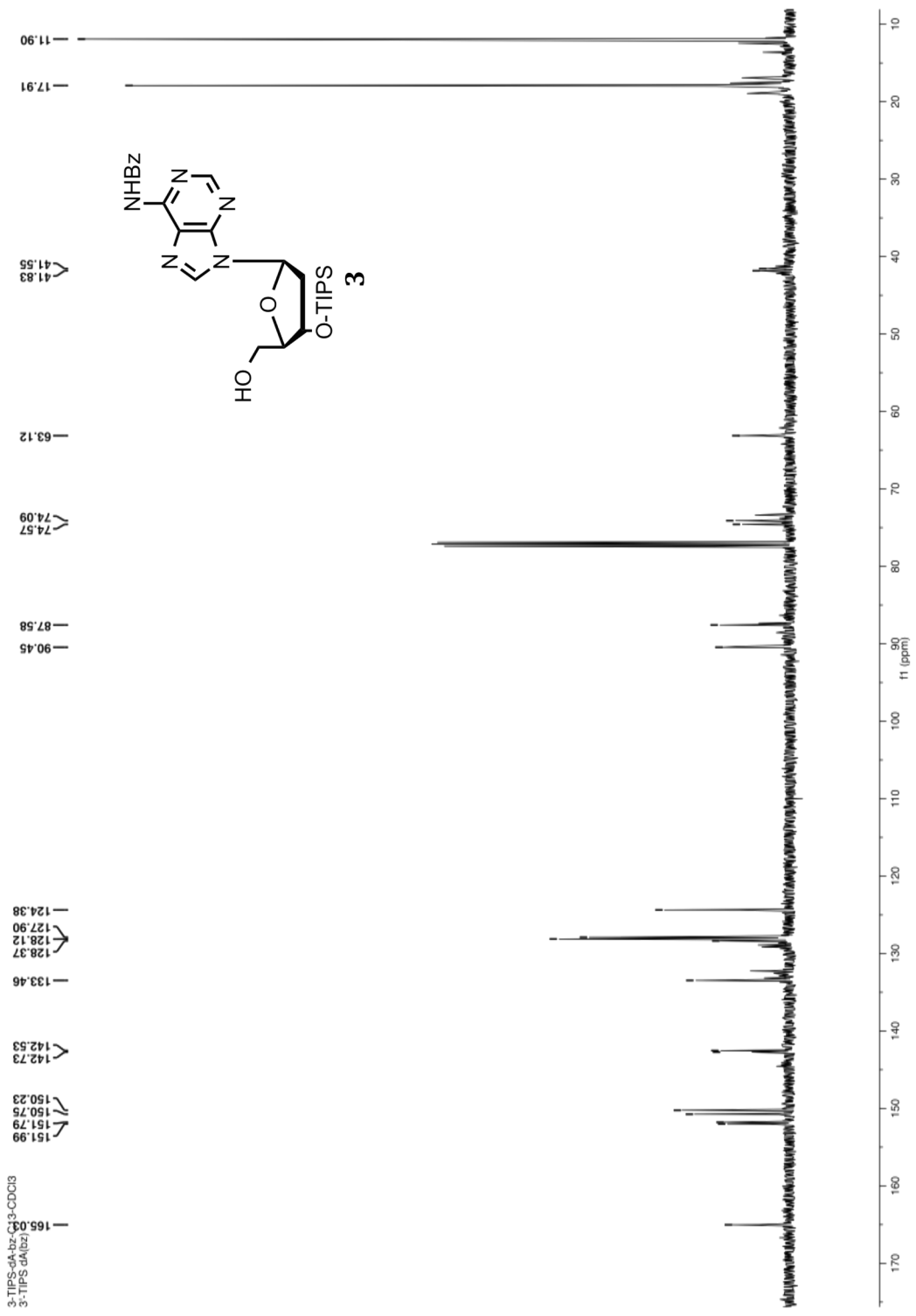
3-TIPS-dA-bz-C13-CDCl3
3-TIPS dA(bz)
165.03
151.99
151.79
150.75
150.23
142.73
142.53
133.46
128.37
128.12
127.90
124.38
90.45
87.58
74.57
74.09
63.12
41.83
41.55
17.91
11.90
NHBz
HO
O-TIPS
3
f1 (ppm)

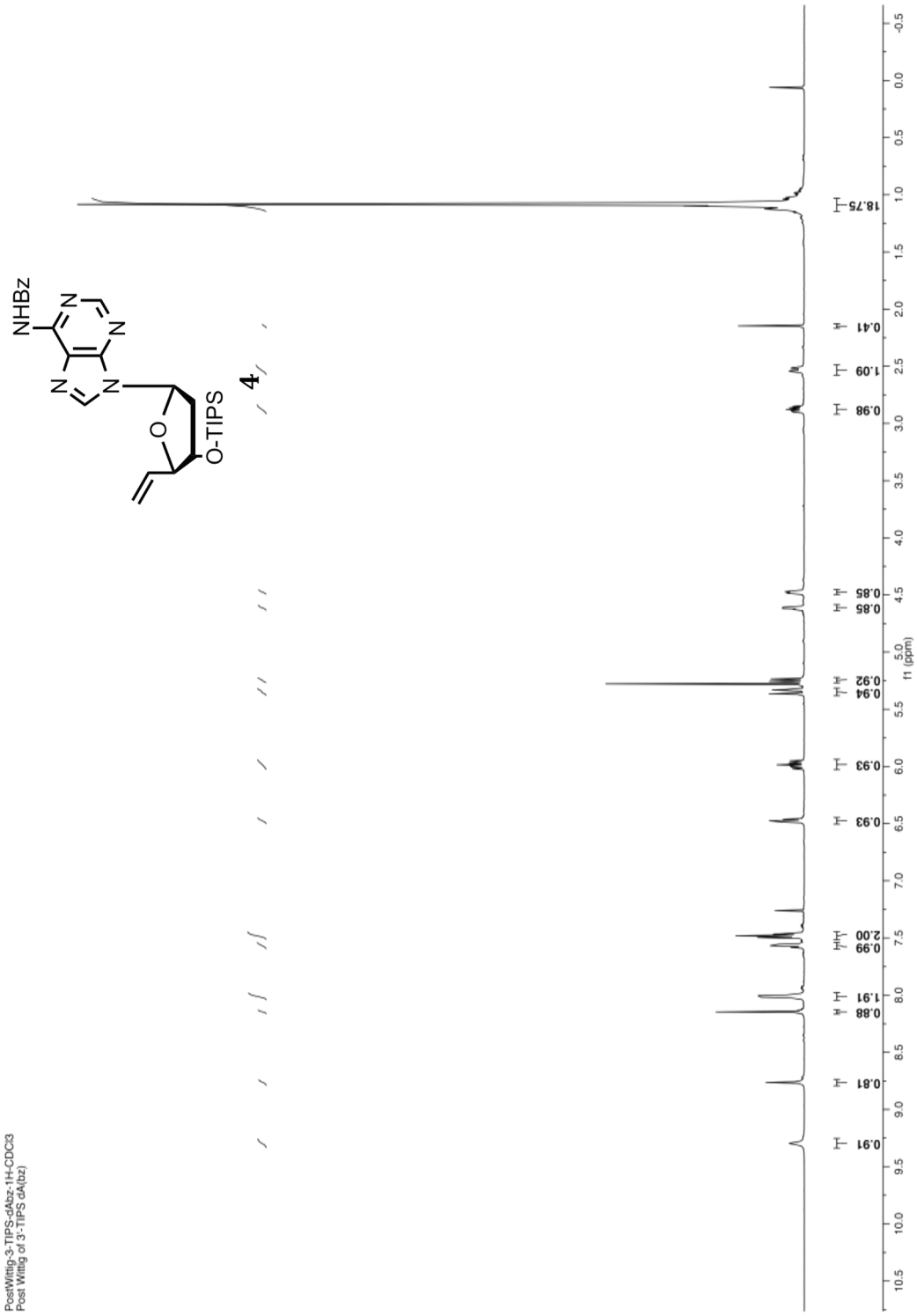
PostWittig-3-TIPS-dAbz-1H-CDCl3
Post Wittig of 3'-TIPS dA(bz)
NHBz
O-TIPS
4
18.75
0.41
1.09
0.98
0.85
0.85
0.94
0.92
0.93
0.93
0.99
2.00
0.88
1.91
0.81
0.91
f1 (ppm)

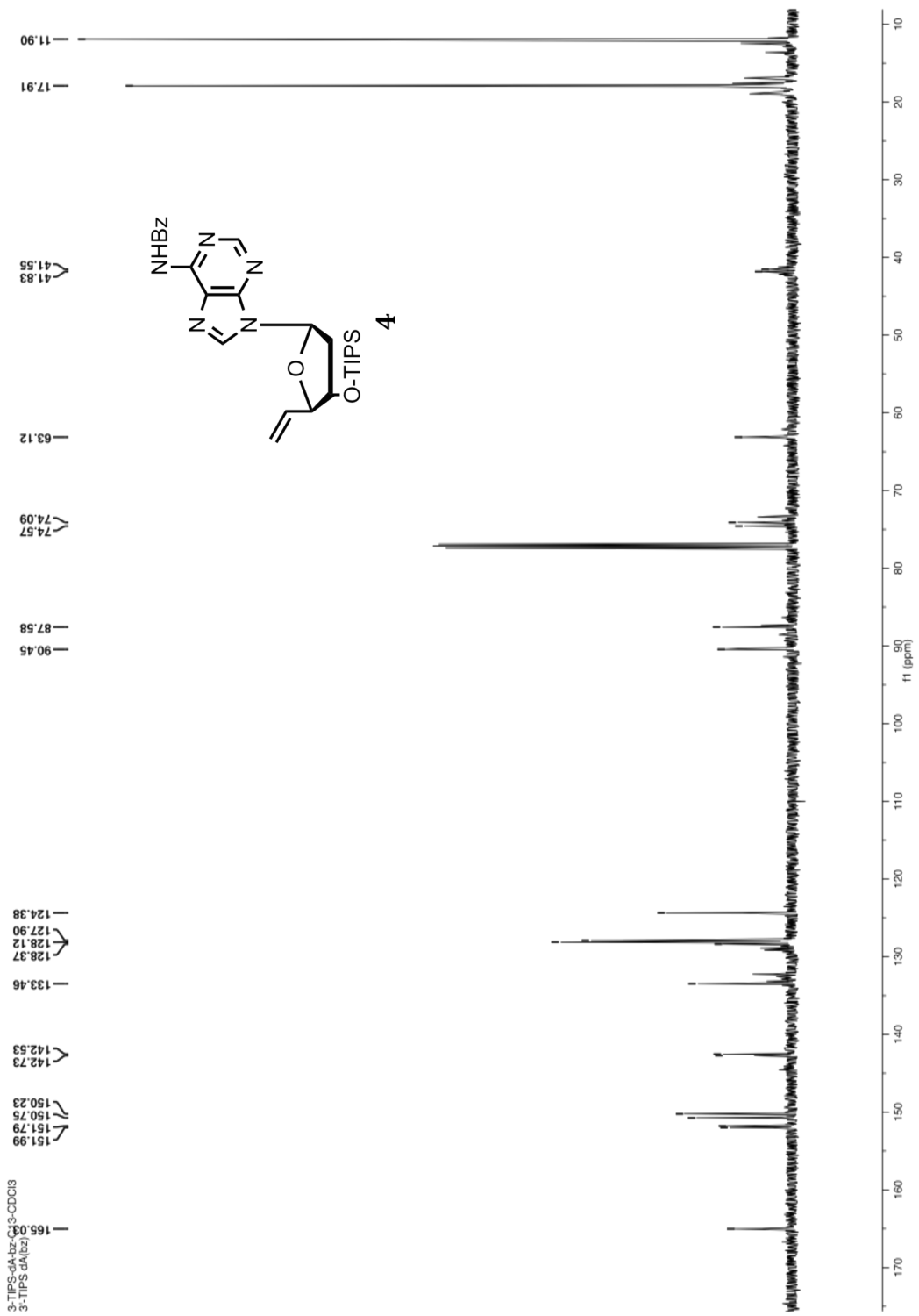
3-TIPS-dA-bz-C13-CDCl3
3-TIPS dA(bz)
11.90
17.91
41.83
41.55
63.12
74.57
74.09
87.58
90.45
124.38
127.90
128.12
128.37
133.46
142.53
142.73
150.23
150.75
151.79
151.99
165.03
NHBz
O-TIPS
4
f1 (ppm)

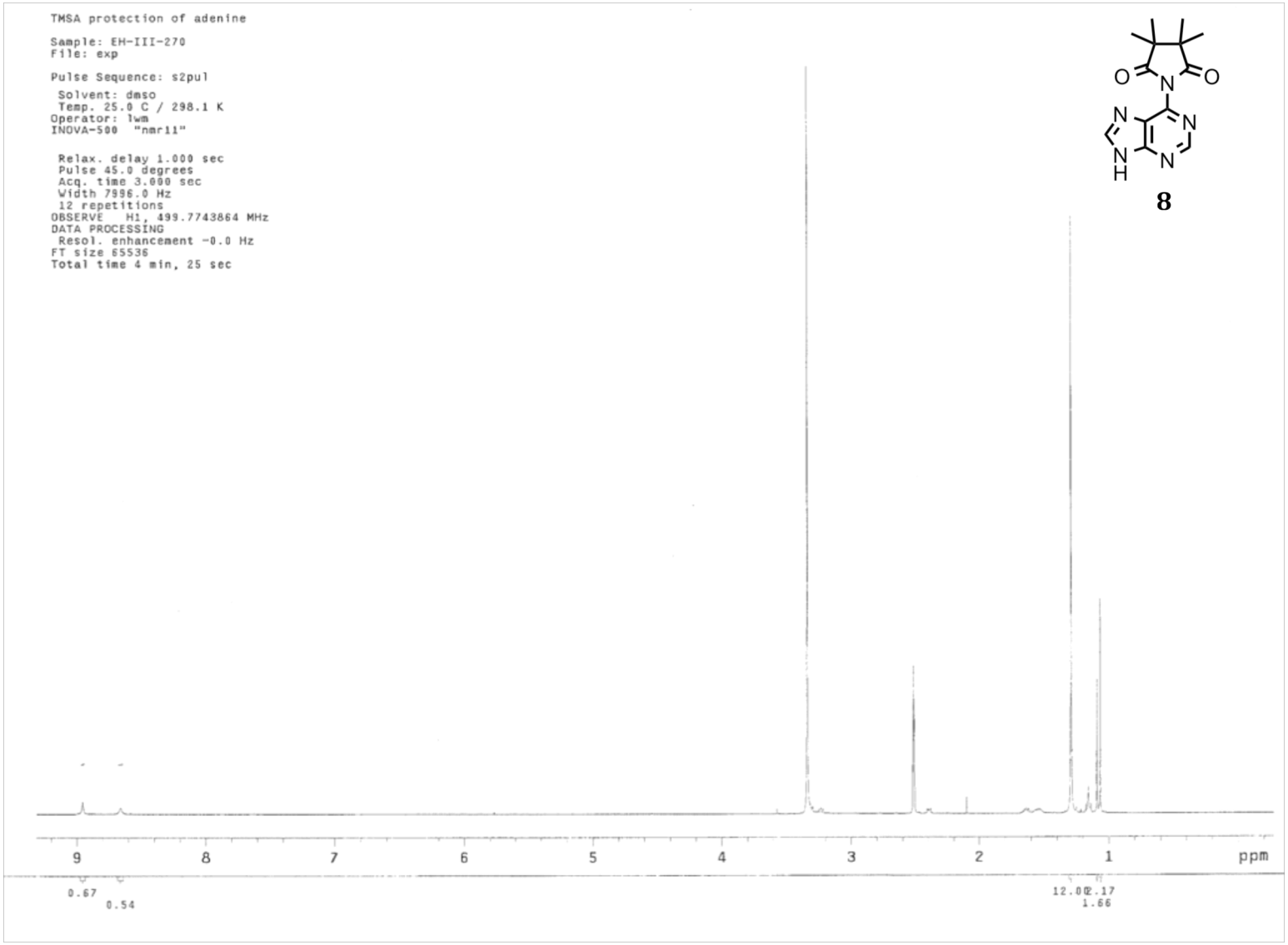
TMSA protection of adenine
Sample: EH-III-270
File: exp
Pulse Sequence: s2pul
Solvent: dmso
Temp. 25.0 C / 298.1 K
Operator: lwm
INOVA-500 "nmr11"
Relax. delay 1.000 sec
Pulse 45.0 degrees
Acq. time 3.000 sec
Width 7996.0 Hz
12 repetitions
OBSERVE H1, 499.7743864 MHz
DATA PROCESSING
Resol. enhancement -0.0 Hz
FT size 65536
Total time 4 min, 25 sec
O
N
O
N
N
N
H
8
9
8
7
6
5
4
3
2
1
ppm
0.67
0.54
12.00
2.17
1.66

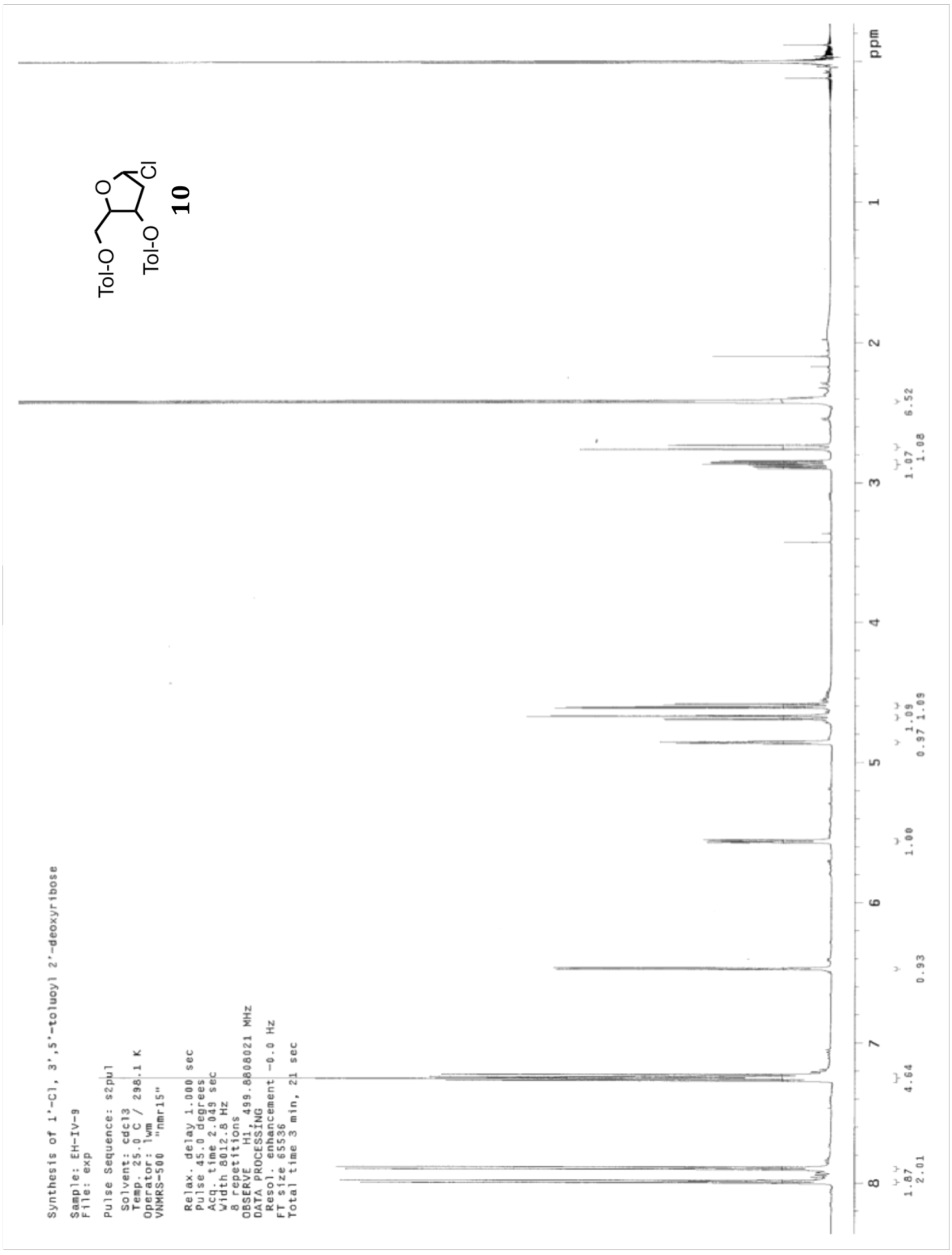
Synthesis of 1'-Cl, 3',5'-toluoyl 2'-deoxyribose
Sample: EH-IV-9
File: exp
Pulse Sequence: s2pul
Solvent: cdcl3
Temp. 25.0 C / 298.1 K
Operator: lwm
VNMRS-500 "nmr15"
Relax. delay 1.000 sec
Pulse 45.0 degrees
Acq. time 2.049 sec
Width 8012.8 Hz
8 repetitions
OBSERVE H1, 499.8808021 MHz
DATA PROCESSING
Resol. enhancement -0.0 Hz
FT size 65536
Total time 3 min, 21 sec
Tol-O
Tol-O
Cl
10
ppm

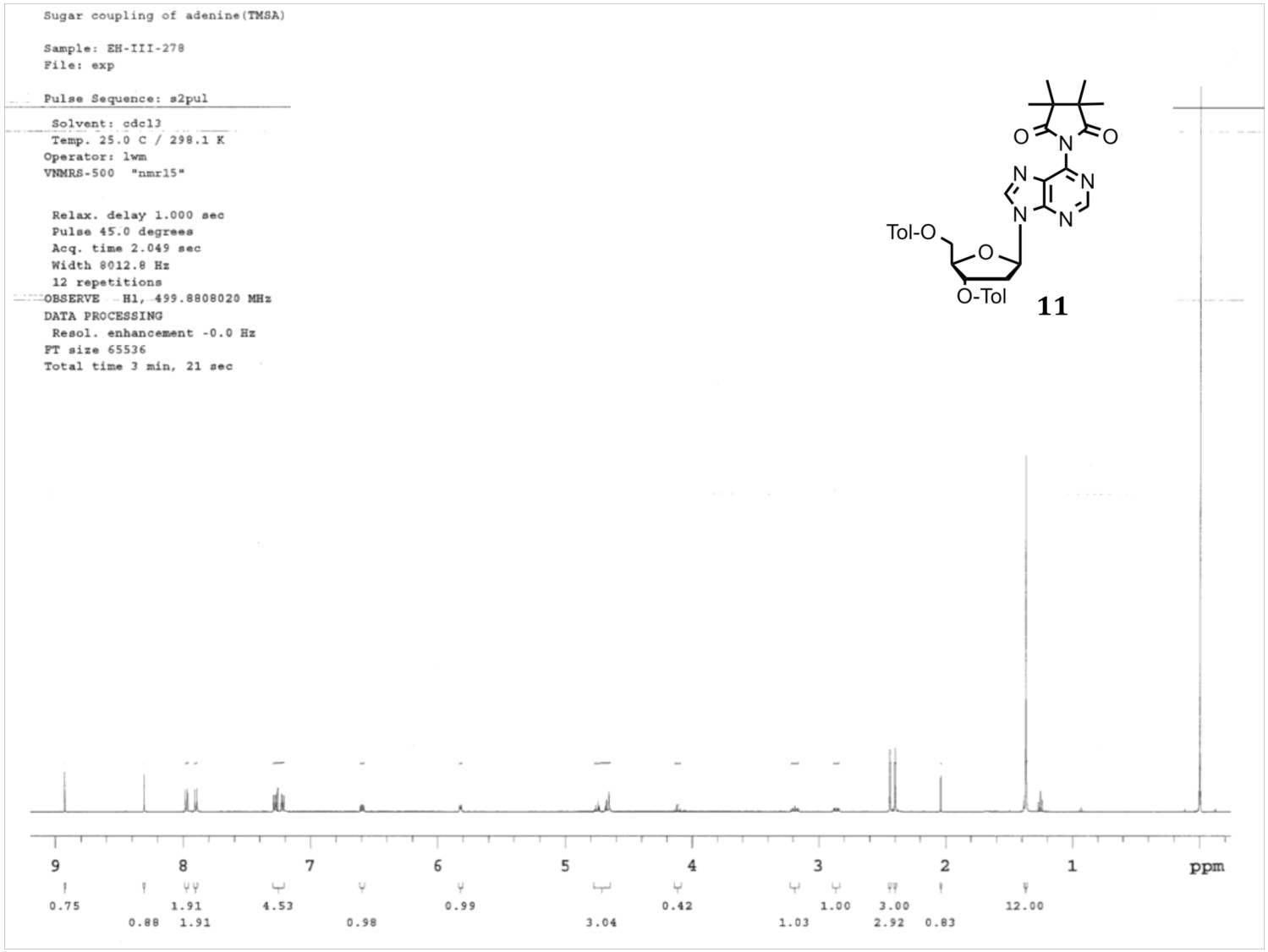
Sugar coupling of adenine(TMSA)
Sample: EH-III-278
File: exp
Pulse Sequence: s2pul
Solvent: cdcl3
Temp. 25.0 C / 298.1 K
Operator: lwm
VNMRS-500 "nmr15"
Relax. delay 1.000 sec
Pulse 45.0 degrees
Acq. time 2.049 sec
Width 8012.8 Hz
12 repetitions
OBSERVE H1, 499.8808020 MHz
DATA PROCESSING
Resol. enhancement -0.0 Hz
FT size 65536
Total time 3 min, 21 sec
Tol-O
O-Tol
11
9
8
7
6
5
4
3
2
1
ppm
0.75
0.88
1.91
1.91
4.53
0.98
0.99
3.04
0.42
1.03
1.00
2.92
3.00
0.83
12.00

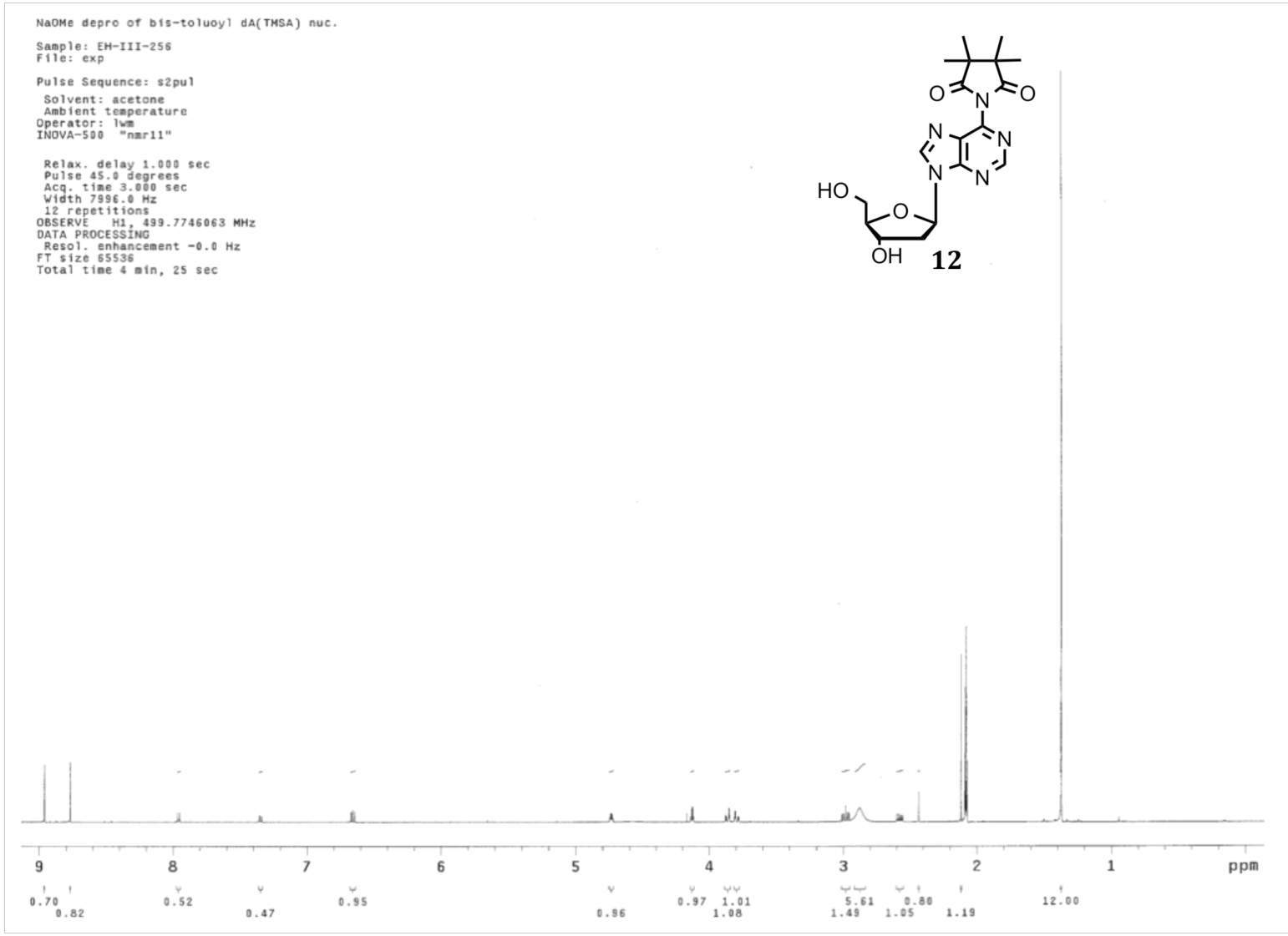
NaOMe depro of bis-toluoyl dA(TMSA) nuc.
Sample: EH-III-256
File: exp
Pulse Sequence: s2pul
Solvent: acetone
Ambient temperature
Operator: lwm
INOVA-500 "nmr11"
Relax. delay 1.000 sec
Pulse 45.0 degrees
Acq. time 3.000 sec
Width 7996.0 Hz
12 repetitions
OBSERVE H1, 499.7746063 MHz
DATA PROCESSING
Resol. enhancement -0.0 Hz
FT size 65536
Total time 4 min, 25 sec
HO
O
OH
12
9
8
7
6
5
4
3
2
1
ppm
0.70
0.82
0.52
0.47
0.95
0.86
0.97
1.01
1.08
5.61
1.49
0.80
1.05
1.19
12.00

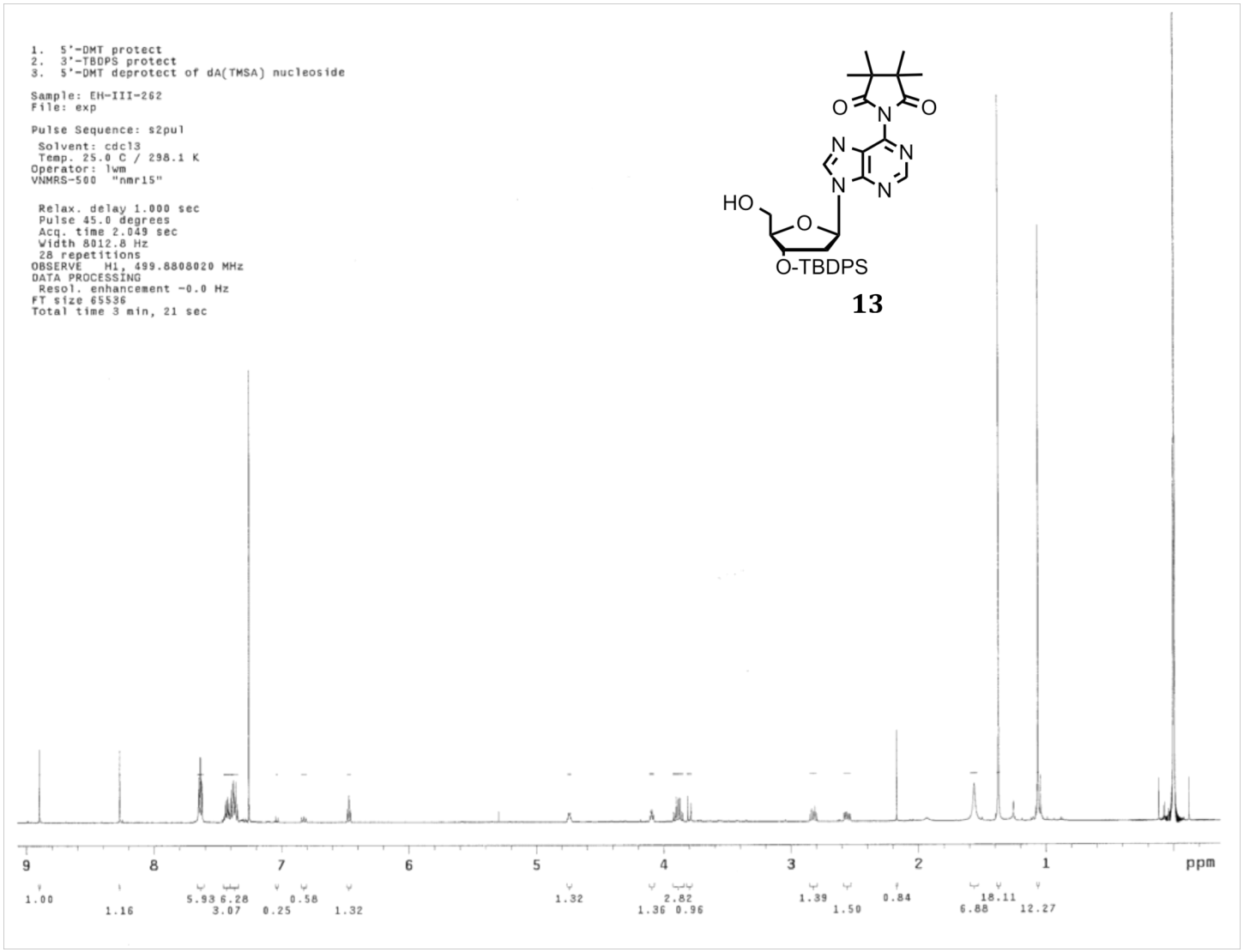
1. 5'-DMT protect
2. 3'-TBDPS protect
3. 5'-DMT deprotect of dA(TMSA) nucleoside
Sample: EH-III-262
File: exp
Pulse Sequence: s2pul
Solvent: cdcl3
Temp. 25.0 C / 298.1 K
Operator: lwm
VNMRS-500 "nmr15"
Relax. delay 1.000 sec
Pulse 45.0 degrees
Acq. time 2.049 sec
Width 8012.8 Hz
28 repetitions
OBSERVE H1, 499.8808020 MHz
DATA PROCESSING
Resol. enhancement -0.0 Hz
FT size 65536
Total time 3 min, 21 sec
HO
O
O-TBDPS
13
9
8
7
6
5
4
3
2
1
ppm
1.00
1.16
5.93
6.28
3.07
0.58
0.25
1.32
1.32
2.82
1.36
0.96
1.39
1.50
0.84
18.11
6.88
12.27

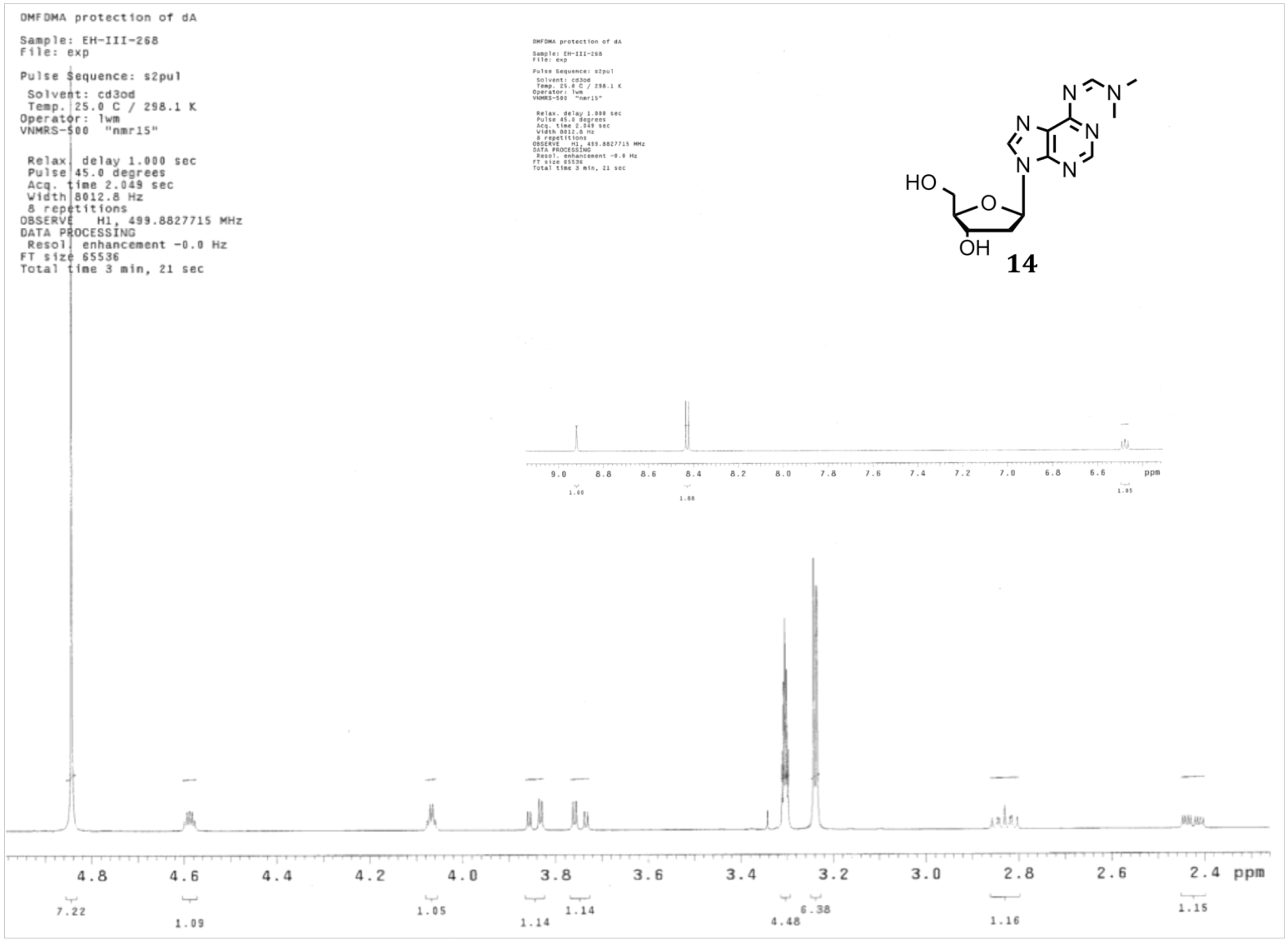
DMFDMA protection of dA
Sample: EH-III-268
File: exp
Pulse Sequence: s2pul
Solvent: cd3od
Temp. 25.0 C / 298.1 K
Operator: lwm
VNMRS-500 "nmr15"
Relax. delay 1.000 sec
Pulse 45.0 degrees
Acq. time 2.049 sec
Width 8012.8 Hz
8 repetitions
OBSERVE H1, 499.8827715 MHz
DATA PROCESSING
Resol. enhancement -0.0 Hz
FT size 65536
Total time 3 min, 21 sec
HO
O
OH
14
ppm
7.22
1.09
1.05
1.14
1.14
4.48
6.38
1.16
1.15

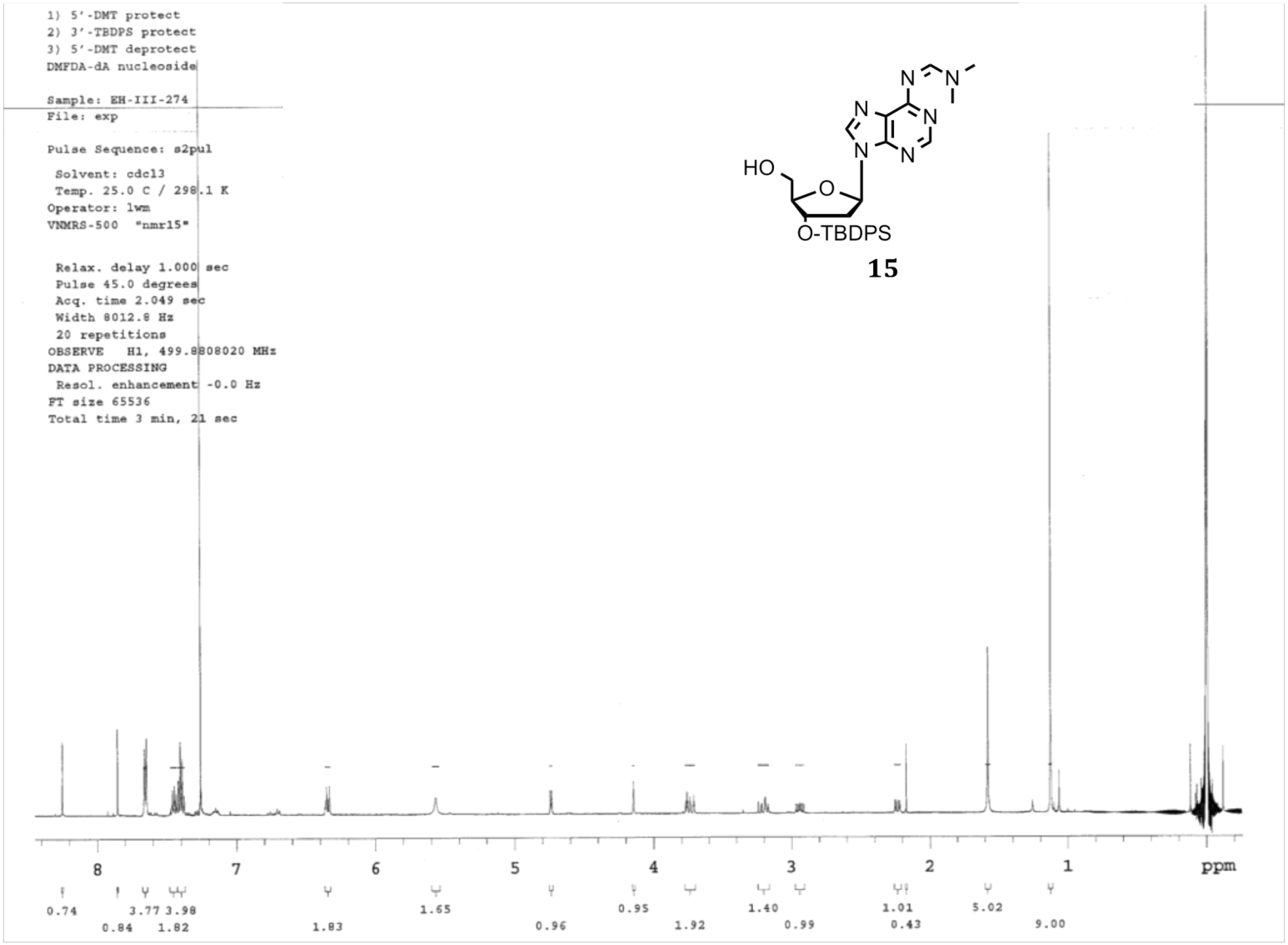
1) 5'-DMT protect
2) 3'-TBDPS protect
3) 5'-DMT deprotect
DMFDA-dA nucleoside
Sample: EH-III-274
File: exp
Pulse Sequence: s2pul
Solvent: cdcl3
Temp. 25.0 C / 298.1 K
Operator: lwm
VNMRS-500 "nmr15"
Relax. delay 1.000 sec
Pulse 45.0 degrees
Acq. time 2.049 sec
Width 8012.8 Hz
20 repetitions
OBSERVE H1, 499.8808020 MHz
DATA PROCESSING
Resol. enhancement -0.0 Hz
FT size 65536
Total time 3 min, 21 sec
HO
O
O-TBDPS
15
8
7
6
5
4
3
2
1
ppm
0.74
0.84
3.77
3.98
1.82
1.83
1.65
0.96
0.95
1.92
1.40
0.99
1.01
0.43
5.02
9.00

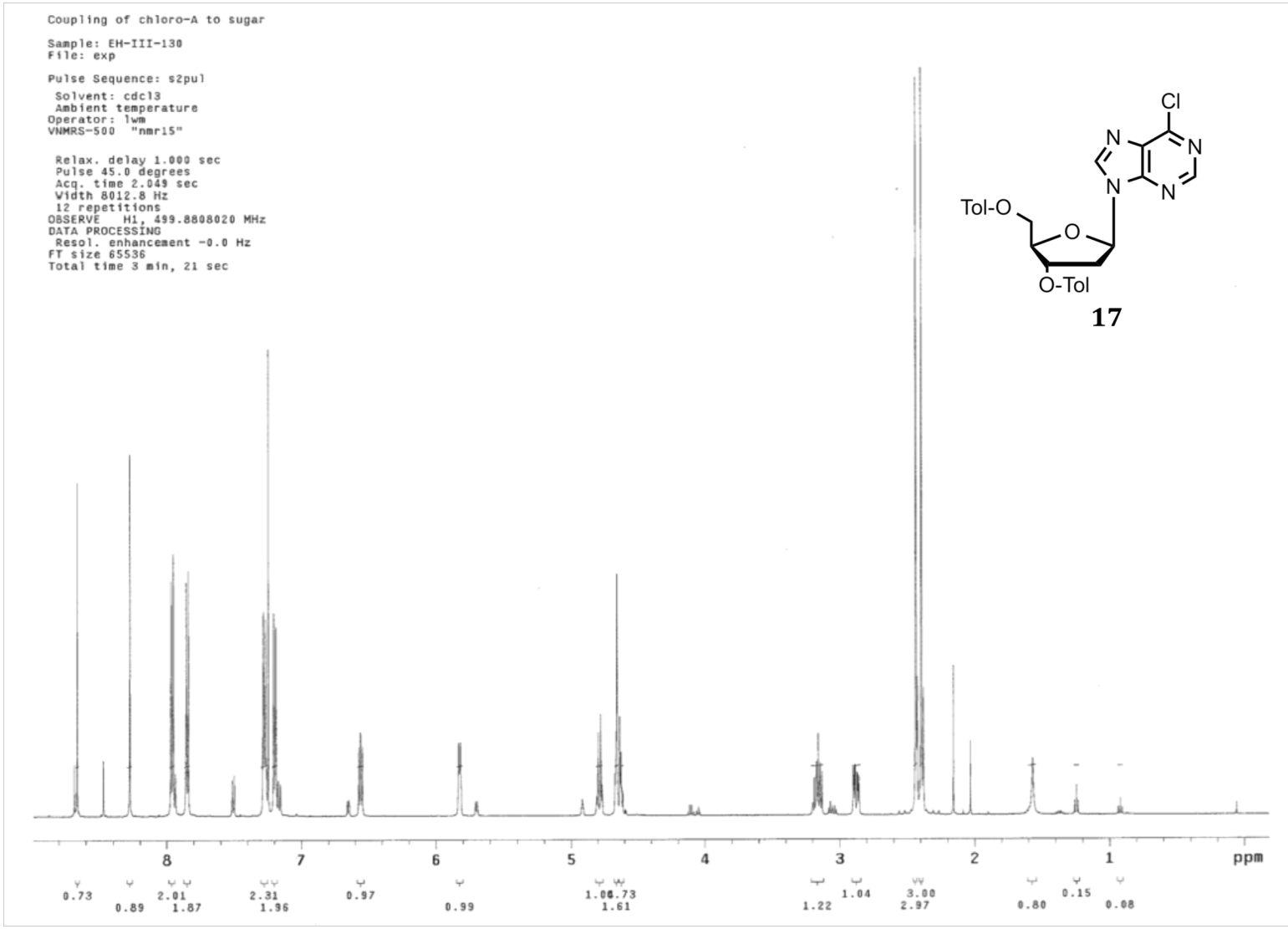
Coupling of chloro-A to sugar
Sample: EH-III-130
File: exp
Pulse Sequence: s2pul
Solvent: cdcl3
Ambient temperature
Operator: lwm
VNMRS-500 "nmr15"
Relax. delay 1.000 sec
Pulse 45.0 degrees
Acq. time 2.049 sec
Width 8012.8 Hz
12 repetitions
OBSERVE H1, 499.8808020 MHz
DATA PROCESSING
Resol. enhancement -0.0 Hz
FT size 65536
Total time 3 min, 21 sec
Cl
N
N
N
N
Tol-O
O
O-Tol
17
8
7
6
5
4
3
2
1
ppm
0.73
0.89
2.01
1.87
2.31
1.96
0.97
0.99
1.61
1.22
1.04
3.00
2.97
0.80
0.15
0.08

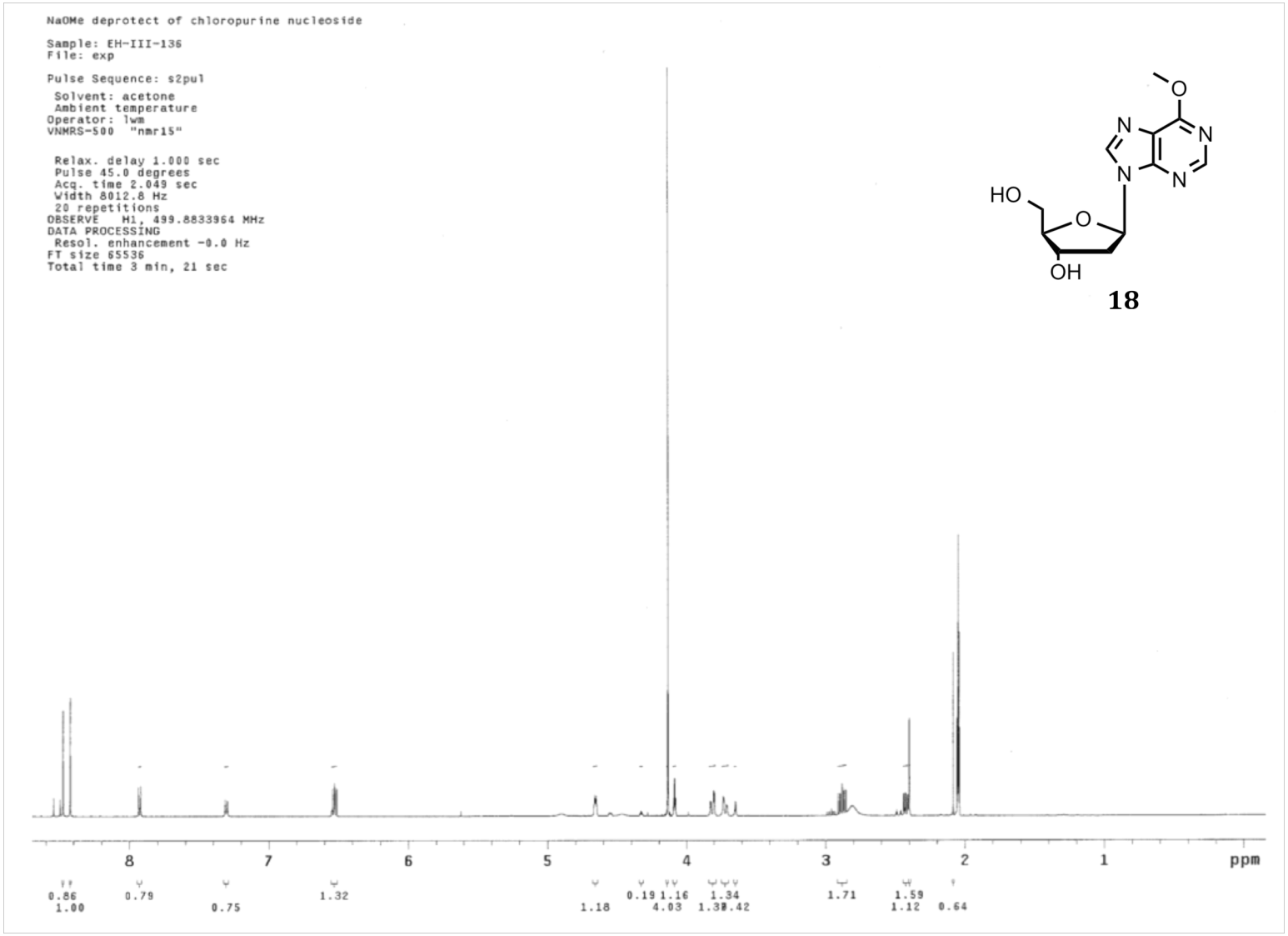
NaOMe deprotect of chloropurine nucleoside
Sample: EH-III-136
File: exp
Pulse Sequence: s2pul
Solvent: acetone
Ambient temperature
Operator: lwm
VNMRS-500 "nmr15"
Relax. delay 1.000 sec
Pulse 45.0 degrees
Acq. time 2.049 sec
Width 8012.8 Hz
20 repetitions
OBSERVE H1, 499.8833964 MHz
DATA PROCESSING
Resol. enhancement -0.0 Hz
FT size 65536
Total time 3 min, 21 sec
HO
O
OH
N
N
N
N
O
18
8
7
6
5
4
3
2
1
ppm
0.86
1.00
0.79
0.75
1.32
1.18
0.19
1.16
4.03
1.34
1.38
2.42
1.71
1.59
1.12
0.64

9-BBN of post wittig 3'-TBS chloro-dA

Sample: EH-III-180
File: exp

Pulse Sequence: s2pul
Solvent: cdcl3
Temp. 25.0 C / 298.1 K
Operator: lwm
VNMRS-500 "nmr15"

Relax. delay 1.000 sec
Pulse 45.0 degrees
Acq. time 2.049 sec
Width 8012.8 Hz
16 repetitions
OBSERVE H1, 499.8808021 MHz
DATA PROCESSING
Resol. enhancement -0.0 Hz
FT size 65536
Total time 3 min, 21 sec

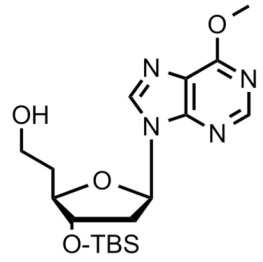

21

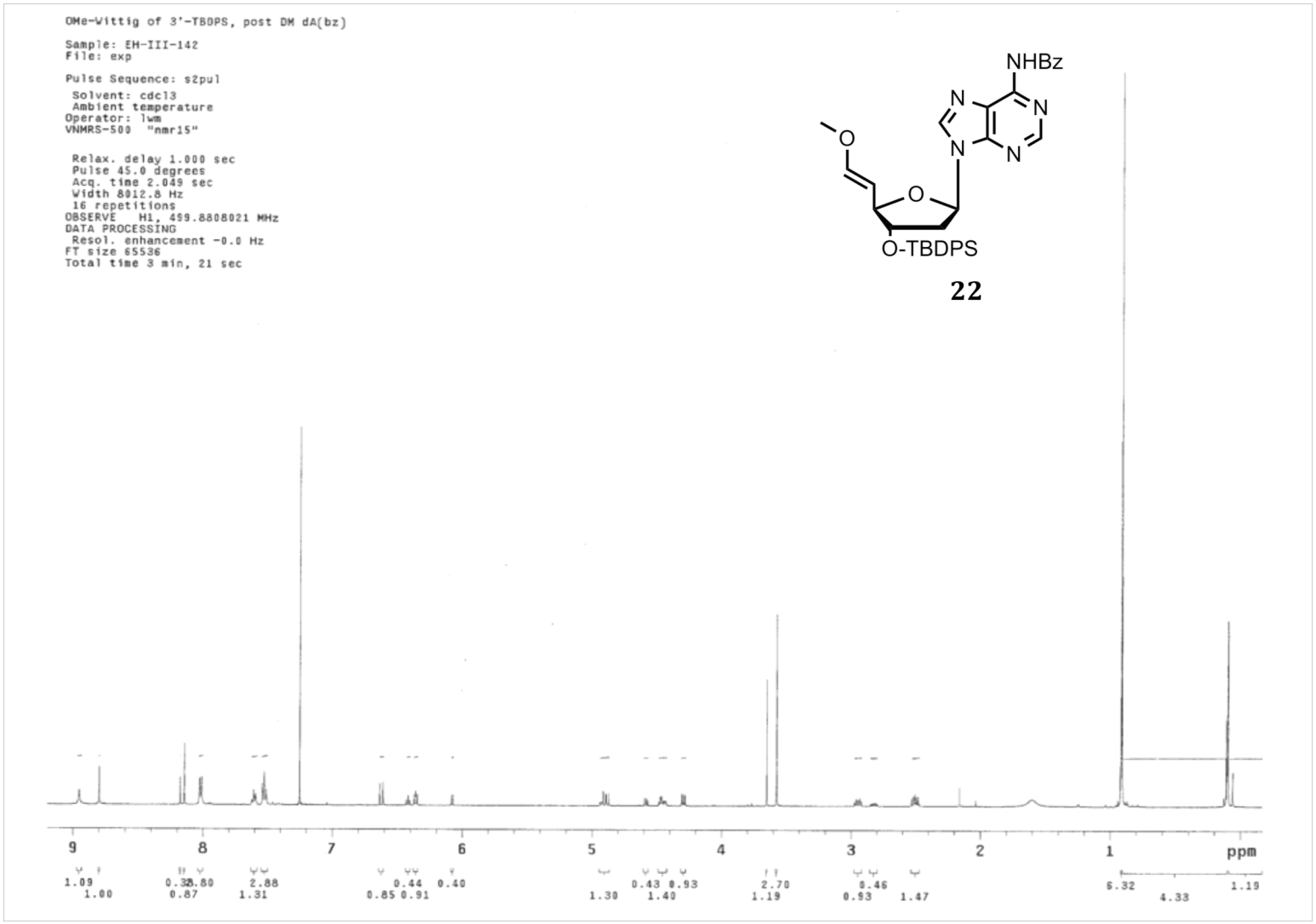
OMe-Wittig of 3'-TBDPS, post DM dA(bz)
Sample: EH-III-142
File: exp
Pulse Sequence: s2pul
Solvent: cdcl3
Ambient temperature
Operator: lwm
VNMRS-500 "nmr15"
Relax. delay 1.000 sec
Pulse 45.0 degrees
Acq. time 2.049 sec
Width 8012.8 Hz
16 repetitions
OBSERVE H1, 499.8808021 MHz
DATA PROCESSING
Resol. enhancement -0.0 Hz
FT size 65536
Total time 3 min, 21 sec
NHBz
N
N
N
N
O
O
O-TBDPS
22
9
8
7
6
5
4
3
2
1
ppm
1.09
1.00
0.38
0.87
0.80
2.88
1.31
0.44
0.85
0.91
0.40
1.30
0.43
1.40
0.93
2.70
1.19
0.46
0.93
1.47
6.32
4.33
1.19

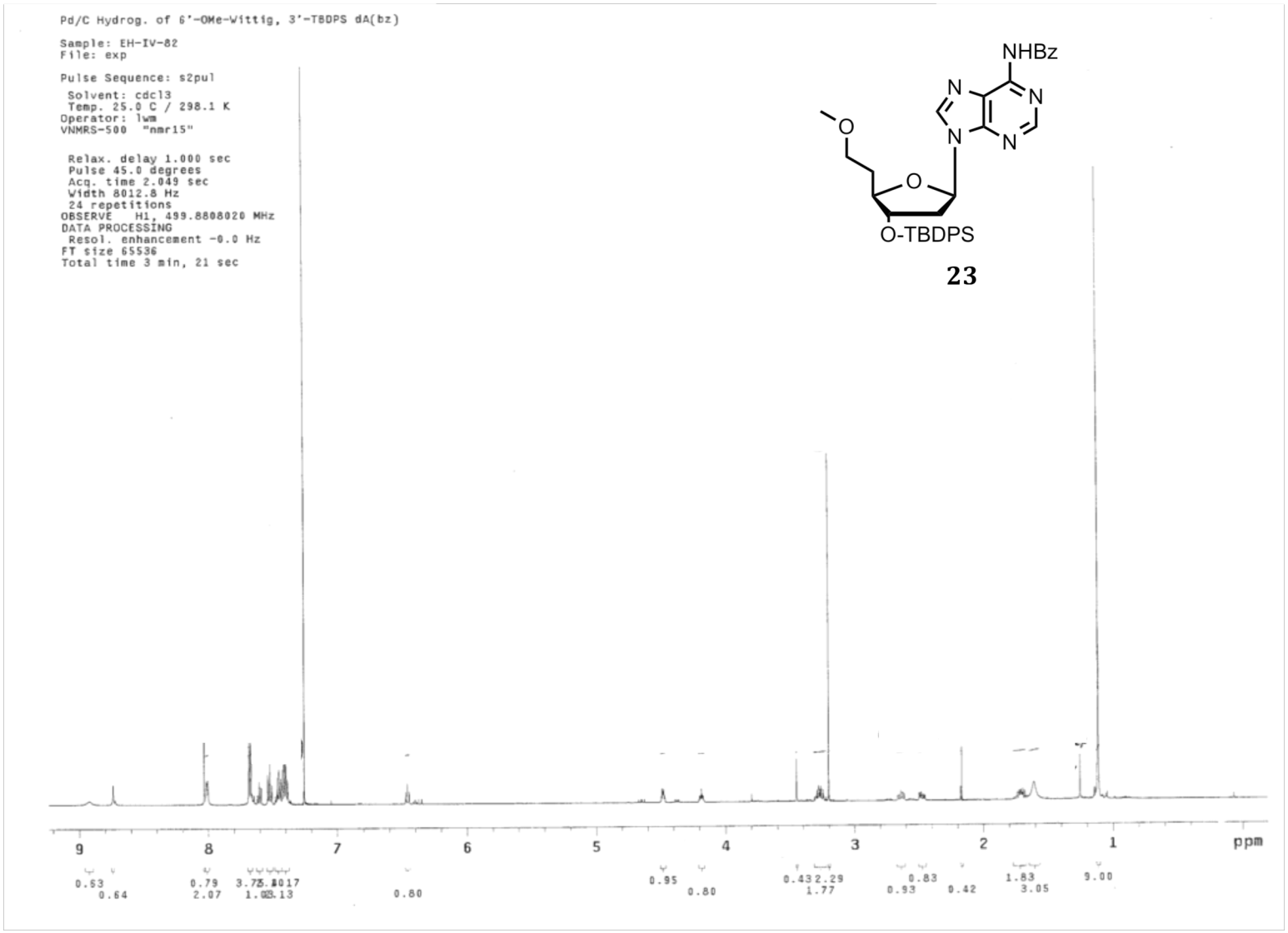
Pd/C Hydrog. of 6'-OMe-Wittig, 3'-TBDPS dA(bz)
Sample: EH-IV-82
File: exp
Pulse Sequence: s2pul
Solvent: cdcl3
Temp. 25.0 C / 298.1 K
Operator: lwm
VNMRS-500 "nmr15"
Relax. delay 1.000 sec
Pulse 45.0 degrees
Acq. time 2.049 sec
Width 8012.8 Hz
24 repetitions
OBSERVE H1, 499.8808020 MHz
DATA PROCESSING
Resol. enhancement -0.0 Hz
FT size 65536
Total time 3 min, 21 sec
NHBz
N
N
N
N
O
O
O-TBDPS
23
9
8
7
6
5
4
3
2
1
ppm
0.53
0.64
0.79
2.07
0.80
0.95
0.80
0.43
2.29
1.77
0.83
0.93
0.42
1.83
3.05
9.00

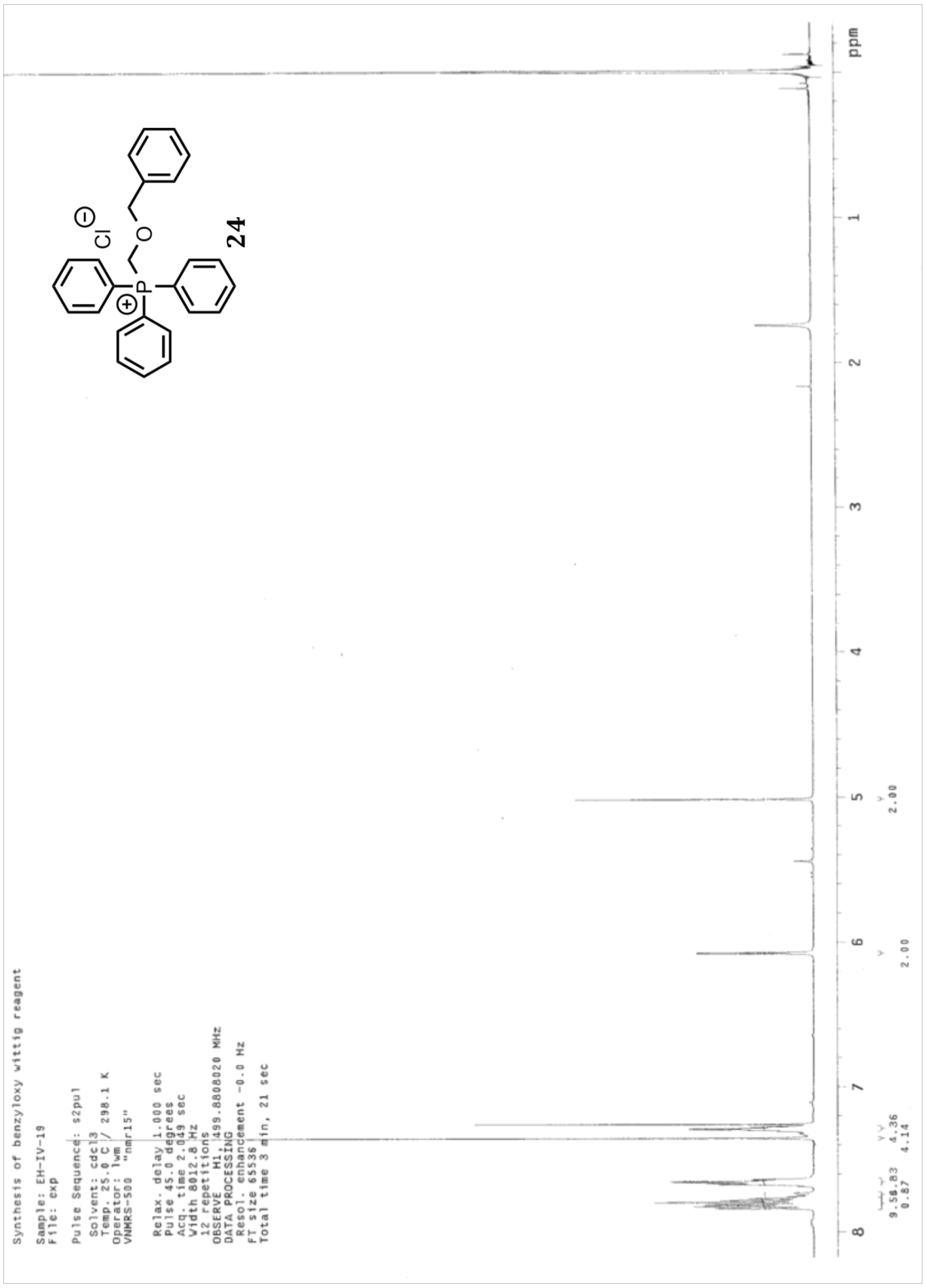
Synthesis of benzyloxy wittig reagent
Sample: EH-IV-19
File: exp
Pulse Sequence: s2pul
Solvent: cdcl3
Temp. 25.0 C / 298.1 K
Operator: lwm
VNMRS-500 "nmr15"
Relax. delay 1.000 sec
Pulse 45.0 degrees
Acq. time 2.049 sec
Width 8012.8 Hz
12 repetitions
OBSERVE H1, 499.8808020 MHz
DATA PROCESSING
Resol: enhancement -0.0 Hz
FT size 65536
Total time 3 min, 21 sec
Cl
O
P
24
ppm
9.58
8.83
0.87
4.36
4.14
2.00
2.00

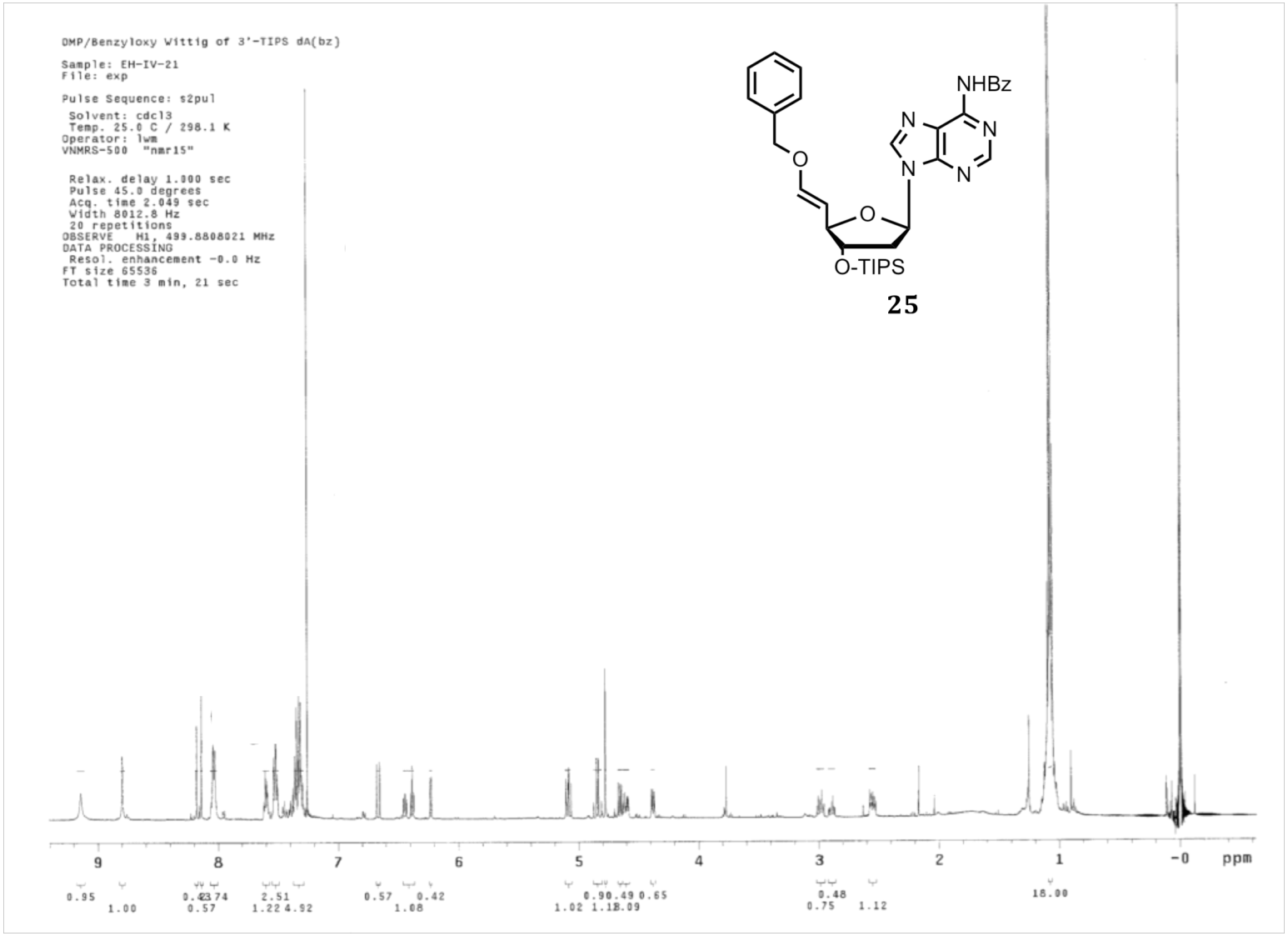
DMP/Benzyloxy Wittig of 3'-TIPS dA(bz)
Sample: EH-IV-21
File: exp
Pulse Sequence: s2pul
Solvent: cdcl3
Temp. 25.0 C / 298.1 K
Operator: lwm
VNMRS-500 "nmr15"
Relax. delay 1.000 sec
Pulse 45.0 degrees
Acq. time 2.049 sec
Width 8012.8 Hz
20 repetitions
OBSERVE H1, 499.8808021 MHz
DATA PROCESSING
Resol. enhancement -0.0 Hz
FT size 65536
Total time 3 min, 21 sec
NHBz
N
N
N
N
O
O
O-TIPS
25
9
8
7
6
5
4
3
2
1
-0
ppm
0.95
1.00
0.42
0.57
3.74
1.22
2.51
4.92
0.57
0.42
1.08
0.90
1.02
0.49
1.18
0.65
1.09
0.48
0.75
1.12
18.00

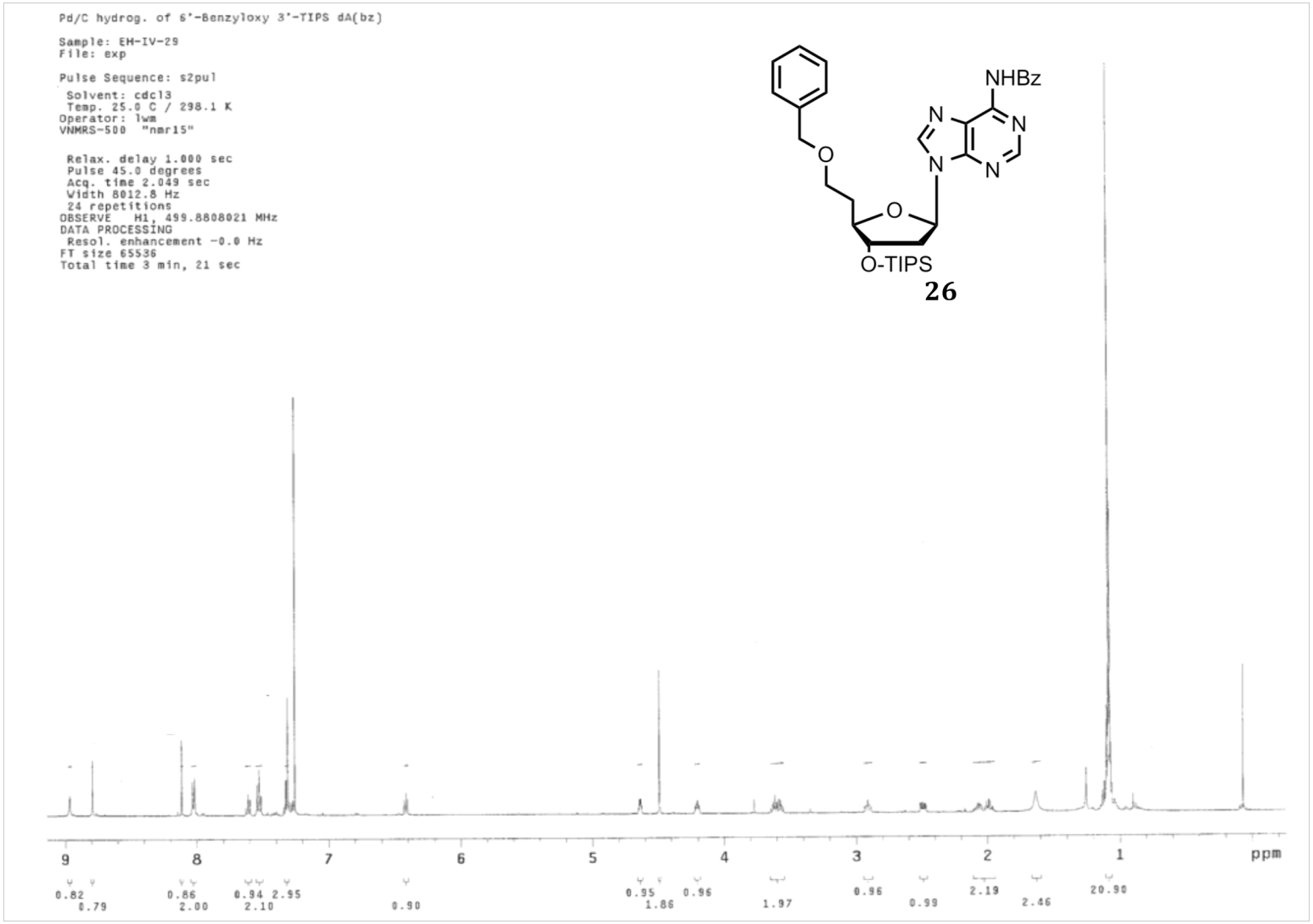
Pd/C hydrog. of 6'-Benzyloxy 3'-TIPS dA(bz)
Sample: EH-IV-29
File: exp
Pulse Sequence: s2pul
Solvent: cdcl3
Temp. 25.0 C / 298.1 K
Operator: lwm
VNMRS-500 "nmr15"
Relax. delay 1.000 sec
Pulse 45.0 degrees
Acq. time 2.049 sec
Width 8012.8 Hz
24 repetitions
OBSERVE H1, 499.8808021 MHz
DATA PROCESSING
Resol. enhancement -0.0 Hz
FT size 65536
Total time 3 min, 21 sec
NHBz
N
N
N
N
O
O
O-TIPS
26
9
8
7
6
5
4
3
2
1
ppm
0.82
0.79
0.86
2.00
0.94
2.10
2.95
0.90
0.95
1.86
0.96
1.97
0.96
0.99
2.19
2.46
20.90

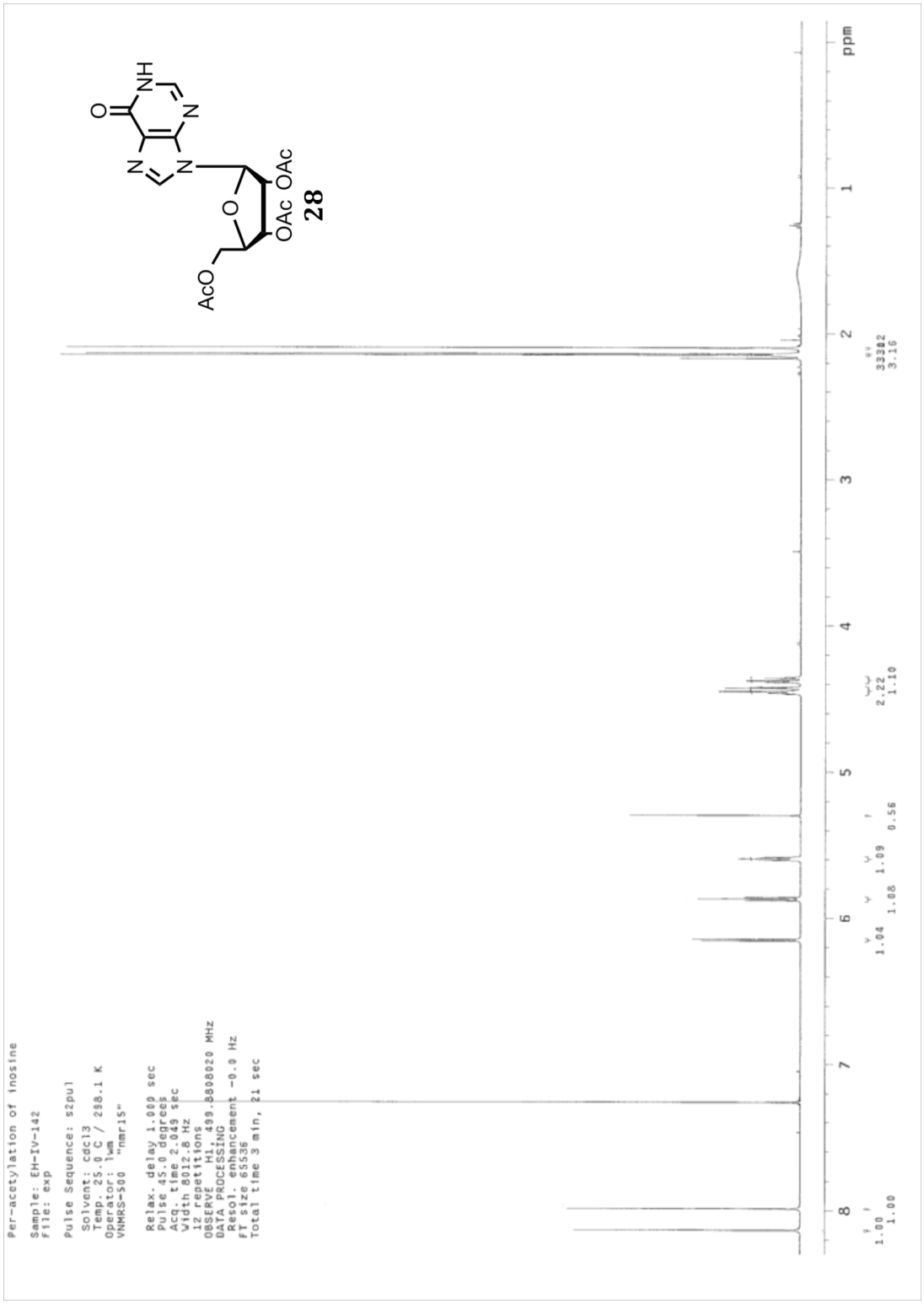
Per-acetylation of Inosine
Sample: EH-IV-142
File: exp
Pulse Sequence: s2pul
Solvent: cdcl3
Temp. 25.0 C / 298.1 K
Operator: lwm
VNMRS-500 "mar15"
Relax. delay 1.000 sec
Pulse 45.0 degrees
Acq. time 2.049 sec
Width 8012.8 Hz
12 repetitions
OBSERVE H1, 499.8808020 MHz
DATA PROCESSING
Resol enhancement -0.9 Hz
FT size 65536
Total time 3 min, 21 sec
NH
O
N
N
N
N
O
AcO
OAc OAc
28
ppm
1.00
1.00
1.04
1.08
1.09
0.56
2.22
1.10
33382
3.16

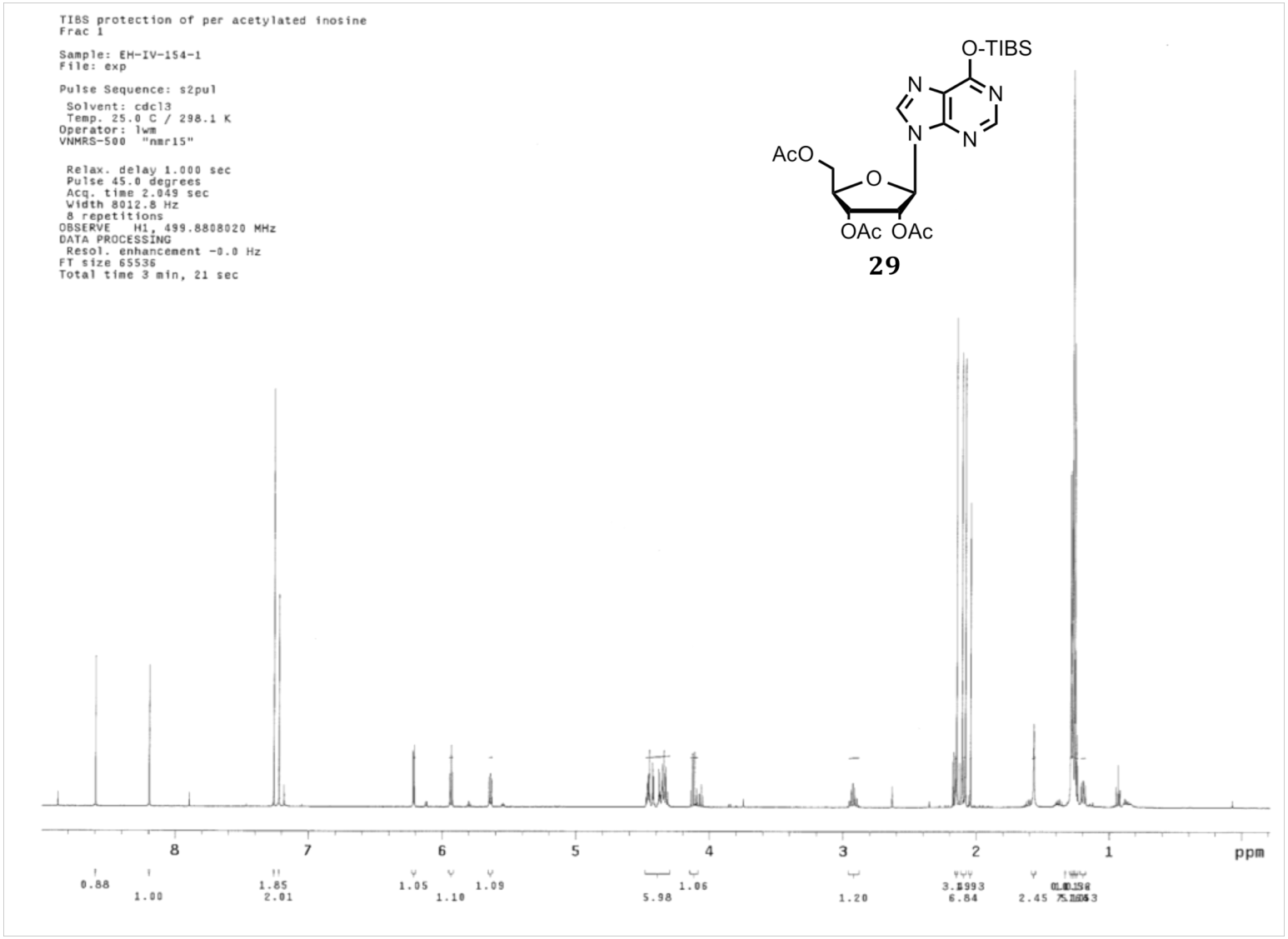
TIBS protection of per acetylated inosine
Frac 1
Sample: EH-IV-154-1
File: exp
Pulse Sequence: s2pul
Solvent: cdcl3
Temp. 25.0 C / 298.1 K
Operator: lwm
VNMRS-500 "nmr15"
Relax. delay 1.000 sec
Pulse 45.0 degrees
Acq. time 2.049 sec
Width 8012.8 Hz
8 repetitions
OBSERVE H1, 499.8808020 MHz
DATA PROCESSING
Resol. enhancement -0.0 Hz
FT size 65536
Total time 3 min, 21 sec
O-TIBS
N
N
N
N
AcO
O
OAc OAc
29
8
7
6
5
4
3
2
1
ppm
0.88
1.00
1.85
2.01
1.05
1.10
1.09
5.98
1.06
1.20
6.84
2.45

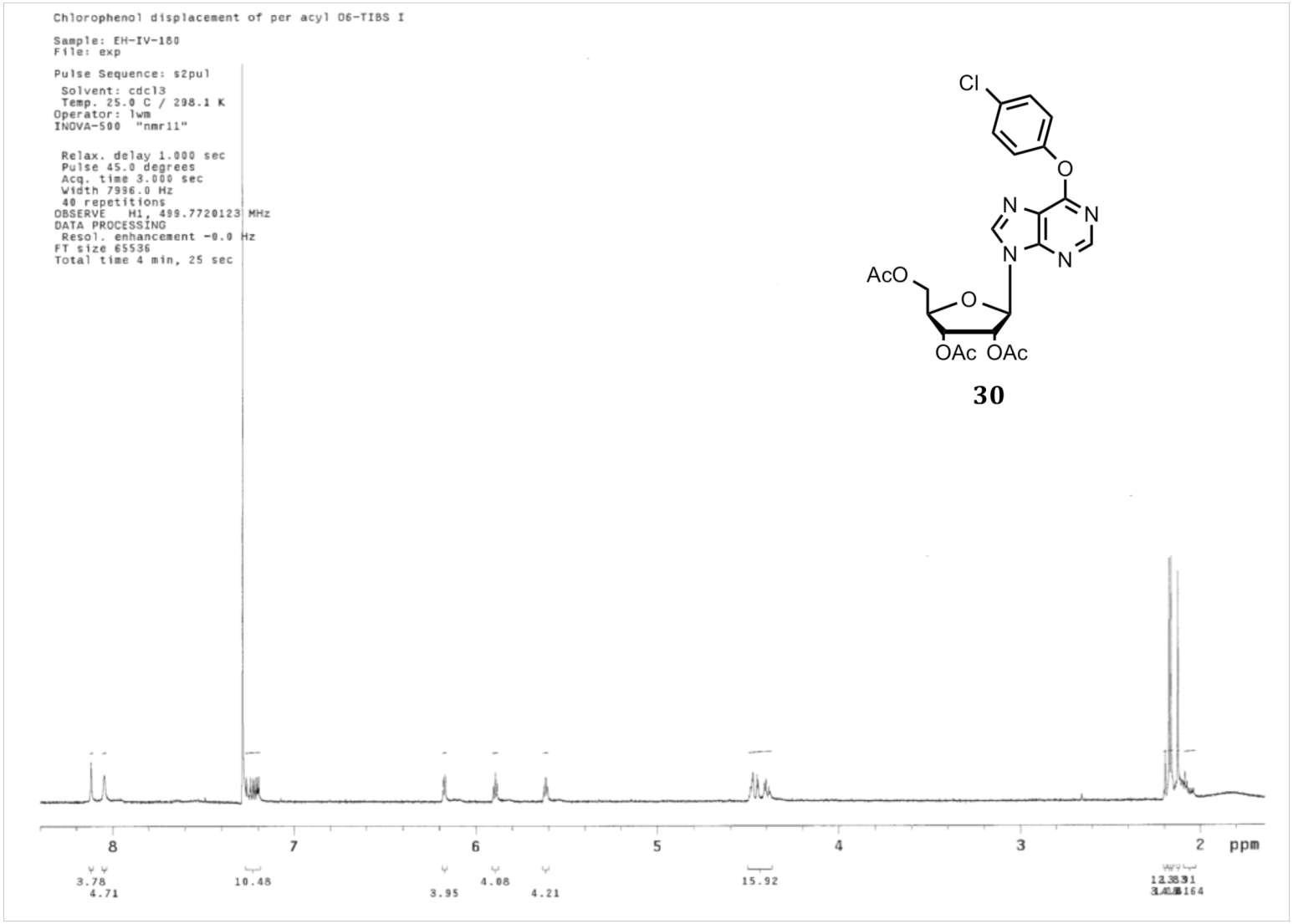
Chlorophenol displacement of per acyl O6-TIBS I
Sample: EH-IV-160
File: exp
Pulse Sequence: s2pul
Solvent: cdcl3
Temp. 25.0 C / 298.1 K
Operator: lwm
INOVA-500 "nmr11"
Relax. delay 1.000 sec
Pulse 45.0 degrees
Acq. time 3.000 sec
Width 7996.0 Hz
40 repetitions
OBSERVE H1, 499.7720123 MHz
DATA PROCESSING
Resol. enhancement -0.0 Hz
FT size 65536
Total time 4 min, 25 sec
Cl
O
N
N
N
N
AcO
O
OAc OAc
8
7
6
5
4
3
2
ppm
3.78
4.71
10.48
3.95
4.08
4.21
15.92

30

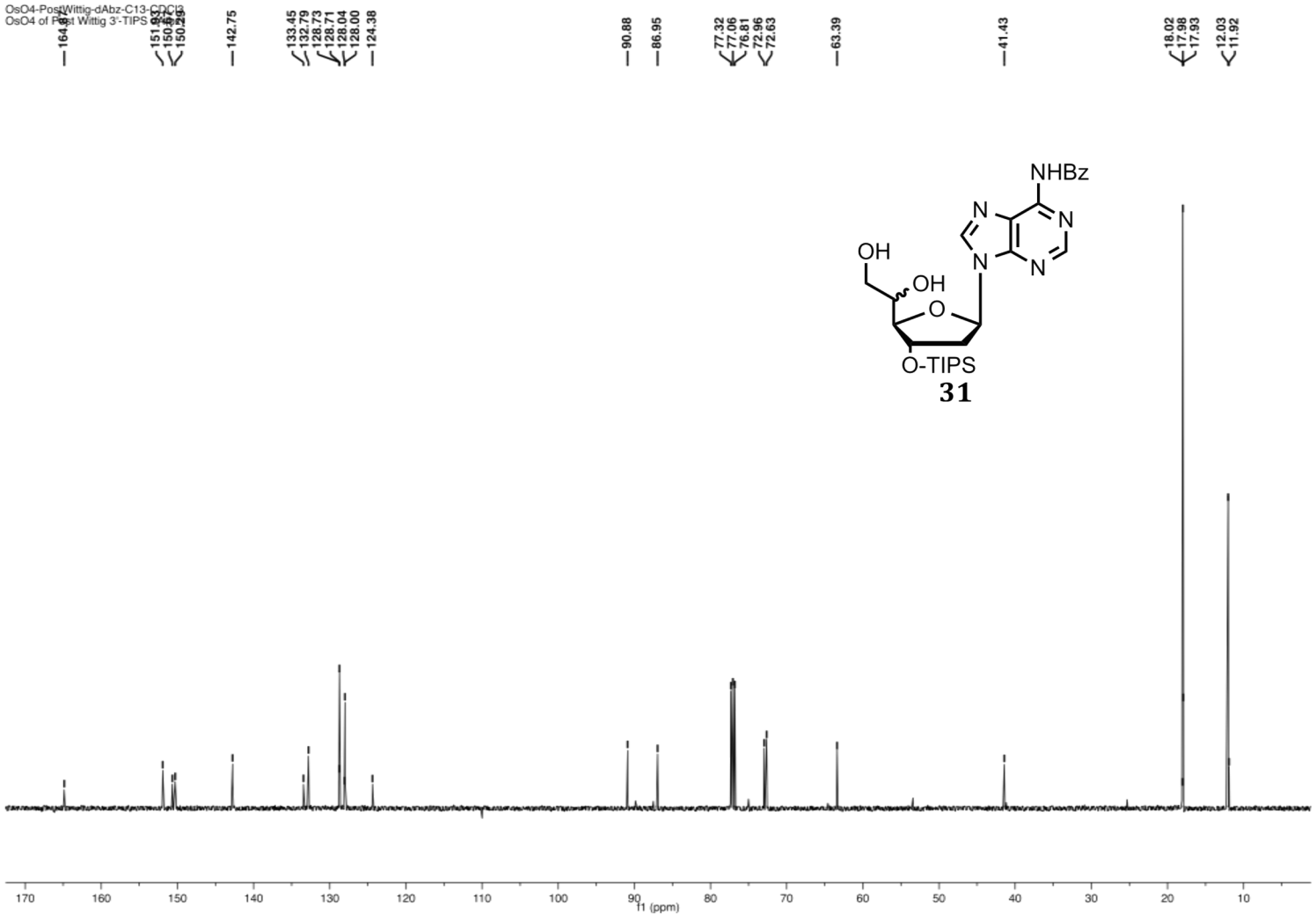
OsO4-PostWittig-dAbz-C13-CDCl3
OsO4 of Post Wittig 3'-TIPS
164.87
151.93
150.47
150.23
142.75
133.45
132.79
128.73
128.71
128.04
128.00
124.38
90.88
86.95
77.32
77.06
76.81
72.96
72.63
63.39
41.43
18.02
17.98
17.93
12.03
11.92
NHBz
N
N
N
N
OH
OH
O
O-TIPS
31
170
160
150
140
130
120
110
100
90
80
70
60
50
40
30
20
10
f1 (ppm)

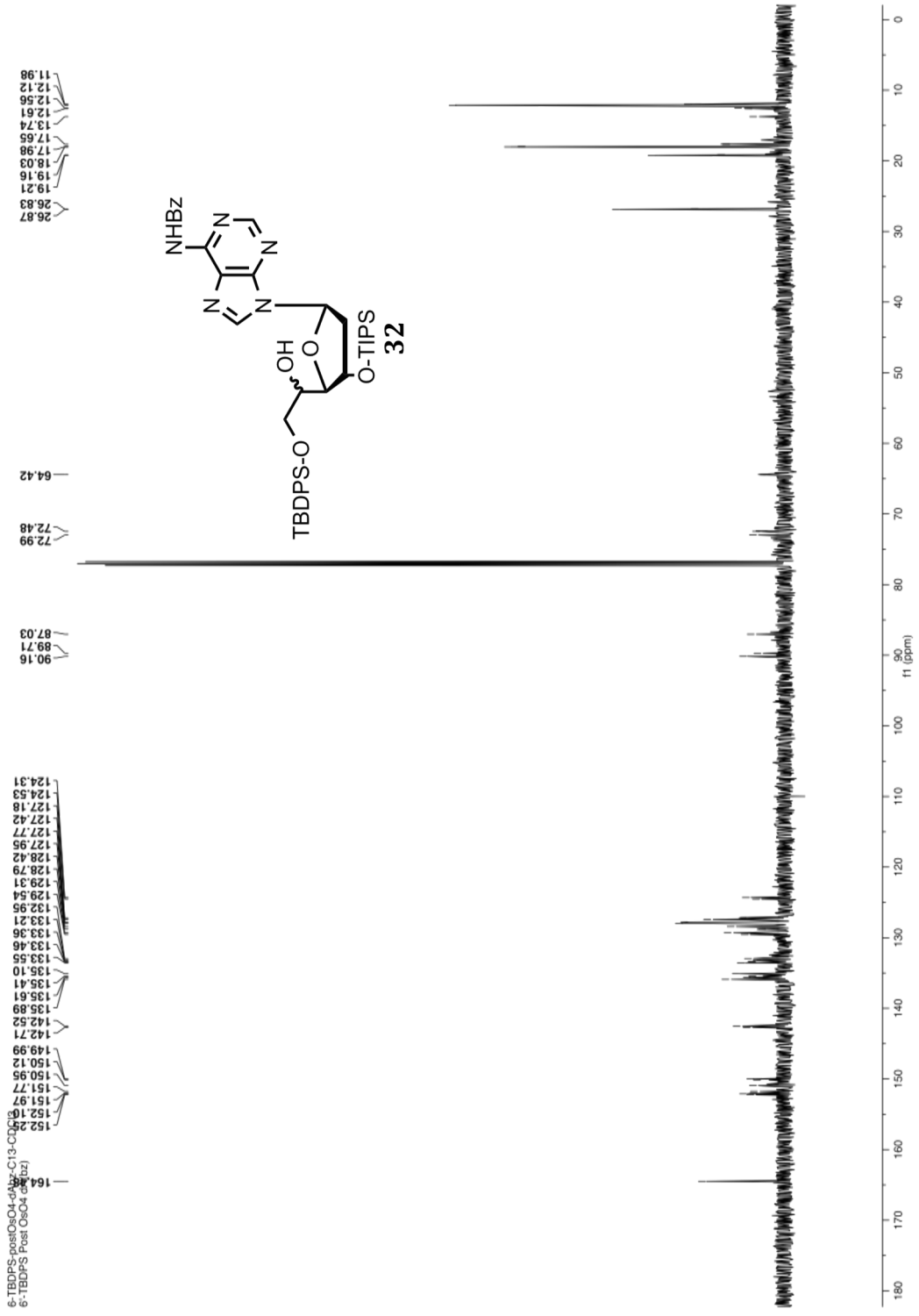
6-TBDPS-postOsO4-dAbz-C13-CDCl3
6-TBDPS Post OsO4 (dAbz)
NHBz
TBDPS-O
OH
O
O-TIPS
32
f1 (ppm)

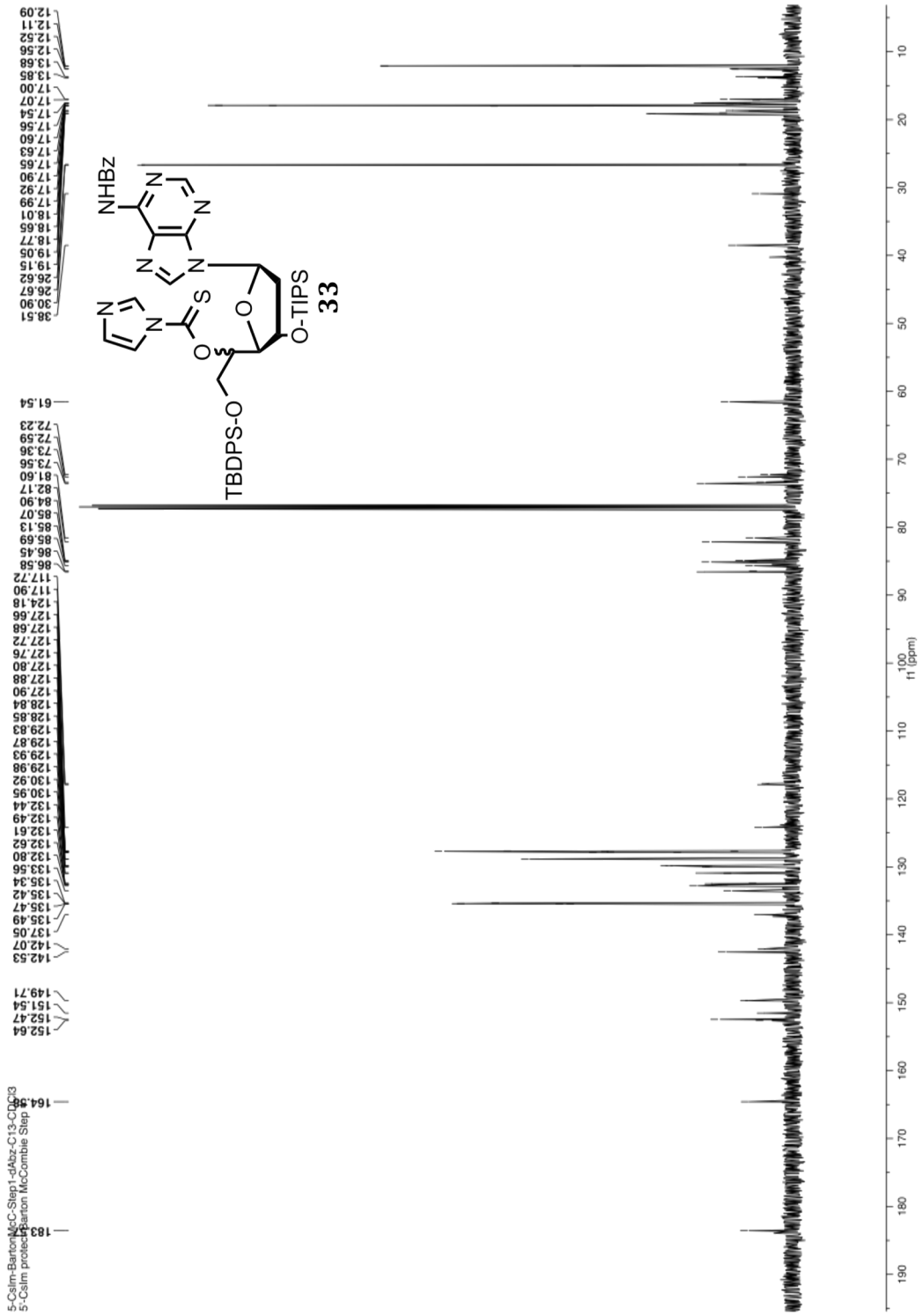
5-CsIm-BartonMcC-Step1-dAbz-C13-CDCl3
5'-CsIm protected Barton McCombie Step
NHBz
TBDPS-O
O-TIPS
33
f1 (ppm)

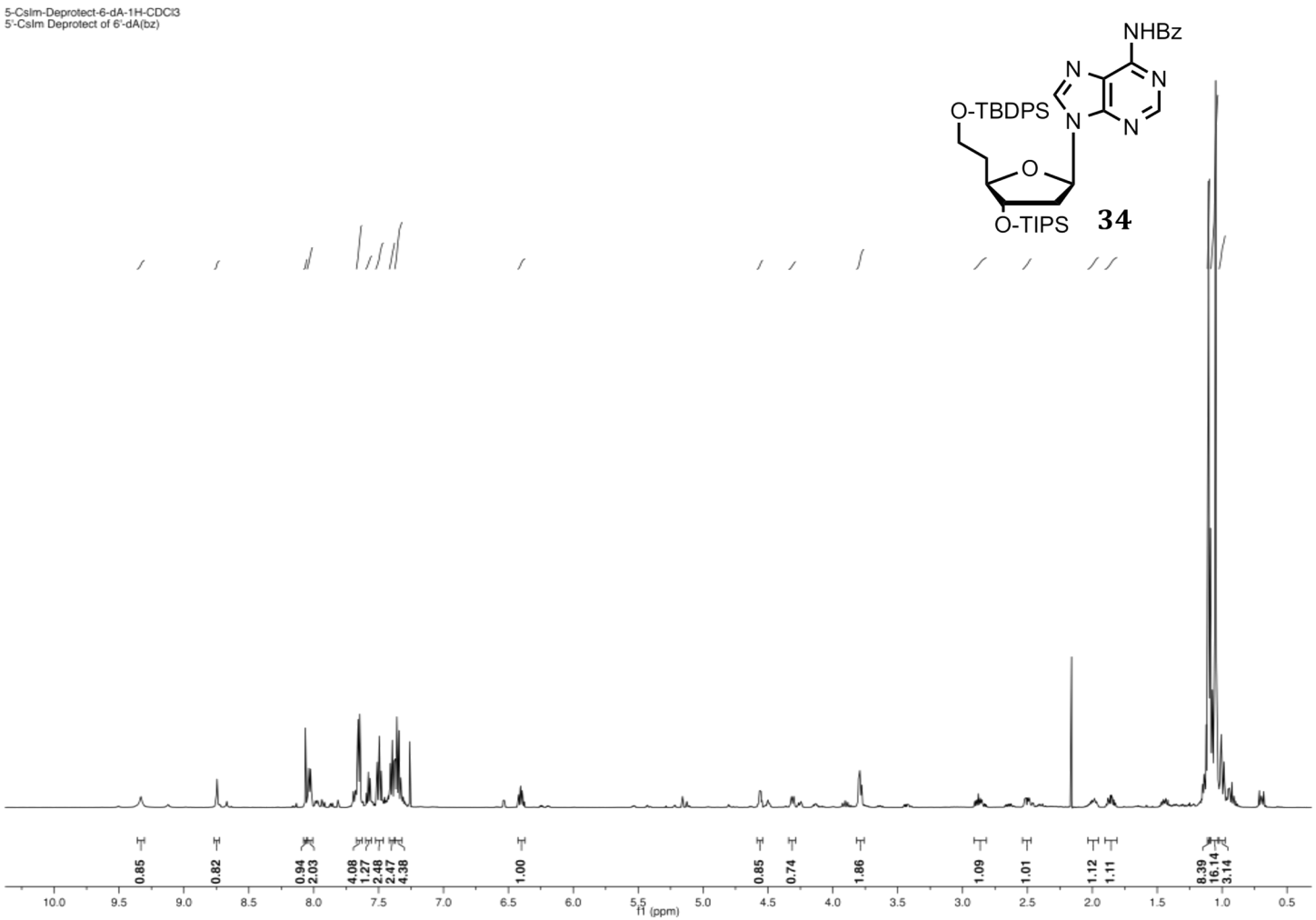
5-Cslm-Deprotect-6-dA-1H-CDCl3
5'-Cslm Deprotect of 6'-dA(bz)
NHBz
N
N
O-TBDPS
N
N
O
O-TIPS
34
0.85
0.82
0.94
2.03
4.08
1.27
2.48
2.47
4.38
1.00
0.85
0.74
1.86
1.09
1.01
1.12
1.11
8.39
16.14
3.14
10.0
9.5
9.0
8.5
8.0
7.5
7.0
6.5
6.0
5.5
5.0
4.5
4.0
3.5
3.0
2.5
2.0
1.5
1.0
0.5
f1 (ppm)

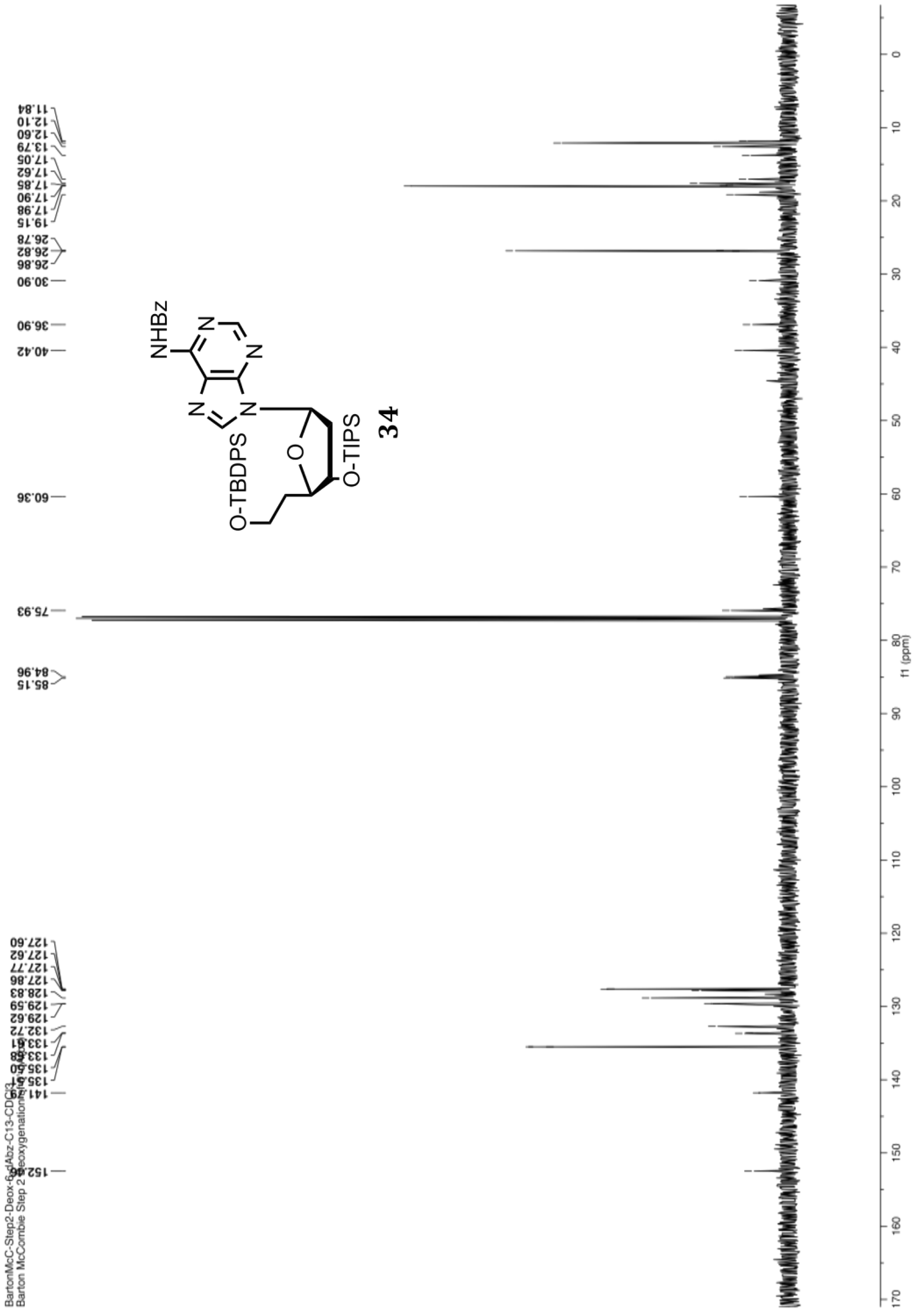
NHBz
O-TBDPS
O-TIPS
34
BartonMcC-Step2-Deox-6-dAbz-C13-CDCl3
Barton McCombie Step 2 deoxygenation.esp
f1 (ppm)

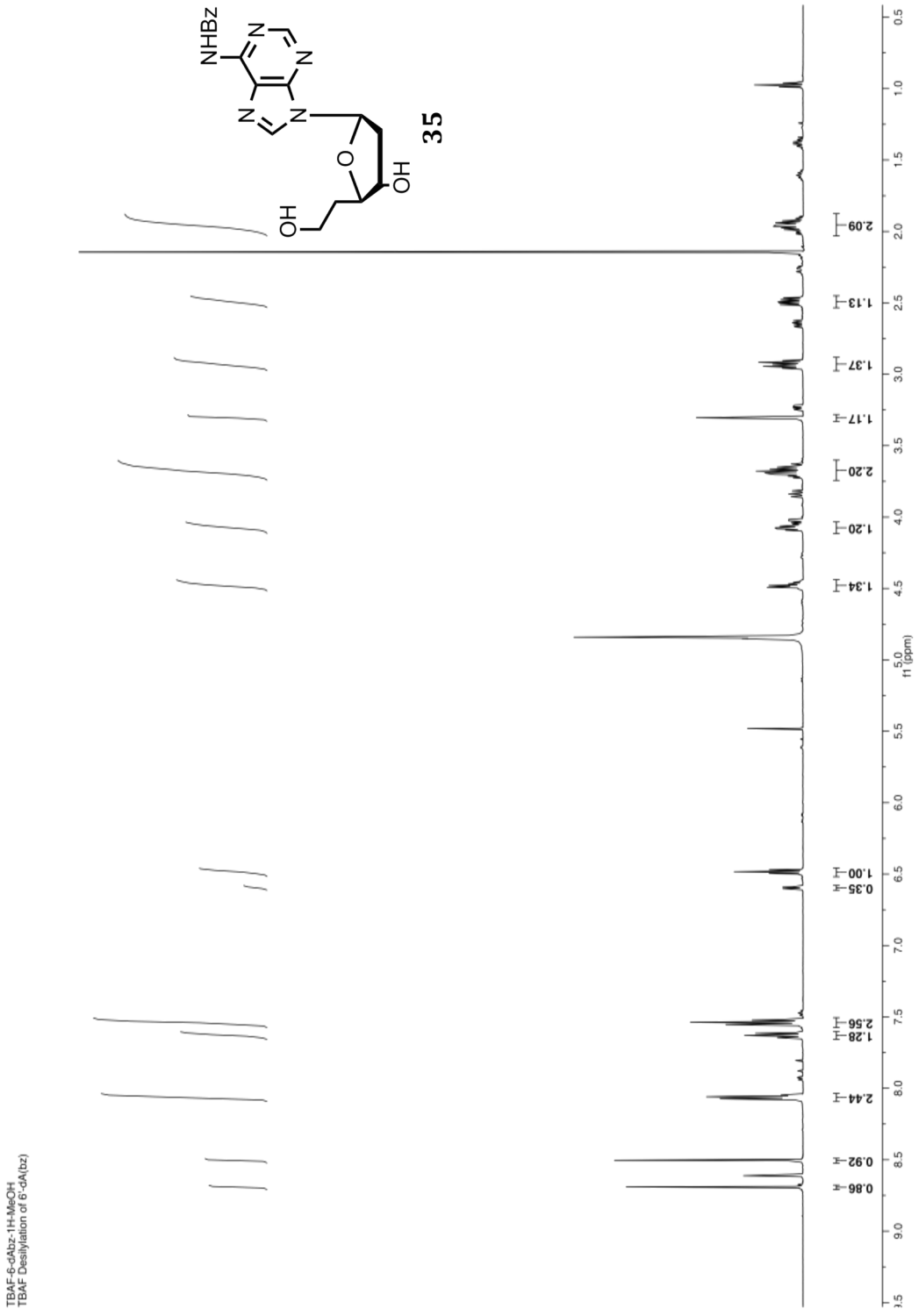
TBAF-6-dAbz-1H-MeOH
TBAF Desilylation of 6'-dA(bz)
NHBz
N
N
N
N
O
OH
OH
35
0.86
0.92
2.44
1.28
2.56
0.35
1.00
1.34
1.20
2.20
1.17
1.37
1.13
2.09
f1 (ppm)

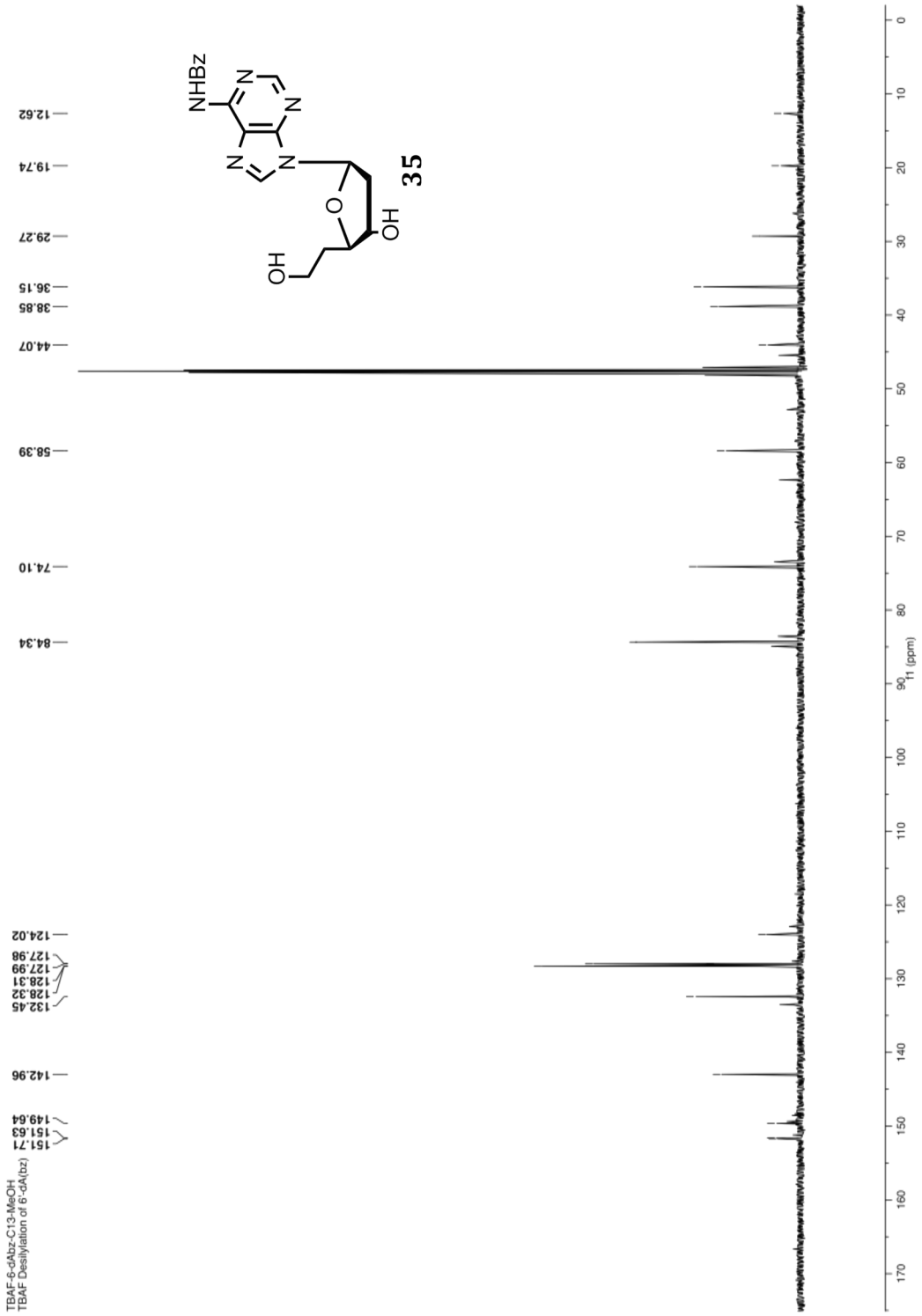
TBAF-6-dAbz-C13-MeOH
TBAF Desilylation of 6'-dA(bz)
151.71
151.63
149.64
142.96
132.45
128.32
128.31
127.99
127.98
124.02
84.34
74.10
58.39
44.07
38.85
36.15
29.27
19.74
12.62
NHBz
N
N
N
N
O
OH
OH
35
f1 (ppm)

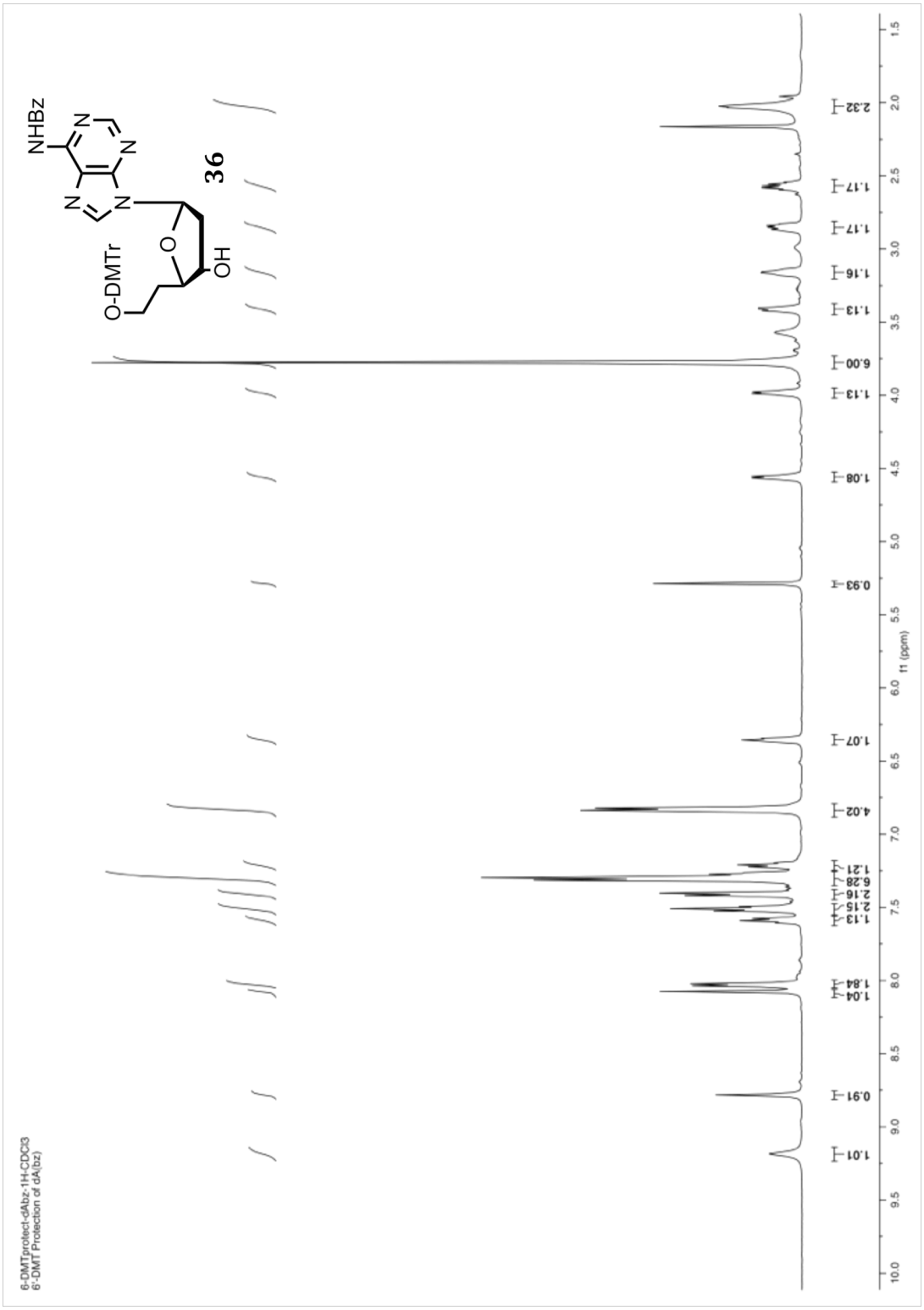
6-DMTprotect-dAbz-1H-CDCl3
6'-DMT Protection of dA(bz)
NHBz
O-DMTr
OH
36
f1 (ppm)

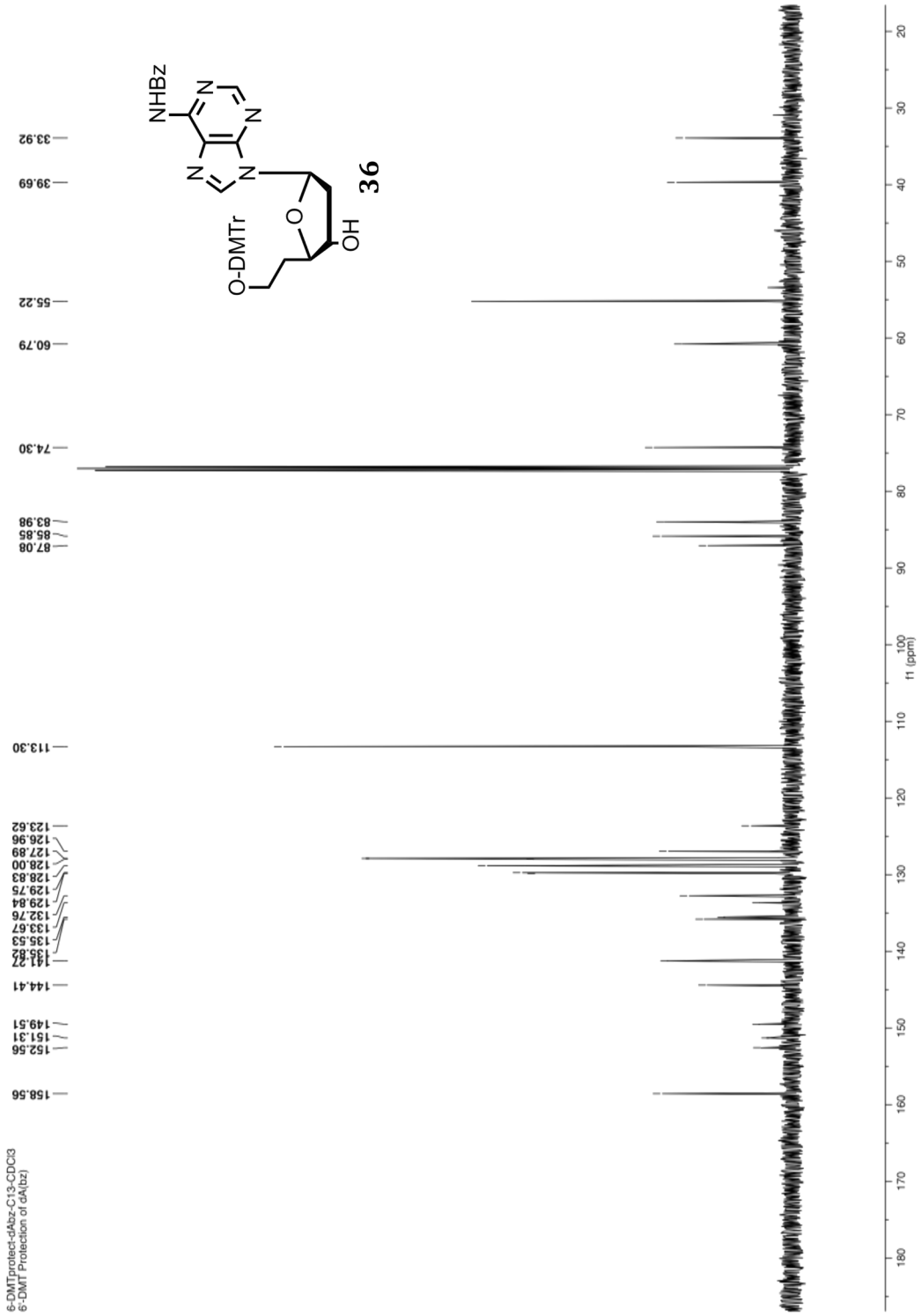
6-DMTprotect-dAbz-C13-CDCl3
6'-DMT Protection of dA(bz)
158.56
152.56
151.31
149.51
144.41
141.27
135.82
135.53
133.67
132.76
129.84
129.75
128.83
128.00
127.89
126.96
123.62
113.30
87.08
85.85
83.98
74.30
60.79
55.22
39.69
33.92
NHBz
O-DMTr
OH
36
f1 (ppm)

EH-4-298-1H
6'-dA bis phosphite phosphitylation

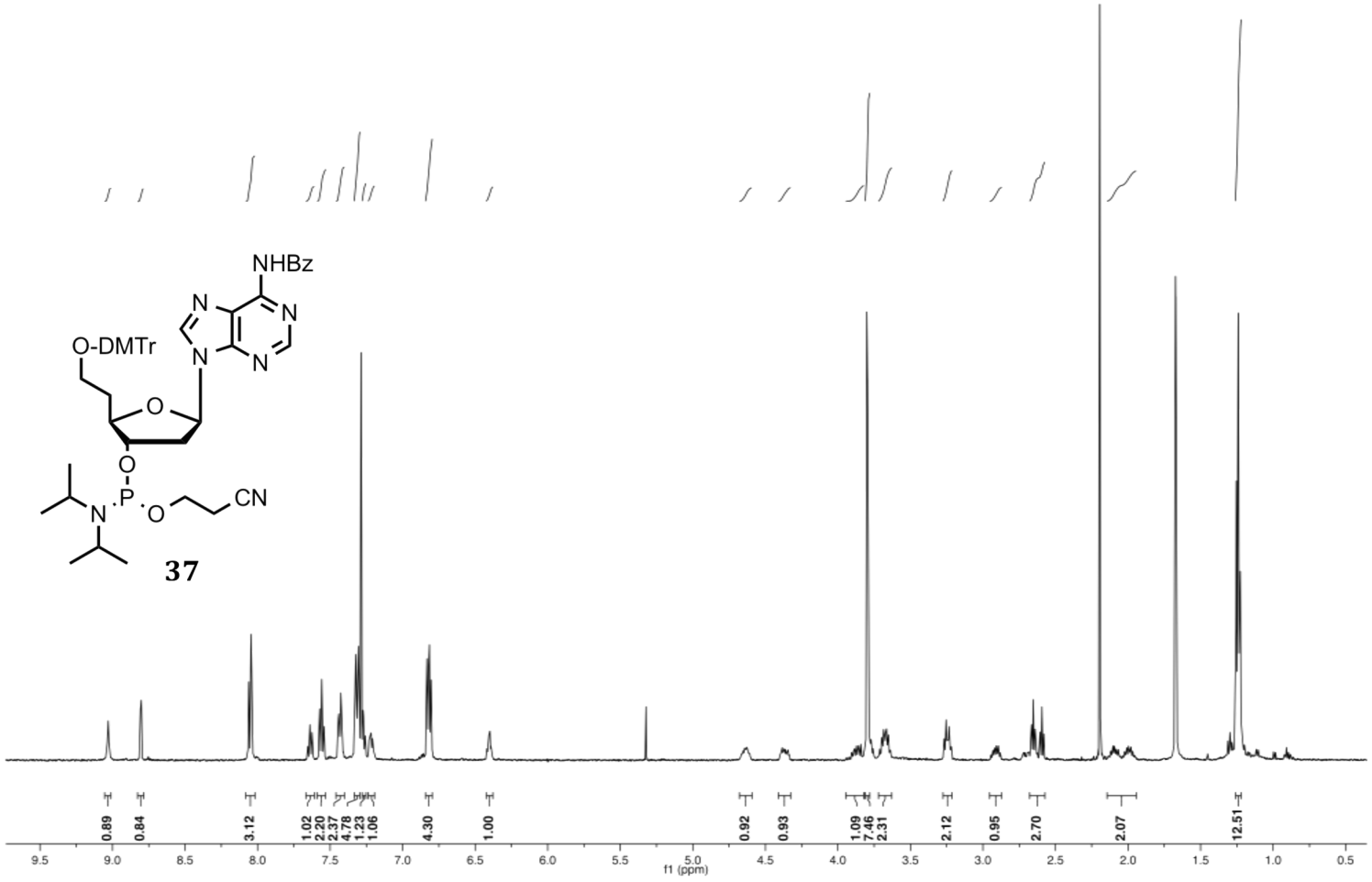

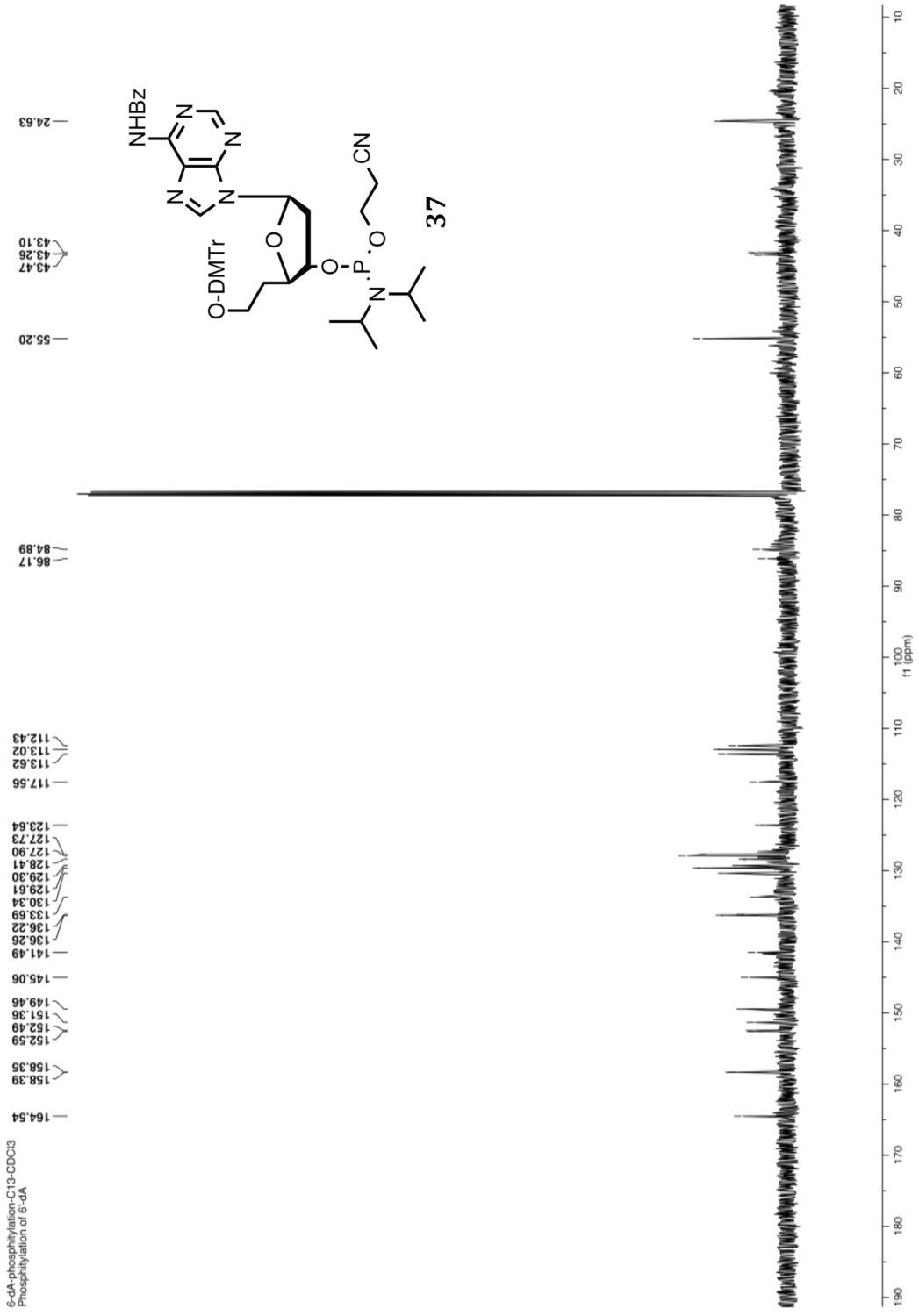
6-dA-phosphitylation-C13-CDCl3
Phosphitylation of 6'-dA
24.63
43.47
43.26
43.10
55.20
84.89
86.17
112.43
113.02
113.62
117.56
123.64
127.73
127.90
128.41
129.30
129.61
130.34
133.69
136.22
136.26
141.49
145.06
149.46
151.36
152.49
152.59
158.35
158.39
164.54
NHBz
O-DMTr
CN
37
f1 (ppm)

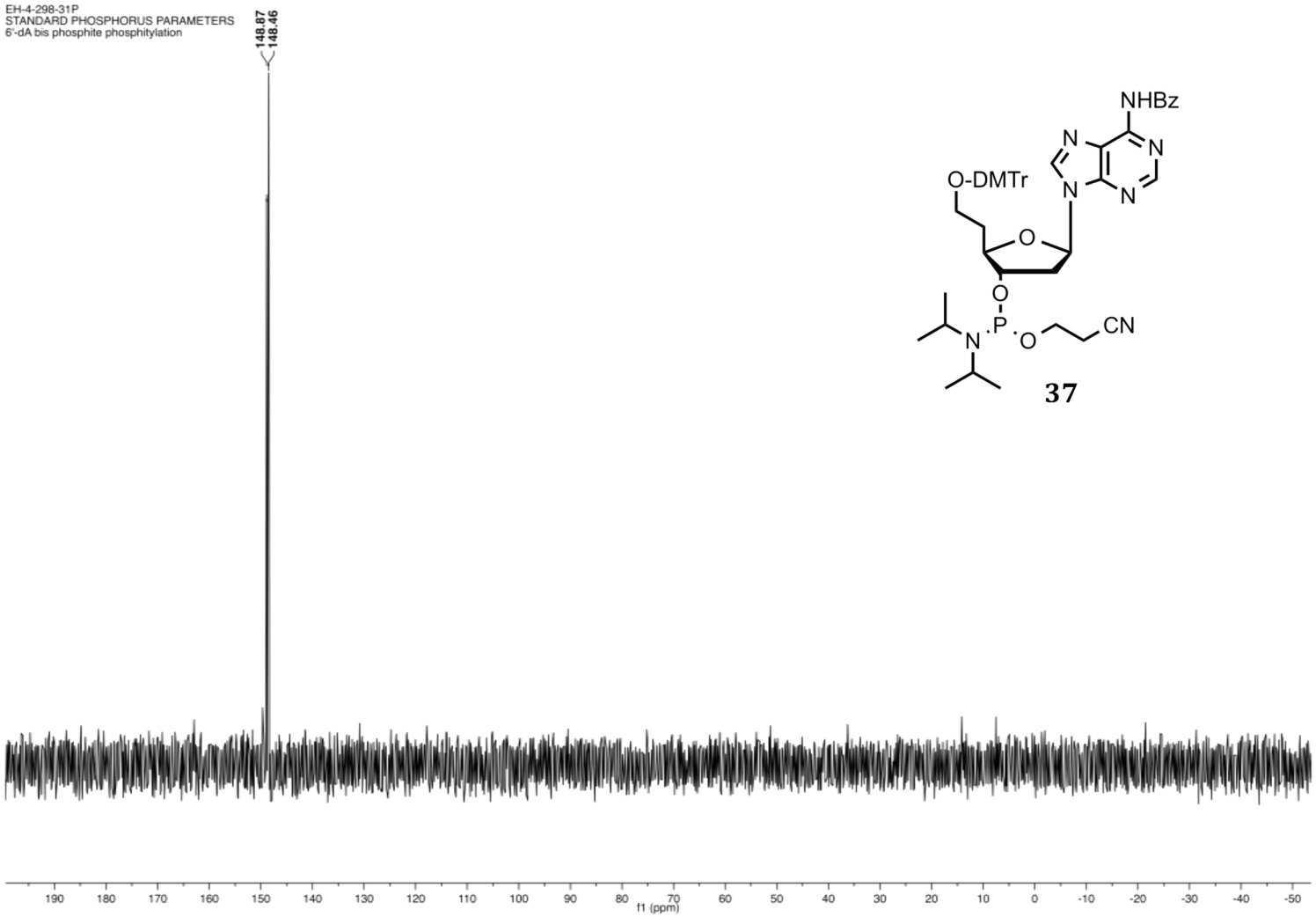
EH-4-298-31P
STANDARD PHOSPHORUS PARAMETERS
6'-dA bis phosphite phosphitylation
148.87
148.46
NHBz
N
N
N
N
O-DMTr
O
O
P
O
N
CN
f1 (ppm)

37

3.17 Mass Spectra

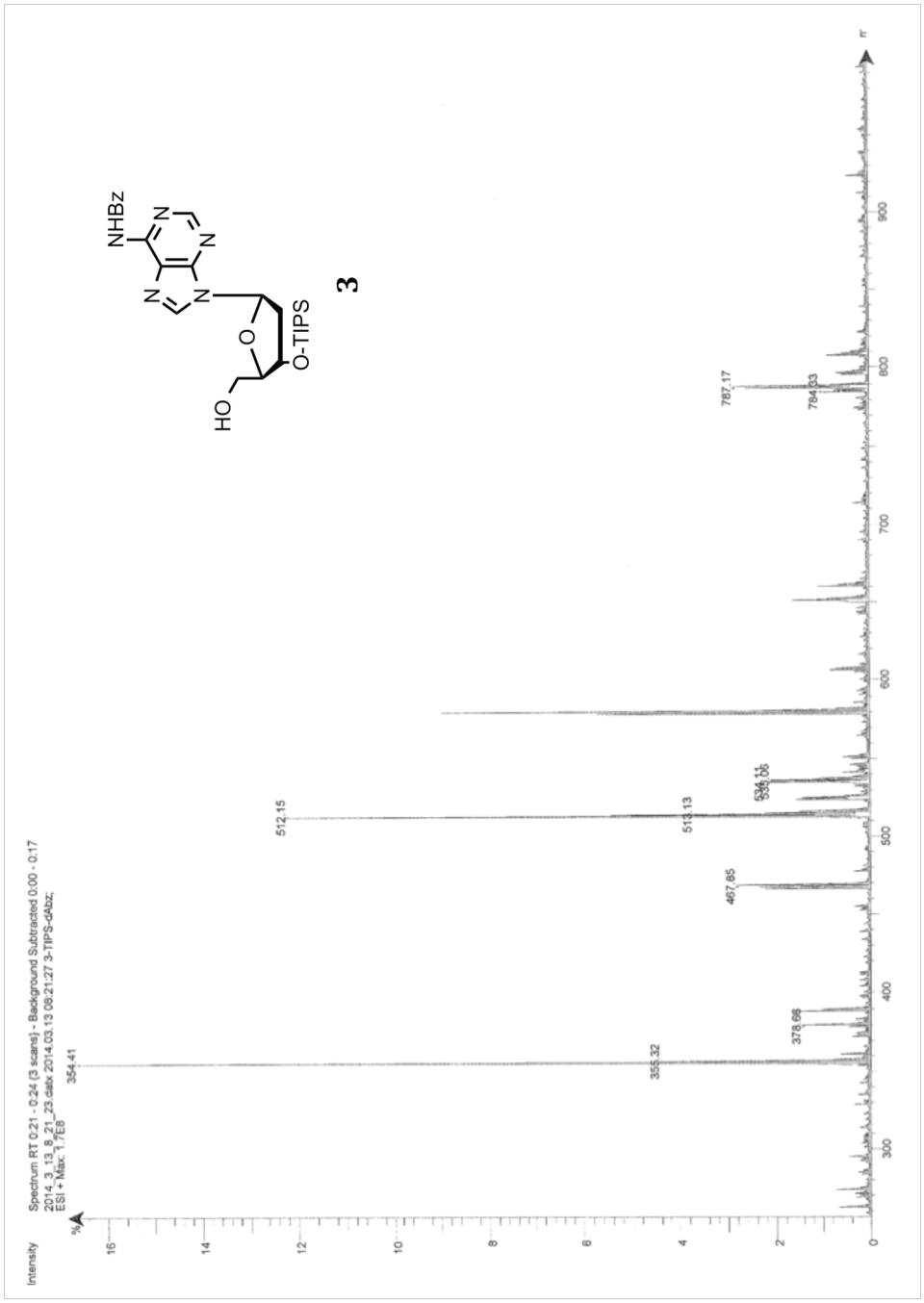

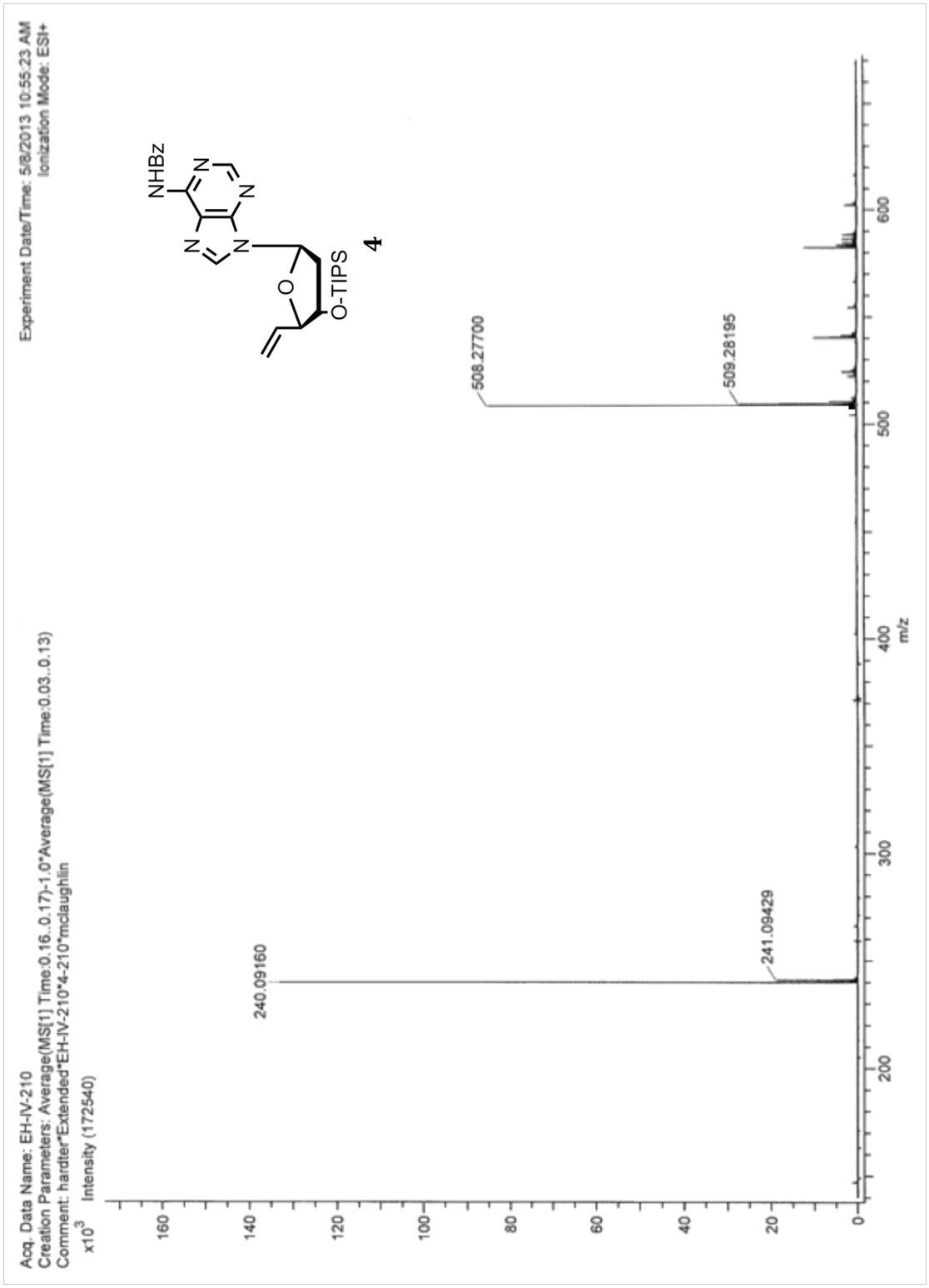
Acq. Data Name: EH-IV-210
Creation Parameters: Average(MS[1] Time:0.16..0.17)-1.0*Average(MS[1] Time:0.03..0.13)
Comment: hardter*Extended*EH-IV-210*4-210*mclaughlin
Experiment Date/Time: 5/8/2013 10:55:23 AM
Ionization Mode: ESI+
x10^3 Intensity (172540)
240.09160
241.09429
508.27700
509.28195
m/z
NHBz
O-TIPS
4

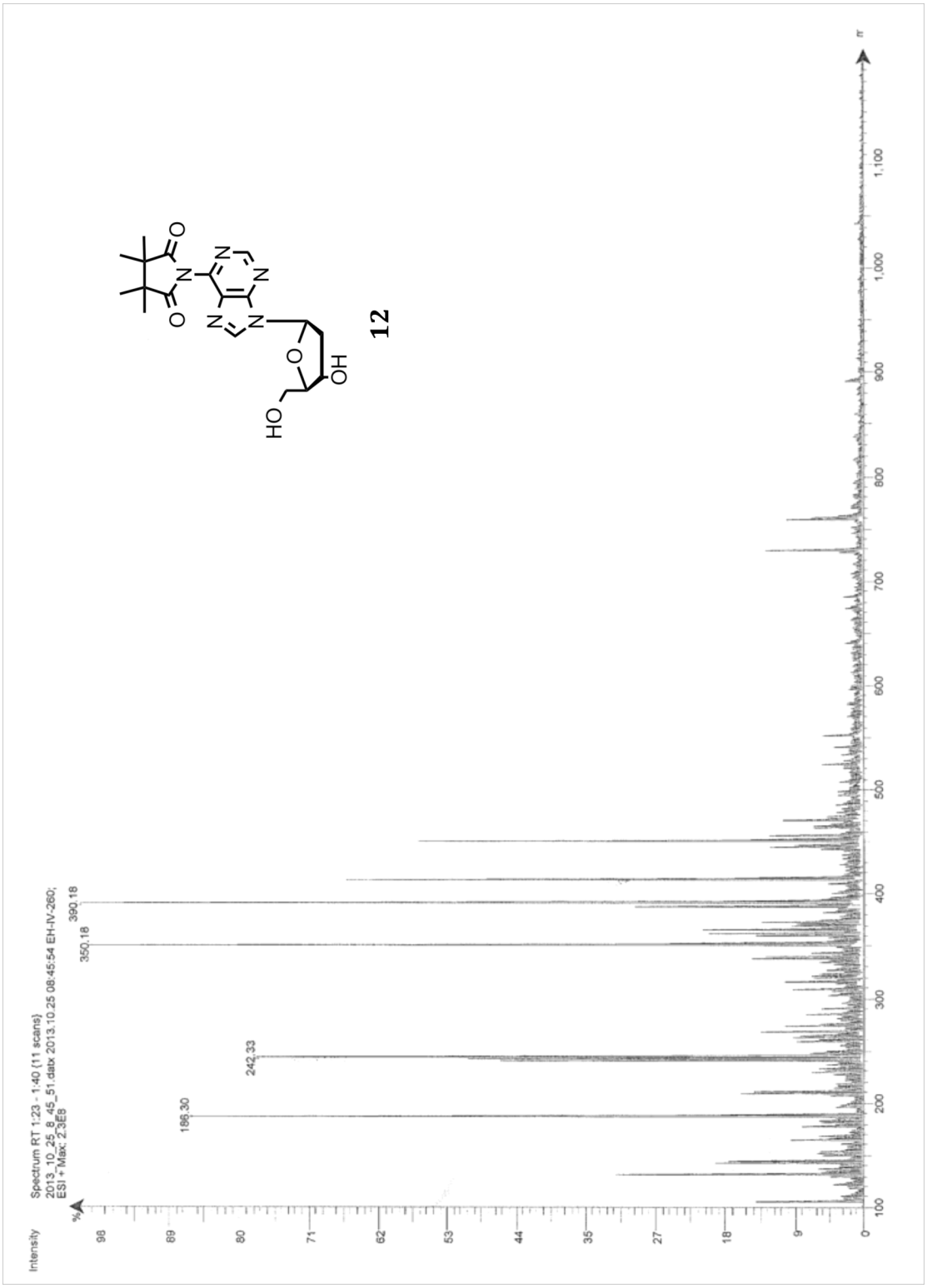
Intensity
Spectrum RT 1:23 - 1:40 (11 scans)
2013_10_25_8_45_51.datx 2013.10.25 08:45:54 EH-IV-260;
ESI + Max: 2.3E8
390.18
350.18
242.33
186.30
%
m/z
12

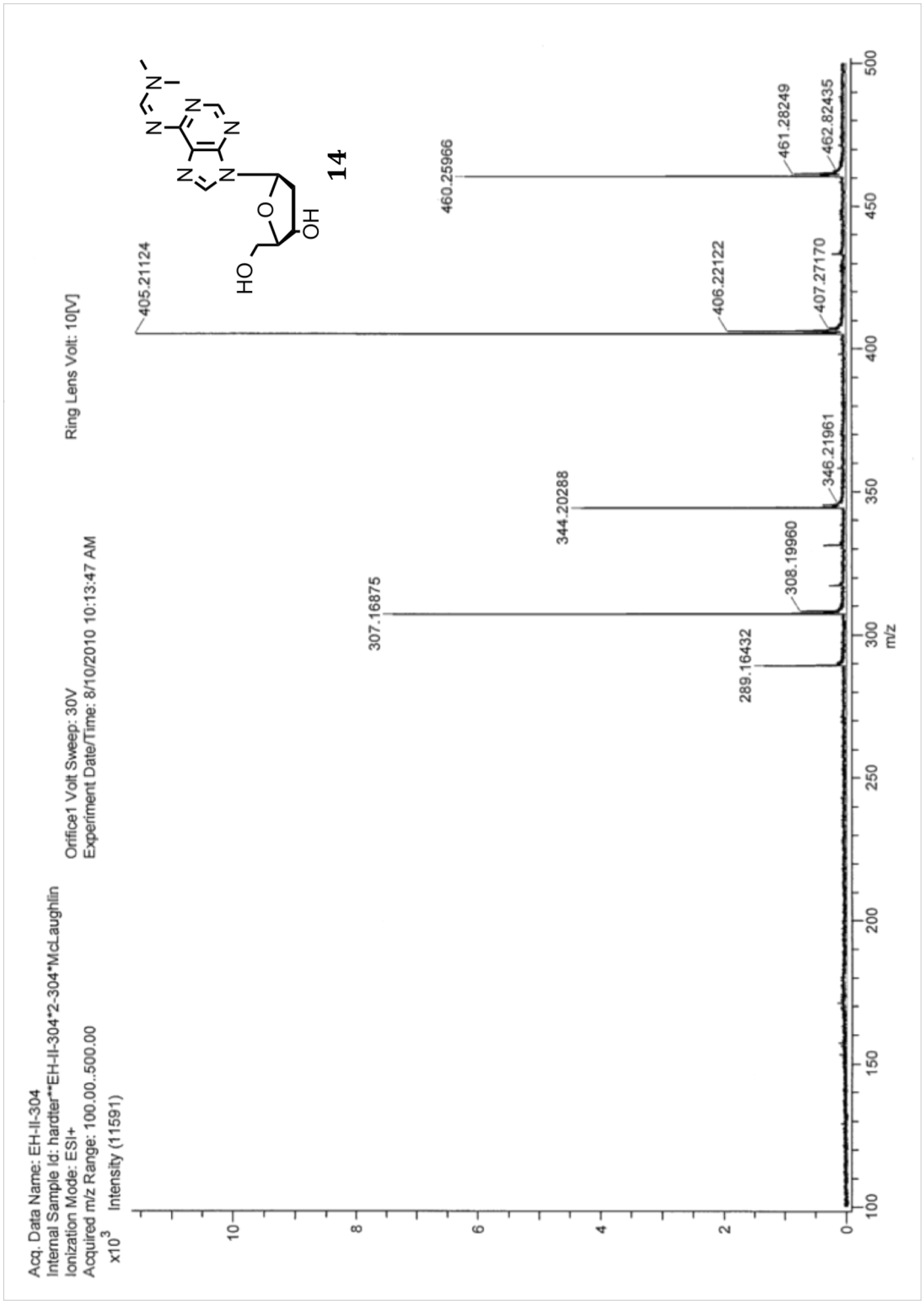
Acq. Data Name: EH-II-304
Internal Sample Id: hardtier**EH-II-304*2-304*McLaughlin
Ionization Mode: ESI+
Acquired m/z Range: 100.00..500.00
x10^3 Intensity (11591)
Orifice1 Volt Sweep: 30V
Experiment Date/Time: 8/10/2010 10:13:47 AM
Ring Lens Volt: 10[V]
405.21124
460.25966
461.28249
462.82435
406.22122
407.27170
346.21961
344.20288
308.19960
307.16875
289.16432
m/z
14

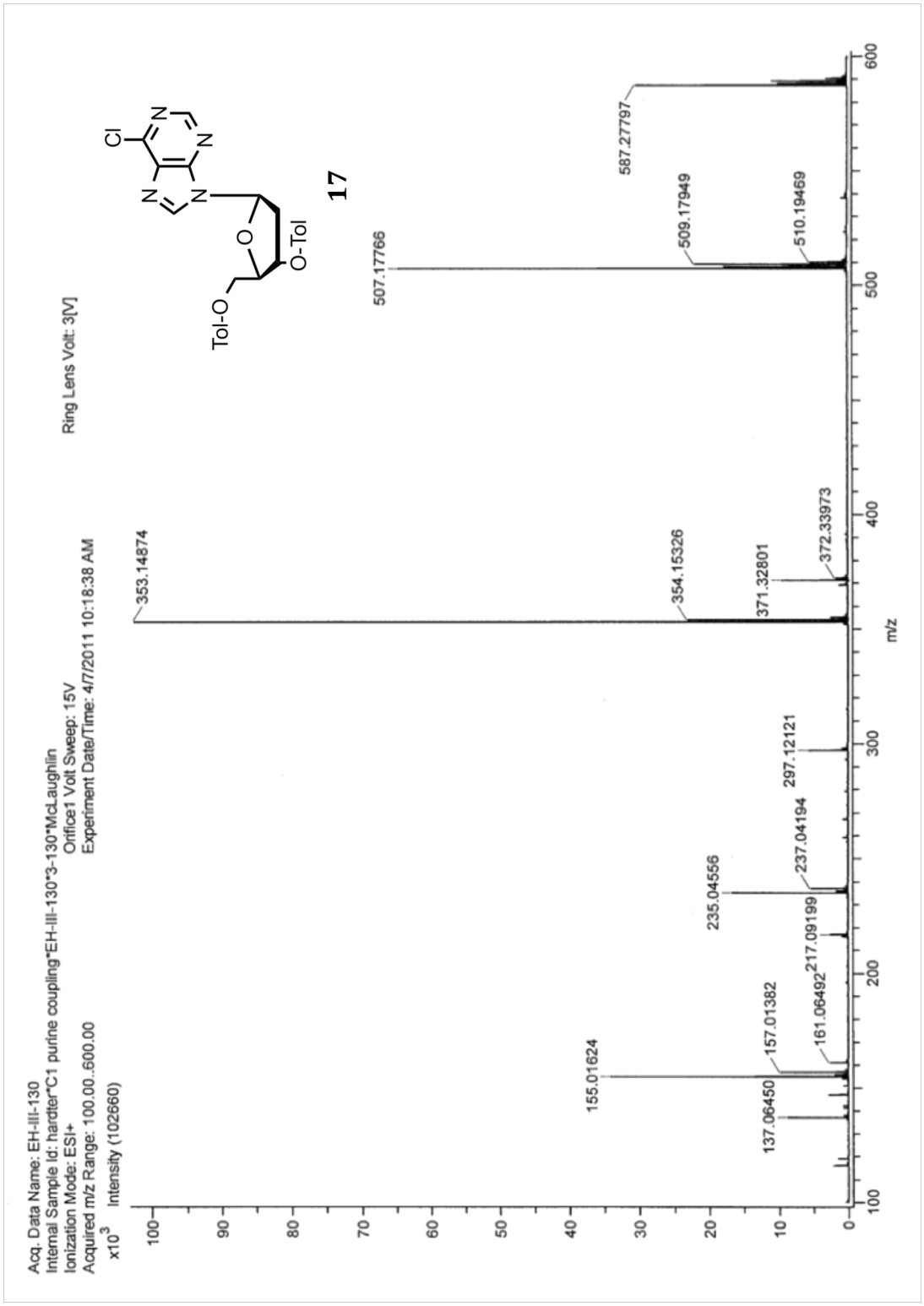
Acq. Data Name: EH-III-130
Internal Sample Id: hardter*C1 purine coupling*EH-III-130*3-130*McLaughlin
Ionization Mode: ESI+
Acquired m/z Range: 100.00..600.00
Orifice1 Volt Sweep: 15V
Experiment Date/Time: 4/7/2011 10:18:38 AM
Ring Lens Volt: 3[V]
x10^3 Intensity (102660)
Tol-O
O-Tol
17
353.14874
354.15326
371.32801
372.33973
507.17766
509.17949
510.19469
587.27797
155.01624
137.06450
157.01382
161.06492
217.09199
235.04556
237.04194
297.12121
m/z

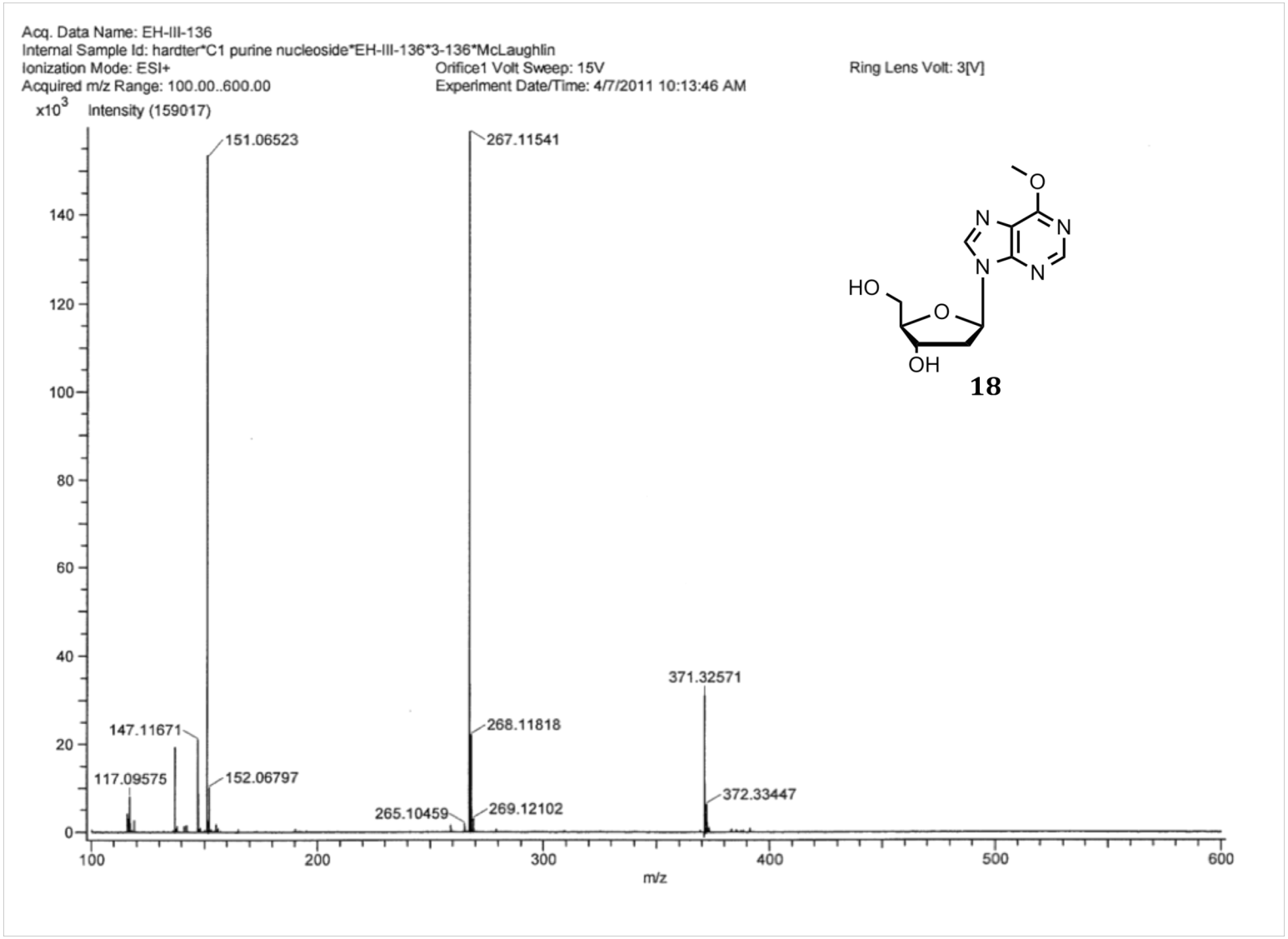
Acq. Data Name: EH-III-136
Internal Sample Id: hardter*C1 purine nucleoside*EH-III-136*3-136*McLaughlin
Ionization Mode: ESI+
Orifice1 Volt Sweep: 15V
Ring Lens Volt: 3[V]
Acquired m/z Range: 100.00..600.00
Experiment Date/Time: 4/7/2011 10:13:46 AM
x10^3 Intensity (159017)
151.06523
267.11541
147.11671
117.09575
152.06797
268.11818
265.10459
269.12102
371.32571
372.33447
m/z
18

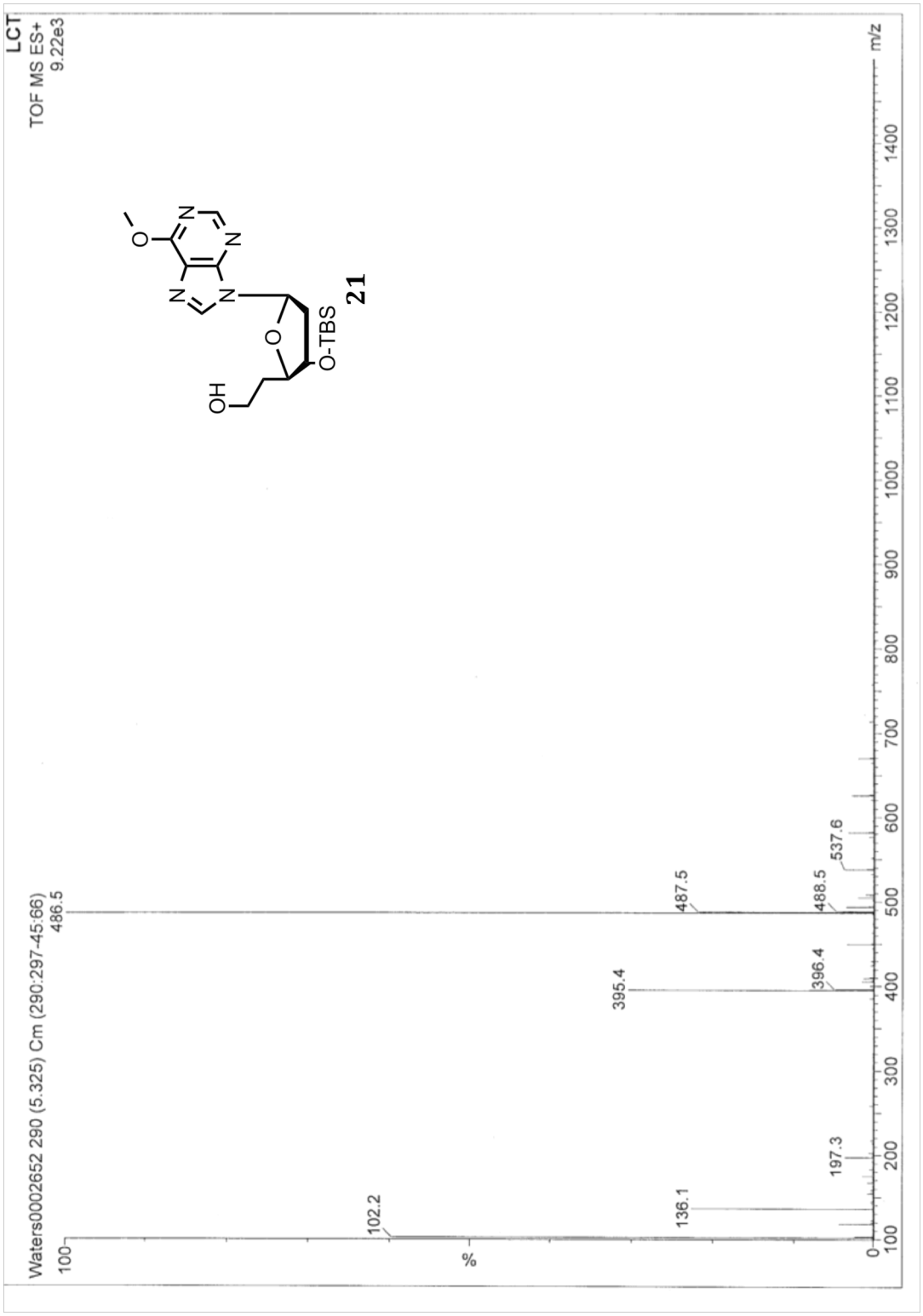
LCT
TOF MS ES+
9.22e3
Waters0002652 290 (5.325) Cm (290:297-45:66)
486.5
487.5
488.5
537.6
395.4
396.4
102.2
136.1
197.3
100
%
0
100
200
300
400
500
600
700
800
900
1000
1100
1200
1300
1400
m/z
O
N
N
N
N
O
O-TBS
OH
21

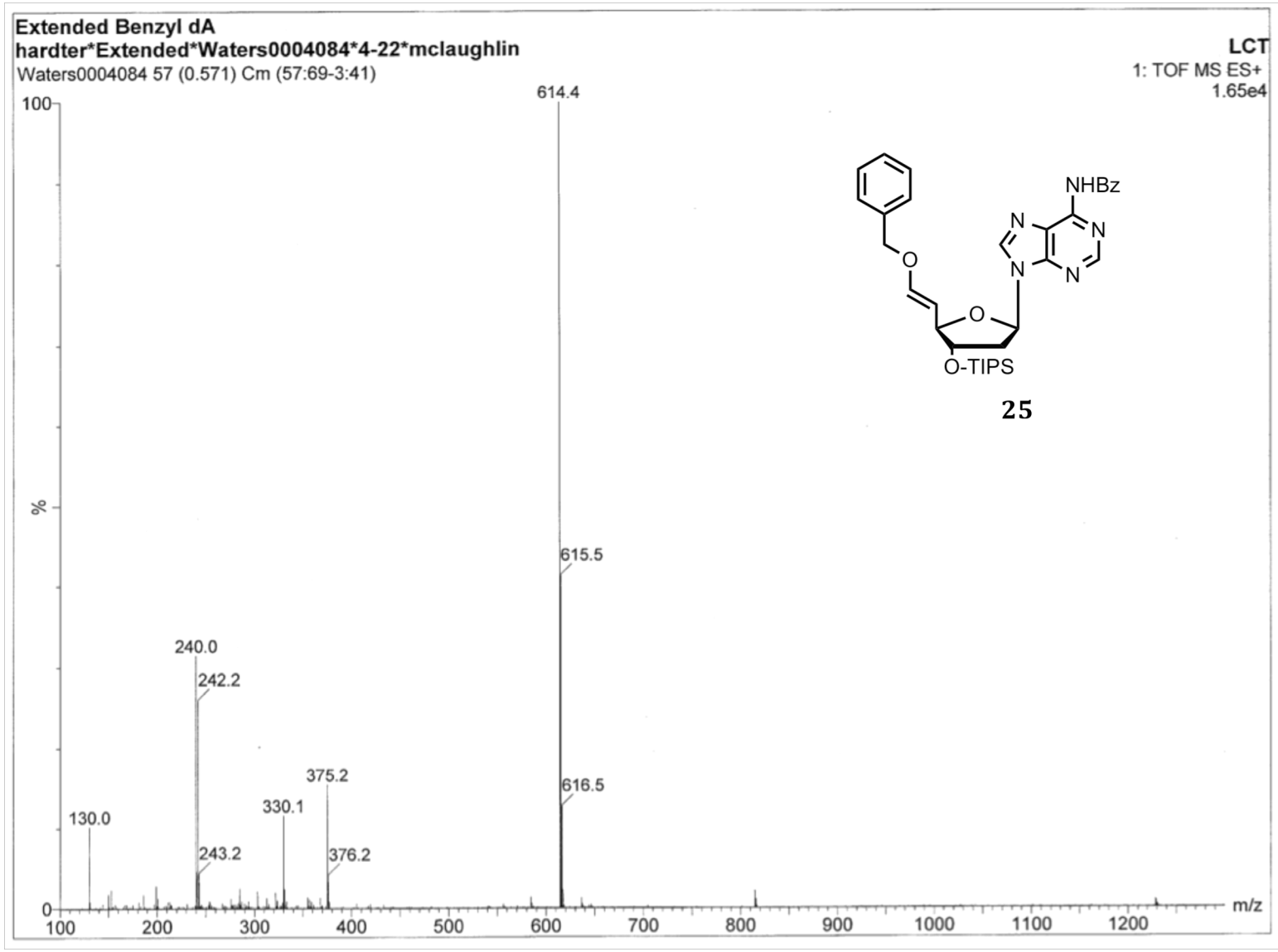
Extended Benzyl dA
hardter*Extended*Waters0004084*4-22*mclaughlin
Waters0004084 57 (0.571) Cm (57:69-3:41)
LCT
1: TOF MS ES+
1.65e4
100
%
0
614.4
615.5
616.5
240.0
242.2
243.2
375.2
376.2
330.1
130.0
100
200
300
400
500
600
700
800
900
1000
1100
1200
m/z
NHBz
N
N
N
N
O
O
O-TIPS

25

Elemental Composition Report

Single Mass Analysis
Tolerance = 10.0 PPM / DBE: min = -50.0, max = 100.0
Isotope cluster parameters: Separation = 1.0 Abundance = 1.0%

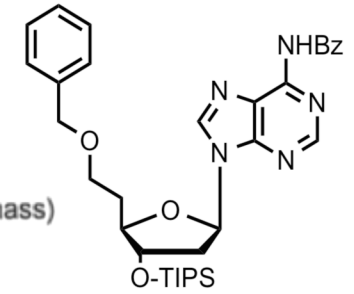

26

Monoisotopic Mass, Odd and Even Electron Ions
63 formula(e) evaluated with 3 results within limits (up to 50 closest results for each mass)

EH-IV-47
hardter*Extended*Waters0004341*4-47*mclaughlin
Waters0004341 54 (0.542) AM (Cen,4, 90.00, Ht,5000.0,594.25,0.70); Cm (49:65-3:39)

LCT
1: TOF MS ES+
380

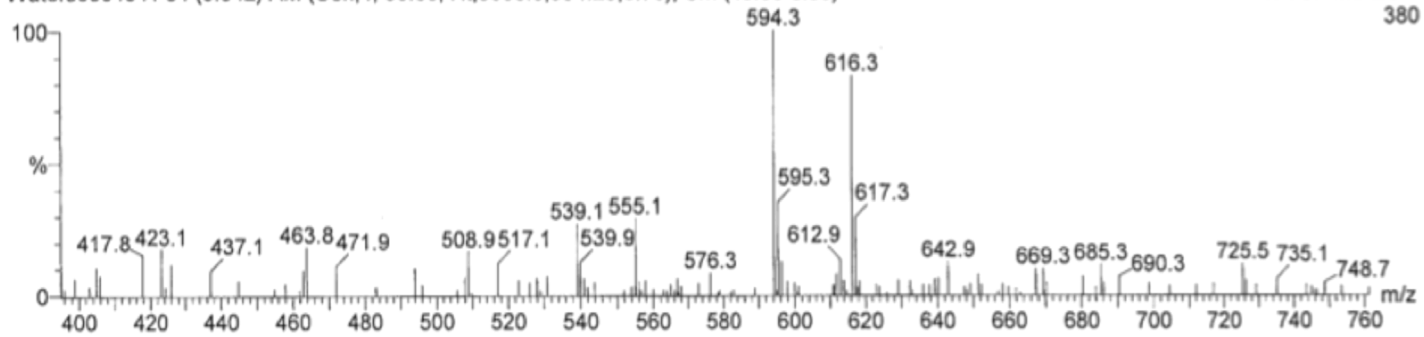

Minimum:				-50.0		
Maximum:		50.0	10.0	100.0		
Mass	Calc. Mass	mDa	PPM	DBE	Score	Formula
594.2531	594.2537	-0.6	-0.9	19.5	1	C33 H36 N5 O4 Si
	594.2568	-3.7	-6.2	14.5	2	C29 H40 N5 O5 Si2
	594.2482	4.9	8.2	19.0	3	C33 H38 N4 O3 Si2

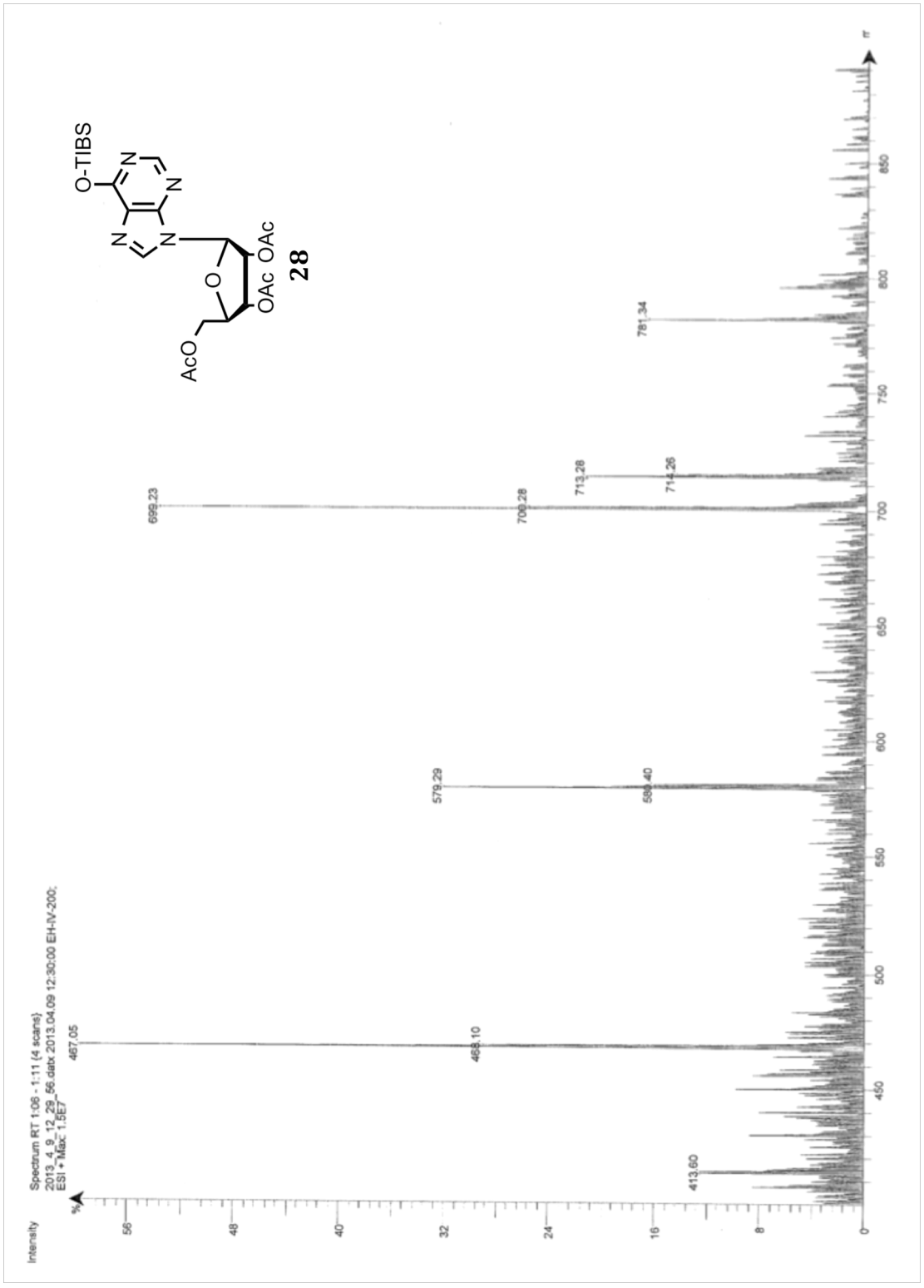
O-TIBS
AcO
OAc OAc
28
Intensity
Spectrum RT 1:06 - 1:11 (4 scans)
2013_4_9_12_29_56.datx 2013.04.09 12:30:00 EH-IV-200:
ESI + Max. 1.5E7
467.05
468.10
413.60
579.29
580.40
699.23
700.28
713.28
714.26
781.34
%
m/z

Data:EH-IV-196
Sample Name:hardter*Extended*EH-IV-196*4-196*mclaughlin
Description:
Ionization Mode:ESI+
History:Determine m/z[Peak Detect[Centroid,30,Area];Correct Base[];Smooth[5]];...

Acquired:4/2/2013 10:34:55 AM
Operator:AccuTOF
Mass Calibration data:DART-2
Created:4/2/2013 10:38:21 AM
Created by:AccuTOF

Charge number:1 Tolerance:5.00(ppm), 5.00 .. 15.00(m... Unsaturation Number:-1.5 .. 50.0 (Frac...
Element:^{12}C:1 .. 100, ^{1}H:1 .. 100, ^{14}N:1 .. 5, ^{16}O:1 .. 5, ^{28}Si:1 .. 1

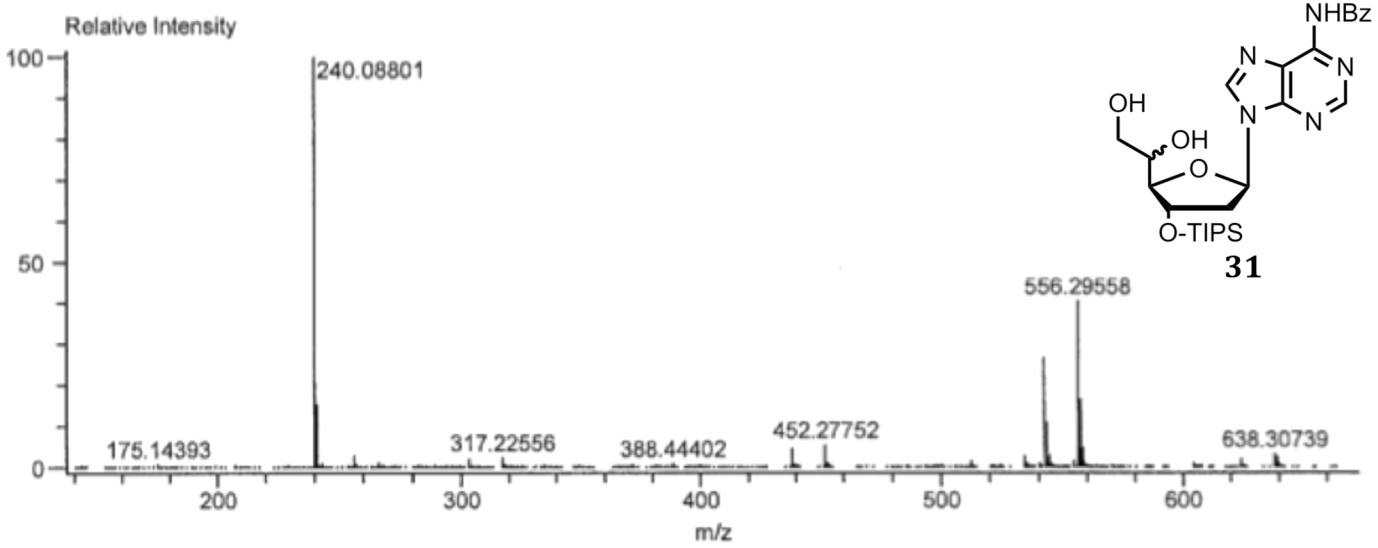

31

Mass	Calc. Mass	Mass Difference (mmu)	Mass Difference (ppm)	Possible Formula	Unsaturation Number
542.28097	542.27987	1.10	2.04	$^{12}C_{27}{}^{1}H_{40}{}^{14}N_5{}^{16}O_5{}^{28}Si_1$	11.5
	542.28389	-2.92	-5.38	$^{12}C_{32}{}^{1}H_{40}{}^{14}N_3{}^{16}O_3{}^{28}Si_1$	15.5

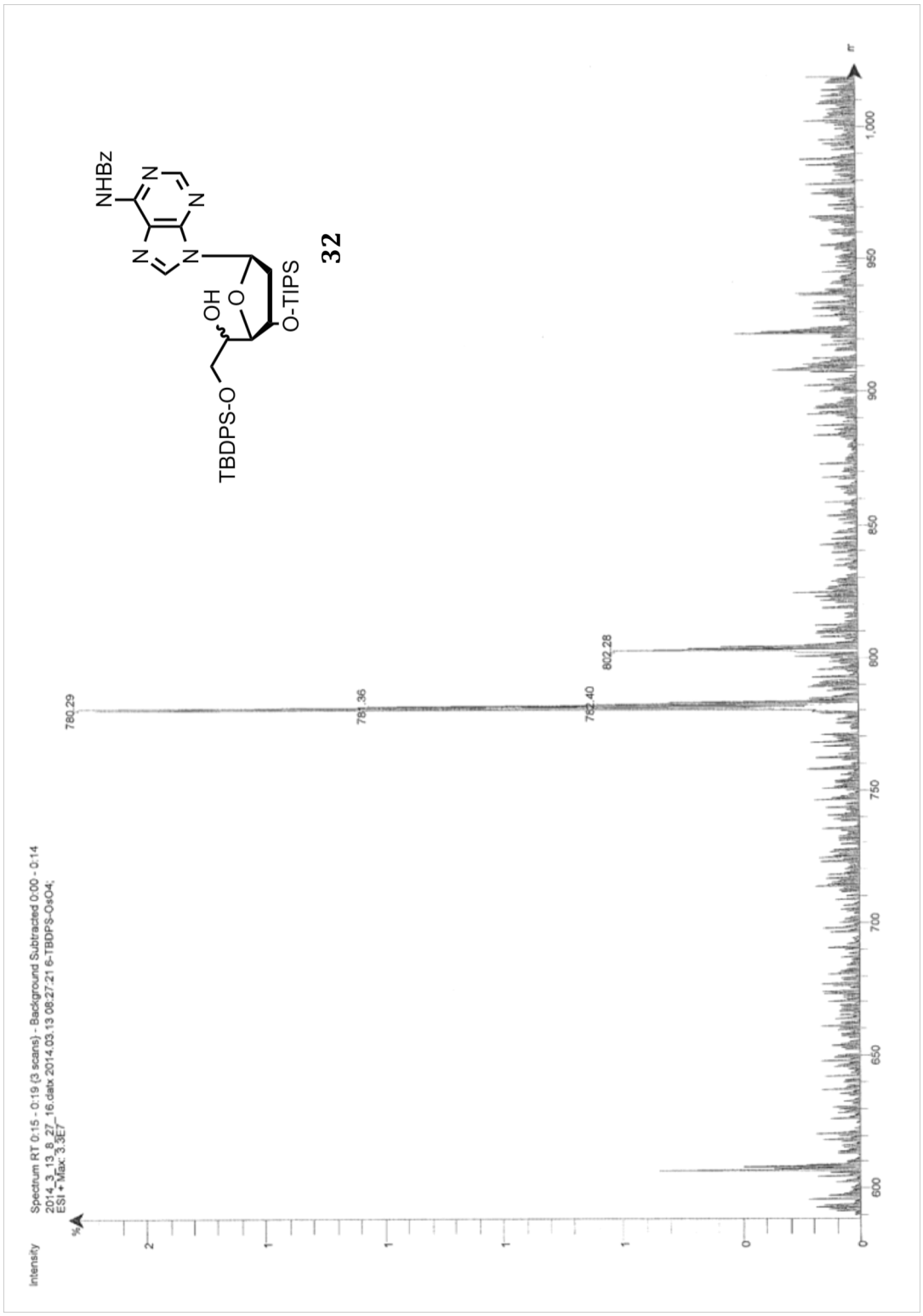
Intensity
Spectrum RT 0:15 - 0:19 (3 scans) - Background Subtracted 0:00 - 0:14
2014_3_13_8_27_16.datx 2014.03.13 08:27:21 6-TBDPS-Os04;
ESI + Max: 3.3E7
%
m/z
780.29
781.36
782.40
802.28
NHBz
N
N
N
N
OH
O
O-TIPS
TBDPS-O
32

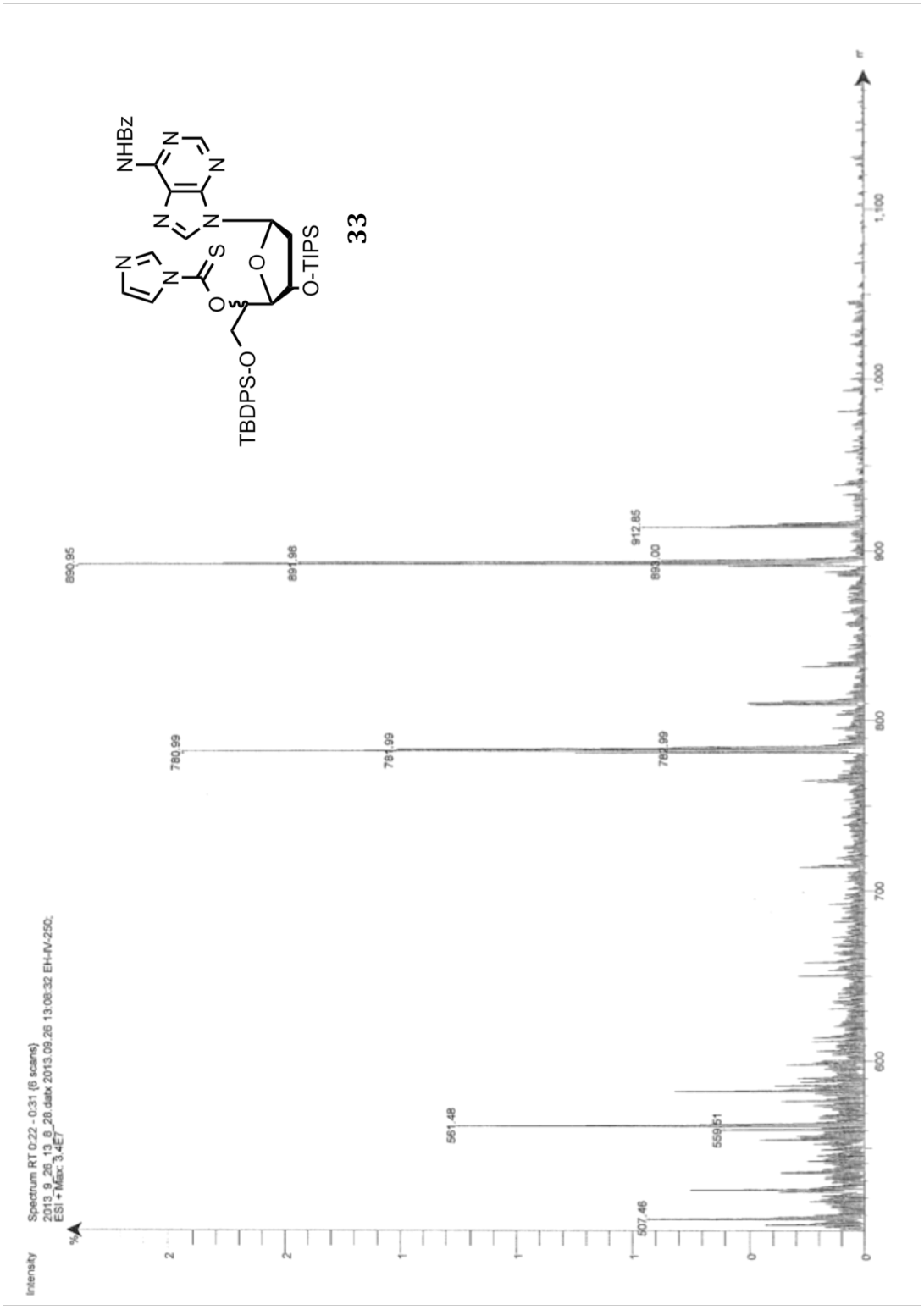
NHBz
TBDPS-O
O-TIPS
33
Intensity
Spectrum RT 0:22 - 0:31 (6 scans)
2013_9_26_13_8_28.datx 2013.09.26 13:08:32 EH-IV-250;
ESI + Maz 3.4E7
%
m/z
507.46
559.51
561.48
780.99
781.99
784.99
890.95
891.98
893.00
912.85
600
700
800
900
1,000
1,100

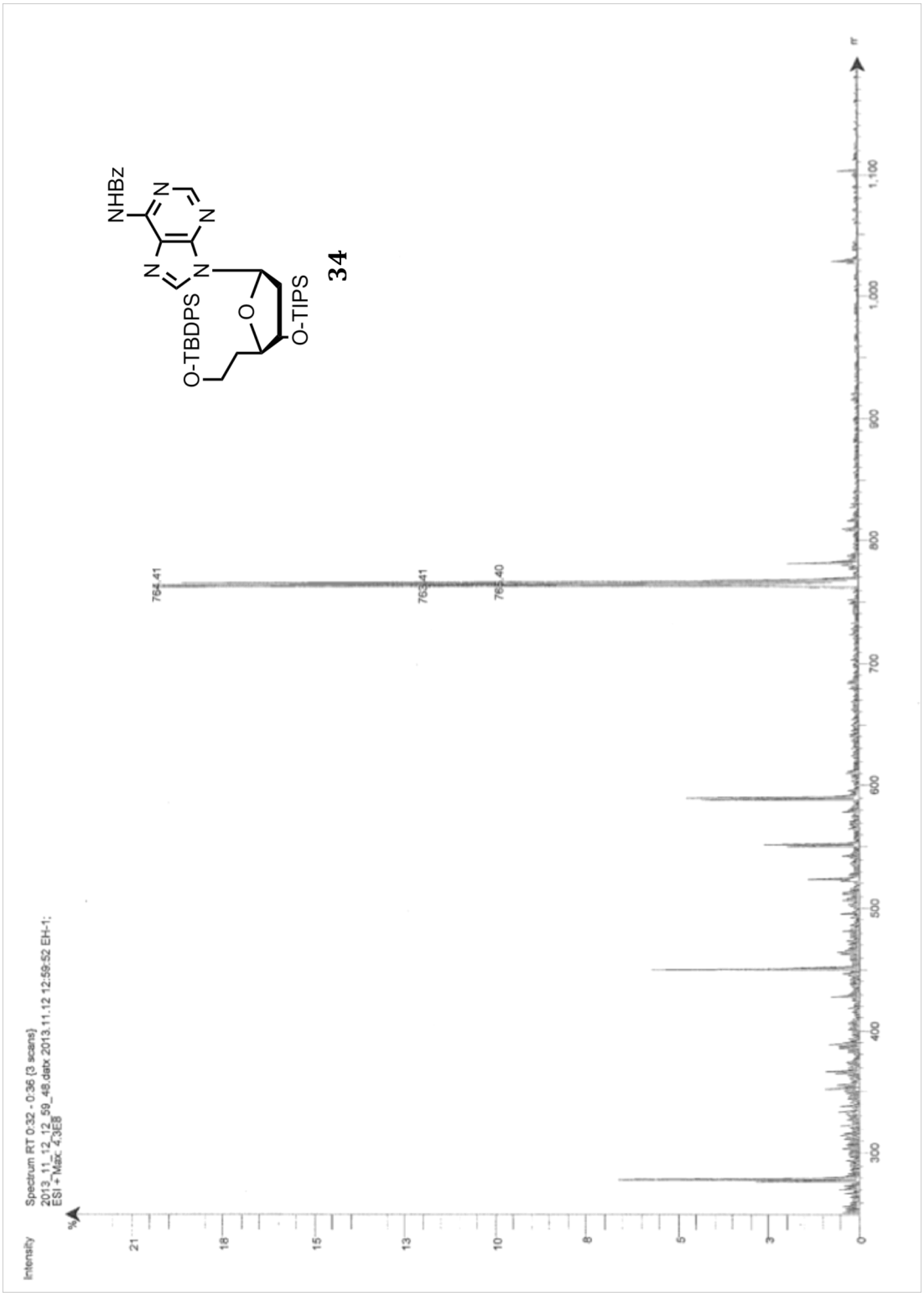
NHBz
O-TBDPS
O-TIPS
34
Intensity
Spectrum RT 0:32 - 0:36 (3 scans)
2013_11_12_12_59_48.datx 2013.11.12 12:59:52 EH-1:
ESI + Max: 4.3E8
764.41
763.41
765.40

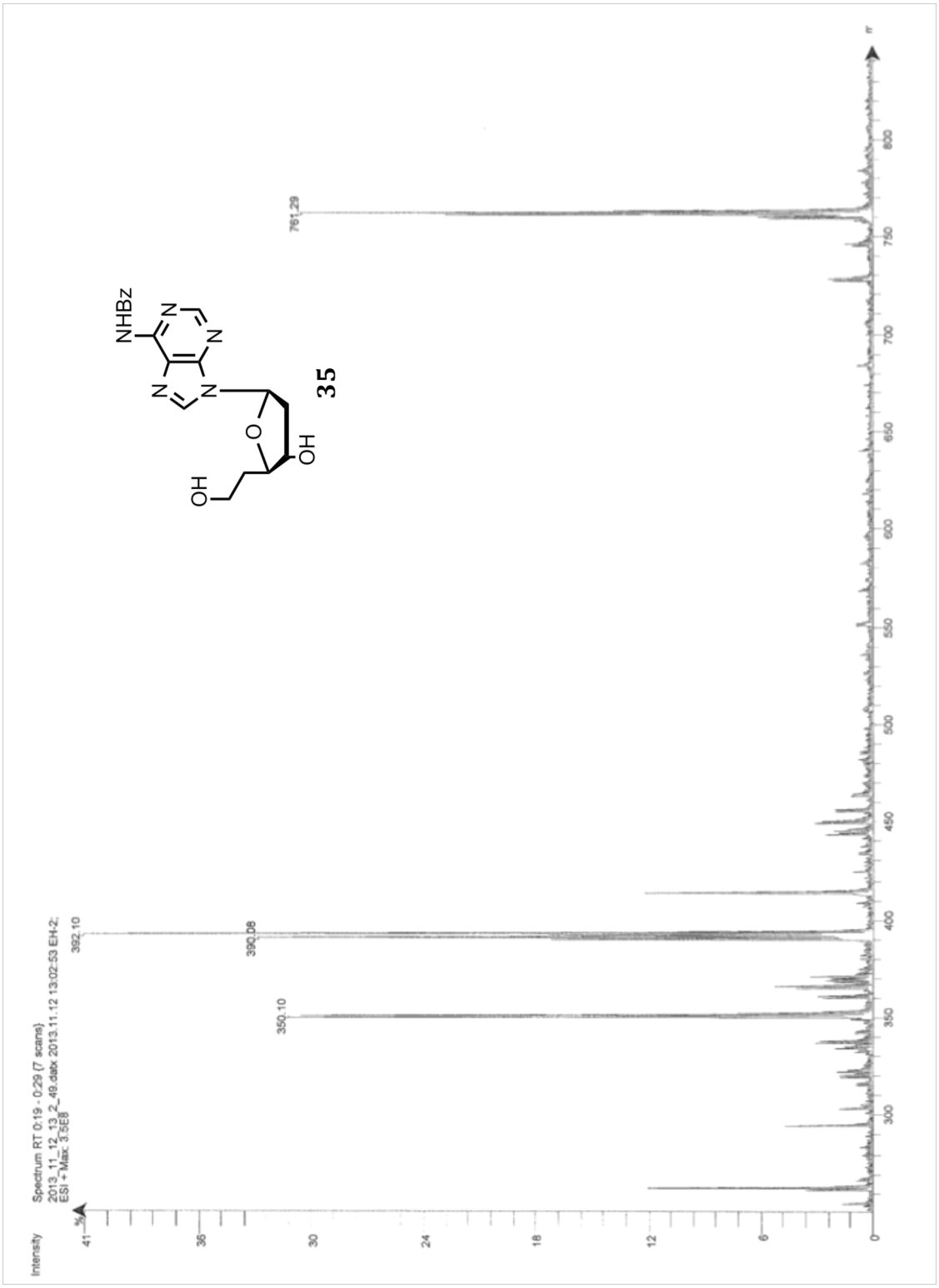
Intensity
Spectrum RT 0:19 - 0:29 (7 scans)
2013_11_12_13_2_49.dax 2013.11.12 13:02:53 EH-2:
ESI + Max. 3.5E8
%
41
36
30
24
18
12
6
0
392.10
390.08
350.10
761.29
300
350
400
450
500
550
600
650
700
750
800
m/z
NHBz
N
N
N
N
O
OH
OH
35

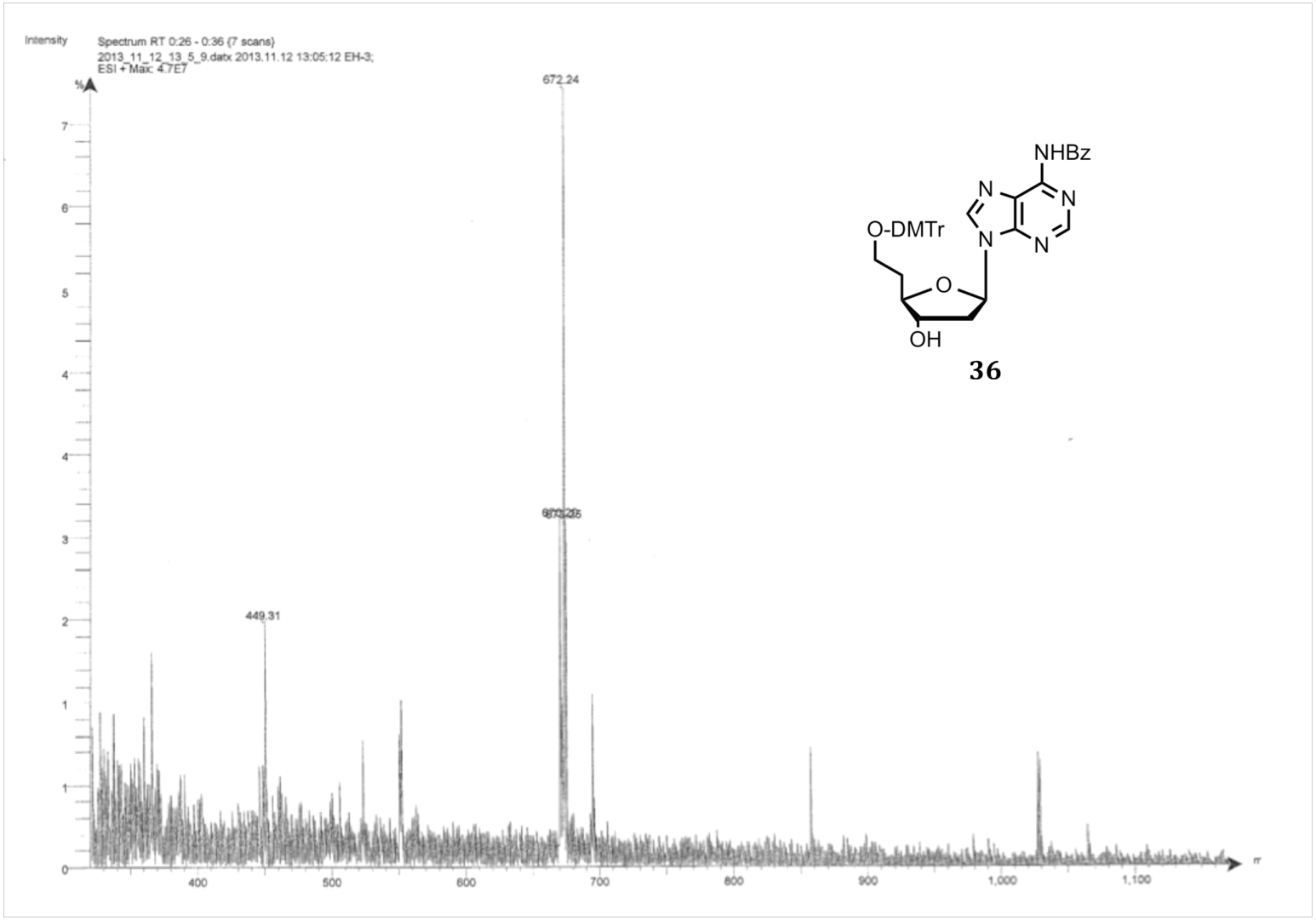
Intensity
Spectrum RT 0:26 - 0:36 (7 scans)
2013_11_12_13_5_9.datx 2013.11.12 13:05:12 EH-3;
ESI + Max: 4.7E7
%
672.24
449.31
O-DMTr
NHBz
N
N
N
N
O
OH
m/z
400
500
600
700
800
900
1,000
1,100

36

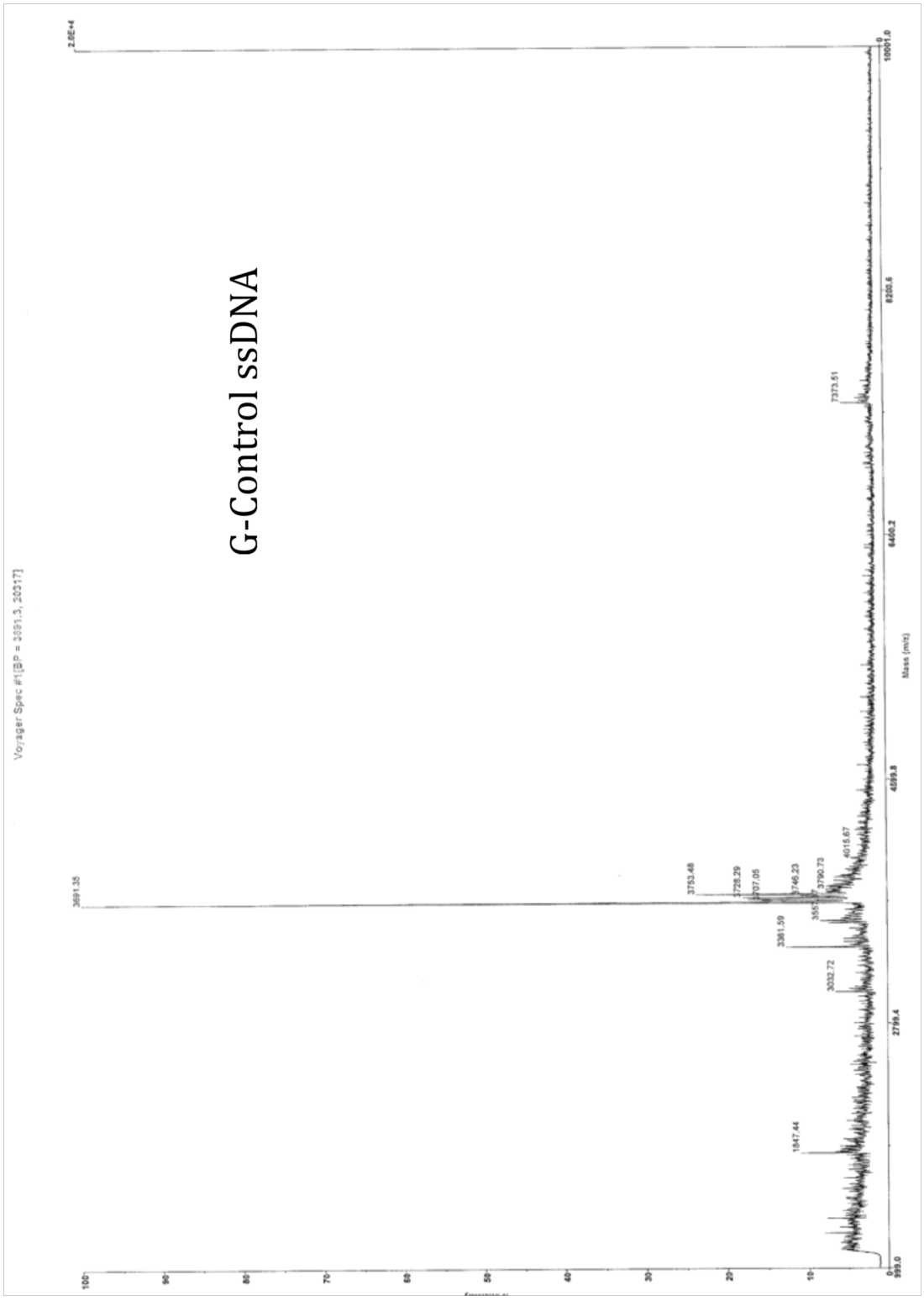
G-Control ssDNA
Voyager Spec #1[BP = 3691.3, 20317]
3691.35
3753.48
1728.29
1707.05
3746.23
3790.73
4015.67
3361.59
3032.72
1547.44
7373.51
2.0E+4
10001.0
8200.8
6460.2
4599.8
2799.4
999.0
Mass (m/z)

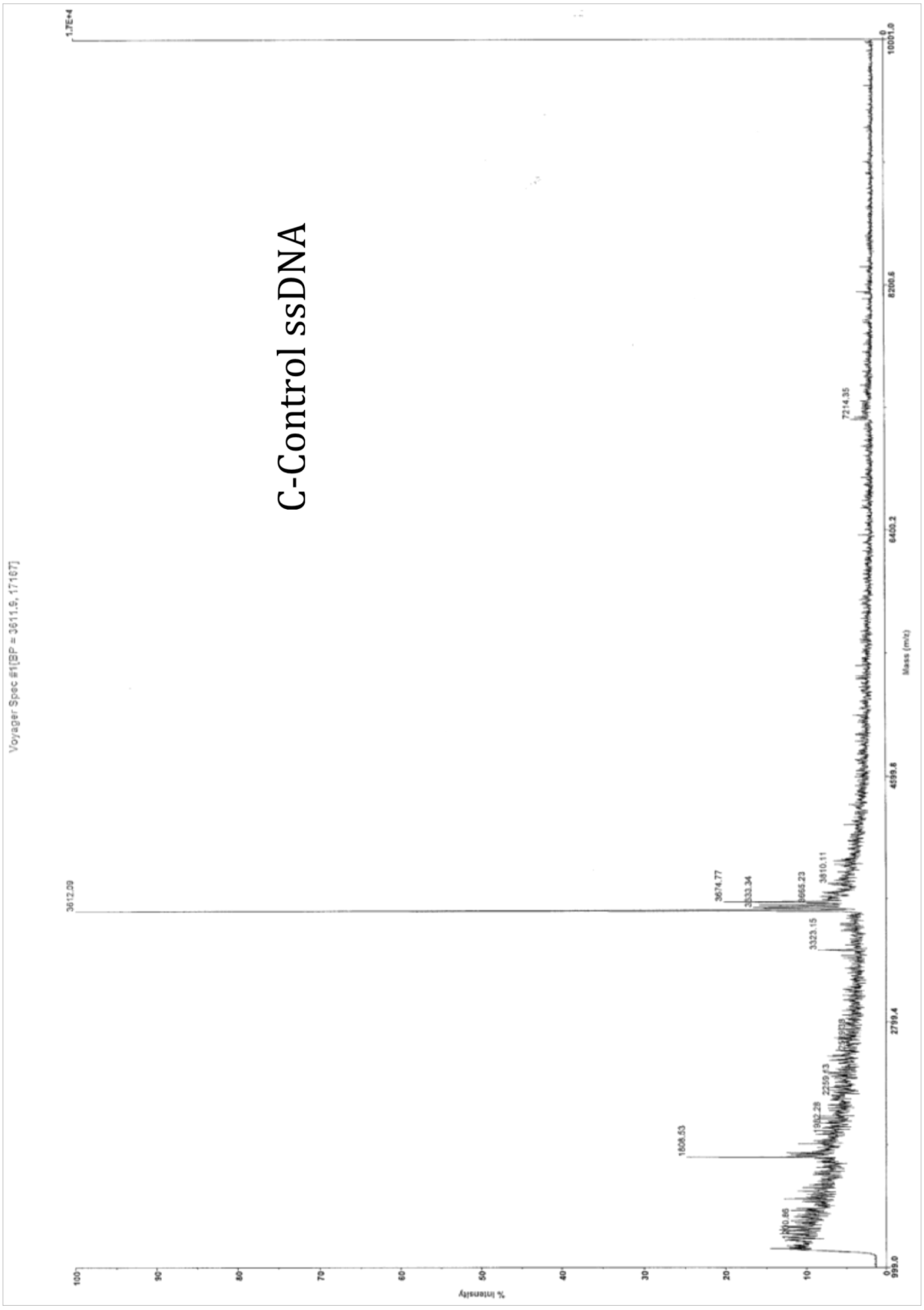
C-Control ssDNA
Voyager Spec #1[BP = 3611.6, 17107]
% Intensity
Mass (m/z)
3612.09
3674.77
3333.34
3323.15
1608.53
7214.35

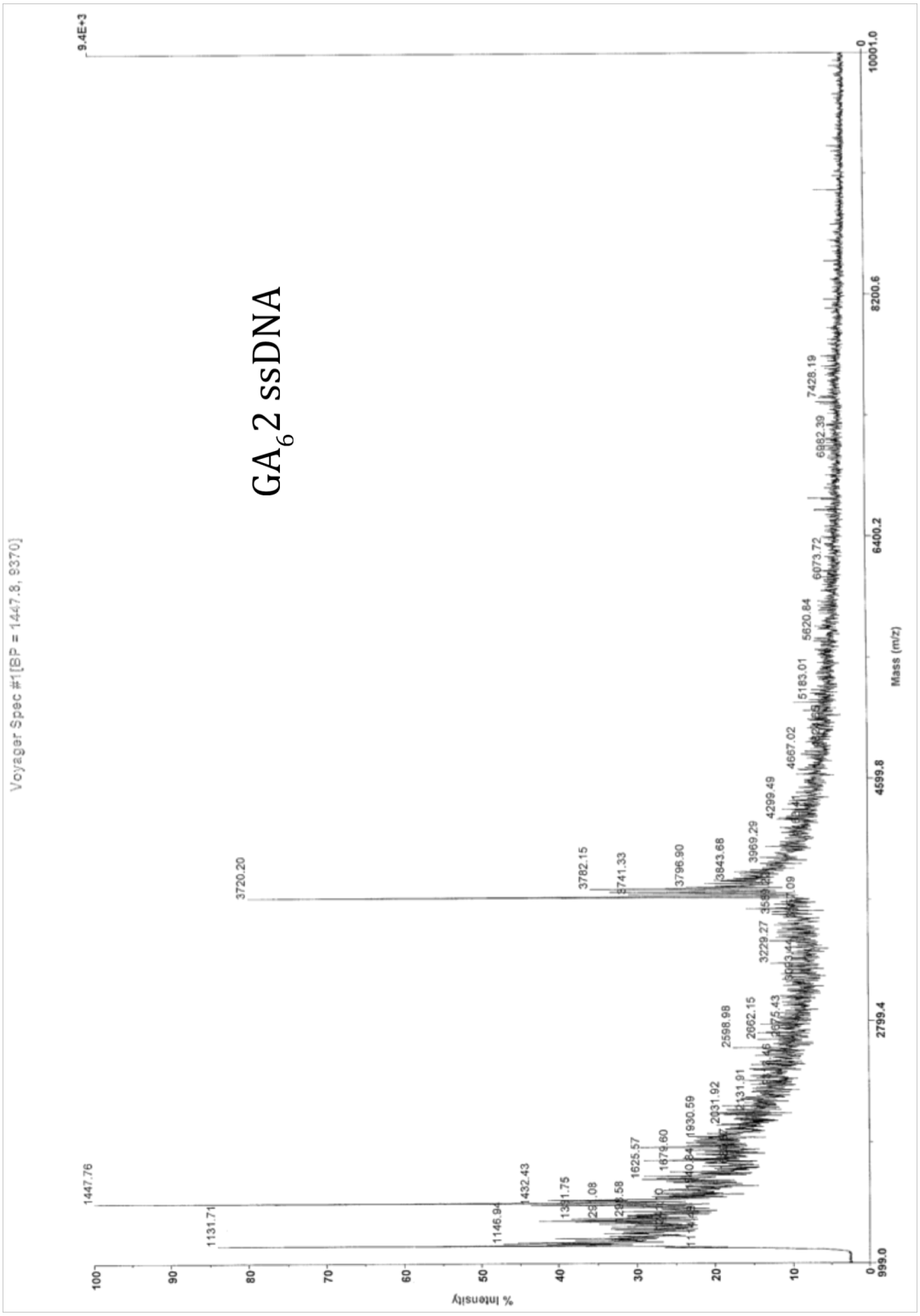
GA6 2 ssDNA
Voyager Spec #1[BP = 1447.8, 9370]
% Intensity
Mass (m/z)
9.4E+3
1447.76
1131.71
1146.94
3720.20
3782.15
3741.33
3796.90
3843.68
3969.29
4299.49
4667.02
5183.01
5620.84
6073.72
6982.39
7428.19
999.0
2799.4
4599.8
6400.2
8200.6
10001.0

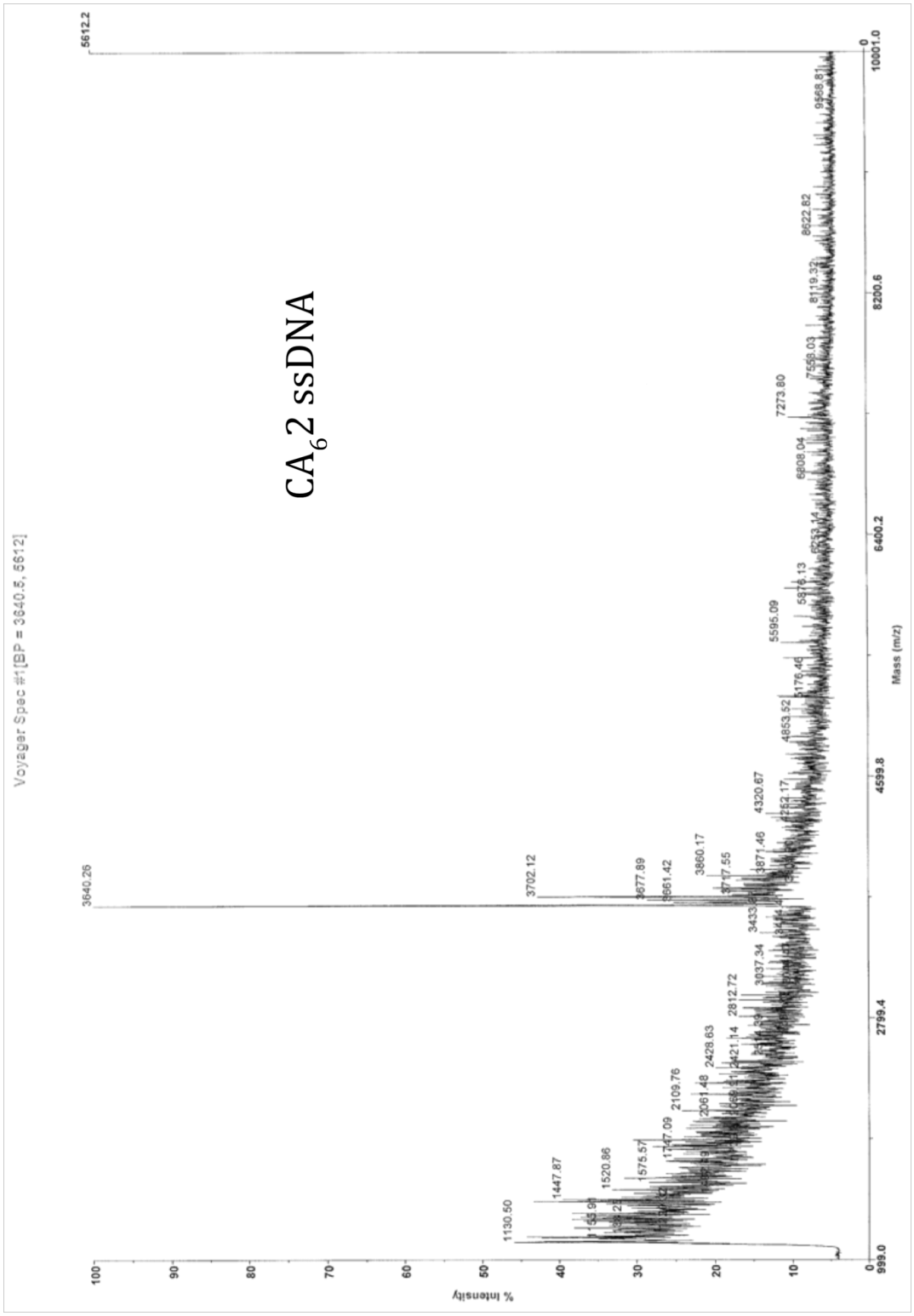
Voyager Spec #1[BP = 3640.5, 5612]
% Intensity
Mass (m/z)
3640.26
3702.12
1130.50
1447.87
1520.86
1575.57
2109.76
2428.63
2812.72
3860.17
4320.67
4853.52
5595.09
7273.80
5612.2

$CA_6 2$ ssDNA

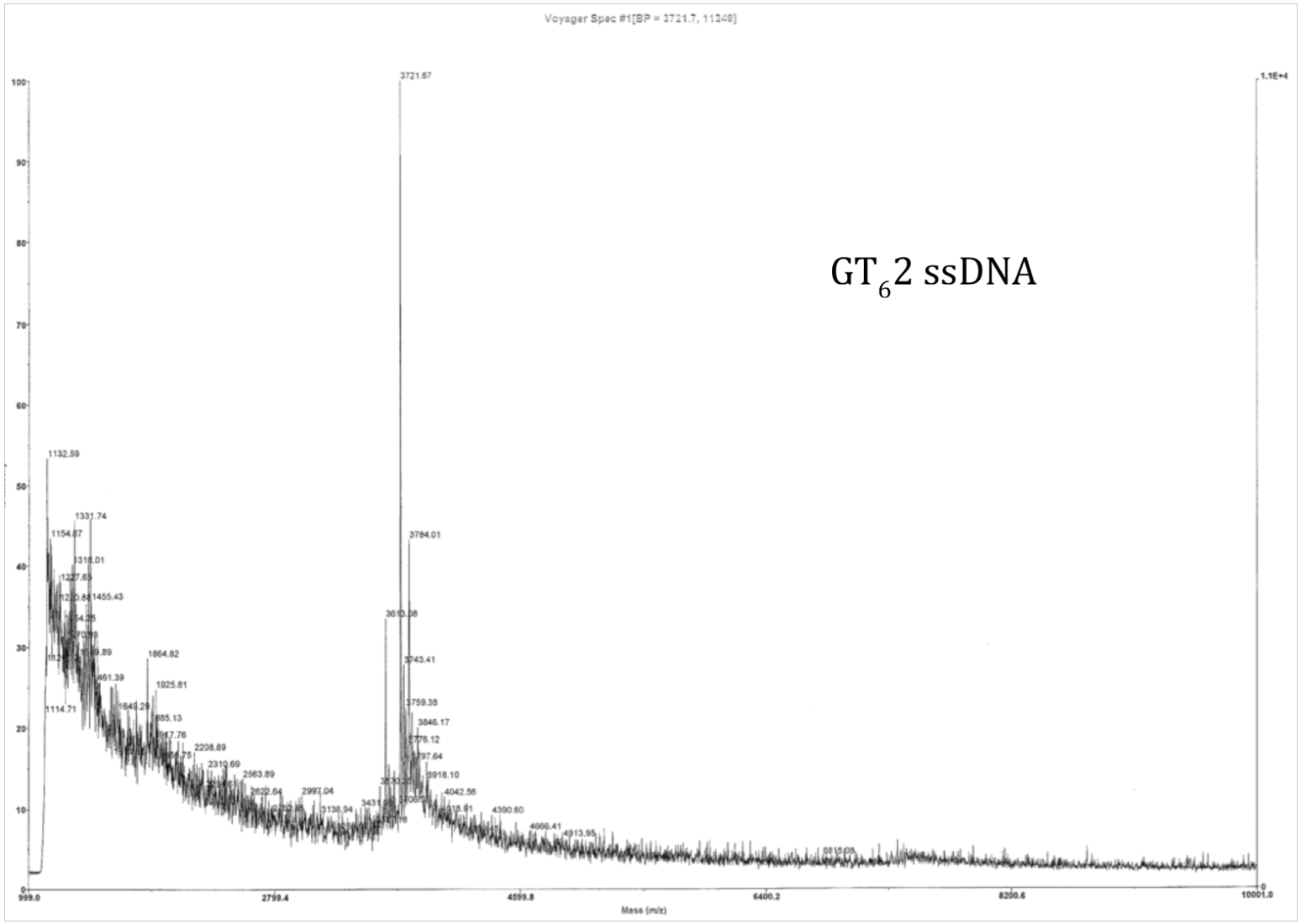
Voyager Spec #1[BP = 3721.7, 11249]
GT6 2 ssDNA
3721.67
1132.59
1331.74
1154.87
3784.01
1316.01
1227.65
1455.43
1864.82
1925.81
1114.71
3743.41
3759.38
3846.17
2208.89
2310.69
2583.89
2997.04
4042.56
4390.60
4666.41
4913.95
Mass (m/z)

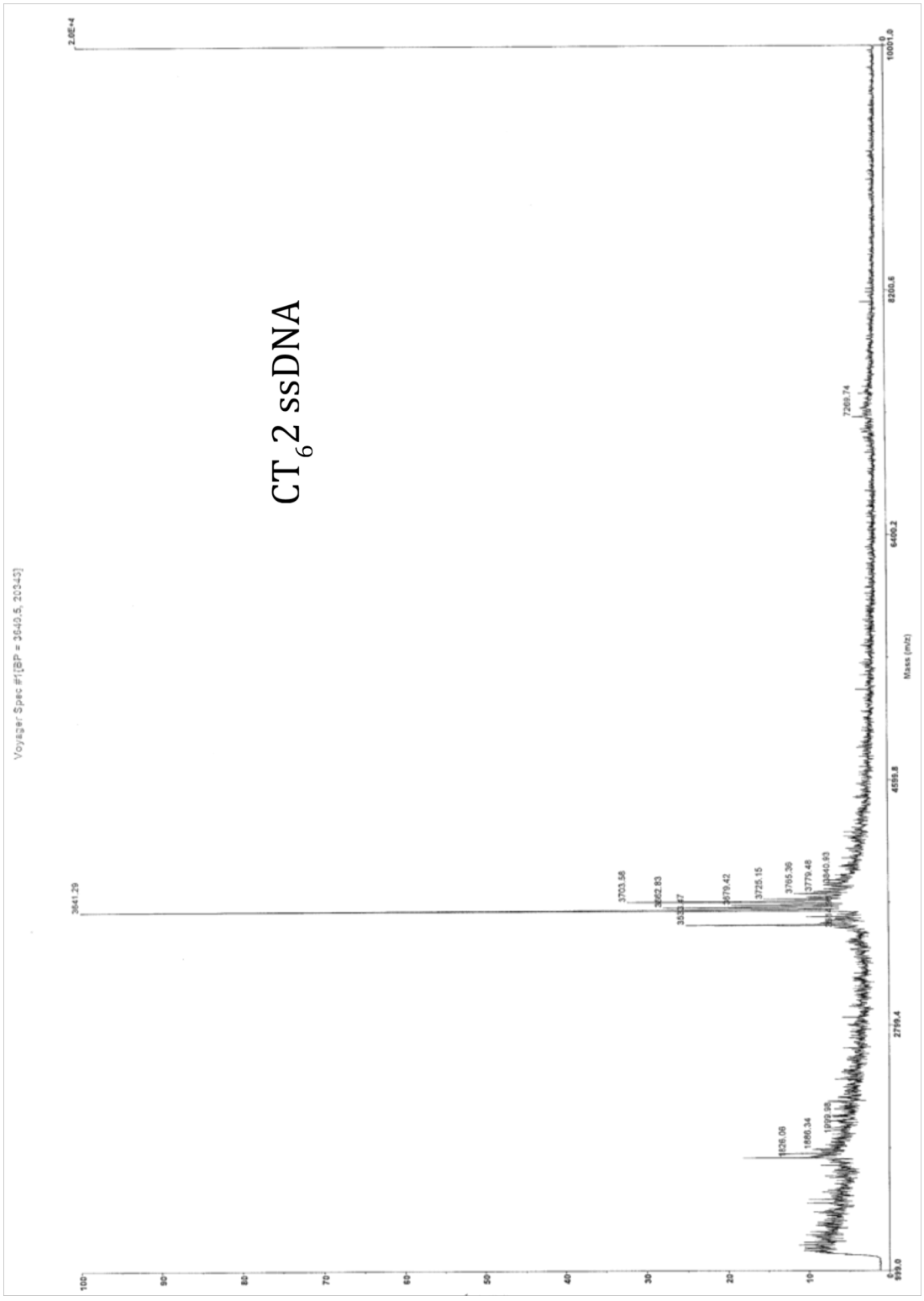
Voyager Spec #1[BP = 3640.5, 20043]
3641.29
3703.56
3862.83
3579.42
3725.15
3785.39
3779.49
3040.93
1520.06
1686.34
1919.95
7269.74
100
90
80
70
60
50
40
30
20
10
0
859.0
2759.4
4659.8
6460.2
8260.6
10061.0
Mass (m/z)
2.0E+4
0

$CT_6 2$ ssDNA

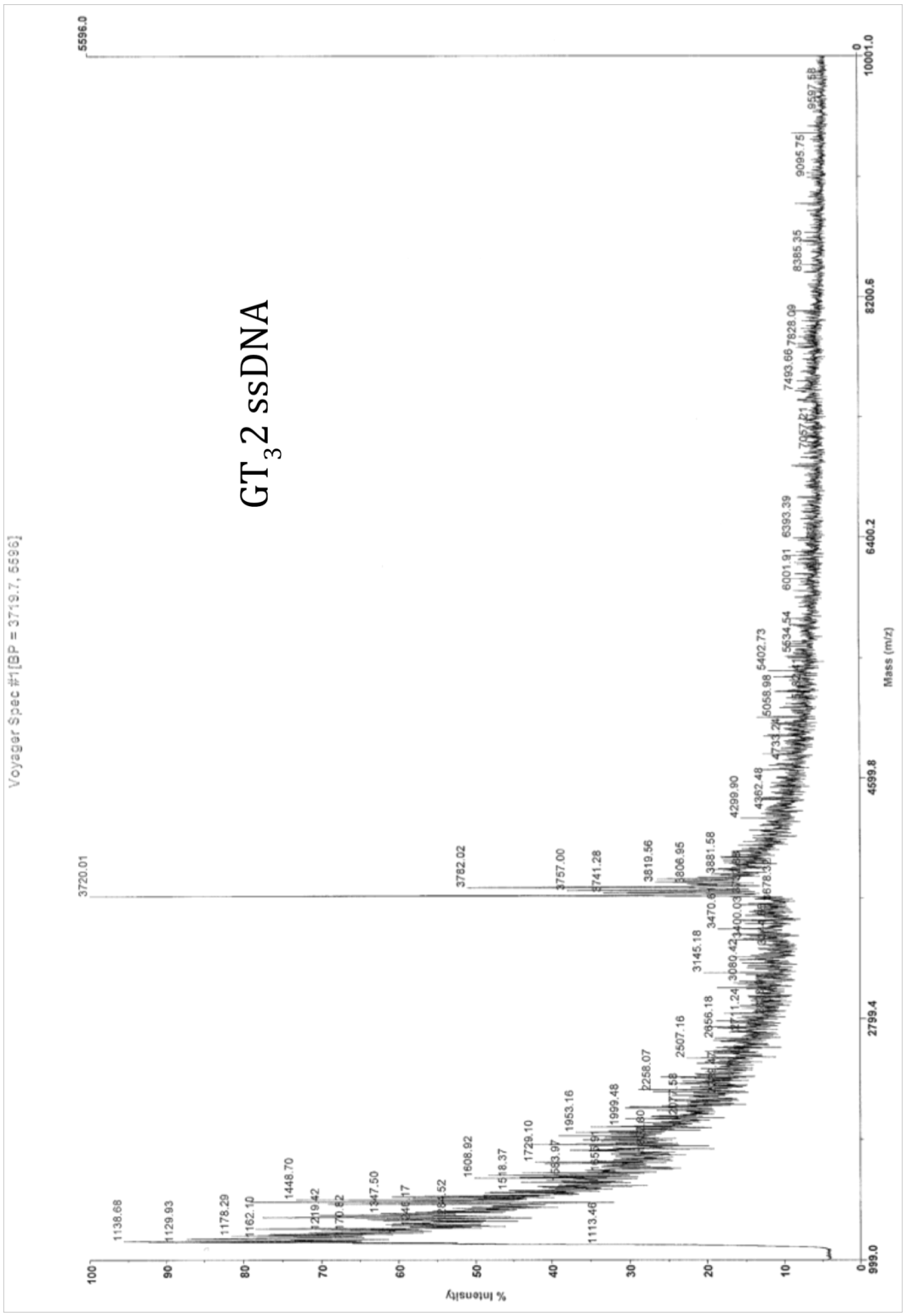
GT3 2 ssDNA
Voyager Spec #1[BP = 3719.7, 5596]
% Intensity
Mass (m/z)
3720.01
3782.02
5596.0

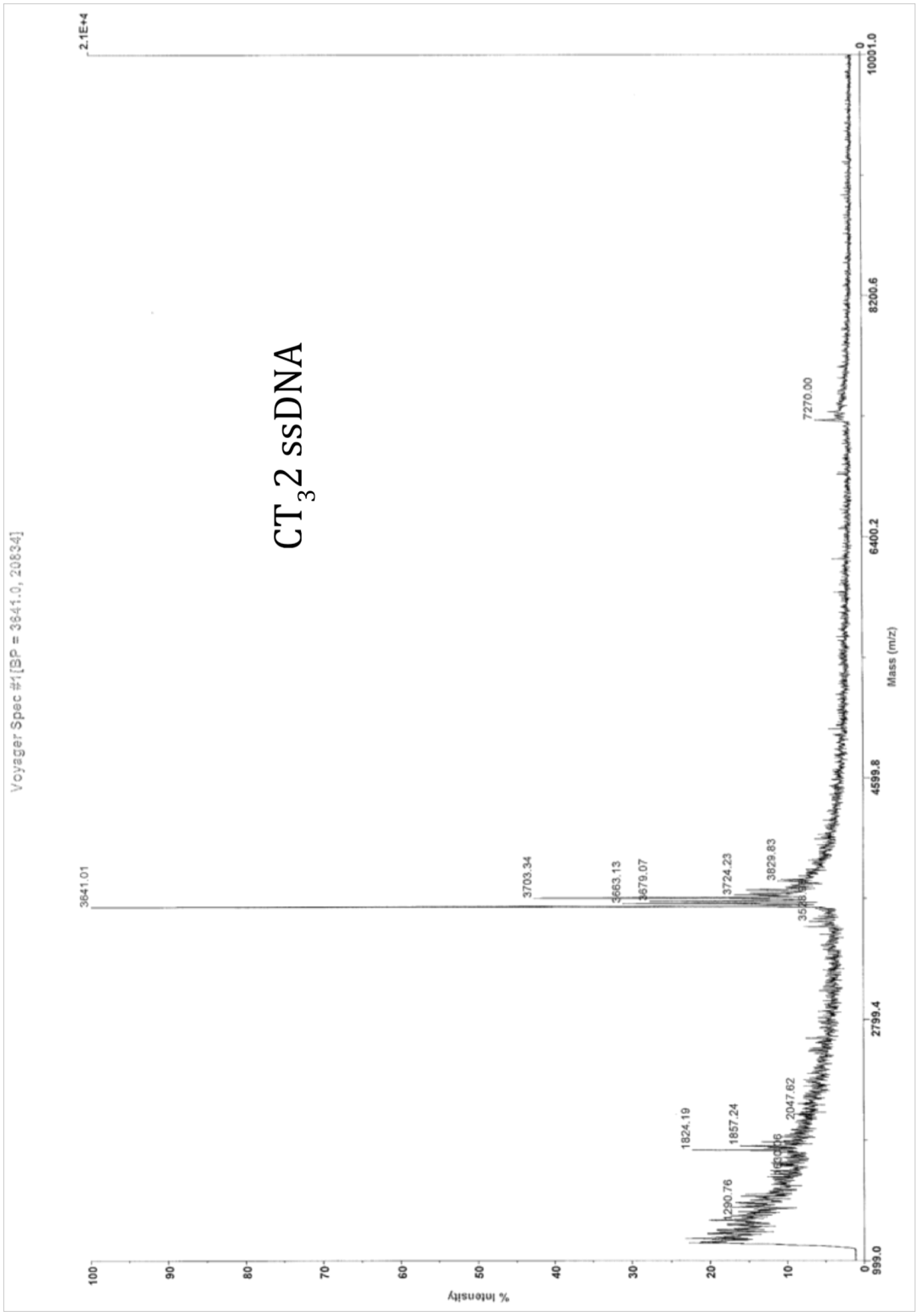
Voyager Spec #1[BP = 3641.0, 20834]
$CT_3 2$ ssDNA
% Intensity
Mass (m/z)
3641.01
3703.34
3663.13
3679.07
3724.23
3829.83
7270.00
1824.19
1857.24
2047.62
1290.76
2.1E+4
100
90
80
70
60
50
40
30
20
10
0
999.0
2799.4
4599.8
6400.2
8200.6
10001.0